Process modelling and economic evaluation of waste tyres to limonene via pyrolysis

by

Lusani Mulaudzi

Thesis presented in partial fulfilment
of the requirements for the Degree

of

MASTER OF ENGINEERING
(CHEMICAL ENGINEERING)

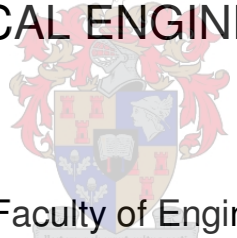

in the Faculty of Engineering
at Stellenbosch University

Supervisor

Professor Percy van der Gryp

Co-Supervisor/s

Professor Cara Schwarz

December 2017

DECLARATION

By submitting this thesis electronically, I declare that the entirety of the work contained therein is my own, original work, that I am the sole author thereof (save to the extent explicitly otherwise stated), that reproduction and publication thereof by Stellenbosch University will not infringe any third party rights and that I have not previously in its entirety or in part submitted it for obtaining any qualification.

Signature: Lusani Mulaudzi

Date: December 2017

ABSTRACT

It is estimated that there are 60 million waste tyres disposed of across South Africa, with approximately 11 million waste tyres added each year. Most of the waste tyres end up being dumped in landfills and stockpiles; the dumps and stockpiles present a series of environmental and human health problems. Processes such as incineration, material recovery, re-treading and energy recovery have mostly been used as current pathways to deal with the waste tyre problem. Current processes have shown to be environmentally unfriendly and/or economically unattractive due to emissions, low demand and low market prices of their associated products.

Pyrolysis has emerged as a potential process that can be used to tackle the problem of waste tyre disposal by valorisation through conversion into gas, liquid, and char products. The liquid product of tyre pyrolysis contains compounds like limonene, benzene, toluene, xylene, and styrene, which could be valuable chemical feedstock due to their market values. Pyrolysis processes that focus on recovery of valuable products are greatly desired to improve the economics of waste tyre pyrolysis.

The main objective of this study was to investigate the economic feasibility of using the pyrolysis technology for upgrading low-value waste tyres to high-value chemicals. Limonene was chosen as the valuable compound of interest in this study. Using literature sources, a seven-step/level hierarchical method with mostly Douglas approach logic was used to develop and evaluate the process for upgrading the waste tyres into limonene.

A literature-based Aspen Plus® simulation model was developed to evaluate the technical performance of the process, and the model was also used as a tool to ascertain the economic feasibility of the process. The PR-BM and NRTL property models were used for conventional components in the simulation model, with the UNIFAC property model used to estimate missing binary parameters for the NRTL model. The HCOALGEN and DCOALIGT property models were used for non-conventional components in the simulation model.

The discounted cash flow method was used to evaluate the economic feasibility of a 30 tons/day waste tyres to limonene process, producing limonene at a rate of 672 kg/day and a purity of 95 wt.%. The residual TDO from the waste tyres to limonene process (at 523 L/hr) was also sold to generate income. The waste tyres to limonene process was then compared with a 30 tons/day conventional process of tyre

pyrolysis for TDO production on the basis of economic performance. The tyres to limonene process was found to be more economically feasible than the tyres to TDO process at the end of a 10 year plant life.

The tyres to limonene process had an IRR of 30%, NPVs of 6.3 and 1.1 MM$ at 12% and 25% discount rates respectively, and a payback period of just under 3 years, at a current limonene selling price of $12/kg. The process had capital investment requirements of 7.6 MM$. Sensitivity analysis showed that the process is most sensitive to changes in the cost of distillation columns, limonene selling price, and the yield of limonene. To achieve 25% IRR for economic attractiveness, a maximum column cost of 2.5 MM$, a minimum limonene selling price of $10/kg, or a minimum limonene yield of 2.1 wt.% are required. For the process to achieve the minimum required IRR of 12% to ensure feasibility, a maximum column cost of 5.3 MM$, a minimum limonene selling price of $5/kg, or a minimum limonene yield of 1.1 wt.% are required.

The tyres to TDO process showed that an IRR of 17% can be achieved, with a payback period of 4.4 years and an NPV of 0.71 MM$ at 12% discount rate, at a current TDO selling price of $0.27/L. A capital investment of 3.3 MM$, and annual total operating cost of $525 323 will be required for the process.

Keywords: Waste tyres, Pyrolysis, Limonene, Aspen Plus® simulation, Economic feasibility, NPV, IRR.

OPSOMMING

Dit word beraam dat daar 60 miljoen bande bestaan regoor Suid-Afrika en elke jaar word daar ongeveer 11 miljoen afval bande bygevoeg. Meeste van die afval bande beland in stortingsterreine; hierdie stortingsterreine veroorsaak n reeks van omgewings- en menslike gesondheidsprobleme. Prosesse soos verbranding, die herwinning van materiale, "*re-treading*" en die herwinning van energie word huidiglik uitgelig as behandelingsmetodes van afval bande. Dit is wel bewys dat huidiglike prosesse, as gevolg van emissies, lae vraag en lae markpryse van verwante produkte, onaantreklik is vanaf beide n omgewings en ekonomiese standpunt.

Pirolise word uitgelig as n potensiele proses om die afval band probleem te behandel deur die omskakeling daarvan na n gas, vloeistof of "char" produkte. Die vloeistof produk vanaf die pirolise van bande bevat potensiele waardevolle verbindings soos limonene, benseen, tolueen, xileen en stireen as gevolg van hul hoe markwaardes. Die winsgewendheid van die pirolise van afval bande word verbeter deur fokus te verskuif na die herwinning van waardevolle produkte.

Die hoofdoel van hierdie studie was om die ekonomies vatbaarheid van pirolise tegnologie te ondersoek vir die opgradering van afval bande na waardevolle chemikaliee. Die verbinding van belang vir hierdie studie was gekies as limonene. Die opgraderingsproses van afval bande na limonene was ontwikkel en ondersoek deur gebruik te maak van n sewe-stap/vlak hierargiese metode, gebaseer op die Douglas benadering.

Die tegniese en ekonomiese vatbaarheid van die proses was evalueer deur gebruik te maak van n literatuur-gebaseerde Aspen Plus® simulasie model. Die PR-BM en NRTL eienskap modelle was gebruik vir die bepaling van konvensionele komponente in the die simulasie model. Die UNIFAC eienskap model was gebruik om die onbekende parameters in die NRTL eienskap model te bepaal. Die HCOALGEN en DCOALIGT eienskap modelle was gebruik vir die bepaling van onkonvensionele komponente in die simulasie model.

Die ekonomiese vatbaarheid van die afval band na limonene proses was evalueer deur die '*discounted cash flow method*' met a voer- en produksietempo van onderskeidelik 30 ton/dag en 672 kg/day, met a suiwerheid van 95 wt%. Die TDO oorblyfsel (523 L/hr) vanaf die afval band na limonene proses was verkoop teen n wins. Die proses was vergelyk met die konvensionele proses van TDO produksie deur afval

band verbranding vanaf n ekonomiese perspektief. Dit was bevind dat vanuit n ekonomiese oogpunt, die omskakeling van afval bande na limonene haalbaar was aan die einde van n 10 jaar aanleg leeftyd.

Dit was bevind dat die afval band na limonene proses n IOK van 30%, n NPV van 6.3 en 1.1 MM$ het teen n afslagkoers van 12% en 25%, onderskeidelik, en n terugbetaal periode van net onder 3 jaar met die huidiglike limonene verkoopsprys van $12/kg. Die proses vereis n kapitalbelegging van 7.6 MM$. Dit was bewys deur sensitiwiteitsanalise dat die proses meer sensitief is teenoor veranderinge in the prys van distillasiekolomme, die verkoopsprys van limonene en die proses opbrengs van limonene. Ekonomiese aantreklikheid deur n 25% IRR kan bereik word, deur n maksimum kolom koste van 2.5 MM$, n minimum limonene verkoopsprys van $10/kg, of n minimum limonene proses opbrengs van 2.1 wt.% te vereis. Vir die proses om vatbaarheid te verseker deur a minimum IRR van 12% te bereik, n maksimum kolom koste van 5.3 MM$, n minimum limonene verkoopsprys van $5/kg, of n minimum limonene proses opbrengs van 1.1 wt.% word vereis.

Daar was bevind dat die pirolise van bande vir die produksie van TDO n IOK van 17% en n NPV van 0.71 MM$ kan behaal met n terugbetaal periode van 4.4 jaar met die huidiglike TDO verkoopsprys van $0.27/L. Hierdie proses vereis n kapitaalbelegging van 3.3 MM$ en n total bedryfskoste van $525 323.

Sleutelwoorde: Afval bande, Pirolise, Limonene, Aspen Plus® simulasie, Ekonomiese vatbaarheid, NPV, IOK.

ACKNOWLEDGEMENTS

I would like to sincerely thank the following people for their enormous contribution towards the success of this study:

- The Lord Jesus Christ for the provision of life, sustaining me up to this point and the countless favours.
- My supervisors, Professor Percy van der Gryp and Professor Cara Schwarz for their patience, guidance, support and critical evaluation of my work throughout.
- The Recycling and Economic Development Initiative of South Africa (REDISA), the National Research Foundation (NRF) and the Technology and Human Resources for Industry Programme (THRIP) for financial support.
- Dr Somayeh Farzad for her immense assistance with the development of Aspen simulation models, economic evaluation and for the countless consultations we had. Your assistance is highly appreciated.
- Dr Bart Danon for his assistance in the early stages of the project especially in selecting the right literatures to use for my simulations. Your assistance is highly appreciated.
- The REDISA research group for their inputs and suggestions during the progress meetings.
- My mom for her love, continuous support and encouragement during the tough times.
- Family and friends for their continuous encouragement.
- Aspen Technology.
- All the many postgrad colleagues from whom I would seek assistance from time to time.

DEDICATION

To my mom Vho-Azwitamisi Joyce Ndiitwani for her love and continual support

Mmawe, heyi ndi yavho!!!!

TABLE OF CONTENTS

NOMENCLATURE

Abbreviation	Definition
BM	Boston-Mathias alpha function
BFD	Block flow diagram
BR	Butadiene rubber
BTX	Benzene, toluene and xylene
CB	Carbon black
CEPCI	Chemical Engineering plant cost index
CPR	Chloroprene rubber
DCFROR	Discounted cash flow rate of return
DCOALGEN	Coal density model
DCOALIGT	IGT coal density model
DEG	Diethylene glycol
DTG	Derivative thermogravimetric
EOS	Equation of state
EU	European union
HCOALGEN	General coal enthalpy model
HETP	Height equivalent to theoretical plate
HFO	Heavy fuel oil
IRR	Internal rate of return
ISBL	Inside battery limits
KEI	Key economic indicator
LLE	Liquid-liquid-equilibrium
LK-PLOCK	Lee-Kesler-Plocker
MM	Million
Mt	Million tons
MT	Metric tons

Abbreviation	Definition
NO_x	Nitrogen oxides
NPV	Net present value
NR	Natural rubber
NRTL	Non-random two-liquid
NTR	Nitrile rubber
OL	Operating labour
OPEX	Operating expenditure
PAHs	Polycyclic aromatic hydrocarbons
PBD	Polybutadiene rubber
PBP	Payback period
PCT	Passenger car tyre
Pet-coke	Petroleum coke
PFD	Process flow diagram
PPC	Pretoria Portland Cement
PR	Peng-Robinson
PENG-ROB	Peng-Robinson
REDISA	Recycling and development initiative of South Africa
RGIBBS	Equilibrium reactor
RKS	Redlich-Kwong-Soave
RK-SOAVE	Redlich-Kwong-Soave
RPLUG	Plug flow reactor
RSTOIC	Stoichiometric reactor
RYIELD	Yield reactor
SBR	Styrene-butadiene rubber
SO_x	Sulphur oxides
SSE	Sum of square of errors

Abbreviation	Definition
STMC	Scrap Tire Management Council
TAC	Total annualised costs
TCI	Total capital investment
TDC	Total direct cost
TDF	Tyre derived fuel
TDO	Tyre derived oil
TFCI	Total fixed capital investment
TGA	Thermogravimetric analysis
TIC	Total indirect costs
TT	Truck tyre
UNIFAC	Universal function activity coefficient
USA	United States of America
VLE	Vapour-liquid-equilibrium
VLLE	Vapour-liquid-liquid-equilibrium
VOCs	Volatile organic compounds
WC	Working capital
WT	Waste tyres

Symbol	Definition	Units
Ash_i	Ash flow rate from component *i*	kg/hr
F_i	Flow rate of component *i*	kg/hr
G	Gas fraction	-
i	Component *i*	-
L	Oil fraction	-
n	Exponential factor	-
N_i	Nitrogen flowrate from component *i*	kg/hr
S	Char fraction	-
S_i	Sulphur flow rate from component *i*	kg/hr
x_i	Yield of component *i* from tyre	wt.%
X_i	Composition of component *i*	wt.%
Y_i	Yield of component *i* from tyre	wt/wt

CHAPTER 1: INTRODUCTION

1.1. Background and motivation

The increase in the demand for tyres has led to a subsequent increase in the amount of tyres reaching their end-of-life. The annual global production of tyres is approximately 1.5 billion with just as many reaching their end-of-life (Williams, 2013; Pilusa *et al.*, 2014; Danon *et al.*, 2015). The United States of America (USA) generated 500 million waste tyres in 2007 whereas the European Union (EU) generated 289 million waste tyres in 2010 (Quek and Balasubramanian, 2013; Danon *et al.*, 2015). In South Africa, annual waste tyre generation is estimated at 11 million tyres (REDISA, 2012; Pilusa *et al.*, 2014).

Most of the waste tyres end up being dumped in landfills and stockpiles and they resist degradation due to their make-up (Martinez *et al.*, 2013; Hita *et al.*, 2016; Wang *et al.*, 2016). The waste tyre dumps and stockpiles present a serious threat to both the environment and human health as they promote the growth of pests and disease carrying insects. Dumps and stockpiles also present a risk of explosive gases as the tyres trap gases while disposed of in landfills (Leung and Wang, 2003; Quek and Balasubramanian, 2013). Waste tyre dumps also present a potential risk of fires that could be difficult to extinguish which would have serious environmental implications (Islam *et al.*, 2011; Choi *et al.*, 2014; Wang *et al.*, 2016).

Different methods have been used as possible pathways for dealing with the problem of waste tyres. Waste tyres have been used in processes like incineration, civil engineering applications, material recovery, re-treading, energy recovery and pyrolysis (Islam *et al.*, 2011; Pilusa *et al.*, 2014). Incineration has drawbacks associated with the disposal of ash, production of toxic emissions and the production of soot (Sharma *et al.*, 2000; Islam *et al.*, 2011). Material recovery methods have drawbacks associated with high energy consumption and a limited market for the associated products (Amari *et al.*, 1999; Sharma *et al.*, 2000; Quek and Balasubramanian, 2013). Re-treading is mainly limited by quality demands, reliability and intricate technical conditions set by the world market (Amari *et al.*, 1999; Sharma *et al.*, 2000; Muzenda and Popa, 2015).

The use of waste tyres as tyre-derived-fuel (TDF) for energy recovery is the major route currently used for treating waste tyres with the majority of TDF used in cement kilns. There are drawbacks associated with this application such as emissions control, product quality control and modifications needed to accommodate TDF (Barlaz *et al.*, 1993; Amari *et al.*, 1999; Giugliano *et al.*, 1999; Conesa *et al.*, 2008).

Environmental concerns, low product demand and low market value of the products are the main limitations and drawbacks associated with the current methods for dealing with waste tyres. These limitations and drawbacks lead to the current pathways being unable to greatly reduce the billions of tyres currently in stockpiles and landfills.

Pyrolysis is a method that could be used to valorise the waste tyres through conversion into valuable products.

Pyrolysis of waste tyres has been gaining popularity as an attractive (alternative) method of recycling waste tyres (Lopez *et al.*, 2010; Islam *et al.*, 2011; Muzenda and Popa, 2015). Pyrolysis is a thermal process that decomposes an organic material into low molecular weight compounds under inert conditions (Cunliffe and Williams, 1998a; Amari *et al.*, 1999). During waste tyre pyrolysis, the organic rubber material is broken down into a gas (pyrolysis gas), liquid (pyrolysis oil/tyre derived oil (TDO)) and a solid product (pyrolysis char) (Kyari *et al.*, 2005; Lopez *et al.*, 2010; Islam *et al.*, 2011; Wang *et al.*, 2016). Waste tyres have a high volatile content, which gives high yields of pyrolysis gas and pyrolysis oil (Williams and Besler 1995; Kyari *et al.*, 2005; Martinez *et al.*, 2013).

The pyrolysis gas has a high calorific value and it is mostly used as alternative fuel for the pyrolysis process (Kyari *et al.*, 2005; Olazar *et al.*, 2008). The pyrolysis char contains the inorganic matter of the tyre (ash, zinc oxide, steel, silicates etc.) and non-volatile carbon black (Amari *et al.*, 1999; Li *et al.*, 2004). The char product can either be used as activated carbon (after activation and upgrading), as a solid fuel or re-used as carbon black in the tyre manufacturing process after upgrading (Wojtowicz and Serio, 1996; Amari *et al.*, 1999). Of the pyrolysis products, the pyrolysis oil/TDO is the most interesting fraction.

TDO is a complex mixture of aliphatic and aromatic compounds which can be attributed to a wide variety of formulations used in tyre manufacturing (Cunliffe and Williams, 1998a; Kyari *et al.*, 2005; Choi *et al.*, 2014). TDO has a high calorific value (about 40-44 MJ/kg) and it has primarily been used as an alternative fuel either directly (in its raw form) or blended with diesel fuel (Muragan *et al.*, 2008; Aydin and Ilkilic, 2012; Martinez *et al.*, 2013; Frigo *et al.*, 2014). However, using TDO as fuel results in low TDO selling prices as raw TDO is generally sold as the equivalence of heavy fuel oil (HFO), which is a very low cost liquid fuel (Pilusa and Muzenda, 2013; Pilusa *et al.*, 2014).

TDO has also been shown to be a potential source of chemical feedstock as it contains valuable chemicals like benzene, toluene, xylene, styrene, ethylbenzene and limonene. These are chemicals that have wide

industrial applications (Williams and Brindle, 2003a; Li *et al.*, 2004; Lopez *et al.*, 2010; Choi *et al.*, 2014). The presence of these various compounds in TDO makes waste tyre pyrolysis an excellent method/pathway for upgrading waste tyres to valuable chemicals.

The low market value of pyrolysis products results in low selling prices, which yields low returns; this could render waste tyre pyrolysis commercially unattractive (Wojtowicz and Serio, 1996; Amari *et al.*, 1999). As such, a process that focuses on recovery of high market value (value-added) products would greatly improve the economic attractiveness of waste tyre pyrolysis (Wojtowicz and Serio, 1996). One interesting valuable chemical of the ones contained in TDO is limonene, and it is the chemical that this study will focus on. The current demand for limonene is mostly catered for by citrus-derived limonene, and the price of citrus-derived limonene can range between 8 and 25 US$ per kilogram depending on product purity (Florida Chemicals Co., 1991a,b,c; Pakdel *et al.*, 2001; Stanciulescu and Ikura, 2007; Danon *et al.*, 2015). It can therefore be expected that targeting the recovery of limonene would improve the economic attractiveness of waste tyre pyrolysis given the potential high selling price of limonene.

Limonene is a monoterpene that is a dimer of two isoprene molecules, and can be obtained from the thermal decomposition of the polyisoprene contained in the tyre according to the reaction scheme represented in Figure 1.

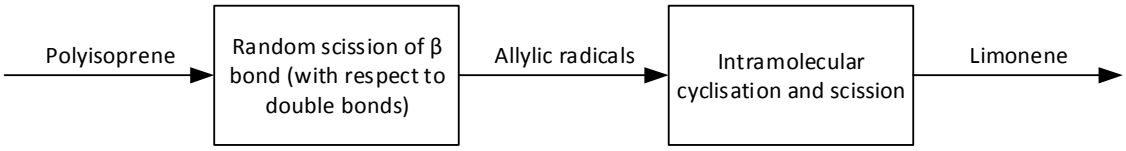

Figure 1: Reaction scheme of limonene formation from polyisoprene (from Chien and Kiang, 1979; Danon *et al.*, 2015)

Limonene is a major component of TDO with common yields of between 2.5 and 5 wt.% on the basis of a steel-free tyre (Lopez *et al.*, 2010; Danon *et al.*, 2015). Limonene has wide industrial applications, and has been used in the formulation of industrial solvents, terpene resins and adhesives, as a cleaning agent, as a dispersing agent for pigment and in the manufacturing of flavouring agents, fragrances and pesticides (Pakdel *et al.*, 2001; Stanciulescu and Ikura, 2007; Williams, 2013; Danon *et al.*, 2015).

This study, therefore, seeks to investigate the economic feasibility of using the pyrolysis technology for upgrading low-value waste tyres to high-value chemicals such as limonene.

1.2. Aims and objectives

Different methods/processes that are currently used for dealing with the problem of waste tyres have shown to be economically unfeasible due to different limitations and drawbacks associated with them and the products they produce. One of the main drivers for recommendation of pyrolysis as a method for dealing with the waste tyre problem is the fact that it produces chemicals that are of high market value (Li *et al.*, 2004; Lopez *et al.*, 2010). It has also been shown that a process that focuses on the recovery of valuable chemicals from waste tyres could greatly improve the economics of waste tyre pyrolysis (Wojtowicz and Serio, 1996). Limonene has been shown to be a high value chemical product of waste tyre pyrolysis with a wide range of industrial applications. Literature studies that have been done on the economics of waste tyres have not focused on the analysis of converting waste tyres into valuable chemicals by pyrolysis. As such, there exists a gap in literature which indicates the economic feasibility of recovering valuable chemicals from waste tyre pyrolysis.

Therefore, this study aims to evaluate the economic viability of different pyrolysis and separation process scenarios that can be used for recovering valuable chemicals from waste tyres.

In order to achieve the aim of this study, four main objectives are defined as follows:

- **Objective 1:** Investigate current technologies available to convert waste tyres into various valuable chemicals.
- **Objective 2:** Propose and develop various conceptual process scenarios for converting waste tyres into targeted valuable chemicals.
- **Objective 3:** Develop Aspen Plus® models/simulations for the scenarios of objective 2.
- **Objective 4:** Evaluate the different scenarios from techno-economic and energy utilisation viewpoints.

1.3. Scope of study and thesis layout

The scope of this study is graphically outlined in Figure 2. This thesis is subdivided into six chapters (including this one) that are set out to achieve the objectives as listed in section 1.2.

Chapter 2 provides details on the methodology that was used to achieve the objectives of this study. Firstly, a brief review of the methodologies commonly used to address process conceptualisation tasks in

literature is provided. Thereafter, focus is then placed on selecting and/or developing a methodology that is specific to this study. Details of the activities performed in each methodology step are presented.

Chapter 3 offers a review of the available literature that has been published with respect to the waste tyre problem. Objective 1 of the study is addressed in this chapter. A general overview of the waste tyre problem and the different methods/processes used to deal with the waste tyres is presented. Pyrolysis of waste tyres as a possible solution to the waste tyre problem is discussed and the valuable chemicals that can be obtained from waste tyre pyrolysis are highlighted. Economics of waste tyre pyrolysis are also discussed. Thereafter, the focus is shifted to the review of modelling/simulation work that has been done for pyrolysis systems in general and in relation to waste tyres. Typical pyrolysis process flow diagrams are also reviewed and a block flow diagram proposed for this study is presented.

Chapter 4 details the development of a proposed base case process scenario for converting waste tyres into a valuable chemical (limonene) through pyrolysis technology. Focus is placed on detailing the development of different sections of the proposed process i.e. pre-treatment, pyrolysis, separation and energy recovery sections. Development of each section of the proposed process is detailed from a technical evaluation and Aspen Plus® modelling/simulation point of view. A complete (combined) process flow diagram of the proposed process is also provided. Objectives 2 and 3 of the study are addressed in this chapter.

Chapter 5 focuses on evaluation of the proposed process developed in chapter 4 from an economic viewpoint thereby addressing objective 4 of the study. An economic model is developed which serves as a guideline for economic evaluation after which results of economic evaluation of the proposed process are presented. Results of economic evaluation of other pre-treatment scenarios (with respect to pre-treatment configuration of the process proposed in chapter 4), energy recovery scenario and the waste tyres to TDO scenario are also presented. Comparison of economic results of the scenario developed in chapter 4 with the other scenarios is performed, after which, sensitivity analysis of the best performing scenario is performed.

Chapter 6 Provides a summary of the main findings of this study and gives recommendations for future work.

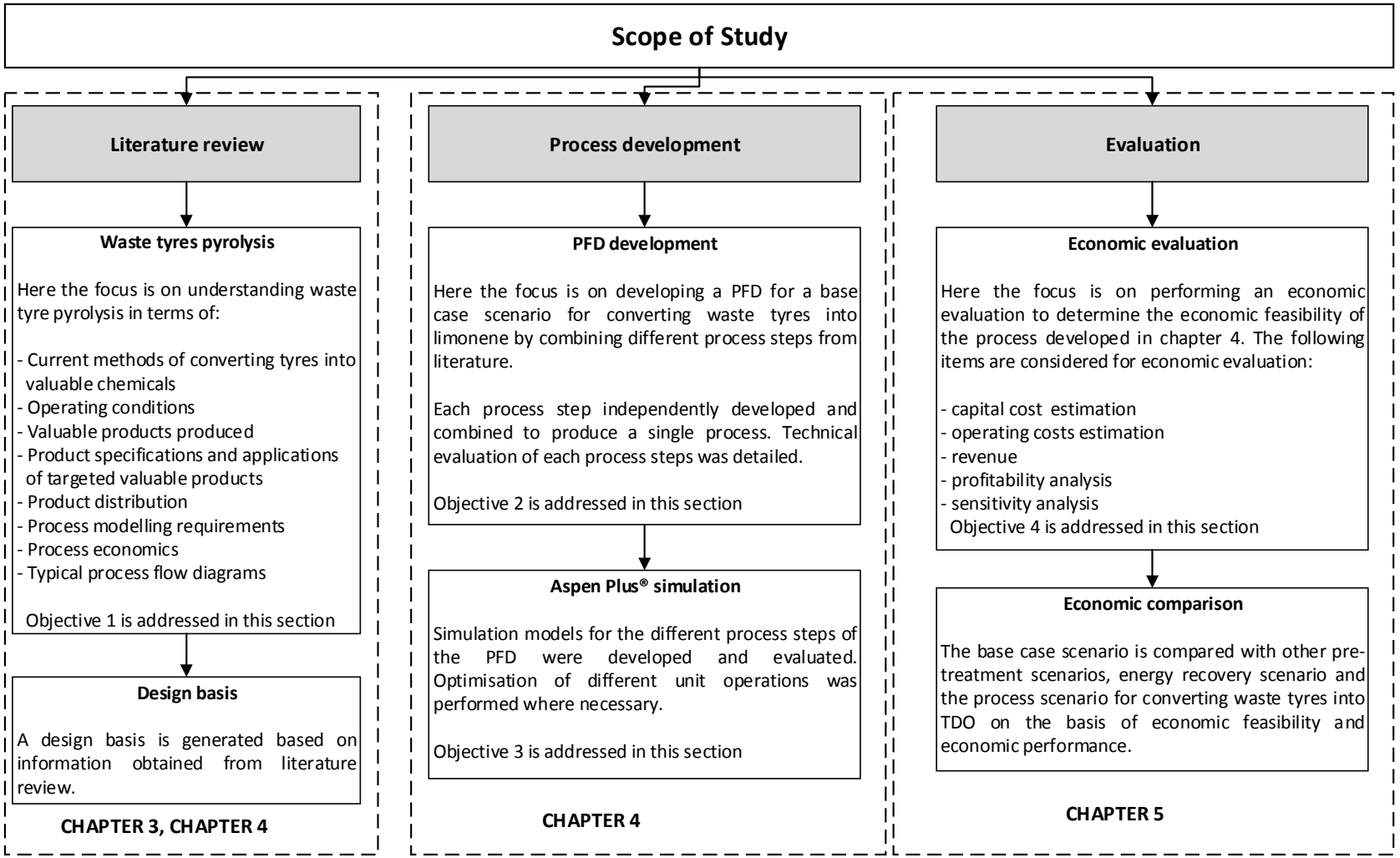

Figure 2: Graphical representation of the scope of this study

CHAPTER 2: FRAMEWORK AND METHODOLOGY

Overview

In this chapter, the methodology that was used to accomplish the objectives of this study is outlined. This chapter is subdivided into 3 sections. Section 2.1 gives a brief review of common literature methodologies used to develop conceptual processes and the most common ways of evaluating conceptual processes. In section 2.2, the methodology used in this study is outlined and the activities carried out in each step of the methodology are provided. Section 2.3 gives a summary of the chapter.

2.1. Synthesis approach and process evaluation

Mapamba (2012) mentioned that according to John Curry (2010), when a problem and its objectives are known, an engineering method can be applied for problem solving. There then exists three key steps between the problem and the solution, which are: generation of possible solutions, testing the solutions, and implementing the most viable solution. For problems that are of a process conceptualisation nature, the three steps can be translated to: identification of candidate processes, evaluation of the candidate processes and presentation of the most viable option. A conceptual design can then be developed for each of the possible/candidate processes. In order to generate an appropriate process configuration for each candidate process, many process flowsheets have to be generated and evaluated during process synthesis to identify those exhibiting better performance indicators (Sanchez and Cardona, 2012). As such, a systematic approach to problem-solving then becomes vital in order to achieve the set objectives (Mapamba, 2012). For problems that involve process simulation, a systematic approach becomes even more important in order to avoid the output from the simulation being misleading or meaningless (Oden *et al.*, 2006).

For design of conceptual processes, there exists a range of process synthesis approaches that have been proposed which are classified into two main approaches i.e. mathematical/optimisation-based approaches and knowledge-based/heuristic approaches (Alqahtani *et al*., 2007; Sanchez and Cardona, 2012).

Optimisation-based approaches involve the formulation of flowsheet synthesis in the form of an optimisation problem and requires explicit representation of a superstructure of process flowsheets from which the optimal solution is selected (Li and Kraslawski, 2004). According to Grossmann *et al*. (2000), there are three main classes of optimisation-based models i.e. aggregated models, short-cut models and rigorous models. Two common features that characterise optimisation-based approaches are formal and mathematical representation of the problem and the subsequent use of optimisation

(Li and Kraslawski, 2004). The main advantage of optimisation-based approaches is the provision of a systematic framework for handling a variety of process synthesis problems, and more rigorous analysis of features such as structure interactions and capital costs (Li and Kraslawski, 2004). The main drawbacks associated with optimisation-based approaches are the lack of ability to automatically generate a flowsheet superstructure, the need for huge computational effort and guarantee of solution optimality only with respect to alternatives that have been considered a priori (Grossmann *et al*., 2000; Li and Kraslawski, 2004).

Knowledge-based (heuristic) approaches have their bases on long-term engineering and research experience and they combine heuristics with an evolutionary strategy for process design (Li and Kraslawski, 2004; Sanchez and Cardona, 2012). The main feature of knowledge-based approaches is the decomposition of the synthesis task into various decision levels for which solutions are separately generated and then combined into a single flowsheet (Grossmann *et al*., 2000; Li and Kraslawski, 2004). The main advantages of knowledge-based approaches are generation of various alternatives that can be economically evaluated using short-cut methods and screening of alternatives which avoids detailed evaluation of each alternative (Grossmann *et al*., 2000; Sanchez and Cardona, 2012). The main disadvantages of knowledge-based approaches include the inability to rigorously produce optimal designs (despite various alternatives generated) and the improper management of interactions between different decision levels (Grossmann *et al*., 2000; Li and Kraslawski, 2004; Sanchez and Cardona, 2012).

Ever since Siirola and Rudd (1971) first made an attempt to develop a systematic heuristic approach for synthesis of a separation sequence for a multicomponent process, several methodologies/approaches have been developed targeting a range of chemical processes (Li and Kraslawski, 2004). Examples include those approaches proposed/developed by Douglas (1988), Jaksland *et al*. (1995), Smith (1995), Seider *et al*. (2004), Alqahtani *et al*. (2007) and Turton *et al*. (2009). Of these knowledge-based approaches, the commonly used approach methods are those of Douglas (1988) and Smith (1995).

The Douglas method is a hierarchical method which breaks down a large complex problem into smaller easier to handle steps (Kusiak and Finke, 1987; Douglas, 1988; Emets *et al.*, 2006). The Douglas method starts by determining the mode of operation and then progresses through various design “hierarchy” levels of the particular mode of operation (Douglas, 1988; Emets *et al.*, 2006).

The method developed by Smith (1995) involves creation of an irreducible structure. The irreducible structure approach creates a structure in its basic form and is based on the “onion” model with each

layer of the onion representing a certain level of design (Smith, 1995; Eriksson *et al.*, 2004; Foo *et al.*, 2005). The onion model is also hierarchical like the Douglas method and emphasises the sequential (hierarchical) nature of process design (Foo *et al.*, 2005; Emets *et al.*, 2006). The advantages and disadvantages of the Smith method and the Douglas method as pointed out by Douglas (1988), Smith (1995) and by Emets *et al.* (2006) are shown in Table 1.

Table 1: Advantages and disadvantages of design approaches developed by Douglas and by Smith

Approach	Advantages	Disadvantages
Douglas hierarchical method	- Enables equipment size calculations and cost estimation throughout hierarchy levels - Decision making at each hierarchy level (allows for generation of process alternatives should design decisions change)	- No distinct reactor design step - Recycling considered a distinct design step
Irreducible structure (Smith method)	- More control of the design process - Inclusion of rational thinking for decision making - More design options can be completed and evaluated	- Early decisions based on incomplete information - Evaluation of many design options that do not guarantee finding an optimal design

When design of conceptual processes is complete, the next step is evaluation of the developed processes (Mapamba, 2012). Evaluation of conceptual processes is commonly accomplished by use of process simulators (Linninger, 2002; Foo *et al.*, 2005; Emets *et al.*, 2006). Process simulation is advantageous over experimental work in that it is not affected by limitations of experimental designs Mapamba (2012). Experimental designs are often constrained by costs, parameter ranges and measuring procedures (Oden *et al*., 2006). Process simulation can also avoid having to rework the experimental work should the candidate process prove to not be the most promising option (Foo et al., 2005).

2.2. Methodology as used in this study

The process of converting waste tyres into limonene carried out in this study will include tyre pre-treatment, pyrolysis, fractionation of the oil product to produce a limonene-rich stream, extractive distillation for limonene recovery and energy recovery. The process in this study is desired to be continuous. The process steps therefore indicate that a simplistic process scheme will be required as

opposed to large complex systems including many process steps required to produce, recover, and purify a wide range of products. In addition to process design, economic feasibility and energy utilisation evaluations will be performed in the current study.

As such, a hierarchical stepwise approach with mostly modified Douglas approach logic is chosen as the methodology to achieve the objectives set out for this study. The need for rational decision making at each level of design and the sequential nature of progression are the main contributing factors to the choice of methodology in this study. Each (major) step in the task of addressing the objectives of this study can then just be represented as a hierarchical level with the hierarchy extended beyond the design phase. The adapted hierarchical and stepwise methodology used in this study is shown in Figure 3. Iterative loops are incorporated in the methodology to account for the iterative nature of using knowledge-based approaches in process design.

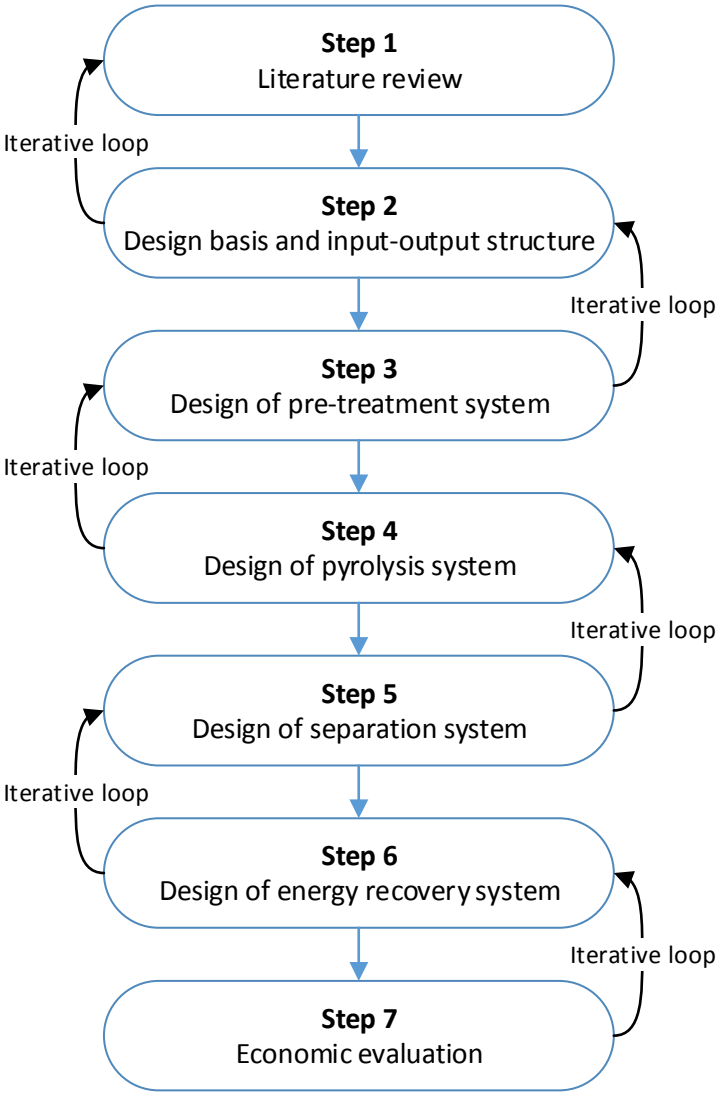

Figure 3: Methodology adopted for use in this study

Details of the activities carried out in each step of the hierarchical sequence shown in Figure 3 are provided in Table 2.

Table 2: Details of methodology steps used in this study

Activity	Sectioned applied	Objectives addressed
Step 1: Literature review		
(a) Current methods of valorising waste tyres	3.1.3	1
(b) Input information	3.2.2	2 and 3
(c) Valuable chemicals from tyre pyrolysis	3.3.3	1
(d) Pyrolysis operating conditions	3.3.4	2
(e) Product distribution	3.3.4	2
(f) Tyre pyrolysis process modelling	3.4.1	3
(g) Typical tyre pyrolysis process flow diagram	3.5	1 and 2
Step 2: Design basis and input-output information		
(a) Design basis	4.1	2 and 3
a.1. Raw materials and production capacity		
a.2. Mode of operation		
a.3. Product target specification		
a.4. Selection of simulation software		
(b) Input-output structure	4.2	2 and 3
b.1. Component selection	4.2	2
b.2. Component specification in Aspen Plus®	4.2.1	3
Step 3: Design of pre-treatment system		
(a) Size reduction requirements and PFD	4.3	2
Step 4: Design of pyrolysis system		
(a) Objective and PFD of the system	4.4	2 and 3
(b) Reactor operating conditions	4.4.1	2 and 3
(c) Reactor product distribution	4.4.2	2 and 3
c.1. Reactor mass balance	4.4.2	
c.2. Yield prediction by correlation equations	4.4.2.1	

Table 2 continued: Details of methodology steps used in this study

Activity	Sectioned applied	Objectives addressed
Step 4: Design of pyrolysis system		
(d) Validation	4.4.3	3
(e) Aspen Plus® simulation	4.4.4	3
e.1. Selection of thermodynamic model	4.4.4.1	
e.2. Flowsheet description	4.4.4.2	
Step 5: Design of separation system		
(a) Objective and PFD of the system	4.5	2
(b) Oil feed temperature determination	4.5.1	2 and 3
(c) Aspen Plus® simulation	4.5.2	3
c.1. Selection of thermodynamic model	4.5.2.1	
c.2. Flowsheet description	4.5.2.2	
c.3. Column optimisation		
Step 6: Design of energy recovery system		
(a) Objective and PFD of the system	4.6	2
(b) Steam generation	4.6	2 and 4
(c) Aspen Plus® simulation	4.6.1	3 and 4
Step 7: Economic evaluation		
(a) Economic model	**5.1**	4
a.2. Economic assumptions	5.1.1	
a.1. Key economic indicators	5.1.2	
(b) Capital costs estimation	**5.2**	
b.1. Aspen Plus® Economic analyser		
b.2. Supplier quotation		
b.3. bare module costing		
b.4. Scale up (sixth-tenths-factor)		

Table 2 continued: Details of methodology steps used in this study

Activity	Sectioned applied	Objectives addressed
Step 7: Economic evaluation		
(c) Operating costs	**5.3**	4
c.1. Variable costs	5.3.1	
c.2. Fixed costs	5.3.2	
(d) Revenue	5.4	
(e) Profitability analysis (DCFROR)	5.5	
(f) Scenario analysis and comparison	**5.6**	
Base case, energy recovery, other pre-treatment scenarios, TDO production scenario		
(g) Sensitivity analysis	**5.7**	
TCI, limonene price, limonene yield, OPEX, TDO price, interest rate, exchange rate		

2.3. Summary

Chapter 2 discussed development of the methodology that was used to achieve the objectives of this study. The methodologies developed by Douglas and by Smith were found to be the most common approaches for design of conceptual processes. Evaluation of conceptual processes is typically achieved by use of processes simulators.

A hierarchical and stepwise methodology with mostly modified Douglas approach logic was developed to achieve the objectives of this study. Literature review forms the basis of conceptual process design in this study, after which, evaluation of the designed conceptual process is achieved by a process simulator. A review of literature with regards to the waste tyre problem, current alternative methods of dealing with waste tyre problem, waste tyre pyrolysis, process modelling of waste tyre valorisation systems and typical process flow diagrams is presented in chapter 3.

CHAPTER 3: LITERATURE REVIEW

Overview

In this chapter, a literature review of upgrading waste tyres to valuable chemicals via pyrolysis will be presented. This chapter aims to address objective 1 of this study (investigation of current technologies available to convert waste tyres into various valuable chemicals). The chapter is subdivided into 6 sections. Section 3.1 discusses the problems that waste tyres pose and the methods that have been used to tackle the problem. Section 3.2 discusses the components that tyres are made of. In section 3.3, pyrolysis of waste tyres is discussed with respect to operating conditions, valuable chemicals produced and the product distribution. A review of current economics of waste tyre pyrolysis is also provided. Section 3.4 discusses the modelling/simulation work that has been done in literature for waste tyre pyrolysis systems. A review of literature on Aspen Plus® modelling/simulation of waste tyre valorisation processes is also provided in section 3.4 and linked to the current study. Section 3.5 gives an overview of typical process flow diagrams of waste tyre pyrolysis processes after which a proposed process for the current study is presented. Section 3.6 gives a summary of the chapter.

3.1. Waste tyre problem

3.1.1. Waste tyre generation

Approximately 1.5 billion new tyres are sold each year worldwide and just as many are categorised as having reached their end-of-life (Williams, 2013). Hita *et al.* (2016) reported that European regulations define end-of-life tyres as those that should either be recycled, valorised or have their usefulness extended (if the intention is to use them again) owing to their physical state and security regulations. The increase in population coupled with economic growth of many nations promote the growth of the automotive industry which in turn increases the number of tyres and subsequently the number of waste tyres discarded annually (Raj *et al.*, 2013). In 2010, 289 million waste tyres were generated in the European Union (EU); 500 million waste tyres were generated in 2007 by the United States of America (USA) and 52.5 million waste tyres were generated in Australia in the years 2007-2008 (Quek and Balasubramanian, 2013; Danon *et al.*, 2015). From a South African context, it is estimated that there are 60 million waste tyres disposed of across the country with approximately 11 million waste tyres added each year (REDISA, 2012; Pilusa *et al.*, 2014).

3.1.2. Disposal of waste tyres

Most of the waste tyres generated end up being dumped in stockpiles and landfills (some illegally); it is estimated that in the developed world 1 car tyre per person is discarded each year (Martinez *et al.*,

2013). It is also estimated that 4 billion waste tyres are currently in landfills and stockpiles worldwide (Martinez *et al.*, 2013).

Tyres are designed to withstand harsh mechanical and weather conditions (such as ozone, light and bacteria) and their complex nature makes them difficult to recycle and/or process further (Adhikari *et al.*, 2000; Leung and Wang, 2003; Raj *et al.*, 2013). Due to their design, waste tyres resist degradation (non-biodegradable) when in landfills and their bulky nature makes them take up a lot of landfilling space (Quek and Balasubramanian, 2013; Pilusa *et al.*, 2014). Waste tyres dumps present a serious threat to both the environment and human health as they promote the growth of pests and disease carrying insects. Waste tyres also pose a high risk of fires that can be difficult to extinguish and could have environmental impacts due to uncontrolled emissions of potentially harmful compounds into the atmosphere, soil and groundwater (Islam *et al.*, 2011). Tyre fires produce toxic gases which contain carcinogenic and mutagenic chemicals, this makes the waste tyre dumps highly undesirable (Quek and Balasubramanian, 2013). Landfilling and stockpiling are thus currently the easiest forms of dealing with waste tyres. However, landfilling and stockpiling fail to utilise the material, energy and chemical potential in waste tyres.

3.1.3. Current methods for treating waste tyres and their challenges

Various processes or methods have been used as alternative pathways for dealing with the problem of waste tyre generation. These pathways are: direct disposal, material recovery and recycling and thermal treatment with energy recovery. Direct disposal includes landfilling and stockpiling. Material recovery and recycling includes processes such as crumbing, milling/grinding, re-treading, devulcanisation, and civil engineering applications (Adhikari *et al.*, 2000; Sharma *et al.*, 2000; Islam *et al.*, 2011; Pilusa *et al.*, 2014). Thermal treatment with energy recovery includes incineration, gasification and pyrolysis (Adhikari *et al.*, 2000; Sharma *et al.*, 2000).

Table 3 shows some of the ways which have been used to deal with waste tyres in several countries. Most of the pathways in Table 3 (except landfilling and stockpiling) are aimed at reducing the amount of waste tyres discarded by converting them into re-usable products or energy.

Table 3: Several methods used for treating waste tyres in different countries (Adhikari *et al.*, 2000)

Country	Re-treading (%)	Recycling (%)	Energy (%)	Landfilling (%)	Export (%)
France (1996)	20	16	15	45	4
Germany (1996)	17.5	11.5	46.5	4	16
Italy (1996)	22	12	23	40	2

Table 3 continued: Several methods used for treating waste tyres in different countries (Adhikari *et al.*, 2000)

Country	Re-treading (%)	Recycling (%)	Energy (%)	Landfilling (%)	Export (%)
UK (1996)	31	16	27	23	2.5
Belgium (1996)	20	10	30	5	25
Netherlands (1996)	60	12	28	0	N/A
Sweden (1996)	5	12.5	64	5	7
USA (1994)	-	28	72	-	-

The direct disposal pathways (landfilling and stockpiling) were discussed in section 3.1.2. In this section, material recovery and recycling and thermal treatment with energy recovery will be briefly discussed. The discussions will highlight the products from each pathway and their common end uses. The drawbacks/limitations associated with the processes in each pathway are highlighted as these bring about the necessity to explore the possibility of using waste tyre pyrolysis for recovery of valuable chemicals. Materials recovery and recycling will be discussed first followed by thermal treatment with energy recovery. The pyrolysis process of thermal treatment will be discussed in detail in section 3.3.

3.1.3.1. Materials recovery and recycling

End-of-life tyres are a potential source of raw materials and as such, several processes have been used for material recovery and recycling from waste tyres. The processes involved in material recovery and recycling ensure conversion of waste tyres into materials that can be used to produce new goods or used for utilitarian purposes (Sienkiewicz *et al.*, 2012; Dabic-Ostojic *et al.*, 2014). In these processes, the waste tyres can undergo size reduction to give products that are similar to the original rubber materials or the tyres can be used as whole (Adhikari *et al.*, 2000; Sharma *et al.*, 2000). Material recovery and recycle processes take advantage of the fact that used tyres are relatively similar to new tyres in composition with slightly less rubber (Sharma *et al.*, 2000; Lebreton and Tuma, 2006). The different processes of material recovery and recycling are briefly discussed below.

Crumbing, milling/grinding

The processes of crumbing and milling/grinding are achieved by mechanical means where rotary blades are used to reduce the size of the tyres, and also help to separate the rubber from other parts of the tyre (Sharma *et al.*, 2000). Tyre crumb rubber (of different sizes) and ground tyre rubber are

produced from these processes based on intended final use (Adhikari *et al.*, 2000; Sharma *et al.*, 2000; Scrap Tire News, 2016). Crumbing is the most common method of waste tyre recycling in South Africa (Nkosi *et al.*, 2013).

Crumb rubber is mainly used in applications such as tyre manufacturing, creation of sports surfaces and a range of civil engineering applications where it has been used as a mixing ingredient with asphalt for highway construction (Amari *et al.*, 1999; Pilusa *et al.*, 2014; Jacob *et al.*, 2014). Ground rubber is mainly used for applications such as filler material in the production of tread and sidewall of new tyres, production of flooring materials, surfacing of recreational facilities, as an additive for asphalt pavement etc. (Amari *et al.*, 1999; Quek and Balasubramanian, 2013; Muzenda and Popa, 2015).

The main drawbacks associated with these size reduction processes is the energy intensity of the processes, the high operational costs and the limited market for the products produced (Sharma *et al.*, 2000; Lebreton and Tuma, 2006).

Re-treading

Re-treading is a process in which the old worn out rubber of the tread section of the tyre is replaced with a new tread section, which regenerates the tyre (Bender, 2007; Zebala *et al.*, 2007). Re-treading is the most resource efficient method of used tyre recovery as the old tyre carcass is not thrown away but only a new tread fused to the old carcass by vulcanisation provided the carcass is not damaged (Amari *et al.*, 1999; Sharma *et al.*, 2000; Jacob *et al.*, 2014). The resource efficiency of re-treading can be seen in the fact that re-treading only consumes about 30% of the energy and 25% of the material needed to produce a new tyre (Lebreton and Tuma, 2006; Sienkiewicz *et al.*, 2012; Dabic-Ostojic *et al.*, 2014).

The use of re-treaded tyres is mainly limited to trucks, buses, airplanes and other heavy vehicles (Sienkiewicz *et al.*, 2012; Dabic-Ostojic *et al.*, 2014). The limitation in use of re-treaded tyres is due to the fact that large re-treaded tyres have a higher quality to price ratio than new tyres of the same class. For passenger car tyres, the quality to price ratio of re-treaded tyres makes them uncompetitive when compared with new tyres as they have been shown to be of lower quality, reliability and safety at high speeds (Sharma *et al.*, 2000; Zebala *et al.*, 2007; Sienkiewicz *et al.*, 2012). Re-treaded products are also faced with a stagnant demand (Xiao *et al.*, 2008). The overall combined effect of the drawbacks discussed above is a low selling price for the associated products.

Devulcanisation

Devulcanisation is a method used to recycle waste tyres by converting the thermoset rubber of tyres into a softer plastic like thermoplastic rubber similar in most properties to virgin rubber. The devulcanised rubber can then be vulcanised again if used in manufacturing of other tyres or it can be mixed with other thermoplastics to produce tougher products (Adhikari *et al.*, 2000; Garcia *et al.*, 2015).

Devulcanisation processes are primarily divided into physical and chemical devulcanisation. Physical devulcanisation employs the use of external energy (thermal and mechanical) where the tyre is crumbed or ground and then converted into devulcanised products. In other instances, liquid nitrogen is required to obtain a fine rubber powder (Adhikari *et al.*, 2000; Seghar *et al.*, 2015). Physical devulcanisation is faced with a drawback of high energy demand as the tyre has to be reduced in size (crumb and ground rubber), and the thermal energy needed to achieve the devulcanisation process is provided externally. The liquid nitrogen required to obtain a fine rubber powder could also add to operational costs (Adhikari *et al.*, 2000).

Chemical devulcanisation agents (mainly organic disulphides or mercaptans) are required for chemical devulcanisation and this poses an economic drawback with the associated costs of the chemicals involved (Adhikari *et al.*, 2000). Another major drawback could be the limitation in the amount of vulcanised rubber that can be mixed with fresh rubber due to quality concerns of the final product e.g. tensile strength, resilience, tear resistance etc. (Adhikari *et al.*, 2000; Garcia *et al.*, 2015; Edwards *et al.*, 2016).

Civil engineering applications

Waste tyres can be utilised in civil engineering applications in a reduced size form (as discussed for crumb and ground products) or as whole. Civil engineering applications include the use of tyres in road and rail foundations, creation of motorway crash barriers, embankments bunds, marine docks etc. (Barlaz *et al.*, 1993; Amari *et al.*, 1999; Islam *et al.*, 2011; Pilusa *et al.*, 2014).

3.1.3.2. Thermal treatment with energy recovery

Waste tyres present a possible energy stream by recovering the energy contained in tyres. Tyres have calorific values of around 31 000 kJ/kg, which makes them an attractive source of energy generation (Adhikari *et al.*, 2000; Pipilikaki *et al.*, 2005; Lebreton and Tuma, 2006). Technologies that are usually used to recover energy from waste tyres include incineration, pyrolysis and gasification (Sharma *et al.*, 2000; Jacob *et al.*, 2014). Thermal treatment has the ability to fully destroy the waste tyres, nett

energy production and the possible reduction of some harmful organic compounds (Amari *et al.*, 1999; Sharma *et al.*, 2000). As mentioned before, in this section, only incineration and gasification will be discussed. Waste tyre pyrolysis is extensively discussed in section 3.3.

Incineration

Incineration of waste tyres involves combustion of the tyres at high temperatures to convert the combustible matter into energy and inert residue (Sharma *et al.*, 2000; Jacob *et al.*, 2014). Waste tyres have been incinerated for energy generation in various applications such as cement kilns, pulp and paper mills, power plants, industrial boilers etc. (Amari *et al.*, 1999; Lebreton and Tuma 2006; Pilusa *et al.*, 2014). Figure 4 shows the market distribution of TDF (use of tyres as a direct energy source) in USA for the year 1996, as reported by Amari *et al.* (1999).

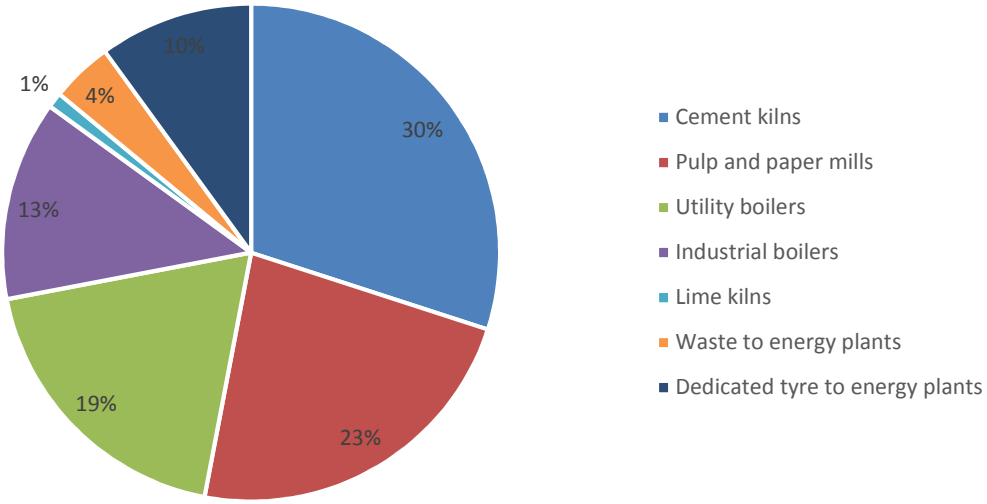

Figure 4: Market distribution of tyre derived fuel in the USA, 1996 (re-drawn from Amari *et al.*, 1999)

The major route for waste tyre incineration has been in use as supplementary fuel in cement kilns (Conesa *et al.*, 2008; Martinez *et al.*, 2013; Jacob *et al.*, 2014). In South Africa, tyres are not yet really used for energy in cement kilns, and only about 6% are recycled (Mahlangu, 2009). The cement manufacturing company Pretoria Portland Cement Limited (PPC Ltd) has an agreement with REDISA to source waste tyres as supplementary fuel for their plant in De Hoek in the Western Cape (PPC Ltd, 2014).

Tyres are a favourable alternative fuel in cement kilns as they have a high energy content compared to some coals. Coal heating values range between 26 000 and 31 000 kJ/kg whereas the heating value

of tyres is about 31 000 kJ/kg (Barlaz *et al.*, 1993). Higher temperatures and longer residence times in cement kilns favour the transformation of the tyres, even the combustion of carbon black (Barlaz *et al.*, 1993; Olazar *et al.*, 2008). The residue of the steel contents of the tyres serves as an iron source, which is required for cement production (Pipilikaki *et al.*, 2005, Lebreton and Tuma, 2006).

The major drawback in using tyres as supplemental fuel is the limitation on the percentage of fuel that can be replaced, due to concerns around cement product quality, emissions, and damage to equipment (Sharma *et al.*, 2000; Pipilikaki *et al.*, 2005; Olazar *et al.*, 2008). The limitation in the amount of tyres that can be used presents an opportunity for utilising the available waste tyres for conversion into high value chemicals.

Gasification

In waste tyre gasification, the tyres are converted to a primarily gaseous product at high temperatures of around 700 °C – 800 °C using reactive agents such as air, steam or oxygen (Raman *et al.*, 1981; Leung and Wang, 2003). Temperatures of as low as 350 °C have been employed at lab scale to study the effects of temperature (Leung and Wang *et al.*, 2003; Xiao *et al.*, 2008). The main product of gasification is syngas even though a carbon black product is also produced (Xiao *et al.*, 2008). The syngas produced is an intermediate product that can be used for energy by combustion or in gas turbines and as a raw material for fuels and chemicals production (Raman *et al.*, 1981).

3.1.3.3. Conclusions on current methods evaluated

From the discussions of section 3.1.3, it can be seen that the current methods used for dealing with the waste tyre problem have not adequately dealt with the problem due to low product quality, low market demands for products and subsequent low selling prices for the products. None of the processes discussed have shown to be a pathway for converting the waste tyres into high value products. This, therefore, presents an opportunity to utilise the waste tyres available for conversion into high value chemicals. This study seeks to address the feasibility of this opportunity.

3.2. Tyre composition

3.2.1. Constituents of a tyre

Tyres contain vulcanised rubber (60-65 wt.%), carbon black (CB) (25-35 wt.%) and the remainder comprises of accelerators, fillers, reinforcing textile cords, fabric belts, steel wire reinforcing beads etc. that are added during the manufacturing process (Kyari *et al.*, 2005; Martinez *et al.*, 2013). These components have varying properties and composition and are individually added to achieve a final tyre product. Each component will give a specific property to the tyre or to the tyre manufacturing

process (Hita *et al.*, 2016). Table 4 shows different elements of the final tyre product and Figure 5 shows the different components that make up a tyre.

Table 4: Typical elements of a tyre and their constituent materials (from Hita *et al.*, 2016)

Element	Composition
Liner	Inner coating of synthetic rubber
Plies	Layers of rubber, nylon and metal reinforced rubber piled together
Bead heel	Ringed steel wires surrounded by hard rubber
Sidewall	Natural and synthetic rubber mixed with small amounts of carbon black and additives
Tread	Natural and synthetic rubber

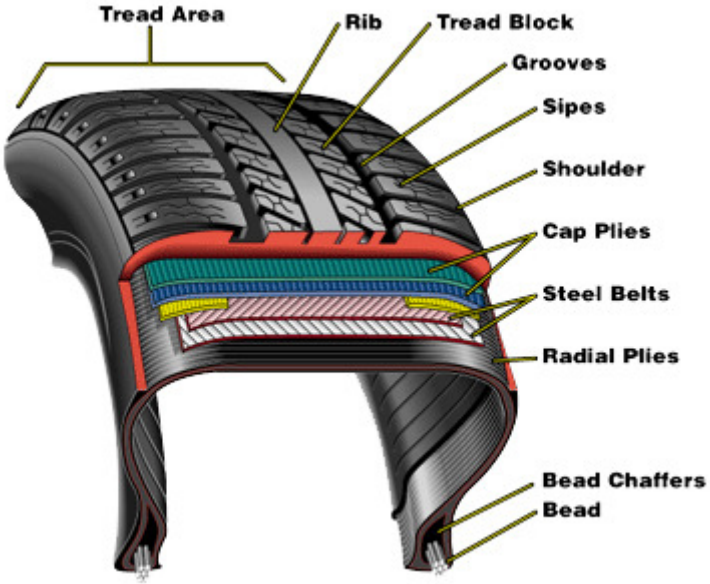

Figure 5: Various components that make up a tyre (Courtesy of CARiD™)

Different natural and synthetic rubber formulations are used for the production of passenger and truck tyres; the tyres are mainly a blend of both rubbers (Kyari *et al.*, 2005; Martinez *et al.*, 2013). The rubbers used in tyre manufacturing are thermoset polymers (Leung and Wang, 2003). The most commonly used of the synthetic rubbers is styrene-butadiene copolymer (SBR) with a styrene content of about 25 wt.%. Other rubbers used in tyre manufacturing are natural rubber (NR) (polyisoprene), polybutadiene rubber (PBD), nitrile rubber (NTR) and chloroprene rubber (CPR) (Mastral *et al.*, 2000). The different rubbers used yield different compounds as degradation products. Isoprene and dipentene (limonene) are the main degradation products of natural rubber whereas styrene, 4-vinylcyclohexene, ethylbenzene and cumene are main degradation products of styrene-butadiene

rubber (Chen and Qian, 2002; Seidelt *et al.*, 2006; Danon *et al.*, 2015). It can then be concluded that tyre formulations that have a high content of natural rubber are desirable for pyrolysis if limonene is to be targeted as a compound of interest. Truck tyres (TT) generally contain more natural rubber content than passenger car tyres (PCT) and the amount of each component added varies from region to region as shown in Table 5.

Carbon black is an amorphous carbon of quasi-graphitic structure and is used in tyre manufacturing to provide strength and aid abrasion resistance of the rubber in the tyre (Mastral *et al.*, 2000; Kyari *et al.*, 2005; Martinez *et al.*, 2013). It is primarily produced by partial combustion of fossil hydrocarbons like petroleum residue (Martinez *et al.*, 2013).

Table 5: Typical composition of passenger and truck tyres (adopted from Hita *et al.*, 2016)

Material (wt.%)	**PCT**		**TT**	
	USA	**EU**	**USA**	**EU**
Natural rubber	14	22	27	30
Synthetic rubber	27	23	14	15
Carbon black	28	28	28	20
Steel	14-15	13	14-15	25
Others[a]	16-17	14	16-17	10

[a] Nylon, fillers, accelerators and sulphur amongst others

An extender oil (a mixture of aromatic hydrocarbons) is added to the tyre during manufacturing to soften and improve workability of the rubber (Kyari *et al.*, 2005). The amount of extender oils added depends on the tyre formulation as shown in Table 6 and Table 7. The constituents (and composition) shown in Table 6 and Table 7 represent just two particular formulations out of a variety of formulations used in tyre manufacturing. It can then be concluded that the amount of extender oil in tyre formulation will have an effect on the quantities of potentially valuable chemicals obtained from pyrolysis as the oil decomposes during pyrolysis.

An accelerator (typically an organo-sulphur compound) is added as a catalyst for the vulcanisation process. Typically, zinc oxide and stearic acid are also added as these compounds control the vulcanisation process and enhance the physical properties of the rubber (Kyari *et al.*, 2005). The different additives can be a variety of compounds as shown in Table 6 and Table 7, however, they still fulfil the same purpose.

Sulphur is added to the tyre to form cross-links between the rubber polymer chains thus also hardening the rubber to prevent excessive deformation at elevated temperatures (Martinez *et al.*, 2013; Hita *et al.*, 2016). The cross-linking of the elastomers gives the rubber materials their thermoset characteristics; the sulphur content is normally up to 1.5 wt.% (Mastral *et al.*, 2000; Martinez *et al.*, 2013).

Table 6: Constituents of a particular tyre formulation (from Kar, 2011)

Component	Composition (wt.%)
SBR	43.5
Carbon black	32.6
Extender oil	21.7
ZnO and sulphur	2.2

Table 7: Constituents of a specific tyre formulation (from Lopez *et al.*, 2010)

Component	Composition (wt.%)
Natural rubber (SMR 5CV)	29.59
Styrene-butadiene rubber (SBR 1507)	29.59
Carbon black (ISAF N220)	29.59
Stearic acid	0.59
IPPD (*n*-isopropyl-*n'*-phenyl-*p*-phenylendiamine)	0.89
Zinc oxide	2.96
Phenolic resin	2.37
Sulphur	0.89
CBS (*n*-cyclohexyl-2-benzothiazol-sulphenamide)	0.89
H-7 (hexamethylentetramine)	0.18
PVI (*n*-cyclohexylthiol-phthalimide)	0.12
Aromatic oil	2.37

3.2.2. Characterisation of a tyre

In literature, tyres are normally characterised using the proximate and ultimate (elemental) analyses. Depending on the intention of the specific literature, calorific values of the tyre can also be included.

Table 8 and Table 9 show the proximate and ultimate analyses of some tyres in literature. It can be seen that the characterisation will depend on the type of tyre material evaluated. The variation in the different components is also a result of different tyre formulation from various tyre brands. A tyre with a high volatile matter content is desirable for pyrolysis processes aiming to recover valuable chemicals from waste tyres, as is explained in section 3.3. For this study, the importance of tyre characterisation is for tyre definition purposes in Aspen Plus® simulation as will be explained in section 3.4 and chapter 4.

Table 8: Typical proximate analysis of a waste tyre

Component (wt.%)	**Literature source**			
	Cunliffe and Williams (1998b)	Rodriguez *et al*. (2001)	Conesa *et al*. (2004)	Choi *et al*. (2014)[a]
Moisture	1.3		0.9	
Volatile matter	62.2	58.8	65.5	73.9
Fixed carbon	29.4	27.7	29.4	21.8
Ash	7.1	3.9	3.7	4.3
Steel		9.6		
Calorific value (MJ/kg)	40	31.8		

[a]Dry basis

Table 9: Typical ultimate analysis of a waste tyre

Element (wt.%)	**Literature source**			
	Cunliffe and Williams (1998b)	Rodriguez *et al*. (2001)	Conesa *et al*. (2004)	Choi *et al*. (2014)[b]
C	86.4	74.2	89.4	89.2
H	8	5.8	7	7.7
N	0.5	0.3	0.2	0.5
S	1.7	1.5	2	2.6
O	3.4	4.7		
Ash	2.4	13.5[a]		

[a]Includes steel, [b]dry and ash free basis

3.3. Pyrolysis of waste tyres

In section 3.3, pyrolysis as an (attractive) alternative method of recycling waste tyres through conversion into valuable products is discussed. Firstly, pyrolysis is defined, then the main product fractions are discussed, the valuable products produced from tyre pyrolysis are highlighted followed by the conditions under which tyre pyrolysis is performed. Lastly, waste tyre economics are discussed, which will relate to the aims of this study.

3.3.1. Definition of waste tyre pyrolysis

Pyrolysis is a thermal process that decomposes an organic material into low molecular weight compounds under inert conditions (Cunliffe and Williams, 1998a; Amari *et al.*, 1999). Pyrolysis breaks down the organic part of a tyre into a gas product, a liquid product and a solid product (Wojtowicz and Serio, 1996; Lopez *et al.*, 2010; Islam *et al.*, 2011; Wang *et al.*, 2016). Figure 6 shows a schematic of a typical waste tyre pyrolysis system.

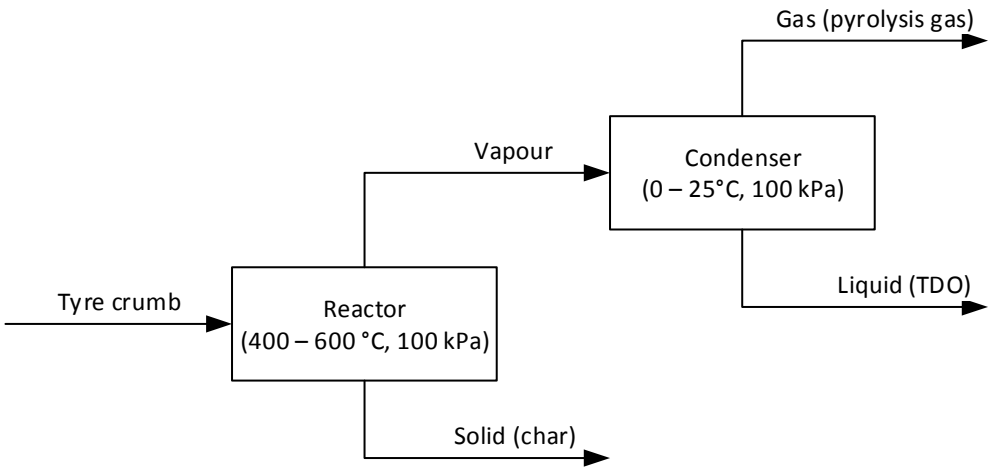

Figure 6: Schematic of a typical waste tyre pyrolysis system

In the typical waste tyre pyrolysis system shown in Figure 6, the tyres (typically in a size-reduced form) are pyrolysed in a reactor (at a specific temperature and pressure) where vapour and solid products are obtained. The vapour product from the reactor is condensed to yield a (non-condensable) gas and a liquid product fraction.

3.3.2. Waste tyre pyrolysis products

3.3.2.1. Gas product

The gas fraction is the gas remaining after condensation of the vapours from the reactor (for liquid recovery) during pyrolysis and it is called pyrolysis gas or pyrogas (Martinez *et al.*, 2013). The gas is typically composed of paraffinic and olefinic compounds that range from C_1 to C_5 (Bennett, 1993;

Rodriguez *et al.*, 2001). Lopez *et al*. (2010) reported finding some aromatic compounds in the pyrolysis gas in addition to paraffinic and olefinic compounds.

The gas is typically composed of hydrogen, carbon monoxide, carbon dioxide, methane, ethane, ethene, propane, propene, butane, butenes and butadiene, with some low concentrations of sulphur and nitrogen compounds (Kyari *et al.*, 2005; Olazar *et al.*, 2008). The presence of C_4 compounds is mainly attributed to the thermal degradation of the rubber as tyres typically contain a mixture of both natural and synthetic rubber of which the latter is mainly SBR or BR (Martinez *et al.*, 2013). Kyari *et al.* (2005) reported pyrolysis gas calorific values of 29.9 – 42.1 MJ/m^3 depending on the tyre brands used in the process. The gas is normally used as fuel for the pyrolysis process (Williams and Besler, 1995).

3.3.2.2. Liquid product

The liquid product (TDO) has a complex composition consisting of both short and long chain carbon molecules and single and multiple ring structures. The proportion of aliphatic and aromatics vary with pyrolysis conditions. Alkylated derivatives of single and multiple ring aromatics are also present in TDO (Kyari *et al.*, 2005; Quek and Balasubramanian, 2013; Choi *et al.*, 2014). TDO is a dark brown/black coloured liquid of medium viscosity and has a sulphur/aromatic smell due to the presence of sulphur containing compounds (Williams, 2013; Frigo *et al.*, 2014). TDO is a combination of the processing oils and organic additives in the original tyres and the products of decomposition of the different rubbers. The composition TDO varies with reactor conditions i.e. temperature, pressure and volatile residence time (Dai *et al.*, 2001; Li *et al.*, 2004; Lopez *et al.*, 2010).

The oil product has high calorific values (around 40 MJ/kg) and can be used as fuel. TDO has a wide boiling point range (about 50 °C to above 350 °C) as shown in Figure 7 from Li *et al.* (2004). The wide boiling point range would require a lot of effort to convert the oil to traditional liquid fuels or make it difficult for its direct application as fuel (Martinez *et al.*, 2013). TDO can be blended with diesel fuel if it is to be used as automotive fuel but only in small proportions to not greatly affect the performance and emissions of standard automotive diesel engines (Quek and Balasubramanian, 2013; frigo *et al.*, 2014). Direct use of TDO as engine fuel can only be in diesel engines that are less fuel-quality demanding and have less stringent emission regulations such as stationary engines and marine propulsion engines (Frigo *et al.*, 2014).

Upgrading of TDO to meet specific fuel requirements is required due to the high contents of aromatics and sulphur and a high viscosity. Depending on the final use of TDO as fuel, different upgrading techniques may be required (Olazar *et al.*, 2008; Lopez *et al.*, 2010; Martinez *et al.*, 2013). The poor

fuel-quality characteristics of TDO oil results in limited application and low selling prices for the oil as compared to traditional fuels from crude oil (Pilusa *et al.*, 2014).

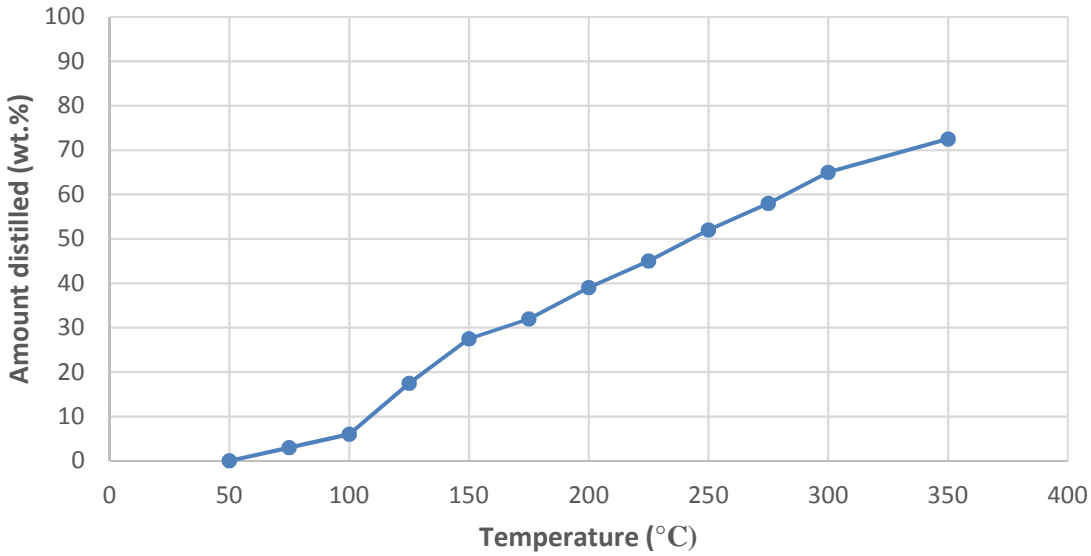

Figure 7: True boiling point curve of TDO obtained at 500 °C (estimation from graph by Li et al., 2004)

TDO can also be used as a source of chemical feedstock due to its various constituent compounds (Li *et al.*, 2004; Kyari *et al.*, 2005). The chemical feedstock potential of TDO is discussed in section 3.3.3. The limited application of TDO as fuel (in its crude form), potentially expensive investment for upgrading TDO to match diesel fuel and consequent low selling price of the oil present an opportunity for converting waste tyres into the high value chemicals found in the oil.

3.3.2.3. Solid product

The solid product is called pyrolysis char; it contains the inorganic matter of the tyre (ash, zinc oxide, steel, silicates etc.) and the non-volatile carbon black added during tyre manufacture (Amari *et al.*, 1999; Li *et al.*, 2004). Sulphur from vulcanisation is mainly retained in this product fraction. Tyre composition and pyrolysis conditions determine the composition of the char product (Lopez *et al.*, 2010; Martinez *et al.*, 2013). Coking or the deposition of degraded tyre material on the carbon black can also form part of the char product, this would be indicated by an amount of char higher than the sum of the carbon black and inorganics in the original tyre (Lopez *et al.*, 2010). The quality of char obtained under vacuum is better than that under atmospheric conditions due to vacuum minimising coking that would block the pores of the char thus minimising its surface area (Lopez *et al.*, 2010).

The char product obtained can be upgraded for use as activated carbon for different applications, as a solid fuel or re-used as carbon black in the tyre manufacturing process. The char product however

needs upgrading to increase surface area, reduce the ash and sulphur contents for use in these applications (Li *et al.*, 2004; Olazar *et al.*, 2008; Lopez *et al.*, 2010).

3.3.3. Valuable chemicals from pyrolysis oil

TDO is a potential source of chemical feedstock as it contains valuable chemicals like benzene, toluene and xylene (BTX), styrene, ethylbenzene and limonene. These are chemicals that have wide industrial applications (Williams and Brindle, 2003a; Li *et al.*, 2004; Lopez *et al.*, 2010; Choi *et al.*, 2014). The yields of these chemicals depend on reactor conditions and the type of tyre used as different studies used different tyre types. Table 10 and Table 11 show the yields (based on tyre feed) of BTX, ethylbenzene, styrene and limonene at 500 °C and 600 °C from different literature sources.

Table 10: Yield of BTX, ethylbenzene, styrene and limonene at 500 °C from different studies

Compound	**Yield from tyre feed (wt.%)**			
	Cunliffe and Williams (1998a)	Williams and Brindle (2003a)	Zhang *et al*. (2008)	Lopez *et al*. (2010)
Benzene	0.04	0.11		0.27
Toluene	0.34	0.61	0.08	1.51
Xylene		0.84	0.21	1.53
Ethylbenzene	0.01	0.11	0.09	1.11
Styrene	0.11		0	6.08
Limonene	1.63	2.00	4.93	10.29

Table 11: Yield of BTX, ethylbenzene, styrene and limonene at 600 °C from different studies

Compound	**Yield from tyre feed (wt.%)**		
	Kaminsky and Mennerich (2001)	Lopez *et al.* (2010)	Choi *et al.* (2014)
Benzene	0.67	0.76	
Toluene	2.1	2.5	
Xylene	0.55	2.11	0.51
Ethylbenzene	1.7	1.35	
Styrene	3.1	4.22	0.09
Limonene		0.94	1.16

As can be seen from Table 10 and Table 11, the potentially valuable chemicals are present in TDO in sufficient quantities given the wide variety of compounds that are present in TDO. Weitkamp *et al.* (2001) reported that in 1999, 6.9 Mt of benzene, 2.3 Mt of toluene and 1.9 Mt of xylenes were produced in Western Europe, and looked at ways of converting BTX into valuable products. BTX compounds are a high value feedstock for the plastic/polymer industry, and the demand for xylene in the industry is growing (Li *et al.*, 2004; Lopez *et al.*, 2010).

Another valuable chemical from waste tyre pyrolysis is limonene, and it is the target chemical in this study. Limonene is a monoterpene that is a dimer of isoprene molecules and can be obtained from the thermal decomposition of the polyisoprene contained in the tyre. The polyisoprene could either be from natural or synthetic rubber (Pakdel *et al.*, 2001; Danon *et al.*, 2015). Limonene is a major component of TDO with common yields of between 2.5 and 5 wt.% on the basis of a steel-free tyre although yields as high as 27 wt.% have been reported (Lopez *et al.*, 2010; Danon *et al.*, 2015). Limonene has wide industrial applications and has been used in the formulation of industrial solvents, terpene resins and adhesives, as a cleaning agent, as a dispersing agent for pigment and in the manufacturing of flavouring agents, fragrances and pesticides (Pakdel *et al.*, 2001; Stanciulescu and Ikura, 2007; Williams, 2013; Danon *et al.*, 2015).

The current demand for limonene is mostly catered for by citrus-derived limonene (Danon *et al.*, 2015). The global production of citrus limonene was estimated at over 70 000 tons in 2013, with both the demand and supply expected to increase constantly in future (Ciriminna *et al.*, 2014). Citrus harvest is a seasonal activity and as such, a drop in supply of citrus-derived limonene can be expected when the citrus season ends. The supply of citrus limonene is subject to agricultural vulnerabilities, which could bring volatility to the price of limonene (Ciriminna *et al.*, 2014). Production and recovery of tyre-derived limonene then become vital to close the potential limonene supply gap given the wide industrial use of limonene.

The price of citrus limonene can range between 8 and 25 US$ per kilogram based on purity (Florida Chemicals Co., 1991a, b, c; Pakdel *et al.*, 2001; Stanciulescu and Ikura, 2007; Danon *et al.*, 2015). To this author's knowledge, there currently is no information available on the price of tyre-derived limonene. Impurities in tyre-derived limonene that were identified by Pakdel *et al.* (2001) include light aromatics and undesirable sulphur containing compounds such as thiophene and benzothiazole. As such, it is necessary to obtain sufficient purity for tyre-derived limonene to minimise the undesirable impurities and to attain a high selling price.

The yields of the valuable chemicals discussed above vary with pyrolysis conditions and the tyre material used. Therefore, it is necessary to optimise the reactor conditions depending on the type of chemical desired. Section 3.3.4 will discuss various important pyrolysis reactor conditions and their effects on reactor product distribution while linking it to limonene as the desired chemical.

3.3.4. Waste tyre pyrolysis operating conditions

Waste tyre pyrolysis is influenced by a variety of parameters with some having a direct and others having an indirect effect. The parameters that mainly influence waste tyre pyrolysis are temperature, pressure, residence time of volatiles in the hot reaction zone and heating rate (Gonzalez *et al.*, 2001; Dai *et al.*, 2001; Leung and Wang, 2003).

3.3.4.1. Temperature

The reactor temperature is an important parameter that has to maintained in order to ensure a constant supply of the heat required to effectively degrade the tyres into various products; it is the main variable affecting pyrolysis (Gonzalez *et al.*, 2001; Diez *et al.*, 2004; Martinez *et al.*, 2013).

Waste tyre pyrolysis has been performed at temperatures ranging from as low as 300 °C to as high as 1000 °C (Williams *et al.*, 1993; Rodriguez *et al.*, 2001; Conesa *et al.*, 2004; Frigo *et al.*, 2014). Thermogravimetric analysis (TGA) studies for most tyre samples that have a combination of different rubber types have shown that initial devolatilisation of the different oils, plasticizers and additives in the tyre occurs in the temperature range of 150 °C to 350 °C. The final weight loss is observed at temperatures of around 450 °C - 500 °C. This has necessitated the opinion that pyrolysis should start around 350 °C and be complete at 500 °C (Williams and Besler, 1995; Leung and Wang, 1998; Senneca *et al.*, 1999; Choi *et al.*, 2014). A study by Rodriguez *et al.* (2001) found that between 300 °C and 400°C, the pyrolysis yields of char were higher than the TGA char results, and the char obtained had a gummy sticky nature. Rodriguez *et al.* (2001) concluded that pyrolysis had not been completed between 300 °C and 400 °C.

Waste tyre pyrolysis is most commonly performed at temperatures of 425 °C to 600 °C, with 500 °C the most commonly used in the range (Benallal *et al.*, 1995; Li *et al.*, 2004; Choi *et al.*, 2014; Wang *et al.*, 2016). Most literature studies have performed their investigations using a range of temperatures depending on the intention of the study. Pyrolysis temperatures of between 400 °C and 500 °C are the most ideal for production of limonene; maximum yields of limonene are mostly obtained in this temperature range (Cunliffe and Williams, 1998a; Zhang *et al.*, 2008; Choi *et al.*, 2014; Danon *et al.*, 2015). Selection of the pyrolysis temperature used in this study is discussed in section 4.4.1.

Effects of temperature on product distribution

An increase in temperature generally results in the increase in gas yield at the expense of the oil yield. This is attributed to the occurrence of secondary thermal cracking reactions of the oil compounds into non-condensable gas compounds at higher temperatures (Williams *et al.*, 1993; Lopez *et al.*, 2010; Choi *et al.*, 2014). In some instances, it has been found that this generic trend is only observed after certain pyrolysis temperatures have been reached. Cunliffe and Williams (1998a) observed that the oil yield increased and reached a maximum at 475 °C when the pyrolysis temperature was increased from 450 °C up to 475 °C. The oil yield from the study by Cunliffe and Williams (1998a) then decreased with temperature from 475 °C up to 600 °C with a corresponding increase in gas yield. This was also attributed to the secondary reactions of breaking down the higher molecular species into gaseous products.

Temperature does not have a significant effect on the yield of char, which will mostly remain at an almost constant value, provided that full devolatilisation has occurred (Lee *et al.*, 1995; Rodriguez *et al.*, 2001). The yield of char can increase slightly with temperature (above the value of original carbon black and inorganics) due to increased deposition of condensed polyaromatic hydrocarbons on the char surface (Lopez *et al.*, 2010). Figure 8 shows the typically observed trends of the effect temperature has on yield of pyrolysis product fractions.

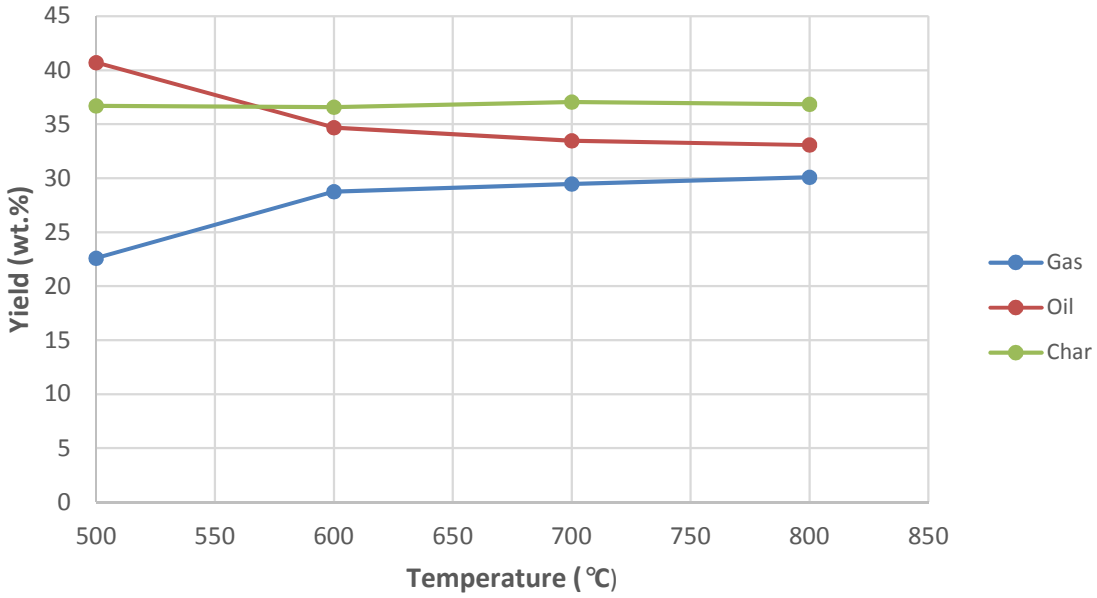

Figure 8: Yields of pyrolysis products with temperature (Choi *et al.*, 2014)

In addition to the effects on the yields of main product fractions, the reactor temperature will also have an effect on composition of each of the product fractions (gas, oil, and char). In the gas fraction, the yield of light gases such as methane and hydrogen increases with temperature while the yield of heavier gas components decreases with an increase in temperature. This is attributed to the decomposition (cracking) of heavier hydrocarbons into lighter hydrocarbons and hydrogen (Lee *et al.*, 1995; Dai *et al.*, 2001; Lopez *et al.*, 2010). An increase in temperature also generally results in an increase of the yield of unsaturated hydrocarbon gases at the expense of saturated hydrocarbon, as consequence of thermal cracking of the saturated hydrocarbons (Lee *et al.*, 1995; Dai *et al.*, 2001). The change in gas composition has an effect on the calorific value of the gas fraction. The calorific value of the gas would increase with temperature due to the subsequent increase in composition of lighter hydrocarbons and hydrogen (Rodriguez *et al.*, 2001).

Reactor temperature also has an effect on the composition of the TDO product and the valuable chemicals in the oil. An increase in temperature results in an increase of the aromatic fraction whereas the aliphatic fraction decreases. This is attributed to higher temperatures favouring aromatic formation reactions like the Diels-Alder reaction, recombination of aliphatics and aromatics free radicals, and the cyclisation of aromatic chains (Williams and Brindle, 2003c; Lopez *et al.*, 2010; Choi *et al.*, 2014; Hita *et al.*, 2016).

An increase in temperature results in a decrease in limonene yield with a noticeable increase in aromatic compounds like BTX. Limonene is unstable at temperatures of above 500 °C and decomposes to form aromatics such as benzene, xylene, toluene, trimethylbenzene, m-cymene and indane (Pakdel *et al.*, 2001; Williams and Brindle, 2003c; Danon *et al.*, 2015). A schematic representation of formation and decomposition of limonene is shown in Figure 9. Some of these aromatic compounds such as cymene, trimethylbenzene and indane have boiling points similar to that of limonene. An increase in the yields of these compounds decreases the purity of the limonene fraction which makes recovery of limonene even more difficult (Pakdel *et al.*, 2001). Figure 10 shows the yield (from tyre feed) of limonene and BTX aromatics with temperature from literature.

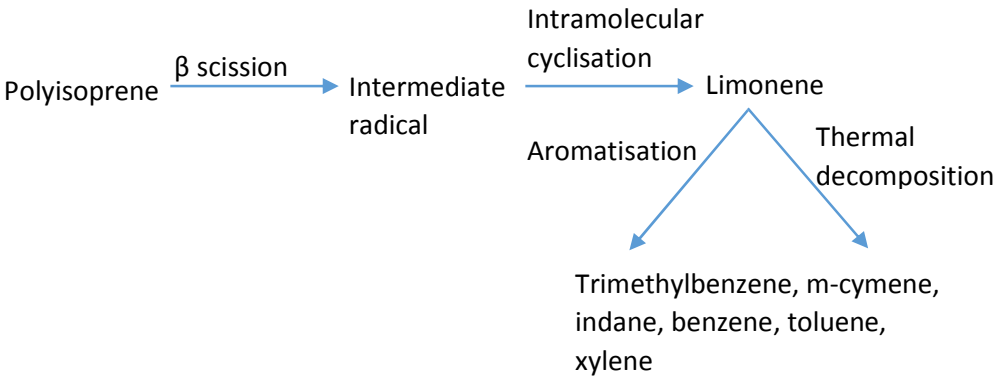

Figure 9: Schematic representation of formation and decomposition of limonene to form aromatics (Pakdel *et al.*, 2001; Williams and Brindle, 2003c; Danon *et al.*, 2015).

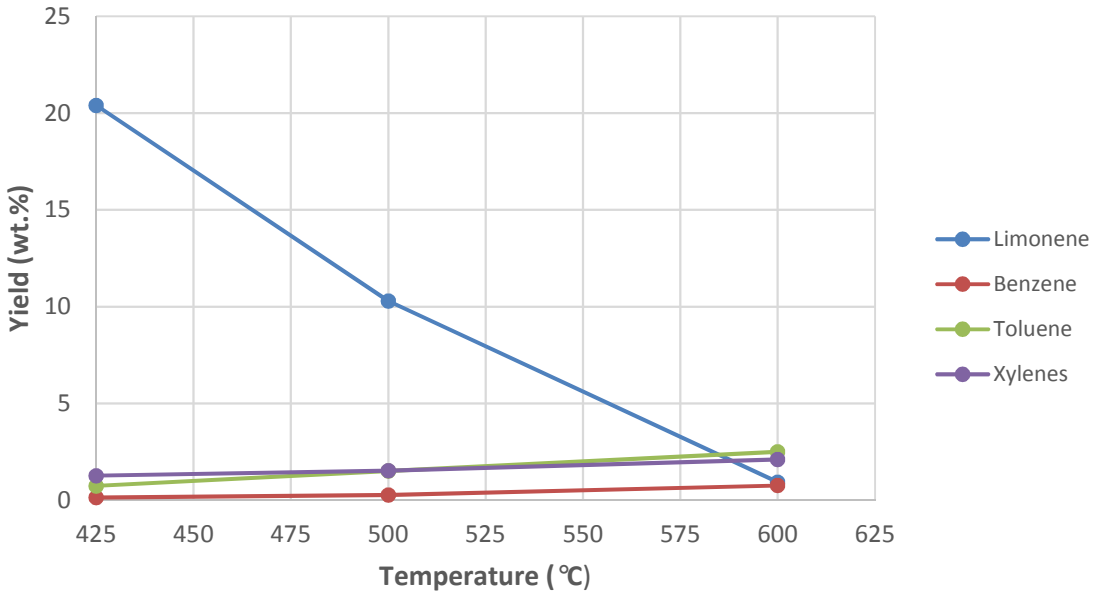

Figure 10: Yields of limonene and BTX aromatics from tyre at various temperatures (Lopez *et al.*, 2010)

In order to maximise the yield of limonene, which is the valuable chemical of interest in this study, it is concluded that pyrolysis reactor temperatures of not more than 500 °C should be used.

3.3.4.2. Pressure

The pressure inside the pyrolysis reactor is another important factor that influences the pyrolysis of waste tyres. Waste tyre pyrolysis has been performed at pressures in the range of 1 to 101 kPa (abs) in literature (Benallal *et al.*, 1995; Pakdel *et al.*, 2001; Zhang *et al.*, 2008; Lopez *et al.*, 2010). Atmospheric pressure (100 kPa (abs)) has been the preferred operational pressure of many studies conducted in literature.

The reactor pressure has an influence on the diffusion of volatiles formed within the tyre particle. This has an effect on the residence time of the volatiles formed, which in turn affects the product distribution (Lopez *et al.*, 2010; Martinez *et al.*, 2013). Pyrolysis under vacuum (pressures lower than 100 kPa (abs)) reduces the residence time of volatiles in that it enhances diffusion of the volatiles towards the outside of the tyre particle owing to the positive pressure gradient created (Zhang *et al.*, 2008; Lopez *et al.*, 2010). The enhanced diffusion causes a rapid removal of volatiles from the reaction zone which reduces the occurrence of secondary decomposition reactions of the products (Mirmiran *et al.*, 1992; Benallal *et al.*, 1995).

Vacuum pyrolysis is preferable for limonene production as the faster removal of volatiles from the reaction zone prevents the secondary cracking reactions which degrade limonene. The typically lower operational temperatures of vacuum pyrolysis also reduce the possibility of limonene degradation (Mirmiran *et al.*, 1992). In a study done by Pakdel *et al.* (2001), vacuum operation was said to improve the yield of limonene at the expense of aromatics due to the rapid removal of volatiles and reduced pyrolysis temperatures, which reduced the occurrence of Diels-Alder type of aromatisation.

Vacuum operation does not have a significant effect on the yield of char (provided pyrolysis is complete) but does have an effect on the quality of the char produced. This is due to the fact that repolymerisation and carbonisation of primary products is minimised under vacuum, which reduces deposition of carbonaceous product material on the char surface (Lopez *et al.*, 2010; Martinez *et al.*, 2013).

3.3.4.3. Volatiles residence time

The residence time of volatiles is influenced by factors such as the flow rate of carrier gas (gas used to sweep pyrolysis vapours from the reaction zone) and the type of reactor used (Martinez *et al.*, 2013). An increase in carrier gas flow rate decreases the volatiles residence time as volatiles are removed faster; the opposite is observed for a decrease in carrier gas flow rate (Martinez *et al.*, 2013). The residence time can also be reduced by operating at vacuum as the positive diffusion gradient around the tyre particle created by vacuum allows for faster removal of volatiles (Pakdel *et al.*, 2001).

Product distribution within the pyrolysis system is also affected by volatiles residence times. Longer residence times favour the occurrence of secondary reactions which have an effect on the final product distribution (Aylon *et al.*, 2008; Martinez *et al.*, 2013). An increase in residence time leads to an increase in the gas yield at the expense of the oil yield due to longer residence times encouraging the occurrence of secondary reactions and cracking of the oil product into gas (Dai *et al.*, 2001; Aylon *et al.*, 2008; Islam *et al.*, 2008). Increasing the volatiles residence time can also lead to a decrease in

char yield due to long contact times between the char product and volatiles, which could lead to secondary reactions like the Boudouard reaction (reaction between carbon and carbon dioxide to yield carbon monoxide) (Dai *et al.*, 2001; Aylon *et al.*, 2008; Islam *et al.*, 2008).

Figure 11 shows the effect of residence time on the yields of pyrolysis products (yield values are estimates from published graph). It can be seen that shorter volatile residence times are preferred for maximising the yield of the liquid fraction, which contains the valuable chemicals that can be targeted for recovery (Mimiran *et al.*, 1992; Pakdel *et al.*, 2001). Shorter residence times are thus preferable for limonene production as occurrence of secondary reactions leading to decomposition of limonene is minimised (Pakdel *et al.*, 2001; Aylon *et al.*, 2008; Martinez *et al.*, 2013).

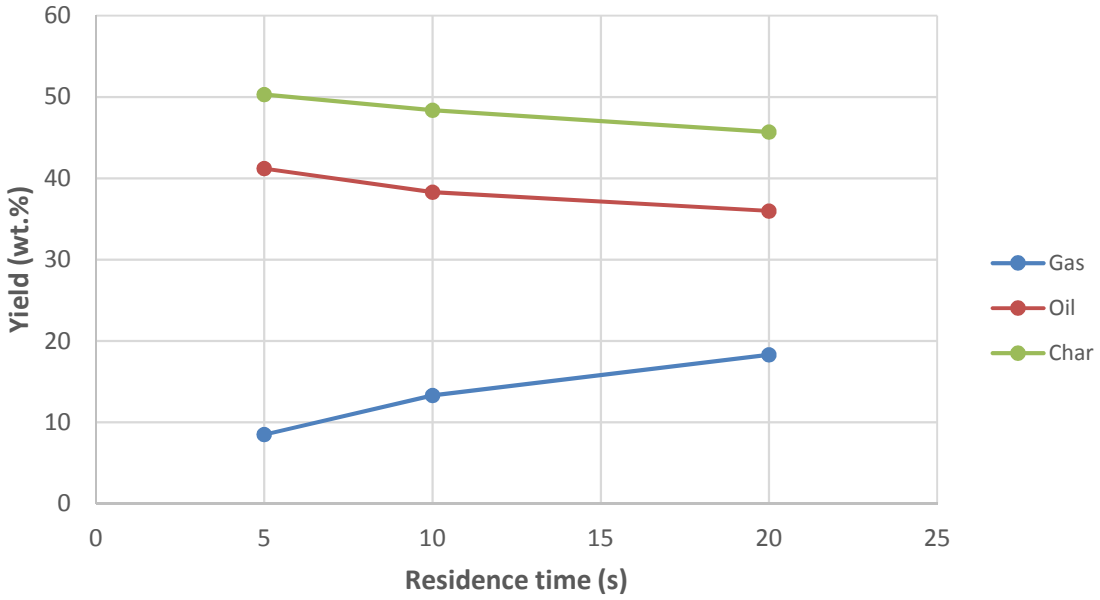

Figure 11: Effect of volatiles residence time on yields of pyrolysis products (re-drawn from Islam *et al.*, 2008)

3.3.4.4. Heating rate

Heating rate is a key variable of pyrolysis as it affects the reaction rate and determines the temperature profile within the particles (Martinez *et al.*, 2013). An increase in heating rate generally increases the temperature at which maximum devolatilisation occurs, which increases the degradation rate (Williams *et al.*, 1990; Leung and Wang, 2003). The shift to higher temperatures of maximum devolatilisation and increased degradation rate is indicated by broadening of the derivative thermogravimetric (DTG) profile with respect to temperature and shrinking of the DTG profiles with respect to time (Senneca *et al.*, 1999). Shifting of thermal decomposition to higher temperatures with an increase in heating rate can be attributed to the combined effects of heat transfer and changes in

the kinetics of devolatilisation which result in delayed decomposition (Williams and Besler, 1995; Martinez *et al.*, 2013).

Operating at higher heating rates leads to higher pyrolysis temperatures, which can result in an increase in the gas yield at the expense of the oil yield due to the occurrence of secondary reaction (Alsaleh and Sattler, 2014). An increase in heating rate increases the yield of primary devolatilisation products at the expense of secondary devolatilisation as maximum devolatilisation is moved to higher temperatures (Senneca *et al.*, 1999).

Dipentene is a major product of primary degradation of natural rubber and it is degraded by occurrence of secondary reactions that form aromatic compounds (Williams and Besler, 1995; Choi *et al.*, 2014). Heating rate has an effect on the characteristics of primary vapour products. Increasing the heating rate increases the yield of aliphatic products while a decrease in the yield of aromatic products occurs (Williams *et al.*, 1990). In order to minimise occurrence of secondary reactions that would crack the oil product and convert primary volatiles into aromatics, faster removal of primary volatiles is essential (Leung and Wang, 1998; Mastral *et al.*, 2000; Naim *et al.*, 2017).

It therefore implies that higher heating rates are favourable for formation of limonene as the rate of reaction is increased, however, faster removal of primary volatiles is required in order to minimise the occurrence of secondary reactions that degrade limonene (shown in Figure 9).

3.3.5. Waste tyre pyrolysis economics

Wojtowicz and Serio (1996) performed a preliminary economic feasibility study for converting waste tyres into carbon black by partial combustion of the oil produced from pyrolysis. They reported that major pyrolysis projects have failed to gain commercial success due to the low market value of the pyrolysis oil and char produced. Wojtowicz and Serio (1996) therefore deemed it necessary to produce carbon black which had a higher market value than pyrolysis oil in order to improve the economics of their process. The preliminary feasibility study by Wojtowicz and Serio (1996) used a tyre flow rate of 100 tons/day and found that the process was economical over a 5 year project life. The process yielded 20% gas, 35% char and 45% oil. The saleable products were carbon black, activated char and Boudard carbon with a tipping fee also adding to the revenue stream. Wojtowicz and Serio (1996) concluded that waste tyre pyrolysis processes are only economical if high value products are produced and recommended recovery of valuable chemicals as a pathway to make waste tyre pyrolysis economically feasible.

Shelly and El-Halwagi (1999) conducted an economic feasibility study for a waste tyre pyrolysis process that converts the pyrolysis oil into a synthetic crude product. The pyrolysis oil obtained was upgraded (hydrotreating and hydrocracking) to produce the synthetic crude product. The study by Shelly and El-Halwagi (1999) found that the process considered was economical having used a tyre feed rate of 100 tons/day. The saleable products from the process were synthetic crude, carbon black and steel; a tipping fee also contributed to the revenue stream. No information was provided about the yields of the different products that were sold. It was however noted by Shelly and El-Halwagi (1999) that a tyre feed rate of 100 tons/day could be difficult to obtain due to transportation costs and/or scheduling conflicts. There is therefore a need to look at waste tyre pyrolysis economic feasibility at lower tyre feed rates. Higher feed rates might have more costs savings due to the effect of economies of scale, however, more realistic flow rates need to be used. The study by Shelly and El-Halwagi (1999) also highlighted the need for upgrading pyrolysis primary products in order to improve process economics.

Pilusa *et al.* (2014) conducted a preliminary economic feasibility study for conversion of waste tyres into fuel in South Africa over a 5 year project life. Similarly to the current study, the study by Pilusa *et al.* (2014) assumed a constant supply of waste tyres from REDISA. The pyrolysis oil obtained was fractionated to produce tyre-derived fuel and heavy fuel oil. The process yielded 10% steel, 45 % oil, 37% char and 8% gas. The saleable products from the process were light diesel-equivalent fuel, refined carbon black, steel and sodium sulphite (a product of scrubbing the flue gases generated in the process using sodium hydroxide solution). The process used a tyre feed rate of 30 tons/day and it was found to be economically feasible. The study by Pilusa *et al.* (2014) highlighted the necessity for upgrading of the pyrolysis primary products to more valuable products in order to achieve economic feasibility for waste tyre pyrolysis processes. Pilusa *et al.* (2014) also concluded that a continuous product market demand is required for economic success of pyrolysis processes.

The economic studies evaluated in this section have highlighted the need for waste tyre pyrolysis processes that are focused on production of high value products as opposed to selling the primary products. The economic evaluation of the current study is therefore focused on the feasibility of recovering valuable products from waste tyres.

3.4. Modelling/simulation of pyrolysis systems

For a lot of processes, numerical simulations become necessary to help identify feasible operating conditions that improve the process performance (Mitta *et al.*, 2006). Process modelling using simulation software provides powerful engineering tools to evaluate the mass and energy balances,

to perform thermodynamic assessment and to optimise the processes (He *et al.*, 2013; Kong *et al.*, 2014). In this section, a general review of process simulation/modelling work that has been done in literature for waste tyre pyrolysis systems is provided.

This section will also provide a review of simulation/modelling of waste tyre valorisation processes using Aspen Plus® simulation package. Aspen Plus® is the simulation package used in the current study. The review of waste tyre valorisation processes will focus on determining the information required to successfully simulate the pyrolysis process in this study using Aspen Plus®. The required information that the review will focus on is: definition/representation of feed material; type of reactor model used; property method used; estimation of reactor product distribution; and model validation. The gaps that currently exist with regards to process modelling of waste tyre pyrolysis processes will also be highlighted.

Aspen Plus® simulation package is a commercial software that has been widely used for modelling, design and process optimisation of steady-state processes of chemical engineering systems including pyrolysis. Aspen Plus® contains various modules, thermodynamic method databases, and extensive physical property models capable of simulating the wide range of chemical process conditions suitable for the pyrolysis process (Yang *et al.*, 2012; Taylor *et al.*, 2013; Visconti *et al.*, 2015). Aspen Plus® has been used to simulate pyrolysis processes of several feedstock such as tyres, coal, biomass, plastics etc. (Yan and Zhang, 1999; Al Amoodi *et al.*, 2013; Hammer *et al.*, 2013; Altayeb, 2015). Therefore, while Aspen Plus® is not the only simulation package available, it is highly suitable for simulation of waste tyre pyrolysis processes.

3.4.1. Modelling/simulation of waste tyre pyrolysis

The open literature has limited work on modelling and simulation of waste tyre pyrolysis systems. During the course of this study, only 2 literature sources that dealt with modelling/simulation of pyrolysis systems were encountered. These sources were a modelling and simulation study for production of liquid fuels by Altayeb (2015) and a study by Ismail *et al*. (2017) where a simulation model was developed to predict yields of various pyrolysis products under varying operating temperatures. Both Altayeb (2015) and Ismail *et al*. (2017) simulated their processes using Aspen Plus®. As such, they will be discussed in section 3.4.2. The acronyms associated with Aspen Plus® used in this study are briefly described in Table 12. According to the knowledge of the author of this current study, no other waste tyre pyrolysis process simulation studies are available in the open literature.

Table 12: Description of Aspen Plus® acronyms used in section 3.4.2

Acronym	Description
DCOALIGT	Density model for coal
FORTRAN	User model for unit operation
HCOALGEN	Enthalpy model for coal
RGIBBS	Multiphase equilibrium reactor model
RPLUG	Reactor model based on plug flow with rate based kinetics
RSTOIC	Reactor model based on reaction stoichiometry
RYIELD	Reactor model based on product yields

3.4.2. Aspen Plus® modelling/simulation of waste tyre valorisation processes

Various studies in literature have developed simulation models for different processes aimed at valorising waste tyres; pyrolysis and gasification are the waste tyre valorisation processes that have commonly been modelled in the open literature using Aspen Plus® (Mitta *et al.*, 2006; Altayeb, 2015; Ismail *et al*., 2017). In developing simulation models of these valorisation processes, definition/specification of the feed material (tyre) and determination of suitable property models are typically amongst the first challenges to be addressed.

Due to the tyre not having a defined molecular structure/formula, and as such, not being in the Aspen Plus® component database, it is characterised as non-conventional, and it is defined using the proximate and ultimate analyses (Taylor *et al.*, 2013; Ismail *et al*., 2017). There has not been much report of the property models that have been used for these processes in literature. The Peng-Robinson with Boston-Mathias alpha function (PR-BM) property model has however been used to calculate physical properties of conventional components by Altayeb (2015). Altayeb (2015) also estimated the density and enthalpy of non-conventional components using the DCOALIGT and HCOALGEN models respectively.

With regards to modelling of the pyrolysis processes, the pyrolysis step is typically divided into 3 steps, which are to simplify the rather complex phenomenon that is tyre pyrolysis (Altayeb, 2015; Ismail *et al*., 2017). Altayeb (2015) divided their pyrolysis reactor into drying, tyre decomposition, and pyrolysis reaction. From the model developed by Altayeb (2015), the drying step was used to reduce the moisture content of the tyre feed. The tyre decomposition step was used to convert (decompose) the non-conventional tyre into its elemental constituents by specifying the output yield of each component based on the ultimate analysis. Finally, Altayeb (2015) used the pyrolysis reaction step to

generate the actual final pyrolysis products of their study using the Gibbs free energy minimisation approach. Ismail *et al*. (2017) used a similar approach to that of Altayeb (2015), where they divided the pyrolysis step of their model into decomposition, kinetic reactions, and combustion. From the model of Ismail *et al*. (2017), the decomposition step performed a similar purpose to that in the model of Altayeb (2015), and the kinetic reaction step was used to generate the actual pyrolysis products using kinetic data obtained from literature. Ismail *et al*. (2017) used the combustion step to generate the heat required for the pyrolysis reactor by combusting part of the char product in a furnace.

For representation of each different step in Aspen Plus®, various reactor models are used, largely depending on the availability of input information required for each reactor model. The reactor models that were used to represent each of the respective 3 steps, and pyrolysis conditions of the models by Altayeb (2015) and by Ismail *et al*. (2017) are shown it Table 13.

Table 13: Aspen Plus® reactor models and pyrolysis conditions of several tyre pyrolysis models in literature

Item	**Altayeb (2015)**	**Ismail *et al*. (2017)**
Drying step	RSTOIC	
Decomposition step	RYIELD	RYIELD
Pyrolysis reaction	RGIBBS	RPLUG
Combustion step		RGIBBS
Pyrolysis conditions	450 °C	300 – 700 °C

For modelling of the waste tyre gasification systems, the actual gasification process (in the gasifier) is also typically divided into 2 – 3 independent steps/stages that represent several phenomena that are hypothesised to be occurring at various points along the gasifier length (Mitta *et al.*, 2006; Taylor *et al.*, 2013).

Mitta *et al.* (2006) divided the gasifier of the model in their study into 3 stages as follows: drying, devolatilisation/decomposition, and gasification-combustion. The drying step in the model of Mitta *et al.* (2006) represented instantaneous moisture removal of the tyre particles, and the devolatilisation step represented decomposition of the non-conventional tyre into its elemental constituents. Finally, the gasification-combustion step in the model of Mitta *et al.* (2006) represented formation of the actual expected gasifier products (compounds in the syngas produced) using Gibbs free energy minimisation. Similarly to Mitta *et al.* (2006), Taylor *et al.* (2013) included the decomposition and gasification steps to represent the actual gasification process in the model of their study. The only

difference between representation of the gasifier between the models of Mitta *et al.* (2006) and Taylor *et al.* (2013) was omission of the drying stage by Taylor *et al.* (2013). The Aspen Plus® reactor models used for representation of the various stages, and the conditions in each step from the models of Mitta *et al.* (2006) and Taylor *et al.* (2013) are shown in Table 14.

Table 14: Aspen Plus® reactor models and conditions of several tyre gasification models in literature

Item	Mitta *et al.* (2006)	Taylor *et al.* (2013)
Drying step	RSTOIC	
Drying conditions	110 °C	
Decomposition step	RYIELD	RYIELD
Decomposition conditions	500 °C	
Gasification step	RGIBBS	RGIBBS
Gasification conditions	900 °C	700 – 800 °C

The last crucial aspect in modelling of the waste tyre pyrolysis and gasification systems is validation of the model-predicted results. This step is typically achieved by comparing the model-predicted reactor or gasifier product distribution with experimental data conducted at the same conditions as those in the models. For validation, experimental data that is readily available in literature or generated specifically for the particular systems modelled in Aspen Plus® is used (Mitta *et al.*, 2006; Taylor *et al.*, 2013; Altayeb, 2015; Ismail *et al.*, 2017).

3.4.3. Observations from studies evaluated

The current study aims to convert waste tyres into valuable chemicals through pyrolysis process by process simulation in Aspen Plus®. From the studies reviewed in section 3.4.2, it can be concluded that the proximate and ultimate analyses will be suitable for definition of the (non-conventional) tyre feed. The studies reviewed in section 3.4.2 also highlighted the importance of properly choosing the approach for prediction/calculation of reactor product distribution. The studies reviewed in section 3.4.2 indicated that the RYIELD reactor model is preferred when yields of the reactor products are known, as product yields are the only requirement for mass balance in such a reactor model. In the current study, reactor product yield information is available. The final choice of reactor model for the current study is explained in chapter 4. Model validation for the current study will be achieved by comparison of product yields results from the model with literature values. The observations from the studies reviewed in 3.4.2 have also been observed in other studies that focused on pyrolysis of biomass (Zhang *et al.*, 2007; Nsaful 2012; Gorling *et al.*, 2013; Shemfe *et al.*, 2015). Biomass pyrolysis

is the most simulated process in Aspen Plus® amongst pyrolysis processed of carbonaceous materials and the observations were found to be applicable to this study.

3.5. Typical process flow diagrams of waste tyre pyrolysis plants

This section gives a brief review of some of the process flow diagrams (PFDs) that have been developed in literature for pyrolysis of waste tyres. The intention of this section is to demonstrate the different process steps that are typically involved during waste tyre pyrolysis; the different process steps will serve as part of a guideline/basis for development of the waste tyres-to-limonene process discussed in chapter 4 of this study.

Wojtowicz and Serio (1996) developed a conceptual PFD of a proposed process for pyrolysis of waste tyres to carbon black, activated char and Boudard carbon. Details about the tyre feed rate and yields of primary products have been discussed in section 3.3.6 and will not be repeated here. The PFD of the process proposed by Wojtowicz and Serio (1996) is shown in Figure 12. In the process shown in Figure 12, tyres are shredded (pre-treatment) before feeding into a pyrolysis reactor (fluidised-bed reactor) operating at 600 °C. A cyclone is required after the reactor in order to separate the volatiles from the char product. The volatiles are condensed to obtain a non-condensable gas product and an oil product. The non-condensable gas product is returned to the reactor as a fluidising medium and as fuel for reactor heating while the oil product is sent to a furnace for conversion into carbon black by partial combustion at 1400 - 1650 °C. The char product from the process in Figure 12 is activated by carbon dioxide at 900 °C to produce activated carbon; the carbon monoxide produced during activation is sent to a Boudard reactor where it is converted to Boudard carbon at 500 - 527 °C.

Fels and Pegg (2009) developed a PFD for evaluation of waste tyre pyrolysis plants operating in Shanghai and Taiwan that process 8000 tons of tyres per year at an estimated operational time of 7680 hours/year. The products from the plants evaluated in the study by Fels and Pegg (2009) are pyrolysis gas, pyrolysis oil, pyrolysis char and steel at yields of 10%, 45%, 35% and 10% respectively. The PFD of the process developed by Fels and Pegg (2009) is shown in Figure 13. It can be seen that shredding of the tyres into 3cm^2 chips is the only major pre-treatment step involved before the tyres are fed into a pyrolysis reactor operating at 425 °C. The volatiles produced in the reactor are cooled in a condenser whereby an oil product is obtained and separated from the non-condensable gases. The oil product is sold as feedstock for an oil refinery. The non-condensable gas product is either combusted for reactor heating (40%), combusted to generate heat for drying (30%) and the remainder is burned in a flare stack. A magnetic separation step is used to separate the steel and the char product that are obtained from the reactor.

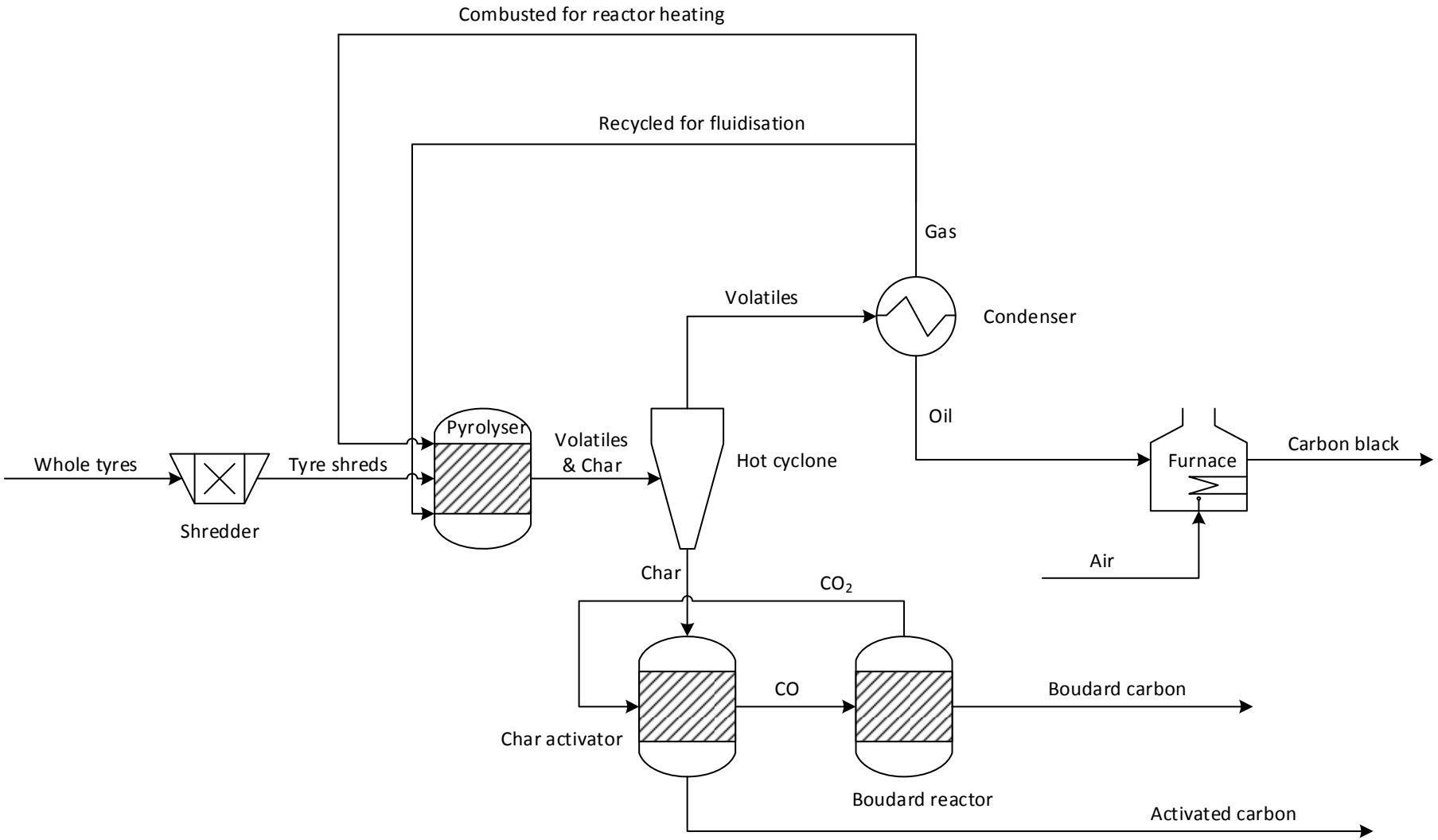

Figure 12: PFD of the process by Wojtowicz and Serio (1996)

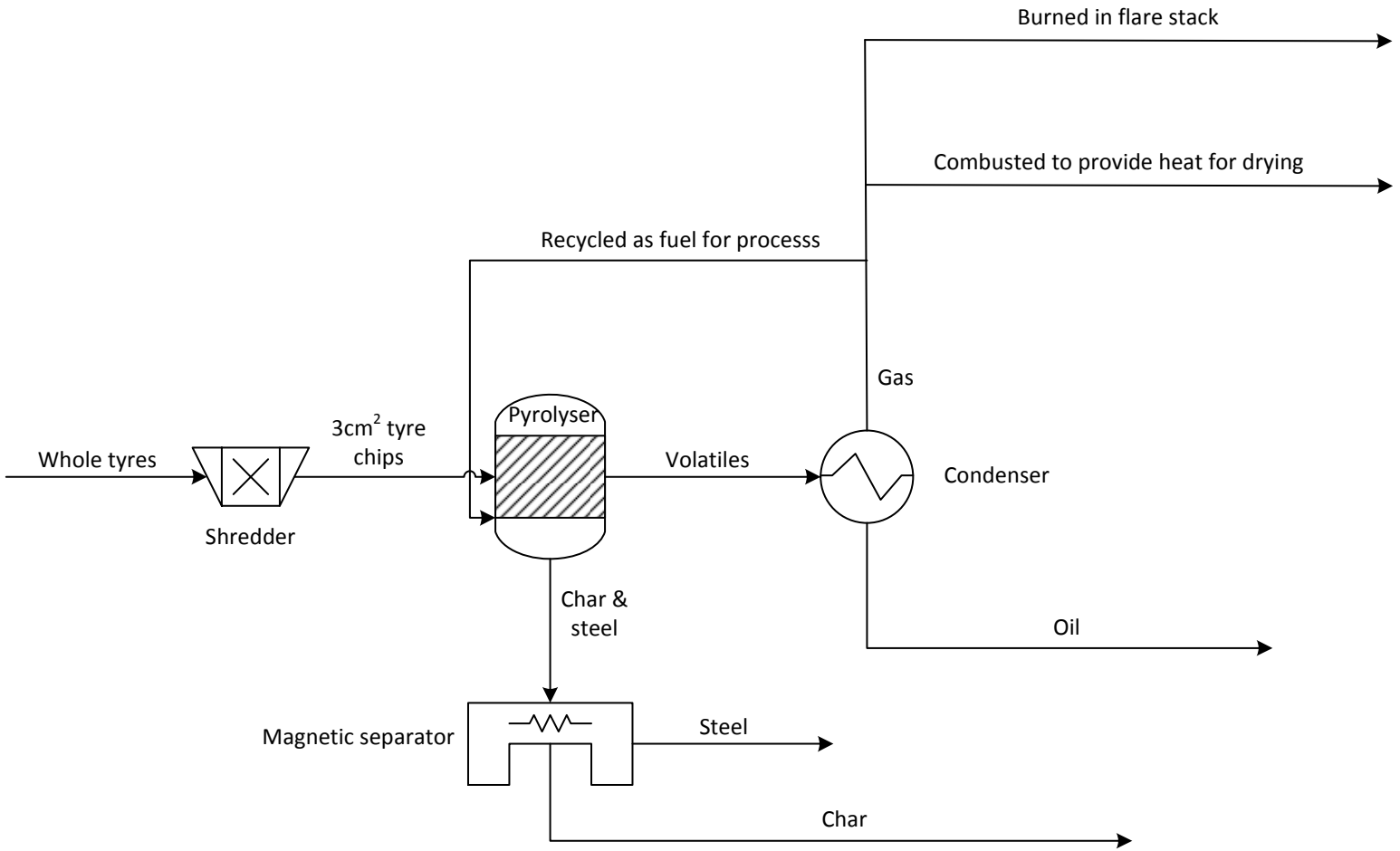

Figure 13: PFD of the process by Fels and Pegg (2009)

Pilusa *et al.* (2014) developed a conceptual PFD for a proposed plant that produces tyre-derived fuel (TDF), refined carbon black, steel and sodium sulphite. Details about process flow rate and reactor product yields have already been discussed in section 3.3.5. The PFD developed by Pilusa *et al.* (2014) is shown in Figure 14. Pre-treatment in Figure 14 includes extraction of the high-tensile bead wires (from trimmed tyre rings) and shredding of the tyres to produce 10-15mm tyre chips. The tyre chips are fed into a pyrolysis reactor operating at 570 °C to produce volatiles, char and steel products. The reactor volatiles are cooled in a condenser to obtain an oil product and a non-condensable gas product. A portion of the non-condensable gas product is combusted for reactor heating and the remaining fraction is compressed and used to run the fork lifts. The oil product from the condenser is sent to a fractionation column where a light diesel-equivalent fuel and an HFO-equivalent fuel are obtained. The light diesel-equivalent fuel is sold and the HFO-equivalent fuel is mixed with diesel and used as fuel for a generator. The char product obtained from the reactor is milled, thickened and filter pressed to produce a refined carbon black product that is sold. The steel obtained from the reactor is also sold together with the steel obtained from pre-treatment. Sodium sulphite is obtained from treatment of the flue gases generated in the process with sodium hydroxide.

From the PFDs reviewed in this section, it can be observed that a PFD of a waste tyre pyrolysis process will depend on the targeted final products. It can also be observed that major differences in the PFDs of tyre pyrolysis plants are mostly due to upgrading of the primary products into the desired final products; minor differences are observed in the PFDs up to recovery of primary products. The major process steps in a PFD of a waste tyre pyrolysis process are pre-treatment (typically shredding), pyrolysis, condensing of reactor volatiles and separation of the resulting oil and non-condensable gases, and separation of the steel from the char product. The PFDs of the processes reviewed in this section have also indicated that while the oil and char products can typically be upgraded to various secondary products, the non-condensable gas is typically combusted for reactor heating and/or is flared.

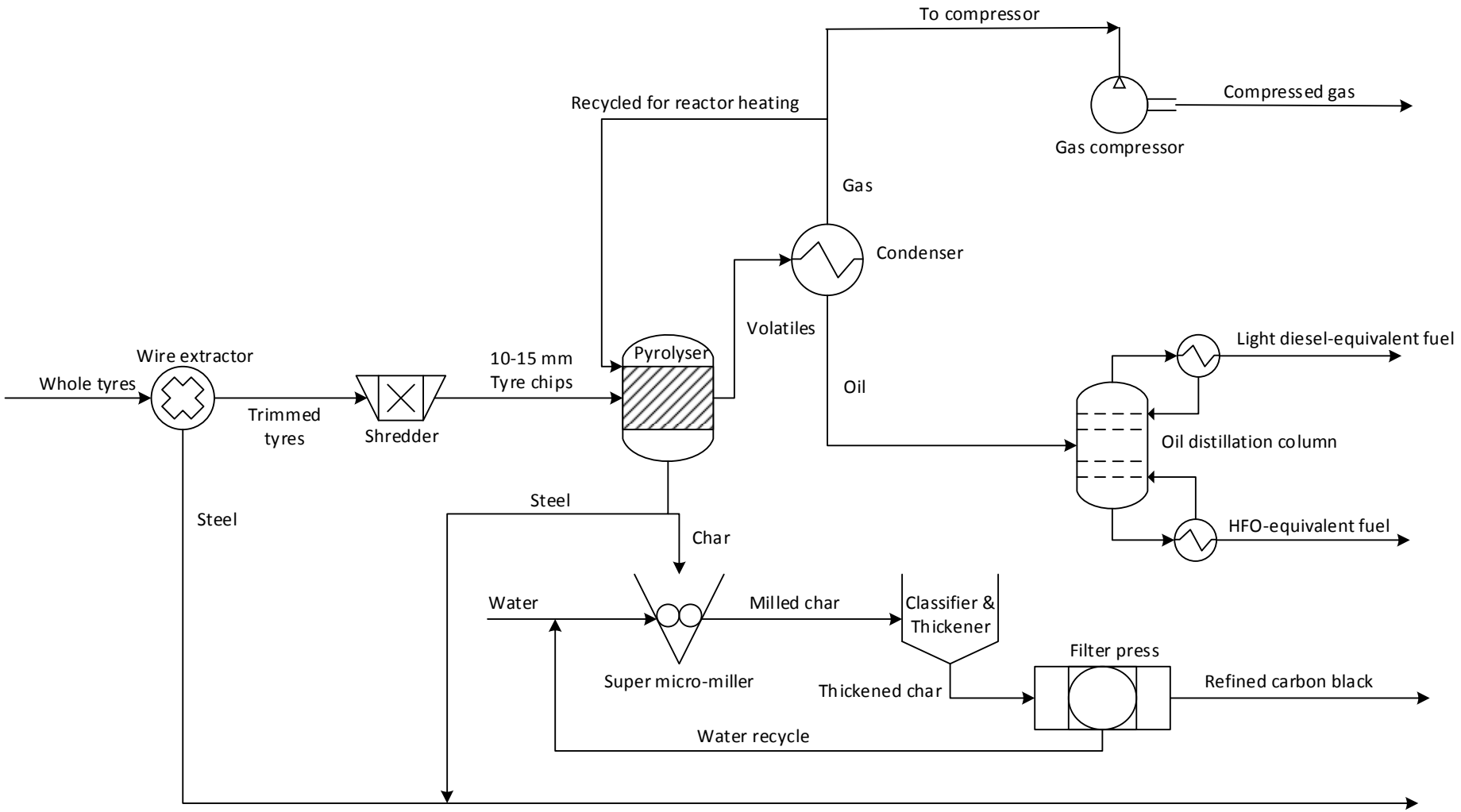

Figure 14: PFD of the process by Pilusa *et al.* (2014)

In this study, a PFD of one main process scenario will be developed, which will serve as the base case scenario for converting waste tyres to limonene by pyrolysis. The main process scenario that will be developed in this study will include de-beading and shredding of whole tyres to tyre chips (pre-treatment), pyrolysis, magnetic separation of the char and steel, condensation of the reactor volatiles, fractional distillation, extractive distillation using a solvent, and solvent regeneration. The process steps (de-beading and shredding, pyrolysis, condensation and magnetic separation) involved up to recovery of primary products (oil, char, non-condensable gas and steel) are based on the PFDs reviewed in section 3.5 and what has been done in other studies (Shelly and El-Halwagi, 1999). In this study, the process steps of fractional distillation, extractive distillation using a solvent and solvent regeneration are adapted from a study done by Ngwetjana (2017) who investigated the recovery of limonene from TDO. The process of limonene recovery from TDO using diethylene glycol (DEG) as the solvent, developed by Ngwetjana (2017), is used in this study. A block flow diagram (BFD) of the proposed main process scenario that will be developed in this study is shown in Figure 15.

An alternative of the process shown in Figure 15 would be a process scenario in which the oil obtained from the condenser is not further upgraded to recover limonene but sold as low value fuel (raw TDO). The use of TDO as low value fuel is currently the most common application. The process scenario of tyre pyrolysis for fuel production purposes would be similar to Figure 15 but without the fractional distillation, extractive distillation and solvent regeneration steps. The process scenario for converting tyres to TDO will be used for purposes of economic comparison (in chapter 5) with the main process scenario in Figure 15 to determine the benefits of upgrading the oil to recover limonene.

Other literature studies have developed processes that include shredding and crumbing of whole tyres to produce steel-free tyre crumbs that are then used as feed to the reactor (Ko *et al.*, 2004, Altayeb, 2015). The pre-treatment to crumb variation of Figure 15 will only be considered for economic comparison in chapter 5 to determine the economic benefits of pre-treating whole tyres to either chips or crumb. Another pre-treatment variation to the one in Figure 15 would be a scenario in which purchased crumb is used as feed for the process (no pre-treatment required). The crumb-purchase variation will also be considered for economic comparison with the main process in Figure 15 to determine if there is any benefit to having no pre-treatment step.

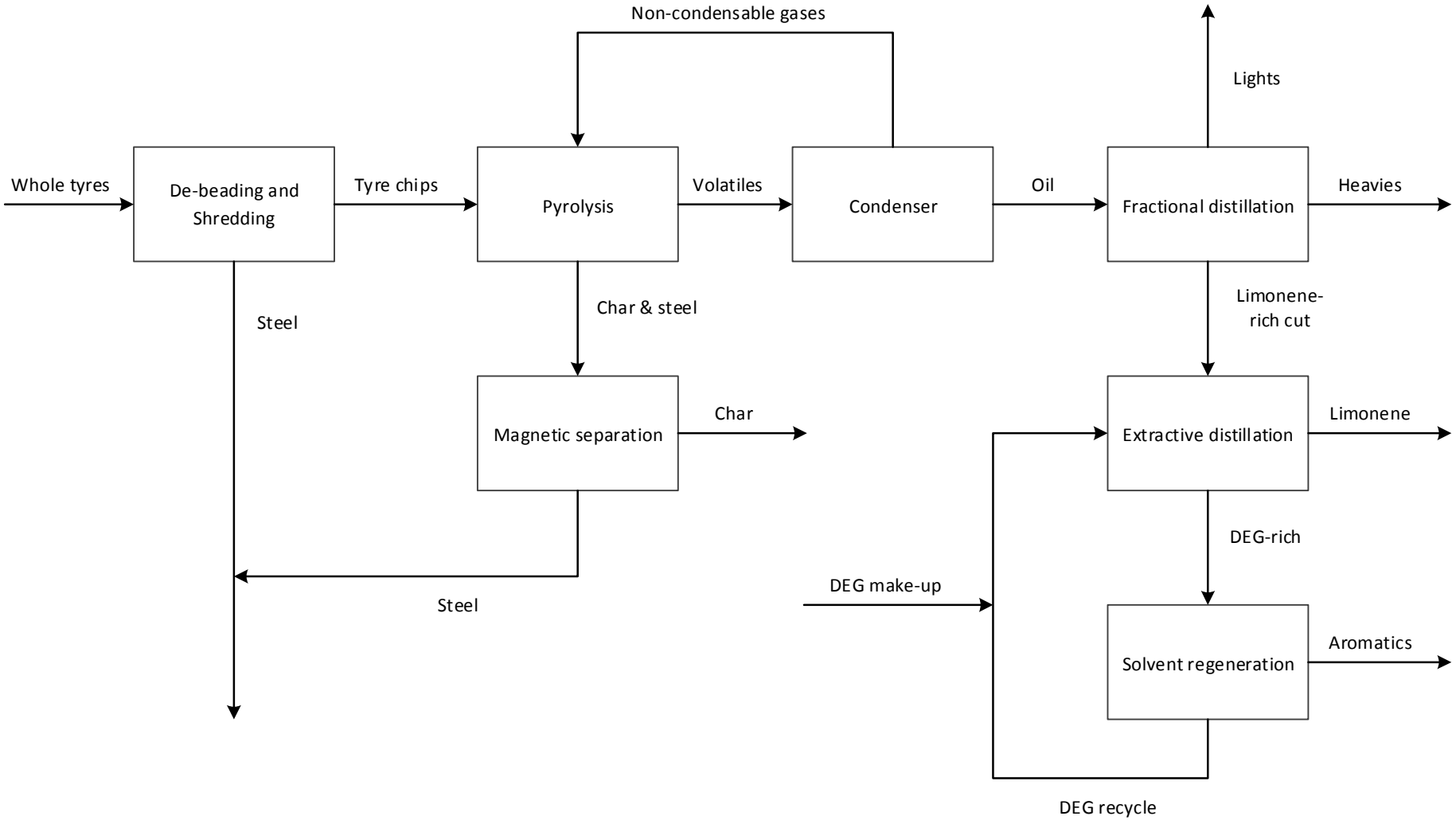

Figure 15: Proposed BFD of the main process scenario for converting waste tyres to limonene in current study

3.6. Summary

In chapter 3, a literature study was conducted with regards to waste tyres and process modelling of waste tyre pyrolysis systems. Landfilling and stockpiling have been shown to be the simplest methods for disposing the waste tyres generated, however, they present serious environmental and human health threats. Several alternative methods that are currently used to deal with the problem of waste tyre produce products that either have low market demands or low market prices mainly due to quality concerns. The current alternative methods have as such failed to greatly reduce the amount of waste tyres in stockpiles and landfills.

Pyrolysis is an attractive alternative method of reducing the amount of waste tyres available. The products of pyrolysis can be independently stored and used as alternative fuels or upgraded to secondary products. Most waste tyre pyrolysis projects have been limited to laboratory or pilot scales with most focus placed on the use of pyrolysis products as alternative fuels.

The literature review also revealed that waste tyre pyrolysis projects have failed to gain commercial success due to low quality of products obtained which results in low selling prices. As such, recovery of high value chemicals from waste tyre pyrolysis is required in order to improve the economics of waste tyre pyrolysis. The current study will address this requirement by performing economic feasibility evaluation of an industrial process aimed at recovering limonene from waste tyre via the pyrolysis process. The feasibility evaluation will demonstrate whether recovering chemicals from waste tyre pyrolysis really has the potential to improve the economic of waste tyre pyrolysis or not.

Pyrolysis seems to be a potential pathway for converting waste tyres into valuable chemicals as the pyrolysis oil contains compounds like limonene, BTX etc. that could command high selling prices should they be recovered. Limonene has been targeted for recovery in this study due to its wide range of industrial applications and potential high selling prices. It was revealed that there currently is a gap with regards to processes being used as pathways for production and recovery of valuable chemicals from waste tyre pyrolysis.

There is limited work in the open literature with regards to process modelling of waste tyre pyrolysis. Aspen Plus® is a simulation software capable of performing process modelling for waste tyre valorisation process such as pyrolysis and gasification. For simulation of waste pyrolysis using Aspen plus®, an RYIELD reactor model is preferred when information about product distribution is available, like in the current study. Process modelling using simulation software can be used as a predictive tool for product distribution at varying reactor conditions. As such, experimental data is always necessary to validate the model-predicted results.

The current study will try to close the literature gap by developing a conceptual base case process scenario aimed at conversion of waste tyres to limonene by pyrolysis using PFDs that have been developed in literature as guideline. The current study will also make a contribution towards the field of process modelling of waste tyre pyrolysis as there currently exists a gap in that particular field. Development of the conceptual base case process scenario (including process simulation in Aspen plus®) is detailed in chapter 4.

CHAPTER 4: PROCESS DEVELOPMENT

Overview

This chapter provides information on development of the conceptual process for conversion of waste tyres to limonene. The development process is described from a technical and Aspen Plus® V8.6 simulation point of view. This chapter aims to address objective 2 (development of various conceptual process scenarios for converting waste tyres into targeted valuable chemicals) and objective 3 (Aspen Plus® simulation of the developed conceptual process scenarios) of this study. This chapter is subdivided into 8 sections. Section 4.1 outlines the design basis of the current study. Section 4.2 describes the input-output structure for the current study. Section 4.3 describes development of the pre-treatment system. In section 4.4, development of the pyrolysis system is detailed, with specific focus on the pyrolysis reactor. The separation system is discussed in section 4.5. Section 4.6 describes the heat recovery system. The final PFD of the conceptual process developed in this study is presented in section 4.7. A summary of the chapter is provided in section 4.8.

4.1. Design basis

The process in this study was developed based on the proposed BFD shown in Figure 15. The design basis of this study is summarised in Table 15.

Table 15: Design basis for the waste tyres to limonene process

Parameter	Value	Motivation	Reference
Raw material	Tyres with 10 wt.% steel content	Typical literature steel content of waste tyres	Fels and Pegg, 2009; Pilusa *et al.*, 2014
Tyre feed rate	30 tons/ day	Typical flow rate for waste tyre pyrolysis plants	Ko *et al.*, 2004; Pilusa *et al.*, 2014; Wiese (2017)
Main product	Technical grade limonene	Market determined	Wilikins Jr, 1999; Ciriminna *et al.*, 2014
Limonene purity	95 wt.%	Market standard for technical grade limonene	Wilikins Jr, 1999; Ciriminna *et al.*, 2014
Mode of operation	24-hour continuous	Shorter reaction times preferred for limonene production	Pakdel *et al.*, 2001; Sinnott and Towler, 2009
Operating hours	8000 h/year	Typical operating time for continuous processes	Sinnott and Towler, 2009; Nsaful, 2012

Table 15 continued: Design basis for the waste tyres to limonene process

Parameter	Value	Motivation	Reference
Simulation software	Aspen Plus®	Widely used for simulation of pyrolysis systems of various carbonaceous feedstock	Yan and Zhang, 1999; Hammer *et al.*, 2013; Altayeb, 2015
Plant location	Cape Town	Close proximity to established network of tyre depots, transporters, processors and potential ease of product distribution	GoIndustry DoveBid, 2016; REDISA, 2016

Raw materials and production capacity

The raw material used for the process in this study is tyres with a steel content of 10 wt.%; truck tyres are preferred in this study as they typically contain more natural rubber content than passenger car tyres. It is assumed that the tyres will be supplied by REDISA. The tyre steel content of 10 wt.% was chosen as it is commonly used in literature for waste tyre pyrolysis studies of both operational and conceptual processes (Fels and Pegg, 2009; Pilusa *et al.*, 2014; Muzenda and Popa, 2015).

The process in this study is based on a tyre feed rate of 30 tons/day. A tyre feed rate of 30 tons/day was chosen based on information obtained from two operational REDISA-affiliated waste tyre pyrolysis plants in South Africa that process an average of 20 - 30 tons/day each. A flow rate of 30 tons/day has also been used in several literature waste tyre pyrolysis feasibility studies (Ko *et al.*, 2004; Fels and Pegg, 2009; Pilusa *et al.*, 2014). A continuous supply of waste tyres is necessary to ensure sustainability of waste tyre pyrolysis plants (Muzenda and Popa, 2015). As such, a tyre flow rate of 30 tons/day was deemed sufficient to ensure sustainability and to sufficiently perform a realistic economic feasibility evaluation.

Mode of operation and processing time

Continuous operation was preferred for the process in this study as lower reaction times are preferred for limonene production and lower residence times will be preferred for the separation steps due to the heat sensitive nature of hydrocarbons (Turton *et al.*, 2009; Martinez *et al.*, 2013). Continuous operation also normally involves less operating and labour costs, and easier control of equipment (due to automation) and product quality (Peters and Timmerhaus, 1991; Sinnott and Towler, 2009).

Continuous operation has also been used for other waste tyre pyrolysis systems in literature (Ko *et al.*, 2004; Fels and Pegg, 2009).

Plant operating times of 7200 - 7900 hours/year have been used in literature studies of waste tyre pyrolysis plants (Ko *et al.*, 2004; Fels and Pegg, 2009; Pilusa *et al.*, 2014). According to Sinnott and Towler (2009), continuous plants usually have 90 - 95% availability, which translates to 7884 - 8332 operating hours/year; 8000 hours were chosen for this study.

Targeted products

The targeted product in the process developed in this study is 95 wt.% purity technical (non-food) grade limonene (main product), with a targeted overall limonene recovery of ±95%. The process also produces TDO, crude char, and steel as by-products, which are sold as well. Limonene purity of 95 wt.% is targeted in this study in order to meet market specifications for technical grade limonene, which is typically 95 wt.% (Wilikins Jr, 1999; Ciriminna *et al.*, 2014). In this study, the remaining 5 wt.% is expected to be compounds such as trimethylbenzene, p-cymene, indene, methylstyrene, butylbenzene etc. that have boiling points similar to, or close to that of limonene. A minimum limonene recovery of ±95% is targeted to ensure high limonene product flow rate given that limonene yields are typically only 2 - 5 wt.% of the tyre feed on a steel-free basis.

Plant location

In this study, it is assumed that the plant will be located in Cape Town as there is an established network of tyre depots, transporters and tyre processors. It is assumed that the close proximity of the plant to tyre depots and availability of transporters will ensure continuous access of raw materials which will ensure sustainability. Cape Town has a major port in South Africa, and it is assumed that the existing goods distribution network/system in Cape Town will enable the products from the process in this study to reach customers.

Selection of simulation software

Various simulation software such as Aspen Plus®, ProSim®, Pro/II®, Hysys®, WinSim DESIGN II®, ProMax® and ChemCAD® are commonly used for simulation of chemical processes (WinSim Inc, 2012; Mocke, 2013; Shoaib *et al.*, 2014). Mocke (2013) reported that according to WinSim Inc (2012), there is little difference between the commonly used chemical engineering simulation software with regards to features such as component libraries, thermodynamic options and recycle convergence. Aspen Plus® is a widely used commercial simulation software and it has also been widely used for simulation of pyrolysis processes of several carbonaceous feedstock such as tyres, coal, biomass etc. (Yan and Zhang, 1999; Al Amoodi *et al.*, 2013; Hammer *et al.*, 2013; Altayeb, 2015). Aspen Plus® offers various

modules, thermodynamic databases and extensive physical property models capable of simulating the wide range of chemical process conditions suitable for the pyrolysis process (Yang *et al.*, 2012; Taylor *et al.*, 2013; Visconti *et al.*, 2015). The Aspen Plus® simulation software will be used for simulation of the base case process scenario developed in this study.

The design basis developed in this section will be expanded on by detail description of development of each section of the proposed BFD shown in Figure 15. Description of how each section of the BFD shown in Figure 15 was developed is detailed in sections 4.3 - 4.6 starting with development of pre-treatment in section 4.3. Development of each section of the proposed base case process scenario will include details about the technical information considered and development of the particular section in Aspen Plus®. The flow of discussion in sections 4.3 - 4.6 follows the hierarchical and stepwise methodology developed in chapter 2.

4.2. Selection of input-output structure information

The input-output structure (Figure 16) shows the main process streams (Linninger, 2002).

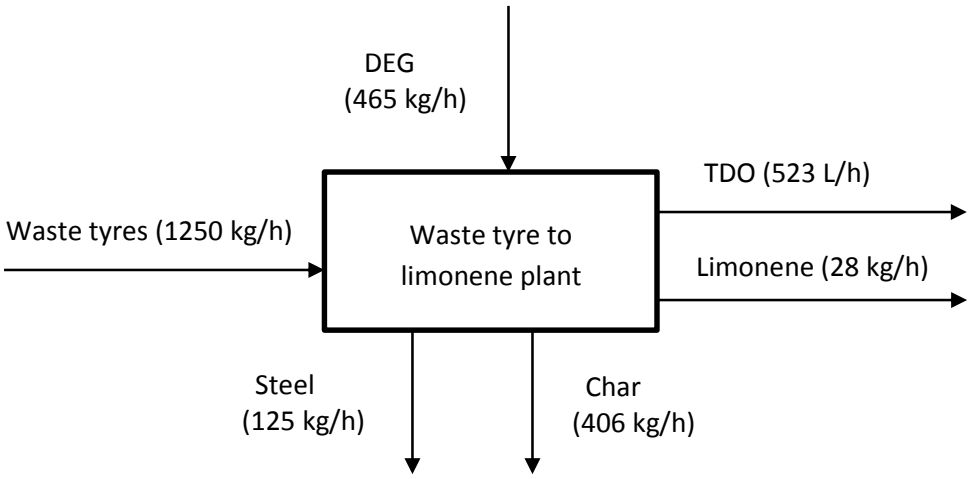

Figure 16: Input-output structure of the waste tyres to limonene process in this study

Compounds that make up the feed or products for the process scenario developed in this study were adopted from studies by Rodriguez *et al.* (2001), Choi *et al.* (2014) and Ngwetjana (2017). The study by Choi *et al.* (2014) was chosen as the base-literature from which feed and product information was adapted. The studies by Rodriguez *et al.* (2001), and by Ngwetjana (2017) were used to provide necessary additional information not available from the study by Choi *et al.* (2014).

In selecting the base-literature source to provide input and output information, a criterion was followed that was twofold: (i) the literature source should have sufficient information necessary for modelling in Aspen Plus® (feed and product characterisation, product distribution and reactor

operating conditions) (ii) the literature source should also have a reported limonene yield of 2 -5 wt.% on the basis of a steel-free tyre feed. The limonene yield criterion is a result of what has been shown in various literature studies that the yield of limonene is typically between 2 and 5 wt.% (Cunliffe and Williams, 1998a; Qu *et al.*, 2006; Frigo *et al.*, 2014; Danon *et al.*, 2015). The study by Choi *et al.* (2014) was found to meet the criteria best as characterisation of both the tyre feed and reactor products was reported. Most importantly, 74 – 79% characterisation of the oil product was reported from the study by Choi *et al.* (2014); significant characterisation of the pyrolysis oil product is rare in literature due to the complexity of pyrolysis oil. The study conducted by Choi *et al.* (2014) was as such deemed suitable for use as the base-literature for input and output information in this study.

The tyre used in the study by Choi *et al.* (2014) was used as reactor feed for the process developed in this study. The char product and the compounds identified in the oil product from the study by Choi *et al.* (2014) were considered as reactor output for this study. All the oxygen and phosphorous containing compounds identified in the oil product from the study by Choi *et al.* (2014) were not considered as reactor output in this study, as the ultimate analysis of the tyre feed used by Choi *et al.* (2014) did not include oxygen and phosphorus.

In a tyre particle, oxygen is normally present due to the moisture contained in the tyre, or the oxygen-containing compounds that are used in tyre manufacturing. Ultimate analyses of various studies have shown the moisture content to typically be a maximum of 1 wt.%, whereas the ultimate analyses show an oxygen content of typically 3 – 5 wt.% on a dry basis (Gonzalez *et al*., 2001; Laresgoiti *et al*., 2004; Banar *et al*., 2012). During pyrolysis, oxygen-containing products can be formed as decomposition products of the organic and inorganic components contained in the tyre such as stearic acid, calcium carbonate, and various other metal oxides (Dai *et al*., 2001; Rodriguez *et al*., 2001). In the pyrolysis gas product, carbon dioxide and carbon monoxide are the most common oxygen-containing compounds, whereas compounds such as stearic acid, 5,5-dimethylhexanal, phthalimide, etc. have been identified in TDO by various authors (Conesa *et al*., 2004; Choi *et al*., 2014; Frigo *et al*., 2014).

Various authors that have identified and quantified oxygen-containing compounds amongst their products have shown that the total combined yield of all these oxygen-containing compounds is mostly less than 1 wt.% on the basis of the tyre feed (Williams and Brindle, 2002; Berrueco *et al*., 2005; Lopez *et al*., 2010). From the study by Choi *et al.* (2014), the oxygen and phosphorous containing compounds identified in the oil accounted for a combined 0.35 wt.% (of the tyre feed) at most, within the temperature range considered. It is as such expected that omission of these compounds would have negligible effect on overall reactor product distribution in this study.

The study conducted by Choi *et al.* (2014) did not report on the characterisation of the (non-condensable) gas fraction (only the gas yield was reported). Gas characterisation from the study conducted by Rodriguez *et al.* (2001) was adapted to represent the gas fraction in this study. The study conducted by Rodriguez *et al.* (2001) was chosen to represent the gas fraction of the study by Choi *et al.* (2014), as similar reactor configurations were used in those studies. All the oxygen-containing gas compounds from the study of Rodriguez *et al.* (2001) were not considered in this study, and the compositions of remaining gas compounds were normalised to represent 100%. The gas compounds from the study of Rodriguez *et al.* (2001) adopted for use in this study were all considered as reactor output.

In this study, benzene and phenanthrene were chosen to represent the uncharacterised fraction of oil and n-eicosane was chosen to represent the distillate residue fraction reported by Choi *et al.* (2014). Benzene was chosen on the basis of high aromatic content of the oil fraction from the study by Choi *et al.* (2014) and that the uncharacterised fraction of oil represented only ±25%. It was assumed that benzene will be a model compound for all unidentified single-ring aromatic compounds. Phenanthrene is chosen as the model compound for all unidentified polycyclic aromatic hydrocarbons (PAHs) in the oil. Cunliffe and Williams (1998a) identified phenanthrenes as having the highest concentration in the oil amongst PAHs that they extensively characterised. As such, phenanthrene was deemed sufficient to represent unidentified PAHs in the oil. n-Eicosane was chosen to represent the distillate residue on the basis that eicosanes were the highest carbon number hydrocarbons identified by Lopez *et al.* (2010) who extensively characterised oil compounds up to C_{20}^{+}. Benzene, phenanthrene and n-eicosane were all considered reactor output compounds as well.

All compounds that form part of the input-output structure for the process in this study are show in Table A.1 and Table A.2 in appendix A, together with Aspen Plus® reactor yields. Table A.2 also shows the original and normalised gas compositions from the study conducted by Rodriguez *et al.* (2001).

4.2.1. Specification of input and output compounds in Aspen Plus®

For the purpose of modelling in Aspen Plus®, tyre and char are regarded as non-conventional components in this study, since they do not have a defined molecular formula; they were defined based on their proximate and ultimate analyses. The proximate and ultimate analyses of tyre and char are shown in Table 16.

Table 16: Proximate and ultimate analyses of tyre and char for definition in Aspen Plus® (Choi *et al.*, 2014)

Proximate analysis			Ultimate analysis		
Component	**Value (wt.%)**		**Component**	**Value (wt.%)**	
	Tyre (dry-basis)	Char		Tyre (dry and ash free basis)	Char
Volatile matter	73.9	0[a]	C	89.2	82.76
Fixed carbon	21.8	87.78[b]	H	7.7[c]	0.55
Ash	4.3	12.21	N	0.5	0.44
Moisture	0	0	S	2.6	4.03
			Ash	0	12.21

[a]Assuming no volatiles are left in char. [b]Sum of C, H, N, S in ultimate analysis. [c]Calculated by difference

All other compounds in this study are regarded and defined as conventional components, as such they were selected from the Aspen Plus® database. Compounds that were reported as a collection of isomers by Choi *et al.* (2014) e.g. xylenes, methylstyrenes etc. were represented by the isomer whose boiling point is closest to that of other isomers. 1,2,4-Tris(methylene)cyclohexane (boiling point of 161.6 °C) and 1,2,5,5-Tetramethyl-1,3-cyclopentadiene (boiling point of 135.9 °C) were not found in the Aspen Plus® database, they were represented by compounds that resembled them closest in molecular formula and boiling point. 3-Ethylytoluene (boiling point of 161.3 °C) and 1-Ethyl-4-methyl-1,3-cyclohexadiene (boiling point of 135.2 °C) were used to represent 1,2,4-Tris(methylene)cyclohexane and 1,2,5,5-Tetramethyl-1,3-cyclopentadiene respectively. For the purposes of modelling in Aspen Plus®, steel was not considered as either input or output in the reactor as the focus in this study is on the decomposition products of the tyre chips fed to the reactor. Table A.1 and Table A.2 in appendix A show all conventional compounds as defined in Aspen Plus®.

The non-conventional solids in this study do not have a particle size distribution, as such, a combined stream class of MIXNC was chosen in Aspen Plus® when simulating the process. The MIXNC stream class is a combination of the MIXED (for conventional components that reach vapour-liquid-solid phase equilibrium) and NC (for non-conventional components) stream classes. MIXNC is recommended for systems with conventional components and non-conventional solids without a particle size distribution (Aspen Technology, 2009).

4.3. Design of pre-treatment system

The aim of the pre-treatment section is to reduce whole tyres that are used as process feed into tyre chips, which will be fed to the pyrolysis reactor. The pre-treatment section in this study consists of a tyre de-beader and a shredder. The PFD of the pre-treatment section is shown in Figure 17.

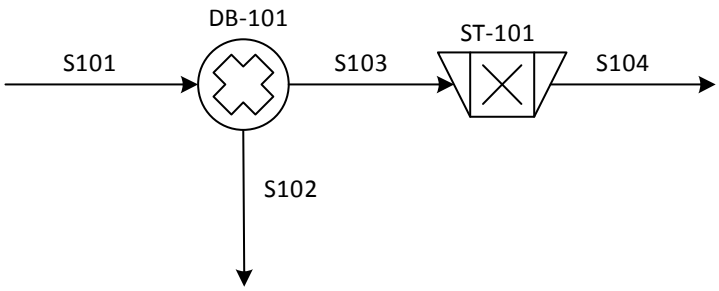

Figure 17: PFD of the pre-treatment system

Following what was done in the study by Pilusa *et al.* (2014), the de-beader (DB-101) in this study is used to remove high tensile reinforcement steel (bead-wire) before the tyres are shredded, so as to prolong the lifespan of shredding equipment. The steel cords removed by the de-beader (S102) are sold as scrap steel. In the shredder (ST-101), whole tyres (S103) are shredded down to 50mm x 50mm chips (S104), which is a tyre chips size commonly used for pyrolysis (Shelly and El-Halwagi, 1999).

The pre-treatment section is not modelled in Aspen Plus® in this study, however, the equipment cost and power requirements of the de-beader and the shredder are taken into account for economic evaluation in chapter 5. Table 17 shows the cost and power requirement of each pre-treatment equipment.

Table 17: Cost and power requirements for pre-treatment equipment

Equipment	Cost ($)	Power requirements (kW)	Reference
DB-101	8000	11	Jiangyin Xinda Machinery (2016)
ST-101	52 200	95	Jiangyin Xinda Machinery (2016)

In terms of energy usage in the pre-treatment section, the shredder accounts for most of the power requirements (86%) due to the energy intensity of tyre size reduction applications. The pre-treatment section accounts for 83% of the overall process power requirements, which could be expected to increase if the tyres chips were to be further reduced in size. It can then be concluded that in order to

minimise electricity costs, size reduction of the tyres fed to the process should only be performed based on process requirements.

4.4. Design of pyrolysis system

The purpose of the pyrolysis system in this study is to pyrolyse the tyre chips from the shredder, in order to obtain the primary pyrolysis products (oil, gas, char) and steel. The tyre chips received from the shredder are pyrolysed to produce a vapour (volatiles) product and a solid product (char). The vapour product is cooled down with cooling water in a condenser from which TDO and the non-condensable gas streams are obtained. The char product (containing steel) is discharged from the reactor, after which magnetic separation is used to separate the char and steel. As such, equipment that forms part of the pyrolysis system in this study is the pyrolysis reactor, reactor volatiles condenser, flash drum, and the magnetic separator that separates the char and the steel. The PFD of the pyrolysis system is shown in Figure 18.

The pyrolysis reactor is the main equipment in the pyrolysis system, and it will be extensively discussed in sections 4.4.1-4.4.3 after which the Aspen Plus® flowsheet of the whole pyrolysis system is presented and discussed in section 4.4.4.

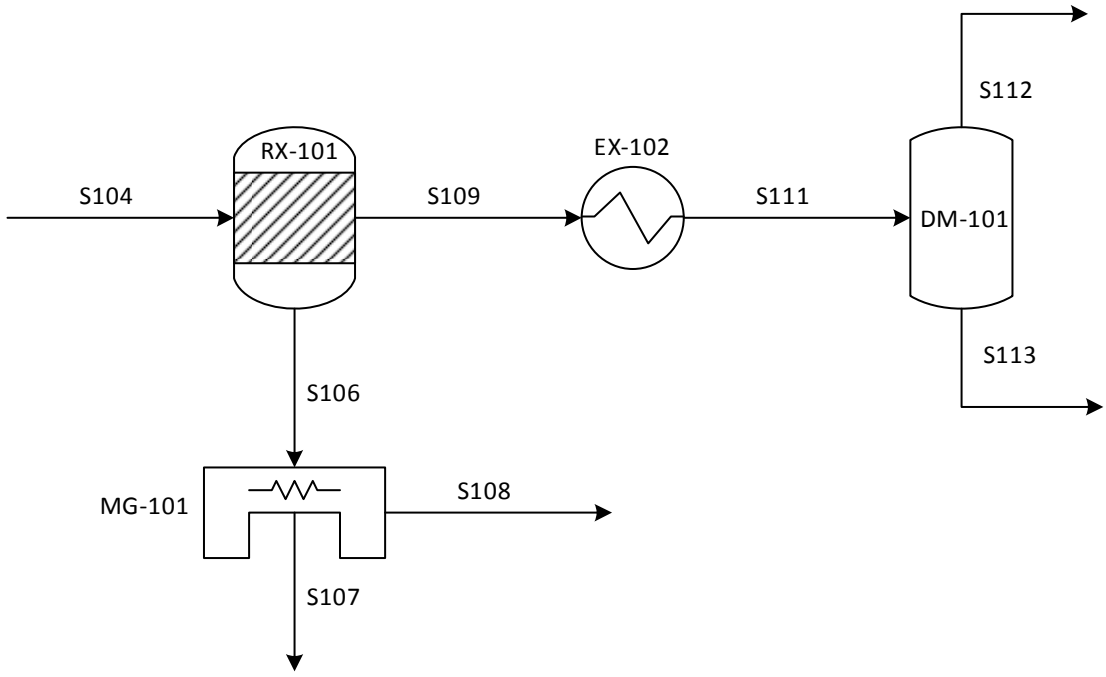

Figure 18: PFD of the pyrolysis system

4.4.1. Selection of reactor operating conditions

The reactor operating conditions in this study are adopted from the base-literature by Choi *et al.* (2014); these were chosen as a temperature of 500 °C and a pressure of 100 kPa (atmospheric pressure).

The intention of this study was to recover limonene, and as such, reactor temperatures that generally result in high limonene yields (on the basis of the tyre feed) had to be considered. In literature, various authors that have varied reactor temperature in their studies have observed maximum limonene yields at varying temperatures that were within the 400 °C - 500 °C range (Cunliffe and Williams, 1998a; Laresgoiti *et al*., 2004; Lopez *et al*., 2010; Choi *et al*., 2014). At even lower pyrolysis temperatures such as 300 °C, the yield of limonene (on the basis of tyre feed) is usually low due to low oil yields, as decomposition of the rubber material would most likely have just begun (Rodriguez *et al*., 2001).

The maximum limonene yields obtained within the 400 °C - 500 °C temperature range have indicated that most authors obtained their highest yields at the lowest temperature used in their studies, provided that it was higher than 400 °C. It is however also evident that some authors obtained maximum limonene yields that were higher than maximum yields obtained at temperatures lower than their corresponding "optimum" temperatures (Cunliffe and Williams, 1998a; Li *et al*., 2004; Choi *et al*., 2014). This could be due to a combination of other variables that affect product distribution (besides temperature), tyre formulation etc., as pointed out by Danon *et al*. (2015).

The study by Choi *et al.* (2014) reported a maximum limonene yield at 500 °C (the lowest in their temperature range), which is higher than maximum yields obtained at temperatures lower than 500 °C in other studies such as those by Laresgoiti *et al*. (2004), Li *et al*. (2004) etc. Based on what is currently available in literature, the temperature of 500 °C was chosen as the reactor temperature for use in this study. Several TGA studies have also indicated that tyre samples with a combination of different rubber types show final weight loss at temperatures of 450 °C - 500 °C, which has necessitated the opinion that pyrolysis should be complete at 500 °C (Leung and Wang, 1998; Senneca *et al*., 1999; Choi *et al*., 2014). It also on the back of this information that 500 °C was selected.

The pressure of 100 kPa was chosen to remain consistent with the pressure at which the experimental results were obtained by Choi *et al.* (2014). A pyrolysis pressure of 100 kPa has also been the preferred operating pressure for several studies in literature (Cunliffe and Williams, 1998a; Rodriguez *et al*., 2001; Conesa *et al*., 2004; Frigo *et al*., 2014).

4.4.2. Reactor product distribution

Reactor product distribution was determined by calculating the yields of all compounds regarded as reactor output in section 4.2. The yields of compounds considered as reactor output were based on the yields of the main pyrolysis product fractions reported by Choi *et al.* (2014), shown in Table 18.

The experimental study conducted by Choi *et al.* (2014) also reports on characterisation of the oil fraction and the composition of the different compounds identified in the oil. The compositions of some of the compounds in the oil and the yield of oil (at 500 °C) were used to calculate the mass yields of the particular compounds (from tyre) for the base case temperature of 500 °C. The yield of oil was calculated using correlation equations that are explained in section 4.4.2.1. The yield of n-eicosane (distillation reside) was used as reported in Table 18 at 500 °C. The yield of char was also calculated from correlation equations that are described in section 4.4.2.1. The normalised gas composition adapted from the study by Rodriguez *et al.* (2001) and the yield of gas from Table 18 were used to calculate the mass yields of gas compounds (except hydrogen sulphide) from tyre at 500 °C.

The yields of benzothiazole and hydrogen sulphide were calculated by performing elemental mass balances for nitrogen and sulphur respectively. Benzothiazole and hydrogen sulphide had the highest mass fractions of nitrogen and sulphur respectively, amongst all nitrogen and sulphur compounds identified. Manipulating the respective yields of benzothiazole and hydrogen sulphide for elemental mass balance calculations would result in minimal deviation from their respective experimentally determined yields. The yield of phenanthrene was specified as 0.0097 (wt/wt) which was the total PAH concentration at 500 °C from the study conducted by Cunliffe and Williams (1998a). The yield of benzene was calculated by closing the overall mass balance within the reactor. The equations used for calculation of the reactor product distribution are shown in appendix B.1.

Table 18: Yields of pyrolysis products with temperature (Choi *et al.*, 2014)

Reaction temperature (°C)	Yields (wt.%)			
	Char	Oil	Gas	Distillation residue
500	36.7	38.3	22.6	2.42
600	36.6	30.9	28.7	3.79
700	37.1	30.5	29.5	3.00
800	36.9	29.8	30.1	3.29

4.4.2.1. Correlation equations for yield prediction

Similarly to the studies of Yan and Zhang (1999) and Abdelouahed *et al.* (2012), correlation equations were developed to express the yields of certain compounds in this study. Both Yan and Zhang (1999) and Abdelouahed *et al.* (2012) developed correlation equations to describe the yields of certain chosen compounds from the pyrolysis reactor as functions of the reactor temperature. The experimental data which was used as input for the models of Yan and Zhang (1999) and Abdelouahed *et al.* (2012) was used to generate the correlation equations. In this study, the reported composition in product fraction and the yields of product fractions from the study by Choi *et al.* (2014) (shown in Table 18) were used to generate correlation equations.

Detailed information of how the correlation equations were developed and the compounds for which the equations were developed is provided in appendix B.2. Yields predicted by correlation equations were compared with literature reported yields for the different compounds, the comparison was used for model validation as is explained in section 4.4.3.

4.4.3. Model validation

Due to the complexity of pyrolysis oil(s) and wide variation in the yields of the pyrolysis products, development of a generic model that can be used to predict the production distribution of a waste tyre pyrolysis reactor is often difficult. The reactor model in this study is thus validated by the accuracy of the correlation equations in predicting the yields of the particular compounds for which correlation equations were developed, within the temperature range of 500 – 800 °C. The product yields calculated from the correlation equations are accepted to within ±10% accuracy of the literature yields of the respective compounds for validation in this study. The product yields predicted by the correlation equations are compared with experimental yields from the study by Choi *et al.* (2014). Results of validation of the model are shown in Figure 19 to Figure 23, and Table 19.

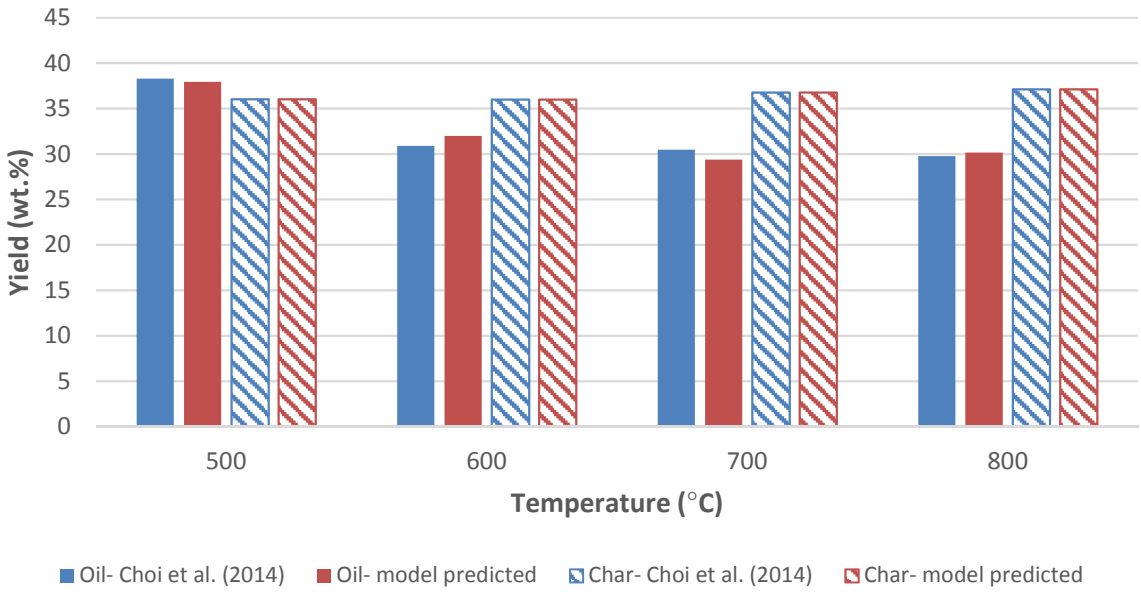

Figure 19: Choi et al. (2014) and model predicted yields of oil and char at various temperatures

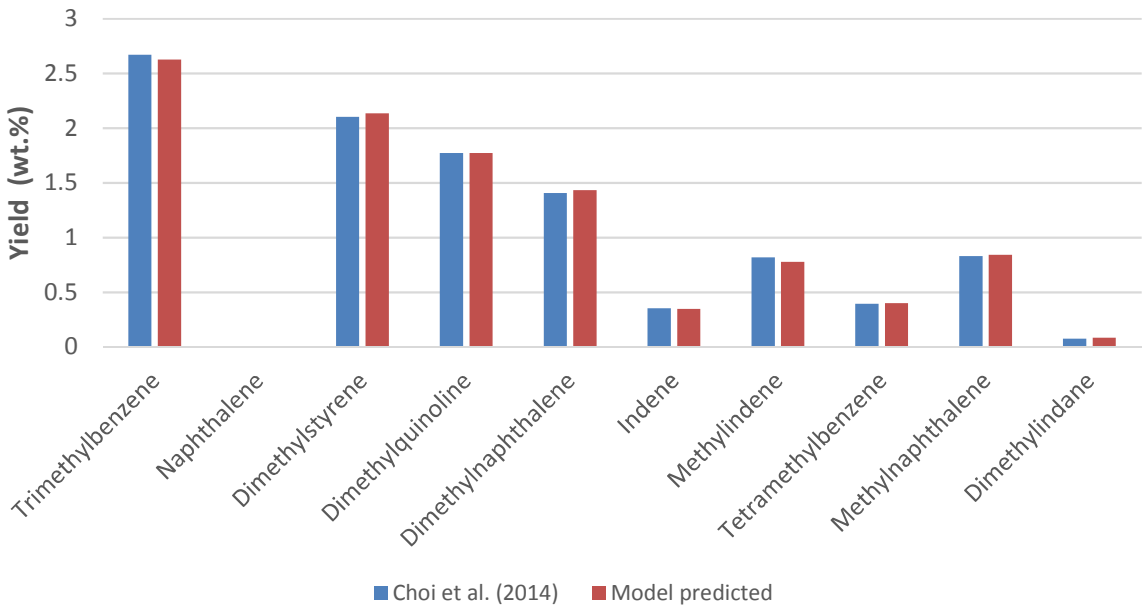

Figure 20: Choi et al. (2014) and model predicted yields of several individual compounds at 500 °C

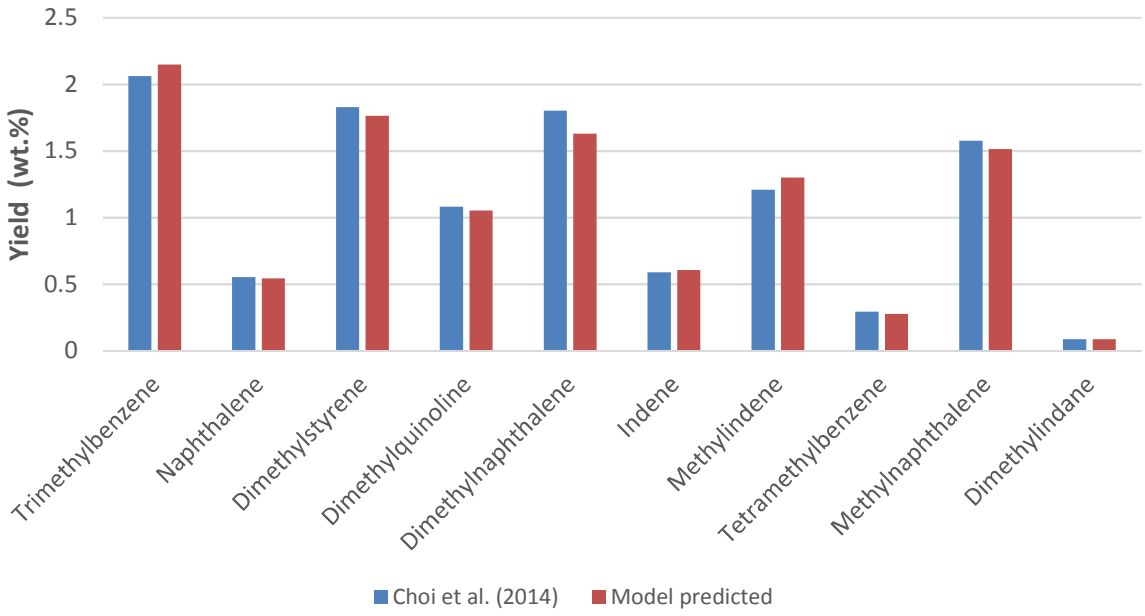

Figure 21: Choi et al. (2014) and model predicted yields of several individual compounds at 600 °C

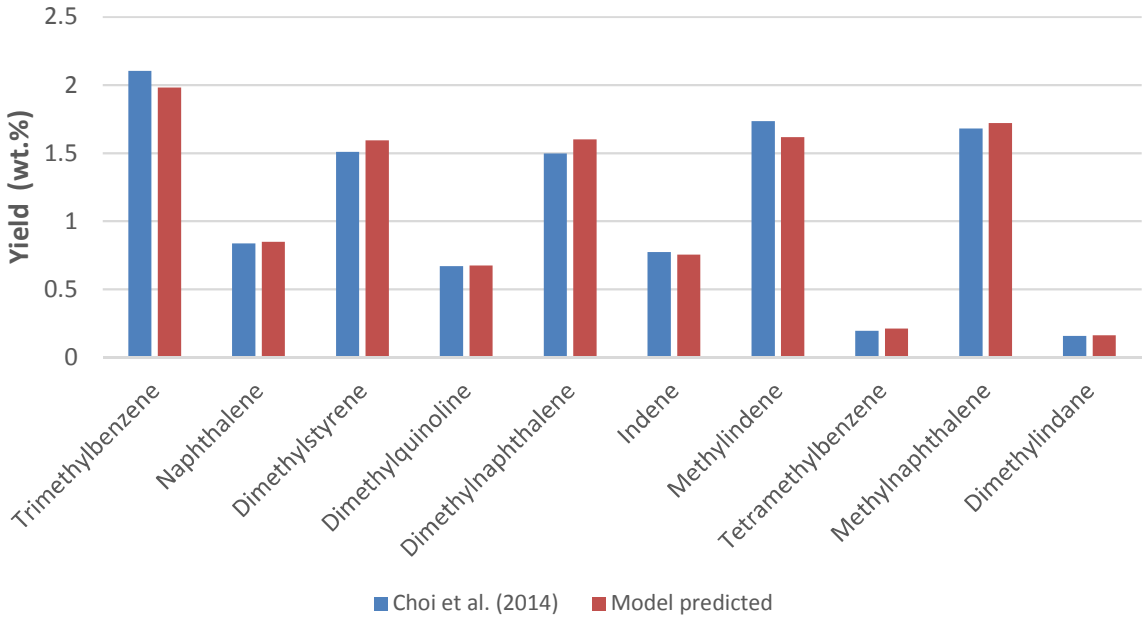

Figure 22: Choi et al. (2014) and model predicted yields of several individual compounds at 700 °C

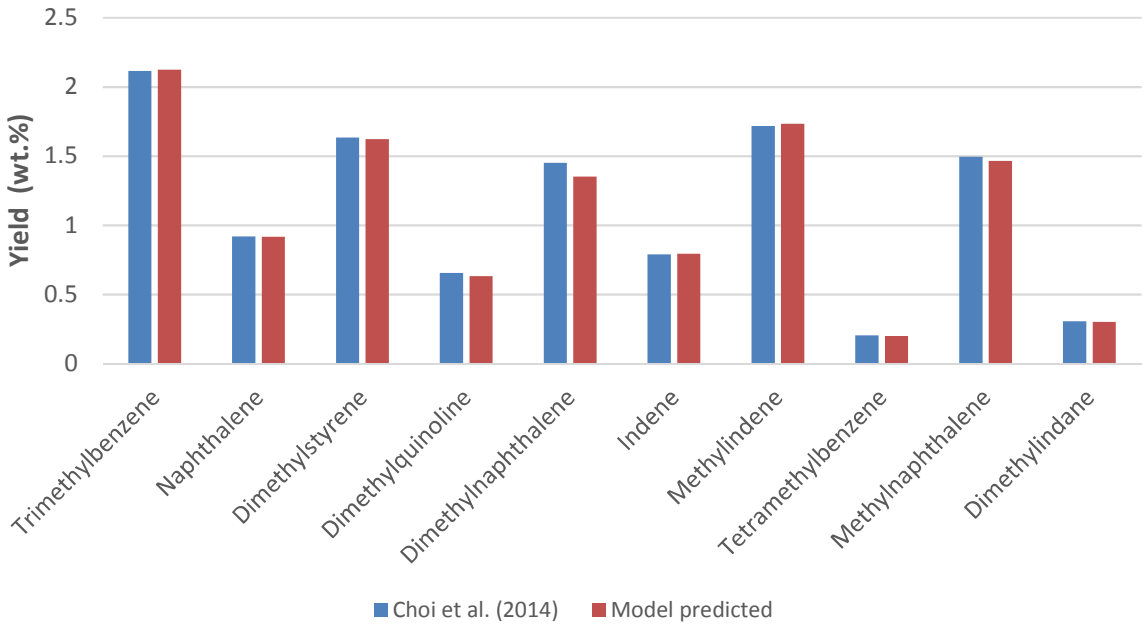

Figure 23: Choi et al. (2014) and model predicted yields of several individual compounds at 800 °C

Table 19: Deviation of model-predicted yields from yields obtained by Choi et al. (2014)

Compound	**Yield prediction error (%)**			
	500 °C	**600 °C**	**700 °C**	**800 °C**
Oil	-0.95	3.51	-3.60	1.23
Char	-1.77	-1.56	-0.76	0.76
Trimethylbenzene	-1.64	4.25	-5.81	0.45
Naphthalene		-1.99	1.33	-0.39
Dimethylstyrene	1.49	-3.56	5.62	-0.70
Dimethylquinoline	0.01	-2.60	0.83	-3.37
Dimethylnaphthalene	1.98	-9.62	6.94	-6.84
Indene	-1.61	2.95	-2.26	0.75
Methylindene	-5.02	7.52	-6.76	0.88
Tetramethylbenzene	1.48	-5.91	8.99	-2.78
Methylnaphthalene	1.29	-3.97	2.46	-1.99
Dimethylindane	8.20	-0.42	2.33	-1.64

From Figure 19, it can be seen that the results of model prediction fit closely with the experimental data for all temperatures considered. It can be inferred from Figure 19 that the model can accurately predict almost all of the product distribution of the main product fractions, as the yield of gas can then

just be calculated by difference (yield of distillate residue is small relative to yield of oil, char and gas). Comparison of literature and model-predicted yields for all other (individual) compounds for which correlation equations were developed is shown in Figure 20 to Figure 23 for various temperatures. It can also be seen from Figure 20 to Figure 23 that the model gives good prediction of the yields of those individual compounds at all temperatures considered.

From Table 19, it can be seen that the differences between all model-predicted yields and experimental yields are within ±10% of the experimental yields, which further proves the accuracy of model prediction. The error in Table 19 was calculated according to Equation 1.

$$\text{Error} = \left(\frac{x_i, \text{model} - x_i, \text{exp}}{x_i, \text{exp}}\right) * 100$$

Equation 1

x_i, model is the model-predicted yield of compound *i,* and x_i, exp is the yield of compound *i* from the literature by Choi *et al.* (2014), both in (wt.%).

4.4.4. Aspen Plus® simulation of the pyrolysis system

For development of the simulation flowsheet of the pyrolysis system, it was assumed that the system is at steady-state. The steady-state assumption is applied for development of simulation flowsheets of all other sections in this study unless otherwise specified.

4.4.4.1. Selection and validation of thermodynamic model

Before a flowsheet can be developed in Aspen Plus®, a thermodynamic model has to be selected. The Peng-Robinson with Boston-Mathias alpha function (PR-BM) thermodynamic model was chosen for calculation of physical properties for all conventional components for the pyrolysis section. The HCOALGEN and DCOALIGT property models were used to calculate the enthalpy and density of the non-conventional components (tyre and char) respectively (based on the proximate and ultimate analyses provided by Choi *et al.*, 2014). The property models used for the pyrolysis section are also used for all other section in this study unless otherwise specified. Detailed description of the procedure followed for selection of the thermodynamic model(s) used in this study is provided in Appendix B.3.

Validation of thermodynamic model

Enthalpy is an important thermodynamic property for calculation of energy balances, with heat capacity data central to calculation of enthalpies of any given system. Cubic equations of state (EOS) like the PR-BM model calculate fluid properties as if the fluid were composed of one (imaginary)

component. For mixtures, properties of the imaginary component are calculated using data of the pure components of which the mixture is composed (Aspen Technology, 2009).

In this study, the PR-BM thermodynamic model is validated by comparing literature and model-predicted pure component heat capacities of limonene, benzene and n-pentane. Limonene is chosen as it is the compound of interest, and benzene and n-pentane are chosen as they represent some of the highest individual product yields from the reactor. The Redlich-Kwong-Soave with Boston-Mathias alpha function (RKS-BM) thermodynamic model (another Aspen Plus® recommended model for pyrolysis systems) is also included for comparison with the PR-BM model. Comparison of the model-predicted and literature (experimental) data is shown in Figure 24 to Figure 26.

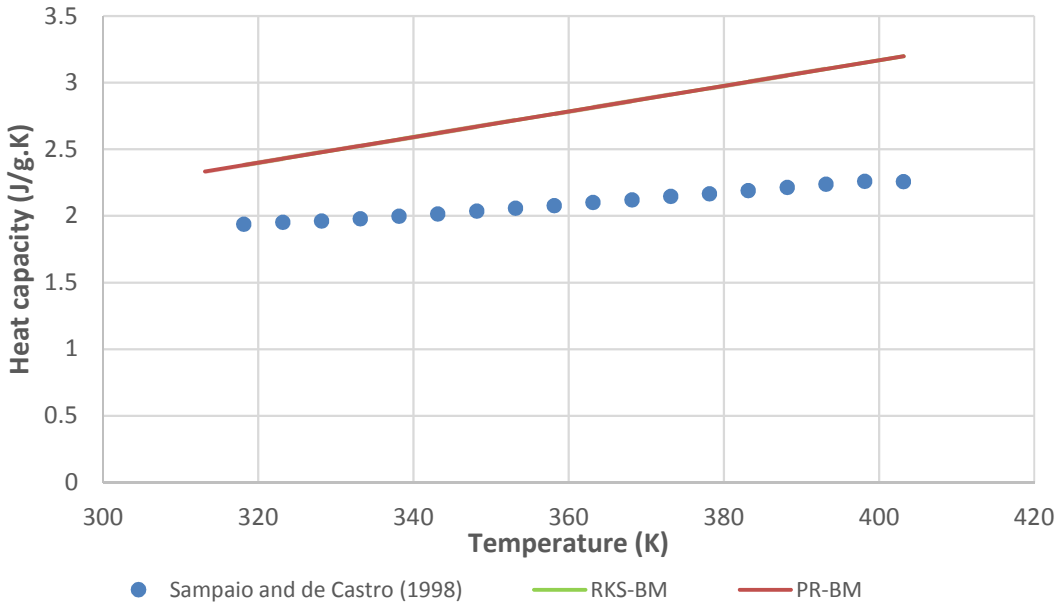

Figure 24: Literature and model-predicted constant pressure heat capacity of limonene

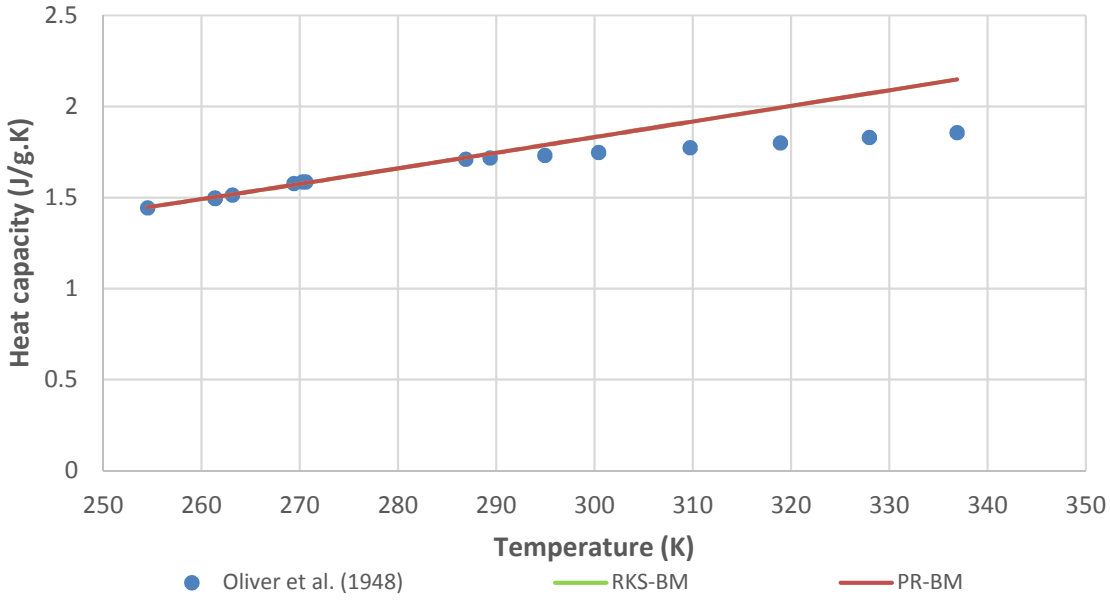

Figure 25: Literature and model-predicted constant pressure heat capacity of benzene

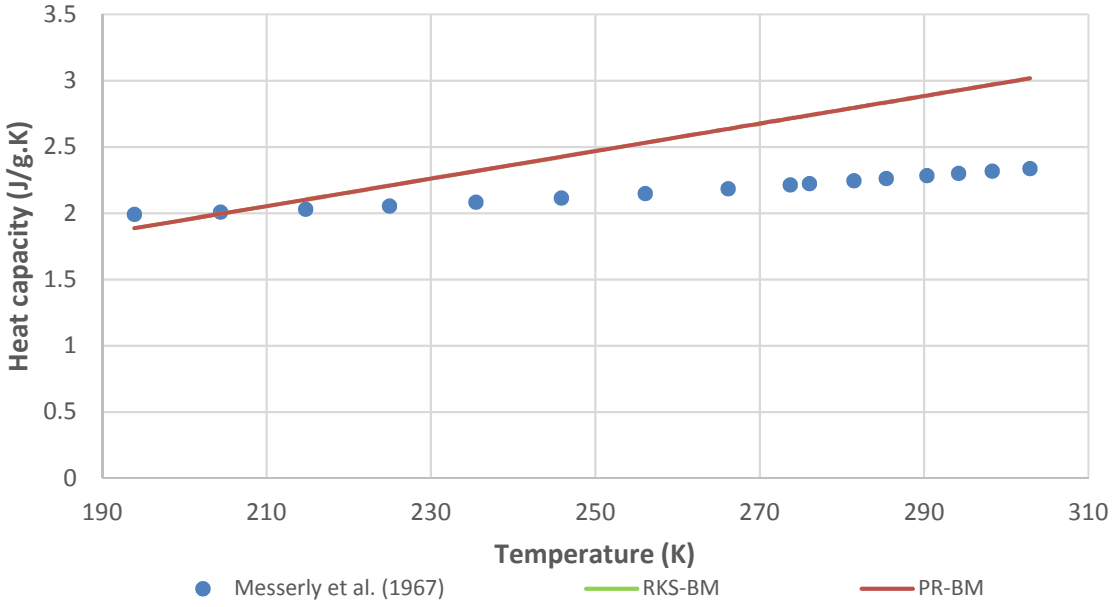

Figure 26: Literature and model-predicted constant pressure heat capacity of n-pentane

Figure 24 to Figure 26 show that there is overestimation of heat capacities of the selected compounds using the PR-BM thermodynamic model; errors in estimation of the pure component heat capacities could result in inaccurate energy balance calculations. As such, the overall energy balance results from the simulation should be used with caution. However, despite the errors in estimating the heat capacities of the selected components, it can be seen that the PR-BM model still does give reasonable estimation for purposes of preliminary feasibility studies such as the current study. Figure 24 to Figure

26 also show that the RKS-BM thermodynamic model gives similar results to those obtained using the PR-BM model (RKS-BM graph subjacent that of PR-BM), which is in agreement with literature (that the PR-BM and RKS-BM methods are comparable) (Aspen Technology, 2009; Ashour *et al.*, 2011).

4.4.4.2. Description of the pyrolysis system flowsheet

The flowsheet and the stream table for the pyrolysis system are shown in Figure 27 and Table 20 respectively. The streams names in Figure 27 correspond to the final PFD of the process in this study, which is provided in section 4.7.

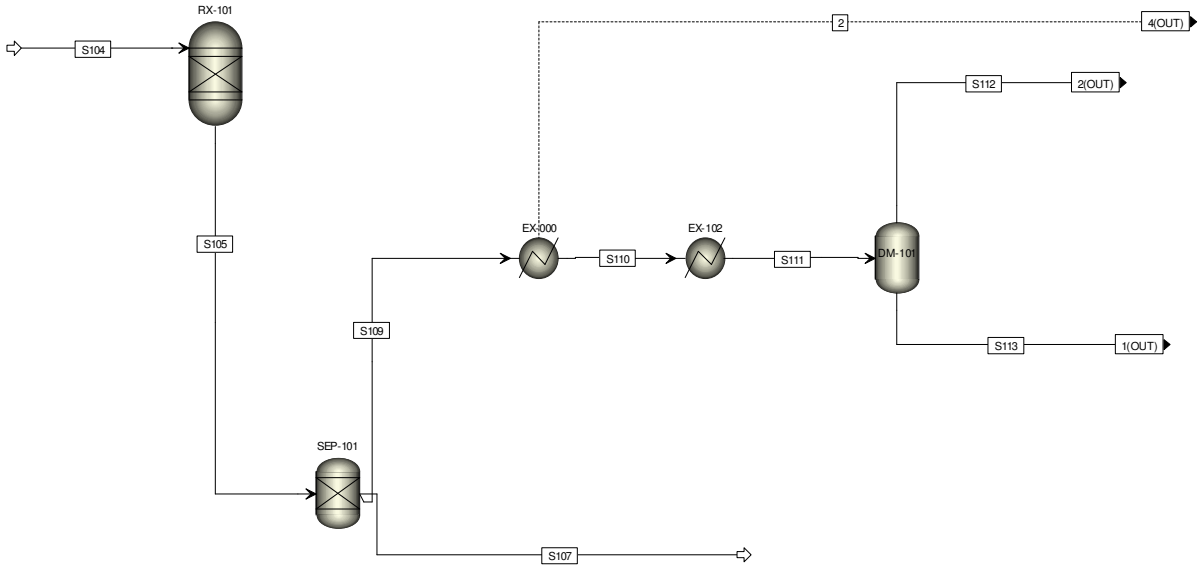

Figure 27: Aspen Plus® flowsheet of the pyrolysis system

Table 20: Stream table for the pyrolysis system

Stream number	S104	S105	S107	S109	S110	S111	S112	S113
Mass flow (kg/hr)	1125.0	1125.0	405.6	719.4	719.4	719.4	231.3	488.1
Mole flow (kmol/hr)		10.0		10.0	10.0	10.0	5.7	4.3
Temperature (°C)	25.0	500.0	500.0	500.0	465.9	35.0	35.0	35.0
Pressure (kPa)	100.0	100.0	100.0	100.0	100.0	100.0	100.0	100.0
Vapour fraction	0.0	0.0	0.0	1.0	1.0	0.6	1.0	0.0
Limonene purity (wt.%)	0.0	2.5	0.0	3.9	3.9	3.9	0.1	5.8

The tyre chips stream (S104) is sent to the reactor at 25 °C and 100 kPa, and a rate of 1125 kg/hr; it is defined by specifying the ultimate and proximate analyses provided in Table 16. The flow rate of

stream S104 has been adjusted to represent 90% of the total tyre feed rate as steel has not been considered for simulation purposes in this study. A very small flow rate of char was also specified in the input sheet of stream S104 to allow activation of the component attribute tab for specification of the proximate and ultimate analysis of char.

The tyre feed is pyrolysed in the reactor (RX-101) which operates at a temperature of 500 °C and a pressure of 100 kPa. A total energy input of 544 kW is required in RX-101 for pyrolysis of the tyre chips at the specified operating conditions. The heating requirements of RX-101 represents all of the heat energy required in the pyrolysis section, and 73% of the final heat energy required by the whole process in this study. The contribution of the pyrolysis reactor to the overall process heat energy requirements in this study is similar to that of Pilusa *et al.*, 2014, who mentioned that the pyrolysis reactor (heat duty of 468 kW) accounted for 70% of the overall heating energy requirements of their waste tyre pyrolysis process. It therefore implies that any feasible opportunity that could minimise utility usage in RX-101 has to be taken into account in order to reduce utility costs for the process in this study.

RX-101 has been modelled as a yield reactor block (RYIELD), which uses specified yields to determine the product distribution. The reactor product distribution was calculated using a calculator block (YIELDS) based on mass balance equations described in section 4.4.2. The RYIELD reactor model was preferred for this study as it is useful when reaction stoichiometry and kinetics are unknown, and yield distribution data or correlations are available (Aspen Technology, 2009). The following assumptions were made for the reactor model:

- Effects of particle size are negligible (feed is of uniform size)
- Reactor is uniformly heated and feed is uniformly distributed in the reactor
- Heat and mass transfer limitations are negligible
- Reaction kinetics are not considered (pyrolysis involves complex reactions, yields are used)
- Gas products are uniformly distributed within the reactor
- No oxygenated compounds are formed (Choi *et al.*, 2014 ultimate analysis does not report oxygen)
- Unknown fraction of oil can be represented by benzene and phenanthrene (major oil fraction is aromatic for temperatures reported by Choi *et al.*, 2014. Unknown fraction only ±25%)

The RYIELD reactor model requires that the sum of all specified yields add up to 1, it is for this reason that the yield of benzene was calculated as the remaining fraction required to add up to 1. The RYIELD reactor model performs an atom balance of all elements specified in the ultimate analysis, elemental

mass balances were performed for sulphur and nitrogen by the calculator block. An allowance of ±5% was given for the elemental mass balances of carbon and hydrogen to allow the overall reactor mass balance to close in order to avoid normalisation of the product yields. As a result of the ±5% allowance, a tolerance of 6% was specified for the reactor mass balance in Aspen Plus®.

The reactor product stream (S105) (char and volatiles) is sent for separation in SEP-101, which has been modelled as a (SEP) separation block. The SEP block separates the feed components based on user-specified split fractions. The non-conventional components (char) report to the char product stream (S107) and all the conventional components report to the volatiles stream (S109). In reality, SEP-101 is not an actual equipment but only represents exit of the volatiles and the char from the reactor via their respective exit channels.

The volatiles stream is then slightly cooled down from 500 °C to 466 °C in EX-000 by exchanging heat with the oil feed to T-101 (S114 in the separation section). EX-000 is in reality not a real heat exchanger, but represents the tube side of EX-101 (shown in the separation flowsheet). The exchange of heat between the volatiles and S114 is represented by heat stream 2, which is sent to the separation section as stream 4(OUT). EX-000 has a heat duty of 19 kW, which means that cooling S109 by heat exchange with S114 saves 19 kW of both cooling and heating utilities that would have additionally been required to cool S109 and heat up S114 respectively.

The volatiles stream exiting EX-000 (S110) is then cooled down to 35 °C in EX-102, and some of the components condense out to give the oil fraction, while the non-condensables remain in the gas phase. Determination of the temperature at which EX-102 should operate is detailed in section 4.5.1 as EX-102 outlet temperature is influenced by the overall recovery of limonene (from the reactor) in the limonene-rich stream in this study. EX-102 has a heat duty of -235 kW, and accounts for all cooling requirements in the pyrolysis section whereas it accounts for 52% of the cooling requirements of the whole process.

The oil-gas mixture stream from EX-102 (S111) is then separated out in a knockout drum (DM-101), which has been modelled using a FLASH 2 separator block, with a specified pressure of 100 kPa and a heat duty of 0 kW. The non-condensables stream (S112) is sent to the heat recovery section as stream 2(OUT) and the condensed oil stream (S113) is sent to the separation section as stream 1(OUT).

4.5. Design of separation system

The purpose of the separation system in this study is to upgrade the raw pyrolysis oil/TDO stream (S113) coming from the pyrolysis section into (the high value) limonene, through various distillation

techniques. The separation system in this study would typically not be found in conventional waste tyre pyrolysis plants that generally only focus on production of primary products. The limonene stream produced in this study is desired to be of at least 95 wt.% purity in order to meet market standards. Any residual liquid streams from the separation system are recombined and sold as TDO product. The PFD and stream names of the separation system are shown in Figure 28 and Table 21 respectively. All equipment names and stream names correspond to the final PFD, equipment list and stream names in section 4.7.

Brief description of the separation system

The separation system is briefly described here; detailed description is presented in section 4.5.2.2, where the Aspen Plus® model of the separation system is discussed. The separation system in this study consists of 4 distillation columns (main unit operations), with accessory (minor) units such as pumps and heat exchangers, in between the columns, depending on process requirements.

The temperature of the feed stream to the separation system (S113) has to be carefully selected as it determines the amount of limonene from the reactor volatiles that gets sent to the separation system, and also has a huge influence on operation of the first fractionation columns (T-101 and T-102). The temperature of stream S113 was determined by a sensitivity analysis of the operating temperature of the reactor volatiles condenser (EX-102 in Figure 27). The procedure for EX-102 sensitivity analysis is explained in section 4.5.1.

Due to the presence of close boiling compounds to limonene in the raw TDO from the pyrolysis reactor, a limonene-rich stream/cut is first produced using fractional distillation. The limonene-rich cut in this study was based on the experimental work of Pakdel *et al.* (2001), which included compounds within around ±8 °C of the boiling point of limonene. Production of the limonene-rich cut is achieved using T-101 and T-102 in the process shown in Figure 28.

The raw TDO from the pyrolysis section is pumped (by PC-101), pre-heated (in EX-101), and is then fed to T-101, where the components lighter than the limonene cut are removed as vapour and liquid distillate streams. The bottoms stream from T-101 is then fed to T-102, where the components heavier than the limonene cut are removed as bottoms products, and the limonene-rich cut is obtained as the distillate product. The liquid distillate from T-101 and the bottoms from T-102 are recombined to form part of the TDO product, which is sold to the market.

The limonene-rich stream is then pumped (by PC-102) and it is fed to an extractive distillation column (T-103), where diethylene glycol (DEG) is introduced to remove most of the impurities, thereby

obtaining a limonene stream of (minimum) 95 wt.% limonene purity as distillate. The solvent (with the entrained impurities) is sent to a distillation column (T-104), where it is regenerated by stripping off the impurities entrained from T-103; the solvent is recovered as bottoms product. A fraction of the regenerated solvent is then purged off to minimise build-up of the remaining impurities in the system. The remaining fraction of the solvent (after purging) is combined with a (fresh) solvent make-up stream, cooled down (in EX-103), and then recycled back for use in T-103. The distillate product from T-104 goes to form the remaining part of the TDO product, which is cooled down in EX-104 before storage.

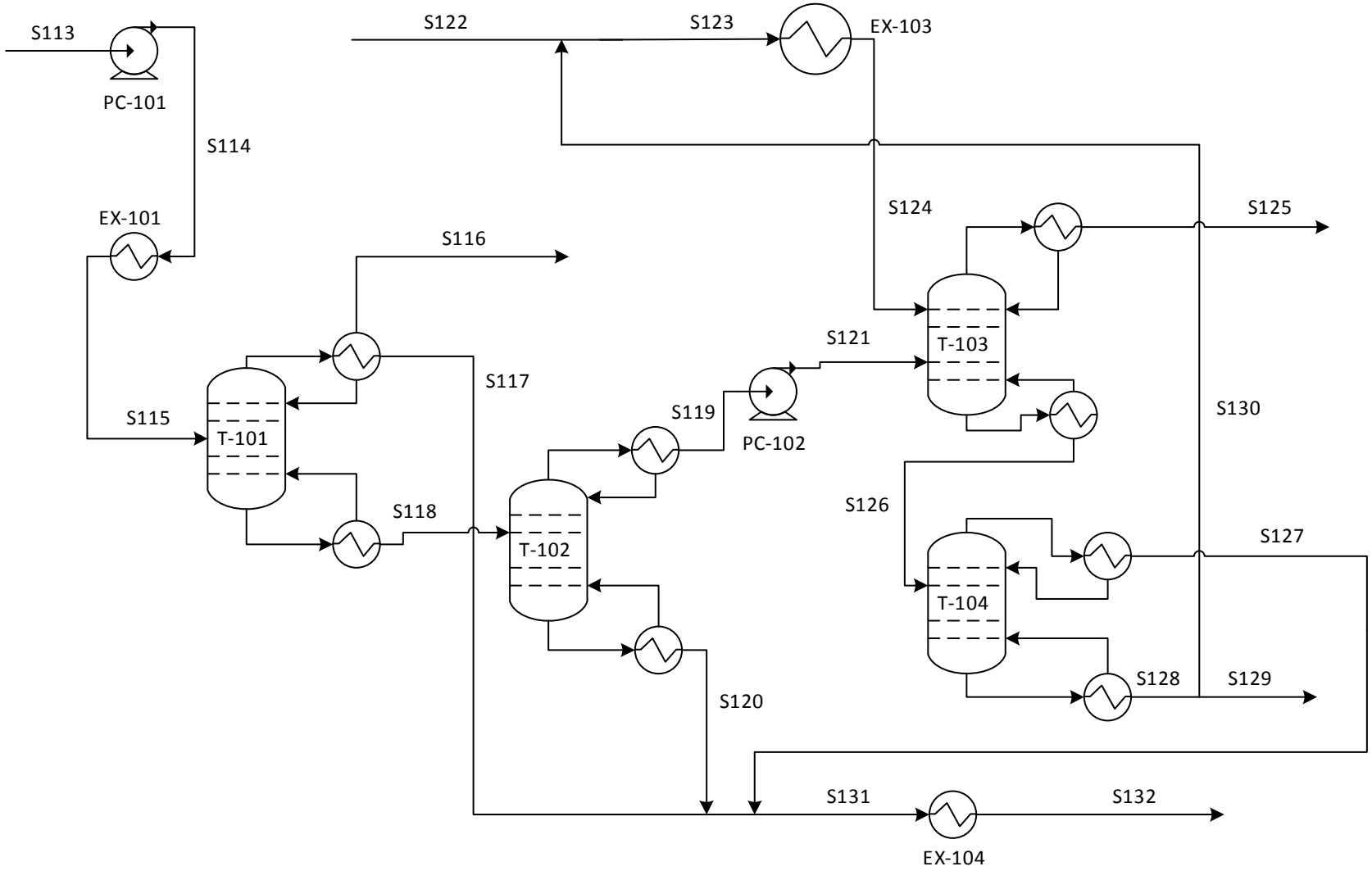

Figure 28: PFD of the separation system

Table 21: Stream names for the separation system

Stream name	Description
S111	Condensed volatiles
S112	Pyrolysis gas
S113	Raw pyrolysis oil/TDO
S114	Pressurised pyrolysis oil
S115	Warm pyrolysis oil feed
S116	T-101 vapour distillate
S117	T-101 liquid distillate
S118	T-101 bottoms product
S119	Limonene-rich stream
S120	T-102 bottoms product
S121	Pressurised limonene-rich stream
S122	DEG make-up
S123	Hot DEG feed
S124	Cool DEG feed
S125	Limonene product
S126	DEG-rich stream
S127	Aromatics product
S128	DEG product
S129	DEG purge
S130	DEG recycle
S131	Hot TDO product
S132	Cool TDO product

4.5.1. Determination of EX-102 operating temperature

For operation of EX-102, two possible scenarios were considered with respect to condenser operation:

Scenario 1: Cooling the hot reactor vapours to a specific temperature in a single condenser to obtain pyrolysis oil, heating the oil up to a specific temperature, and then feeding the oil to the separation columns. The PFD of scenario 1 is shown in Figure 29. The stream names in Figure 29 correspond to those shown in Table 21.

In scenario 1, the hot pyrolysis reactor vapours are cooled down from 500 °C to a temperature range of 35 °C to 210 °C (at 210 °C and above, no oil is condensed) in EX-102, and then the condensed pyrolysis oil is separated from the non-condensable pyrolysis gas in DM-101. The temperature of 35 °C was chosen as the minimum achievable temperature with cooling water, assuming inlet and outlet temperatures of 25 °C and 40 °C respectively for the cooling water, with a 10 °C minimum temperature approach in the heat exchangers. The condensed oil is then sent for separation in T-101 and T-102 with the intention of producing a limonene-rich stream.

The cooling water inlet temperature of 25 °C was chosen as a conservative estimate for this study based on monthly average design wet bulb temperatures for the DF Malan and Cape Town international airport weather stations published by ASHRAE Inc (2005; 2013). According to these publications, the design wet bulb temperatures for the DF Malan and Cape Town international airport weather stations are around 20 °C - 22 °C for the hottest months. For design and sizing of cooling towers, the highest wet bulb temperatures experienced in a particular location would be used as design reference to ensure that the cooling tower can deliver the required cooling even in the hottest months. A cooling water inlet temperature of 25 °C has also been used in other process design studies in literature (Diederichs, 2015). A cooling water temperature increase of 15 °C was adopted from Seider *et al.* (2004).

Scenario 2: Feeding the hot reactor vapours to the separation columns without any cooling stage. Scenario 2 is shown in Figure 30. The stream names in Figure 30 also correspond to those shown in Table 21.

In scenario 2, the hot pyrolysis vapour are sent straight from the reactor (at the reactor temperature) for separation in T-101 and T-102 without any cooling (EX-102 is not required in this scenario).

In both scenario 1 and 2, T-101 is used to separate the components lighter than the limonene cut (taken as distillate) and T-102 is used to separate the components heavier than the limonene cut, with the limonene-rich stream taken as distillate. The choice of column sequencing was based on recommendations from Sinnott and Towler (2009) who recommend that lighter components (and non-condensables) should be separated first. Separating lighter components and non-condensables first avoids the use of refrigerants and high pressures in the whole separation process (Sinnott and Towler, 2009). It is also recommended that desired products be obtained as distillate, as it is easier to control the purity of the distillate stream (Sinnott and Towler, 2009).

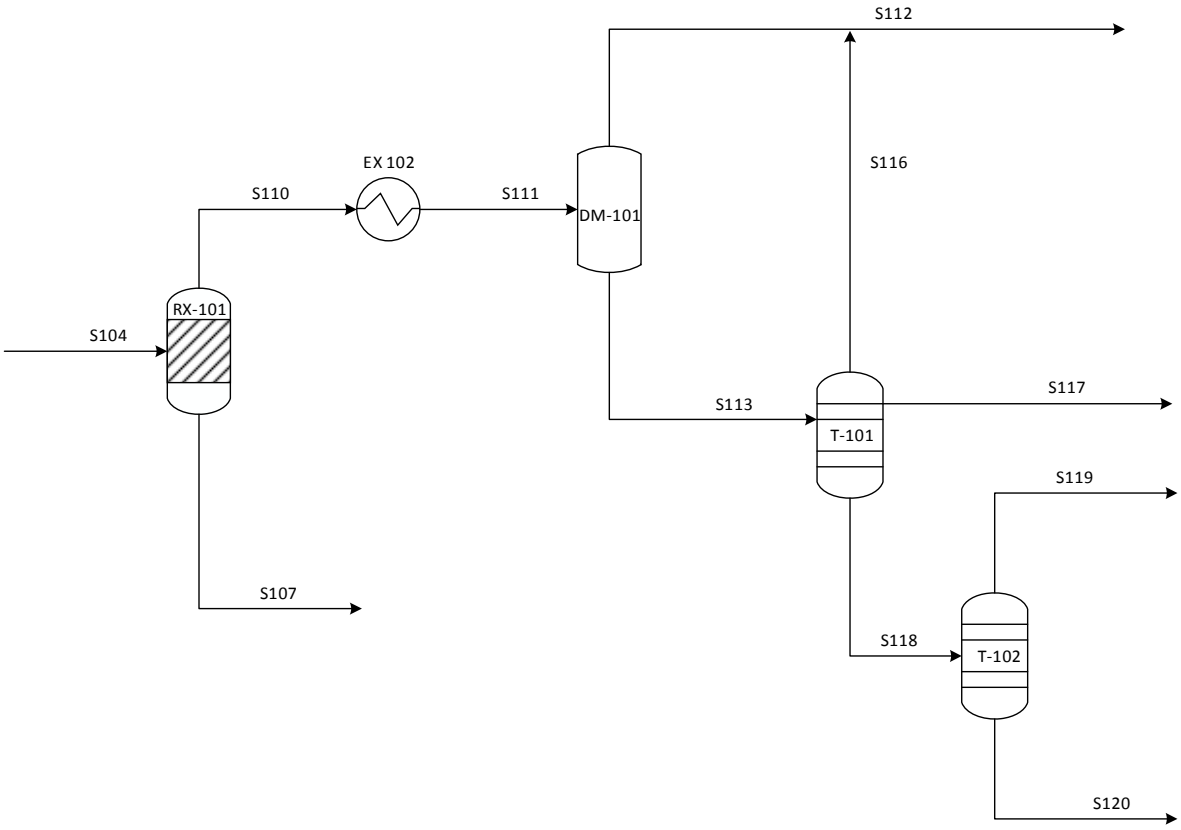

Figure 29: PFD of scenario 1

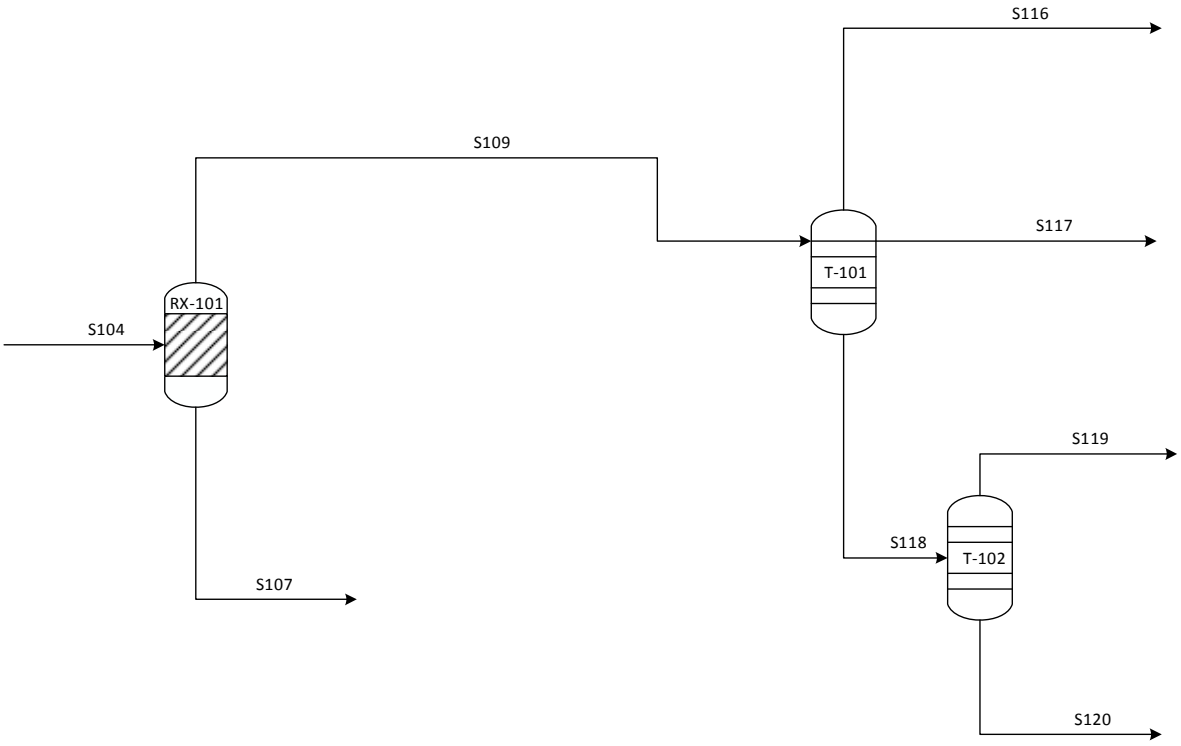

Figure 30: PFD of scenario 2

Scenario 1 and 2 were compared on the basis of limonene recovery (from reactor volatiles) fed to T-101 (S113 in Figure 29 and S109 in Figure 30 respectively), total energy usage, preliminary estimation of subsequent column diameters, and preliminary estimated capital and operating costs. In both scenarios, it is desired to have as much recovery of limonene in the respective feed streams to T-101 as possible (100% ideally). The limonene recovery targets of T-101 and T-102 were similar in both scenarios (99%), hence the recovery of limonene is considered at T-101 feed stream for comparison purposes. A targeted recovery of 99% (in T-101 and T-102) was chosen based on guidelines from Sinnott and Towler (2009) that recovery of key components is typically aimed at 99% for distillation column design purposes. Energy usage for each scenario was calculated using Aspen Plus®, preliminary column diameter sizes were calculated using column sizing guidelines from Sinnott and Towler (2009). Preliminary column costs were calculated using the bare module costing technique from Turton *et al.* (2009), and preliminary operating costs were manually calculated.

Comparison of scenario 1 and 2

The recovery of limonene in T-101 feed stream (S113 in Figure 29) with varying EX-102 temperature for scenario 1 is shown in Figure 31. It can be seen that 99.4% of the limonene from the reactor can be recovered in S113 at the minimum possible temperature of 35 °C, and the recovery decreases sharply with an increase in temperature. Based on Figure 31, it can be concluded that the minimum possible EX-102 temperature of 35 °C is thus desirable for scenario 1, as the limonene recovery is highest at this temperature (since the aim is to maximise limonene recovery).

For scenario 2, the recovery of limonene in T-101 feed stream (S109 in Figure 30) is 100% since the reactor volatiles are sent straight for separation as they come out of the reactor.

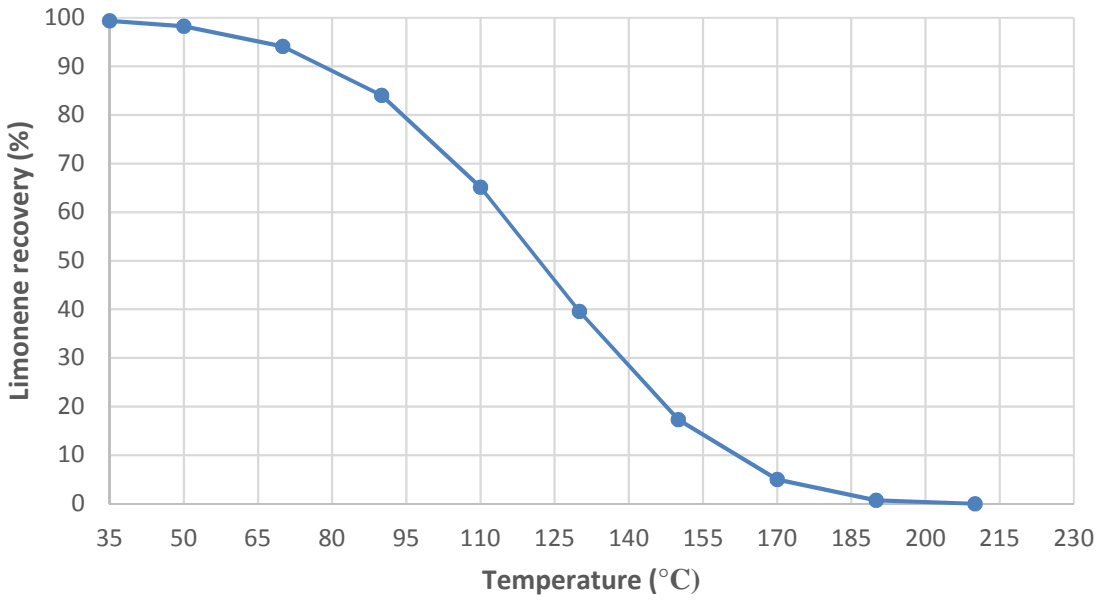

Figure 31: Recovery of limonene in oil stream with EX 102 temperature for scenario 1

Since all the reactor volatiles are sent to T-101 in scenario 2, one challenge becomes operation of the column condenser in such a way that no refrigerants are required to cool the column overhead stream, as the reactor volatiles contain non-condensable gases as well. As such, energy usage and preliminary cost evaluation for T-101 in scenario 2 were performed with a condenser vapour fraction of 0.95, which ensured that cooling in the condenser could be achieved with cooling water. The condenser vapour fraction of 0.95 was determined by a sensitivity analysis of condenser outlet temperature with varying vapour fraction using Aspen Plus®. It should also be taken into account that the high T-101 condenser vapour fraction of scenario 2 could also imply that some compounds that would normally have been in the liquid distillate stream would be lost to the vapour distillate stream. Loss of those compounds to the vapour distillate would mean reduced TDO product flow rate or the need for additional equipment to recover them as liquid product.

The results of comparison between scenario 1 and scenario 2 on an energy usage and cost evaluation basis are shown in Table 22. Similar S118 results are obtained for both scenarios, and as such, T-102 costing and energy usage is not included in Table 22. It can be observed that scenario 2 requires a larger column (T-101), and the total cooling and heating duties for scenario 2 are higher than for scenario 1. The larger column size for scenario 2 can be explained by the large volume of vapour sent to T-101 in that particular scenario as the column size is dependent on the vapour flow rate (Sinnott and Towler, 2009). Results of preliminary cost estimation show that scenario 2 requires higher capital and operating costs due to the larger diameter and higher energy usage as compared to scenario 1.

Table 22: Preliminary energy usage and cost evaluation for scenario 1 and 2

Parameter	Scenario 1	Scenario 2
Column diameter (m)	0.5	0.82
Theoretical number of stages	75	66
EX 102 duty (kW)	-235	0
Condenser duty (kW)	-95	-410
Reboiler duty (kW)	107	203
Estimated capital cost ($)	459 034	505 000
Estimated operating costs ($/year)	214 943	276 240

Based on the recovery of limonene shown in Figure 31, and the results from Table 22, scenario 1 was chosen as the preferred configuration in this study, and it was the configuration used for modelling in Aspen Plus®. Description of the Aspen Plus® flowsheet for the separation system is presented in section 4.5.2.

4.5.2. Aspen Plus® simulation of the separation system

4.5.2.1. Selection and validation of thermodynamic model

Simulation of the separation section in Aspen Plus® involved the use of two thermodynamic models. The PR-BM thermodynamic model was used for estimation of physical properties for unit operations involved in fractional distillation (T-101 and T-102). For the solvent recovery section (T-103 and T-104), the non-random two-liquid (NRTL) property model has been used for prediction of thermodynamic properties of components in this study. The universal function activity coefficient (UNIFAC) property model was used to estimate missing binary parameters for the NRTL property model in this study.

Validation of thermodynamic model

For separation in the TDO (multi-component) system, it would ideally be desirable to accurately account for the equilibrium phase behaviour of each component present in the TDO, and every possible interaction between the components of the TDO. For such, experimentally determined vapour-liquid equilibrium (VLE) and vapour-liquid-liquid equilibrium (VLLE) data would be required; however, such VLE and VLLE data (especially for systems involving limonene) is limited in the open literature.

In this study, the thermodynamic models chosen for the separation section are validated by comparing the model-predicted, and readily available experimental binary VLE data of a p-cymene + limonene

system (at 101 kPa) from the work of Tong *et al*. (2009) (as reported by Ngwetjana, 2017). The PR-BM and NRTL models are tested for validation, and additionally, the RKS-BM and UNIQUAC models are also shown for comparison. For the NRTL and UNIQUAC models, binary interaction parameter estimation is performed using the UNIFAC model. The results of VLE data comparison are shown in Figure 32.

Accurate pure component vapour pressure estimation is also essential in determining the distribution of various species between various phases in a given system, especially when using activity coefficient models (for calculation of activity coefficients using Raoult's law as a basis) (Aspen Technology, 2009). Calculations with Raoult's law will largely be influenced by species that have high concentrations within a particular liquid mixture. In this study, prediction of the pure component vapour pressures of limonene, p-cymene, and the solvent (diethylene glycol) using all the 4 models is performed and compared with experimental data as a further validation step. The results of pure component vapour pressure comparison are shown in Figure 33 to Figure 35.

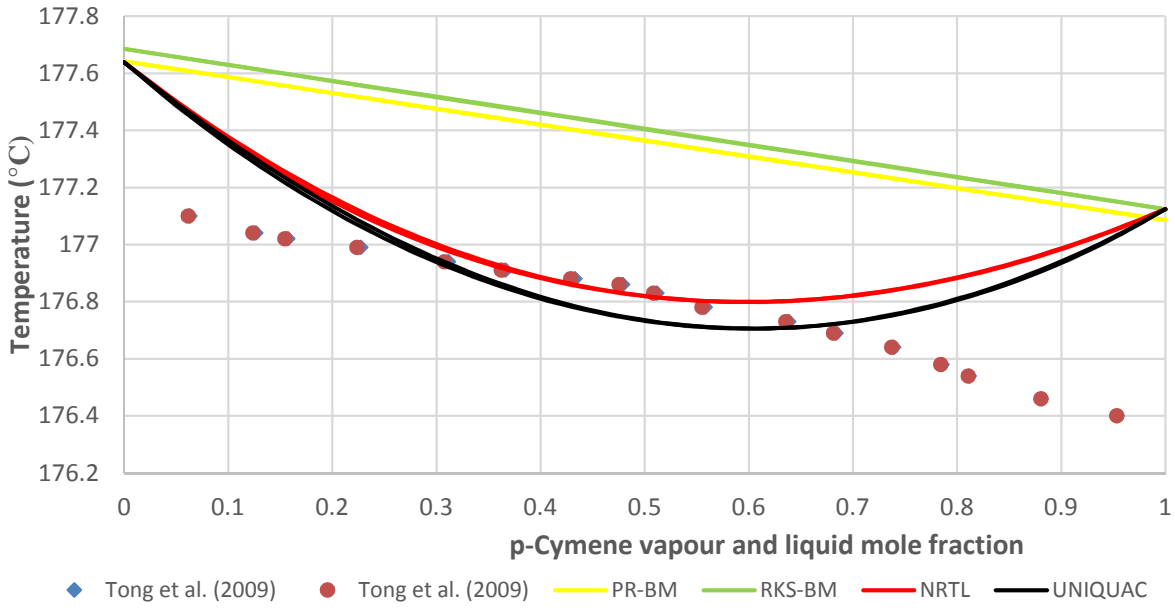

Figure 32: Diagram of binary VLE data of p-cymene + limonene at 101 kPa

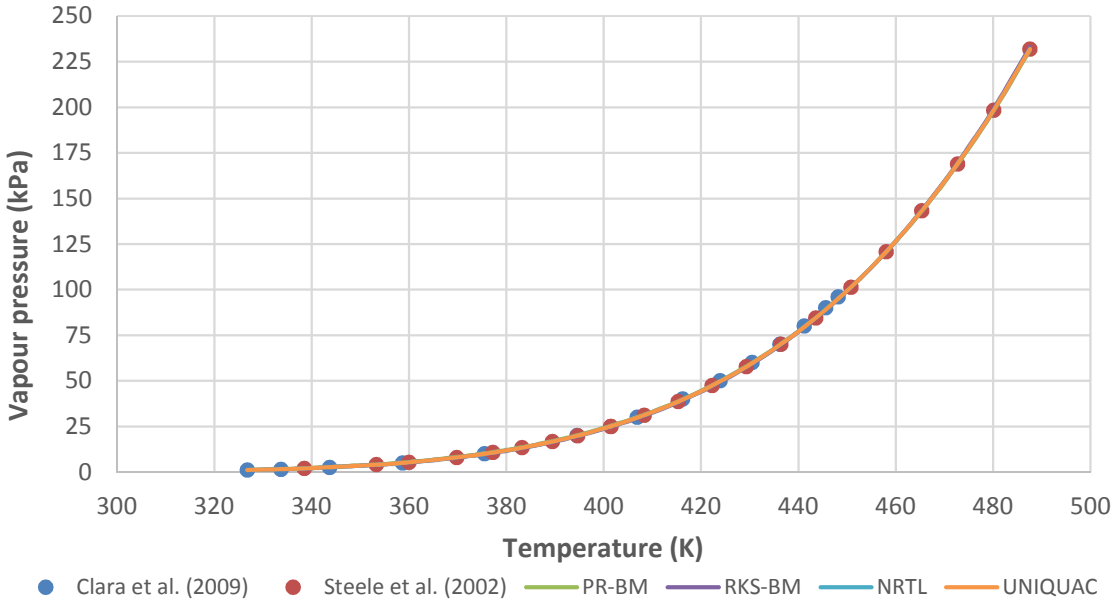

Figure 33: Literature and model-predicted pure component vapour pressure diagram for d-limonene

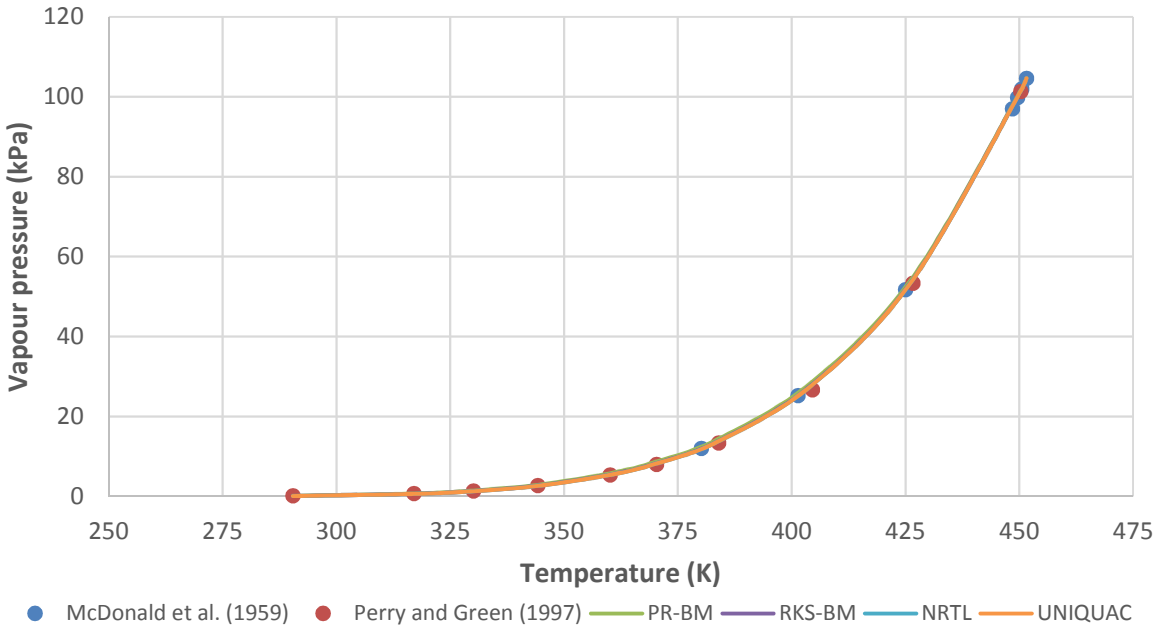

Figure 34: Literature and model-predicted pure component vapour pressure diagram for p-cymene

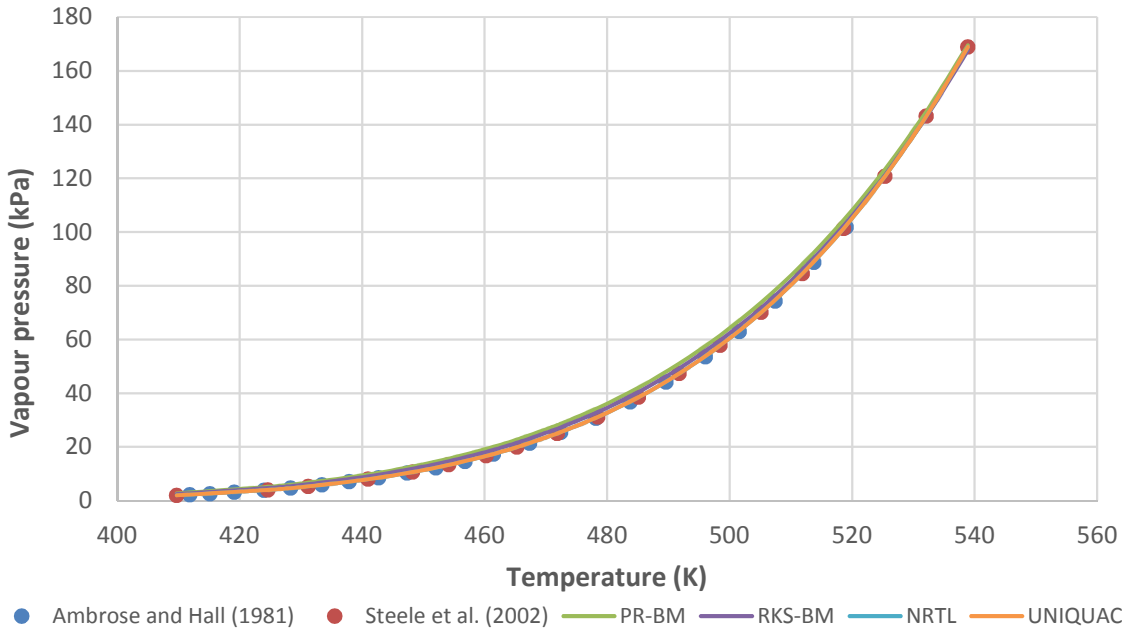

Figure 35: Literature and model-predicted pure component vapour pressure diagram for diethylene glycol

Figure 32 shows that there is a general over prediction of the mole fraction of p-cymene in either fraction when using all the thermodynamic models tested; this could be attributed to estimation of the binary interaction parameters using Aspen Plus®. It can also be seen that the error margin in prediction is lower with activity coefficient models as compared to EOS models, which could be due to that EOS models use less parameters to account for binary interactions (Aspen Technology, 2009). Experimentally determined VLE data of possible binary systems within TDO would then be required to generate accurate interaction parameters, which could be done using regression in Aspen Plus®. However, in the absence of literature binary interaction parameters for TDO components, estimation of binary parameters using Aspen Plus® is deemed acceptable for the purposes of this study.

From Figure 32, it can also be observed that at every temperature point, a constant equilibrium mole fraction of p-cymene (and subsequently of limonene) is obtained in each phase, which indicates difficulty in separating p-cymene and limonene through normal distillation. The difficulty of separating p-cymene and limonene using normal distillation has already been demonstrated in the experimental work of Pakdel *et al*. (2001). It therefore indicates that enhanced distillation techniques are required to separate these two components, hence the use of extractive distillation for limonene recovery from the limonene-rich stream in this study.

Figure 33 to Figure 35 show that all the thermodynamic models tested in this study give accurate pure component vapour pressure prediction for both limonene and p-cymene, and the solvent adopted for extractive distillation in this study. This implies that all the models tested would be able to accurately

predict the equilibrium phase distribution of each of those components in their respective individual pure component systems. Good prediction of their vapour pressures should imply that activity coefficients of a system consisting of these compounds should be well calculated. Experimental VLLE data would however be required to accurately predict the equilibrium phase behaviour of a limonene + p-cymene system when the solvent is introduced, as activity coefficient models are less accurate in predicting ternary systems (Smith *et al,* 2005).

4.5.2.2. Description of the separation system flowsheet

In this section, the separation system is discussed in detailed, with focus placed on detailing the operating conditions of each equipment, the rationale behind each unit model of the Aspen Plus® flowsheet, and the optimisation performed before specific equipment were chosen. This section expands on the brief description given in section 5.1. The Aspen Plus® flowsheet and stream table of the separation system are shown in Figure 36 and Table 23 respectively. The stream names in Figure 36 correspond to those given in Table 21 and the final stream names in section 4.7. Equipment names in Figure 36 correspond to the final equipment names in section 4.7.

In the process shown in Figure 36, the oil feed stream from the pyrolysis section (S113) is pumped to 200 kPa by PC-101 in preparation for the first stage of fractionation in T-101. The oil is pressurised before feeding to T-101 in order to aid with flashing of the light compounds in the oil as they enter a lower pressure zone in the column (Henley *et al.*, 2011).

The pressurised oil from PC-101 (S114) is sent to T-101 feed pre-heater (EX-101) where it is heated to just below its initial boiling point of 105 °C (where the vapour fraction is just above 0) also in preparation for the first stage fractionation in T-101. The oil temperature of 105 °C was determined by a sensitivity analysis of the resulting vapour fraction of EX-101 outlet stream (S115) with varying EX-101 operating temperature. The heat required for pre-heating the oil in EX-101 (19 kW) is provided by contact with the hot reactor volatiles (S109 in Figure 27) from the pyrolysis section; the heat provided by S109 is represented by heat stream 4. A design specification (EX101-T) controls the outlet temperature of EX-101 by varying the outlet temperature of EX-000 from Figure 27.

The pressurised and pre-heated oil stream (S115) is then sent to T-101 at 105 °C and 200 kPa, where the process of upgrading the oil to recover limonene begins. The objective and operation of each separation column will be explained in detail. In this study, the oil feed to the separation section (S113) is assumed to contain no solid material that could cause either plugging or fouling of the trays or packing material in the separation columns (no solids indicated in the oil by Choi *et al.*, 2014). In cases

where the TDO contains such solid material, a solids removal/trapping system such as a strainer or filtration could be required in the TDO feed line to the separation columns.

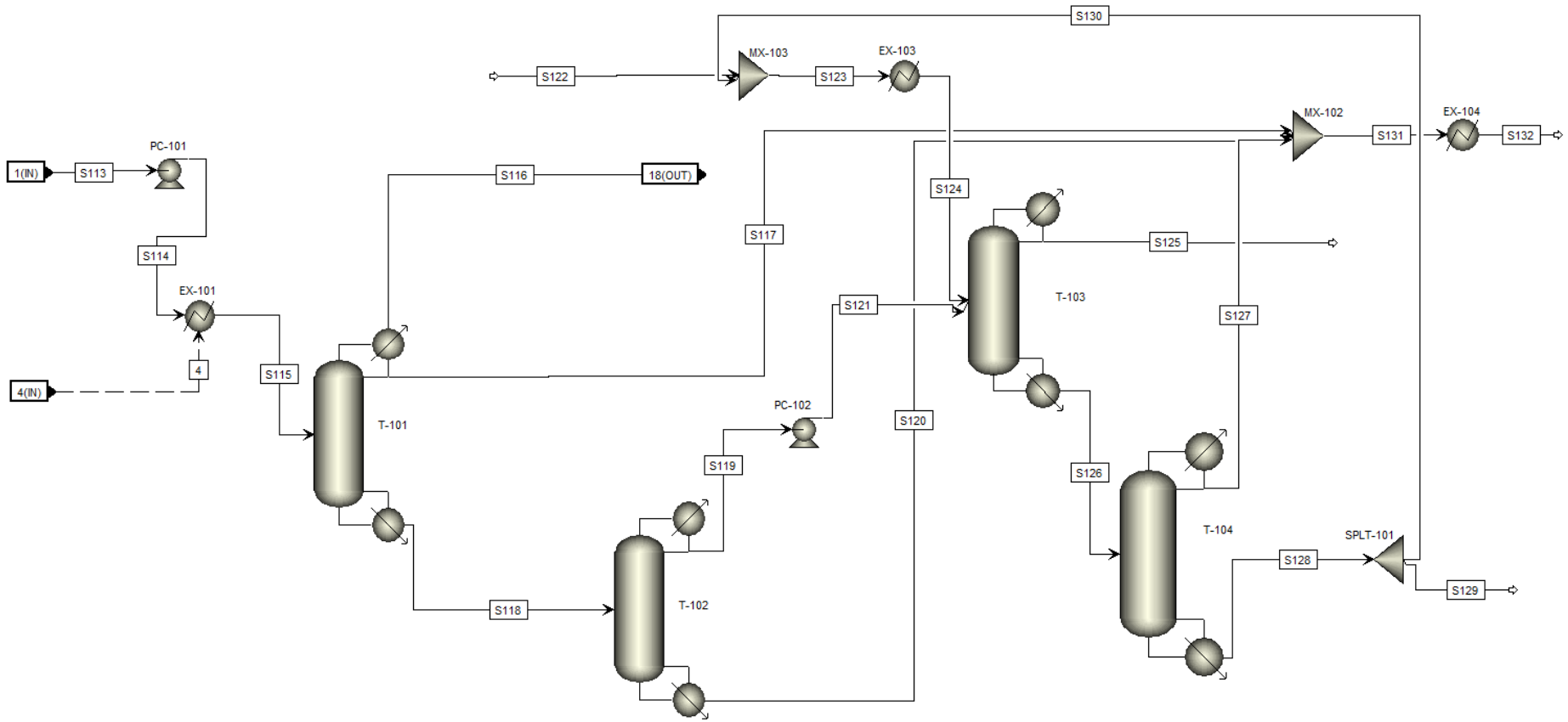

Figure 36: Aspen Plus® flowsheet of the separation system

Table 23: Stream table for the separation system

Stream number	S113	S114	S115	S116	S117	S118	S119	S120	S121	S122	S123	S124	S125	S126
Mass flow (kg/hr)	488.1	488.1	488.1	14.2	187.3	286.5	71.6	214.9	71.6	10.3	464.5	464.5	28.0	508.2

Table 23 continued: Stream table for the separation system

Stream number	S113	S114	S115	S116	S117	S118	S119	S120	S121	S122	S123	S124	S125	S126
Mole flow (kmol/hr)	4.3	4.3	4.3	0.2	2.1	1.9	0.5	1.4	0.5	0.1	4.4	4.4	0.2	4.7
Temperature (°C)	35.0	35.2	105.0	49.7	49.7	208.2	177.0	229.9	177.0	25.0	234.2	100.0	173.5	193.3
Pressure (kPa)	100.0	200.0	200.0	100.0	100.0	103.2	100.0	102.5	105.0	100.0	100.0	100.0	100.0	102.5
Vapour fraction	0.00	0.00	0.06	1.00	0.00	0.00	0.00	0.00	0.00	0.00	0.00	0.00	0.00	0.00
Limonene purity (wt.%)	5.8	5.8	5.8	0.0	0.2	9.7	38.8	0.1	38.8	0.0	0.0	0.0	95.1	0.2
Impurities (wt.%)	94.2	94.2	94.2	100.0	99.8	90.3	61.2	99.9	61.2	0.0	1.0	1.0	0.7	9.5
DEG purity (wt.%)	0.0	0.0	0.0	0.0	0.0	0.0	0.0	0.0	0.0	100.0	99.0	99.0	4.2	90.3

Table 23 continued: Stream table for the separation system

Stream number	S127	S128	S129	S130	S131	S132
Mass flow (kg/hr)	49.3	458.8	4.6	454.2	451.6	451.6
Mole flow (kmol/hr)	0.4	4.3	0.0	4.3	3.9	3.9
Temperature (°C)	175.0	244.5	238.4	238.4	123.6	35.0
Pressure (kPa)	100.0	100.5	100.5	100.5	100.0	100.0
Vapour fraction	0.0	0.0	0.0	0.0	0.3	0.0
Limonene purity (wt.%)	2.4	0.0	0.0	0.0	0.3	0.3
Impurities (wt.%)	88.3	1.0	1.0	1.0	98.6	98.6
DEG purity (wt.%)	9.3	99.0	99.0	99.0	1.0	1.0

T-101

The purpose of T-101 is to remove the components lighter than the limonene-rich fraction from the pressurised and pre-heated oil feed (S115). The components lighter than the limonene-rich fraction are recovered as distillate product whereas the limonene-rich fraction and heavier components are obtained as bottoms product.

T-101 has been modelled using a RADFRAC column model, which can perform rigorous multi-stage distillation calculations (Aspen Technology, 2009). The final input parameters for T-101 were determined by first modelling T-101 using a DSTWU column model, to obtain initial RADFRAC estimate column parameters. Details of determination of DSTWU parameters are provided in Appendix C.1. Table 24 shows the initial input parameters for T-101 (base case) RADFRAC model as obtained from DSTWU results. The boil-up ratio was obtained by running the RADFRAC model with values obtained from DSTWU results.

The initial RADFRAC parameters obtained from the DSTWU model were then used in a base case sensitivity analysis to determine the parameters with the most influence on separation. Optimised column parameters at base case were then used as input for a sensitivity analysis to obtain possible optimum column parameters that could achieve the desired separation for different number of stages. The desired separation in this study is 99% recovery of key components in their respective desired streams, which were selected based on recommendations by Sinnott and Towler (2009), explained in section 4.5.1. Economic analysis (annualised costs) was then performed for the different sets of possible optimum column parameters to determine the final parameters for T-101.

For the RADFRAC column model sensitivity analysis at base case, important column parameters (number of stages feed stage, reflux ratio, boil-up ratio and feed temperature) were varied to determine the optimum parameters at different number of stages.

Table 24: Initial RADFRAC column model input parameters for T-101 (obtained from DSTWU model)

Parameter	Value
Number of stages	75
Reflux ratio	1.8
Distillate to feed ratio	0.49
Feed stage	38
Boil-up ratio	4.6

Sensitivity analysis for T-101 parameters at base case number of stages

Sensitivity analysis was performed to determine the effects that variation of each parameter has on the recoveries of key components (limonene and 2-ethyltoluene) in their desired streams. When the effects of each parameter is investigated, all other parameters are kept at their initial values (shown in Table 24). The intention of sensitivity analysis at the base case number of stages was to determine the parameters that had the most significant effects on the recoveries of both key components. The parameters with significant effects are the ones that are then used to determine various possible number of stages to achieve the desired separation. The results of sensitivity analysis at the base case number of stages are given in Appendix C.2.

From the results obtained for the variation of parameters at the base case number of stages, it was concluded that reflux ratio and boil-up ratio had the most significant effect on the recovery of limonene and 2-ethyltoulene. A column design specification was applied for T-101 at the base case input parameters (number of stages and feed location) to maintain the recoveries of limonene (in the bottoms stream) and 2-ethyltoluene (in the overheads) at 99% using the boil-up ratio and the reflux ratio respectively. The resultant values of reflux ratio and boil-up ratio were 2.39 and 3.19 respectively; the optimum feed location at base case number of stages using these resultant values was stage 38.

Determination of T-101 parameters to achieve 99% recovery at various number of stages

The optimised column parameter values (at base case number of stages) were then used as input to perform sensitivity analysis that would determine the final column parameters that could achieve 99% recoveries for both key components at various number of stages. For this sensitivity analysis, the reflux ratio, boil-up ratio, and feed location were varied. Temperature showed to have negligible effect on the recoveries of both limonene and 2-ethyltoluene at base case, so the (T-101) feed temperature of 105 °C was maintained for the sensitivity analysis. Additional sensitivity analysis results at various number of stages are given in Appendix C.2.

The effect of reflux ratio on the recovery of limonene in the bottoms product stream at various number of stages is shown in Figure 37. It can be seen that for all number of stages, recoveries of more than 95% can be achieved at reflux ratios of around 2.5; over 99% recovery can be achieved with at least 55 stages at reflux ratios of around 2.5. Below 55 stages, reflux ratios of around 3 are required to achieve at least 99% limonene recovery.

The recovery of 2-ethyltoluene in the overheads product with varying reflux ratios is shown in Figure 38, and it can be seen that reflux ratios of below 1.5 are preferred to achieve recoveries of more than

95% for all number of stages. At 55 stages and above, recoveries of 95-99% can still be achieved at a reflux ratios of between 2 and 2.5, with a maximum reflux ratio of 2 required to ensure 99% recovery. Below 55 stages, the reflux ratio should be kept at a maximum of 1 to ensure that 99% recovery is achieved.

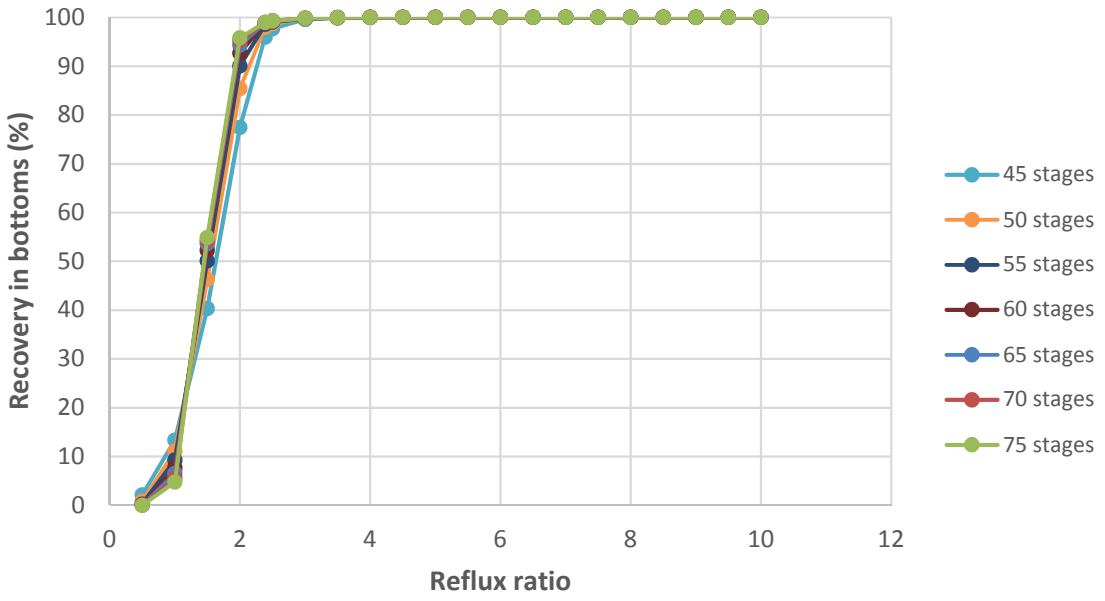

Figure 37: Effect of reflux ratio on the recovery of limonene in the bottoms at various number of stages

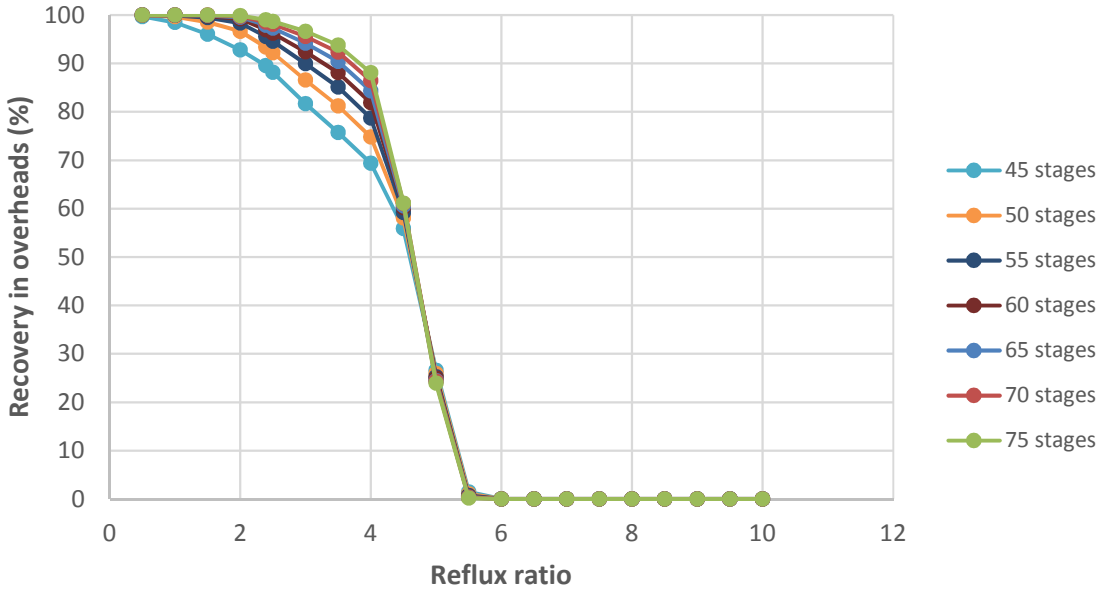

Figure 38: Effect of reflux ratio on the recovery of 2-ethyltoluene in the overheads at various number of stages

Figure 39 shows the effect of boil-up ratio on the recovery of limonene in the bottoms product at various number of stages. It can be observed that lower boil-up ratios are preferred to achieve high limonene recoveries at all number of stages, as vapourisation of limonene recovered in the bottom stages is minimised. Recoveries of 99% can be achieved up to a boil-up ratio of 2.5 for all number of stages, with a further increase in boil-up ratio requiring at least 50 stages to achieve 99% recovery. Above a boil-up ratio of 3, 99% recovery can no longer be achieved for all number of stages.

Figure 40 shows the recovery of 2-ethyltoluene in the overheads with varying boil-up ratio. It can be seen that in order to achieve 99% recovery for 2-ethyltoluene, a boil-up ratio of between 3.5 and 4 is required for 50 stages and above. Below 50 stages, a boil-up ratio of between 4.5 and 5 is required to ensure 99% recovery.

The effect of feed location on the recoveries of limonene and 2-ethyltoluene in their respective desired streams is shown in Figure 41 and Figure 42 respectively. It can be seen from both figures that for 45 to 55 stages, feeding around stages 30 - 32 gives the best recoveries of both compounds; feeding around stages 34 – 36 gives the best separation for 60 - 65 stages. At 65 stages and above, the best separation is obtained with the feed located around stage 38.

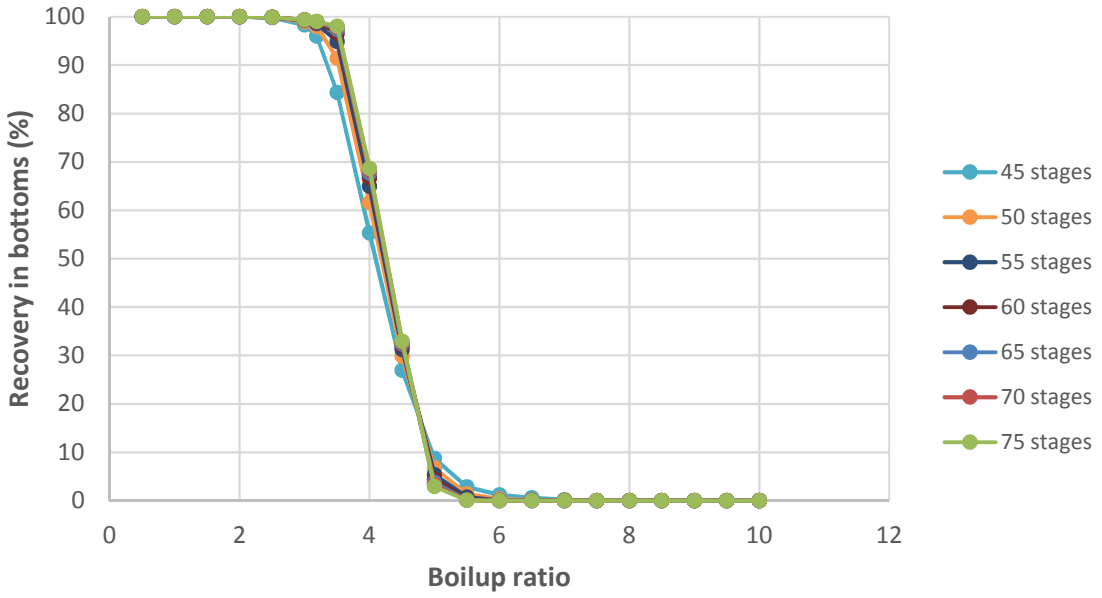

Figure 39: Effect of boil-up ratio on the recovery of limonene in bottoms product at various number of stages

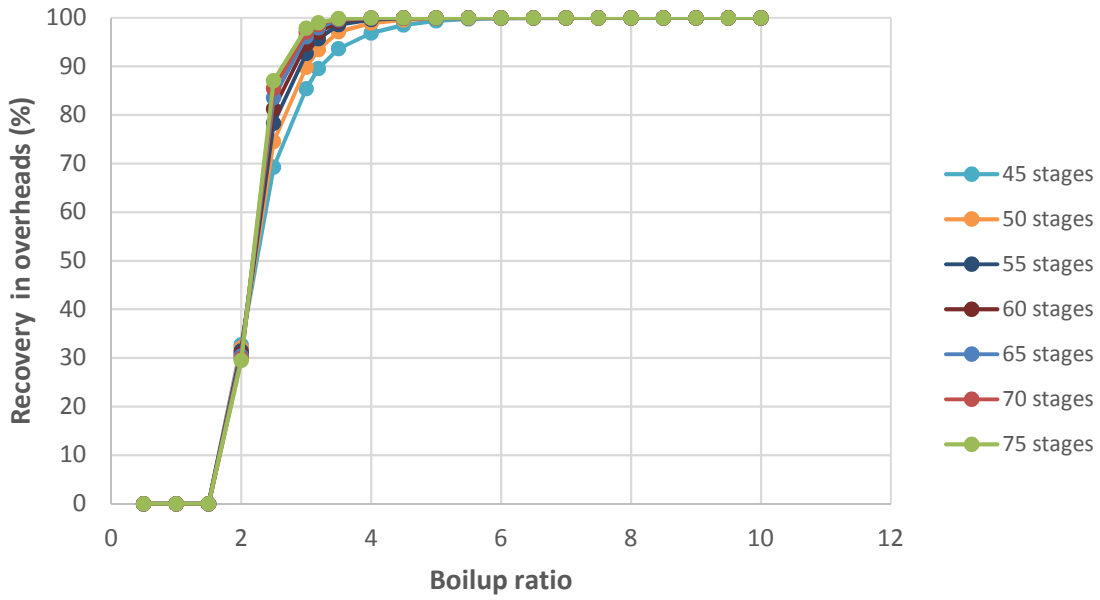

Figure 40: Effect of boil-up ratio on the recovery of 2-ethyltoluene at various number of stages

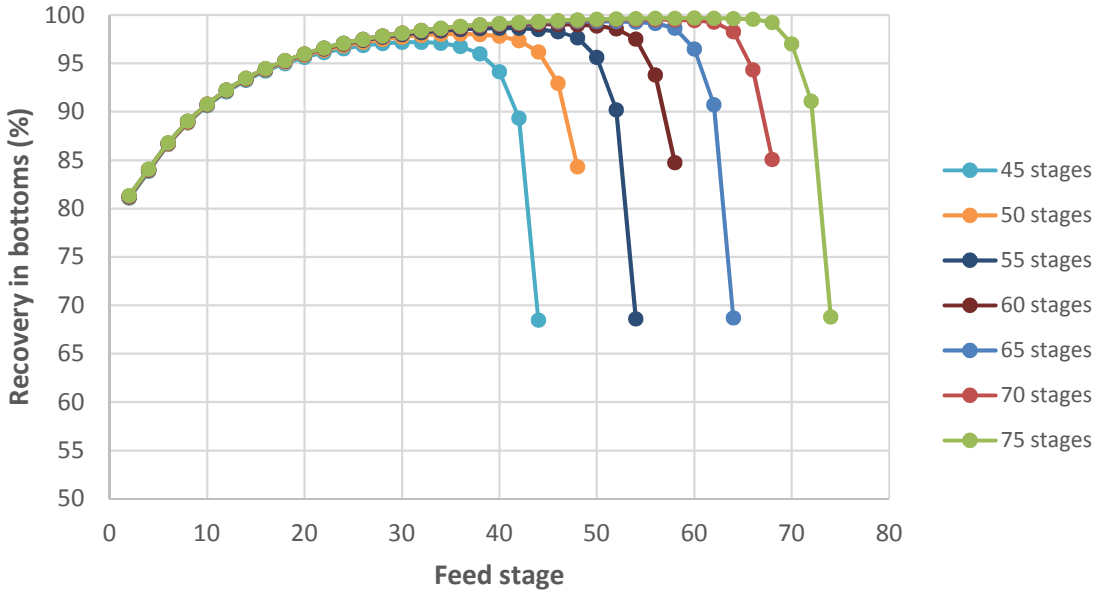

Figure 41: Effect of feed location of recovery of limonene in bottoms product at various number of stages

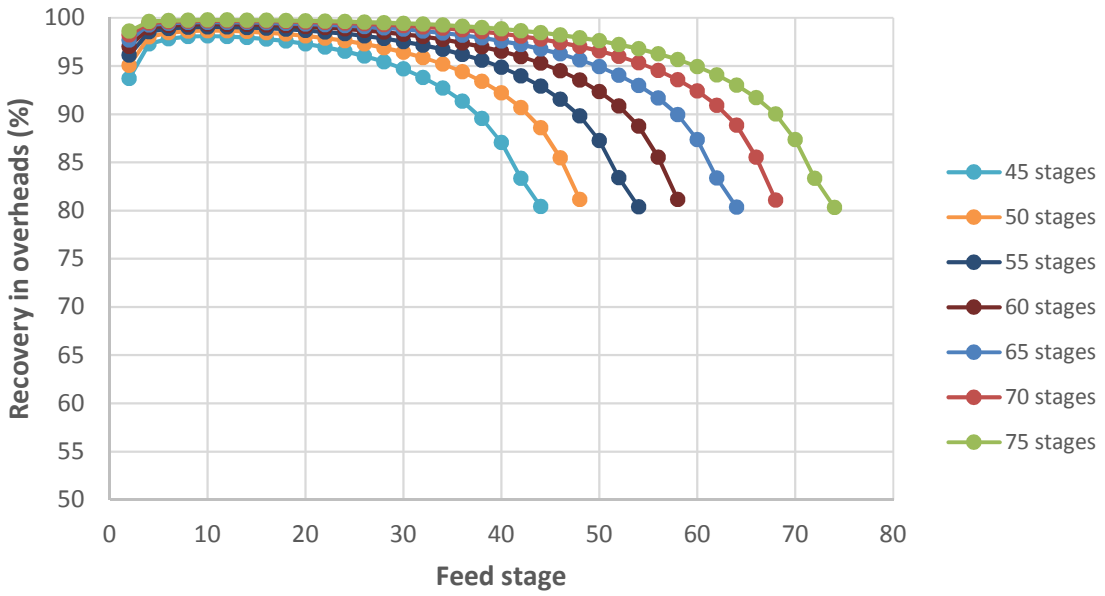

Figure 42: Effect of feed location on recovery of 2-ethyltoluene in overheads at various number of stages

Based on observations from Figure 37 to Figure 42, the final specific reflux and boil-up ratios required to achieve 99% recovery of both limonene and 2-ethyltoluene for each number of stages were adjusted using a column design specification of T-101, at respective optimum feed stages. The resulting reflux and boil-up ratios were used to determine the condenser and reboiler duties for each number of stages; the duties were then used to calculate the operating costs at each number of stages. The Economic Analyzer of Aspen Plus® V8.6 was used to perform column sizing, and the sizing results were used to obtain the column installed (capital) cost for each number of stages, using the bare module technique from Turton *et al.* (2009). A Similar approach is applied for all other columns.

The associated capital and operating costs at each number of stages were then used to calculate total annualised cost for the respective number of stages using Equation 2, which was obtained from Peters and Timmerhaus (1991). According to Peters and Timmerhaus (1991), the optimum reflux ratio occurs at the point where the total annualised cost is minimum. The annualised costs for different number of stages for T-101 is shown in Figure 43.

$$TAC = 0.15 * annual\ fixed\ charges + annual\ operating\ charges$$

Equation 2

TAC is the total annualised cost ($/yr), $annual\ fixed\ charges$ is the annualised sum of the installed cost of the column and the costs of piping, insulation and instrumentation (60% of the cost of installed column) in $/yr; $annual\ operating\ charges$ are the costs of cooling water and steam from the condenser and reboiler respectively ($/yr).

From Figure 43, it can be concluded that 65 stages will give the most economical operation for T-101, as the total annualised costs are lowest. As such, 65 stages were chosen as the final number of stages for T-101. The final RADFRAC column parameters for T-101 used in this study are given in Table 25.

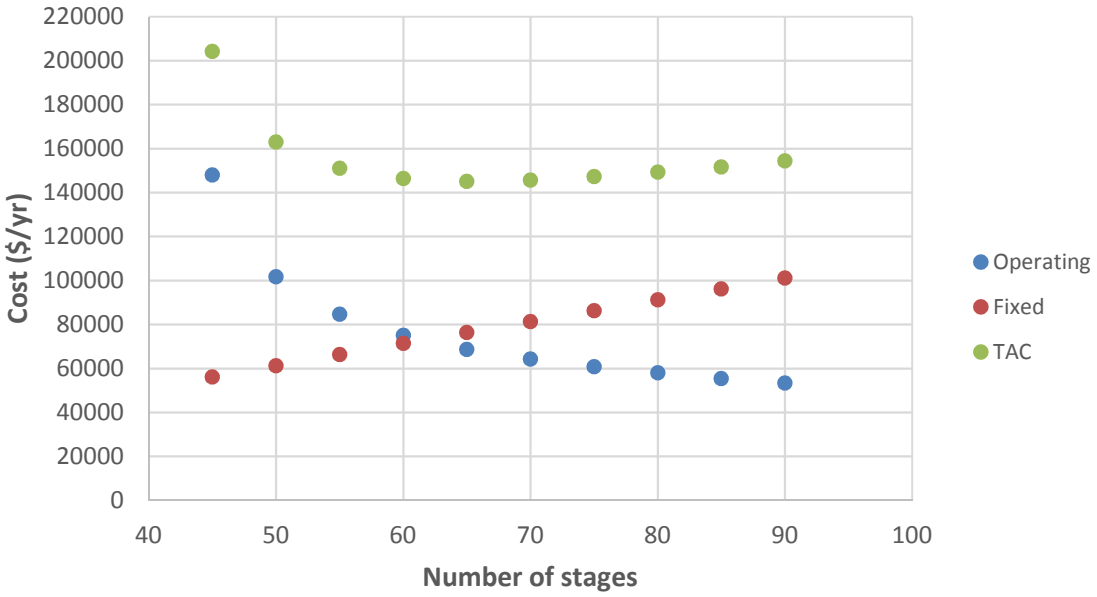

Figure 43: Annualised costs for T-101 at different number of stages

Table 25: Final RADFRAC column model parameters for T-101

Parameter	Value
Number of stages	65
Reflux ratio	2.3
Boil-up ratio	4.1
Feed stage	38
Feed temperature	105 °C

Operation of T-101

T-101 is operated at atmospheric pressure, and the condenser pressure is specified as 100 kPa. Atmospheric pressure operation for T-101 was chosen on the basis that vacuum operation is often costly due to maintenance requirements of the associated equipment needed to create vacuum. Most vacuum is steam induced, which could also increase capital and operational costs. Equipment operating under vacuum might require thicker walls, which would also increase capital cost (Sinnott and Towler, 2009). Vacuum operation would however reduce the operating temperatures and the subsequent duties of the condenser and reboiler.

Based on the preliminary column sizing in section 4.5.1, and the number of theoretical stages required from Table 25, T-101 would preferably have to be a packed column. Packed columns are recommended for small diameters, temperature sensitive material, and for difficult separations that could require a lot of stages (Douglas, 1998; Henley *et al.*, 2011). Structured packings are favourable for such operations as they can give a height equivalent to theoretical plate (HETP) of typically less than 0.5m, and low pressure drop (around less than 100 Pa/m) (Sinnott and Towler, 2009). As such, a stage pressure drop of 50 Pa was specified for T-101 based on these HETP and pressure drop values.

Even though the pressure drop is greatly reduced, operating at atmospheric pressure has resulted in a reboiler temperature of around 210 °C. It is noted that in reality, with these temperatures, thermal degradation of some compounds could be possible, which would cause fouling of the packing material. This would reduce the separation capacity, as the effective cross-sectional area open to vapour flow determines the capacity of a packed column (Lamprecht, 2010; Henley *et al.*, 2011). In such cases, the effects of hold-up will have to be taken into account (Lamprecht, 2010). Liquid hold-up is usually considerably lower for packed columns as compared to plate columns (Sinnott and Towler, 2009).

The lighter components removed from T-101 as overheads are sent to a partial condenser with a vapour fraction of 0.1, to flash some non-condensables, which helps in eliminating the need for refrigerants, and reduces the condenser duty. The condenser has a duty of -91 kW, which accounts for 63% of the cooling requirements of all 4 columns, and 42% of the cooling requirements of the whole separation system. The vapour distillate stream (S116) is sent to the heat recovery section, and the liquid distillate stream (S117) is combined with by-products from T-102 and T-104 to form the TDO product stream (S132).

Limonene and heavier components are drawn off as bottoms product (S118), and the stream is sent to T-102 for further limonene enrichment. T-101 reboiler requires 103 kW of heat input (from high pressure steam at 255 °C), which represents 51% of the steam requirements in the separation section. It implies that T-101 reboiler accounts for 51% of all steam requirements, as steam is only used in the columns in this study. The final mass balance of T-101 is shown in Table 26.

Table 26: Final mass balance of T-101

Stream number	**S115**	**S116**	**S117**	**S118**
Mass flow (kg/hr)	488.1	14.2	187.3	286.5
Mole flow (kmol/hr)	4.3	0.2	2.1	1.9
Temperature (°C)	105.0	49.7	49.7	208.2

Table 26 continued: Final mass balance of T-101

Stream number	S115	S116	S117	S118
Pressure (kPa)	200.0	100.0	100.0	103.2
Vapour fraction	0.06	1.00	0.00	0.00
Limonene purity (wt.%)	5.8	0.0	0.2	9.7

T-102

The purpose of T-102 in this study is to remove the components that are heavier than the limonene cut, from the bottoms product of T-101 (S118), thereby further increasing the purity of limonene in the limonene-rich stream. The limonene-rich stream is collected as distillate product (also following recommendations from Sinnott and Towler (2009) regarding collection of desired products as distillate); the heavier components are collected as bottoms product.

T-102 was also modelled using a RADFRAC distillation column model; the initial and final RADFRAC column parameters were determined in a similar manner to that of T-101. In the case of T-102, limonene and 2,5-dimethlystyrene were specified as light and heavy key components, respectively, for determination of initial input parameters from the DSTWU column model. Recoveries of both key components in their respective desired streams were set at 99% as well. Table 27 shows the initial RADFRAC column parameters for T-102, as obtained from the DSTWU column model. The initial estimate parameters in Table 27 were then used in a sensitivity analysis at the base case number of stages, to determine the optimum base case parameters, similarly to T-101. For the base case sensitivity analysis, all the parameters shown in Table 27 were varied. The results of T-102 sensitivity analysis at the base case number of stages are shown in Appendix C.3.

Table 27: Initial RADFRAC column model input parameters for T-102 (obtained from DSTWU model)

Parameter	Value
Number of stages	68
Reflux ratio	5.1
Distillate to feed ratio	0.27
Feed stage	35
Boil-up ratio	2.46

From the results of sensitivity analysis at the base case number of stages, it was concluded that the optimum base case parameters are a reflux ratio of 5, a distillate to feed ratio of 0.25, and feed location at stage 20. It was also concluded that T-102 feed temperature (S118) should be kept at its value of 208 °C. The RADFRAC input parameters where then changed from those in Table 27 to these optimised values, and a sensitivity analysis to determine the optimum parameters that would achieve the desired separation at various number of stages was performed, similarly to that of T-101. For each number of stages, the reflux ratio, distillate to feed ratio and feed location were varied. The results of T-102 sensitivity analysis at various number of stages are also shown in Appendix C.3.

From the results of sensitivity analysis at various number of stages, it was concluded that maximum recoveries of 75 - 80% can be achieved for 2,5-dimethylstyrene (in the bottoms product) without compromising the recovery of limonene in the distillate product (below 99%). Since a high recovery of limonene is desired, T-102 was designed to achieve a recovery of around 80% for 2,5-dimethylstyrene; the remaining amount is removed by the solvent in T-103.

The results of optimum column parameters at various number of stages were then used to calculate the annualised costs for the respective number of stages, in a similar manner to T-101. The annualised costs for the various number of stages are shown Figure 44, and it can be seen that the total annualised costs are lowest at 50 stages. The final number of stages for T-102 were then chosen as 50, which correspond to a reflux ratio of 5, and a distillate to feed ratio of 0.25. The final RADFRAC column parameters for T-102 are shown in Table 28.

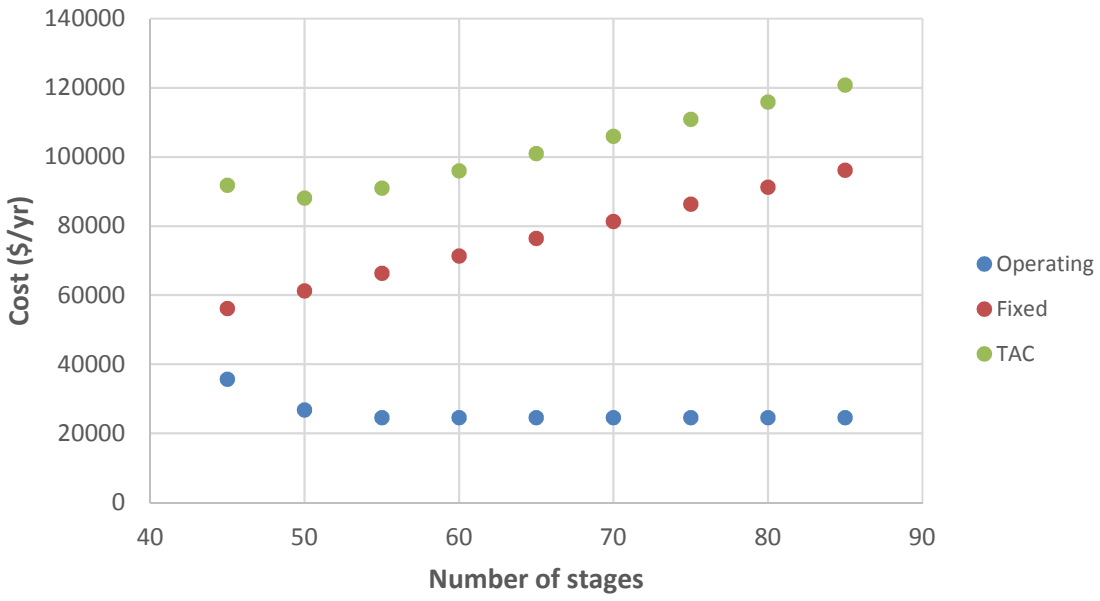

Figure 44: Annualised costs for T-102 at various number of stages

Table 28: Final RADFRAC column parameters for T-102

Parameter	Value
Number of stages	50
Reflux ratio	5
Distillate to feed ratio	0.25
Feed stage	24
Feed temperature	208 °C

Operation of T-102

Just like T-101, T-102 is also desired to be a (structured) packed column, and it is also operated at a condenser pressure of 100 kPa, with a 50 Pa/stage pressure drop. T-101 bottoms stream (S118) is fed to T-102, where removal of the heavier components increases the limonene content of the limonene-rich fraction from 10 wt.% to 39 wt.%. The limonene-rich fraction is recovered as the overheads, with a condenser duty of -36 kW required to condense the overhead vapours. The limonene-rich stream (S119) is then pressurised in PC-102, and is sent to the limonene recovery column (T-103) for the final stage of limonene enrichment/recovery. The outlet pressure of PC-102 has been specified so as to overcome the pressure drop in T-103.

The bottoms stream (S120) is mixed with the liquid distillate of T-101 (S117) and the distillate stream of T-104 (S127) to make the TDO product stream (S132). A reboiler duty of 37 kW is required to supply the heat requirements of T-102, which is considerably lower than what is required for T-101 reboiler. A lower T-102 reboiler duty could be due to the high temperature of S118, which lowers additional heat input requirements. The final mass balance of T-102 is shown in Table 29.

Table 29: Final mass balance of T-102

Stream number	S118	S119	S120
Mass flow (kg/hr)	286.5	71.6	214.9
Mole flow (kmol/hr)	1.9	0.5	1.4
Temperature (°C)	208.2	177.0	229.9
Pressure (kPa)	103.2	100.0	102.5
Vapour fraction	0.00	0.00	0.00
Limonene purity (wt.%)	9.7	38.8	0.1
2,5-dimethlystyrene purity (wt.%)	8.3	6.4	9.0

T-103

The objective of T-103 is to remove the impurities contained in the limonene-rich stream (S119), using extractive distillation, to produce a limonene stream of (minimum) 95 wt.% limonene purity. The limonene product stream is obtained as distillate product, while the solvent, together with the entrained impurities, are obtained as bottoms product.

T-103 is also modelled using a RADFRAC distillation column model. Initial RADFRAC input parameters for T-103 (except for distillate flow rate) are adopted from the work of Ngwetjana (2017). The initial input parameters are shown in Table 30. The final RADFRAC column input parameters were obtained by a sensitivity analysis of the main (initial) column parameters, and a preliminary economic analysis of annualised costs. Main results of sensitivity analysis are presented here; additional results of sensitivity analysis can be found in Appendix C.4.

Table 30: Initial RADFRAC input parameters for T-103 (obtained from Ngwetjana, 2017)

Parameter	Value
Number of stages	55
Reflux ratio	1.8
Distillate rate	28 kg/h
Solvent feed stage	2
Solvent feed temperature	95 °C
Solvent to feed ratio	6
Oil feed stage	24

Determination of T-103 parameters to achieve 95% limonene purity at various number of stages

The initial input parameters for T-103 adopted from Ngwetjana (2017), shown in Table 30, were final optimised parameters in the particular study. As such, the only sensitivity analysis done in this study was to determine the possible number of stages that could achieve 95 wt.% limonene purity, while also monitoring the recovery of limonene in the limonene stream. The following column parameters were varied in the sensitivity study: reflux ratio, oil (limonene-rich fraction) feed location, entrainer/solvent feed location, entrainer flow rate and entrainer feed temperature. When the effect of each of parameter was studied, all other parameters were kept at their base values.

The distillate flow rate of 28 kg/h was specified for T-103 as it represents approximately all the limonene sent to T-103, which is all desired as distillate product in perfect separation. Since the distillate flow rate is specified in the column, the recovery and purity of limonene in the distillate stream will be closely related. As such, only the effects of varying the column parameters on limonene purity are presented here, results of the effects on recovery are presented in Appendix C.4.

Effect of reflux ratio

The effect of variation of reflux ratio on the purity of limonene is shown in Figure 45. It is observed that the purity of limonene decreases with increasing reflux ratio for all number of stages considered. The decrease in limonene purity is due to increased vaporisation of the impurities and possibly the entrainer, as the energy input from the reboiler is increased to make up for the increase in required vapour flow. It can also be observed that in order to achieve 95% purity, it is necessary to have reflux ratios of ≤1, and a column with a minimum of around 50 stages.

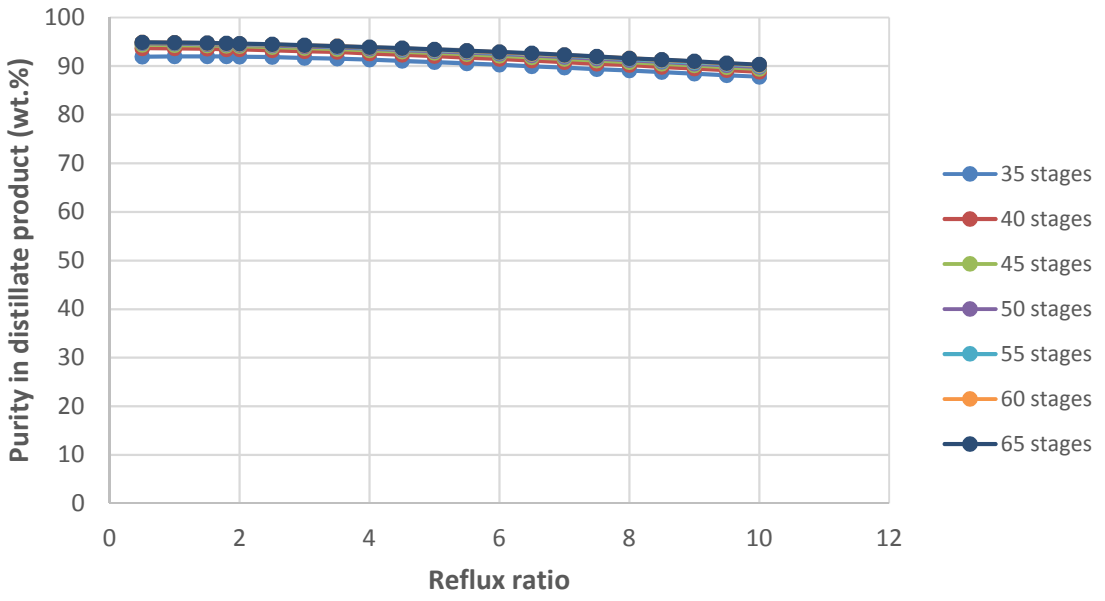

Figure 45: Effect of reflux ratio on limonene purity in distillate product at various number of stages

Effect of oil feed location

The effect of variation in oil feed stage on the purity of limonene is shown in Figure 46. It can be seen that the purity increases with increasing feed location (feed is located further down the column), as more contact area is created for extraction of the impurities in the oil (limonene-rich stream) by the entrainer. The purity then decreases with feeding further down the column, as more impurities (and possibly the entrainer) are stripped and collected as distillate product. In order to achieve maximum

purity, the oil feed should be located between stages 20 and 24, for a column of less than 45 stages. For a column with 45 to 55 stages, the optimum oil feed location is between stages 26 and 34, whereas feeding between stages 36 and 45 gives optimum purity for a column with 60 and 65 stages.

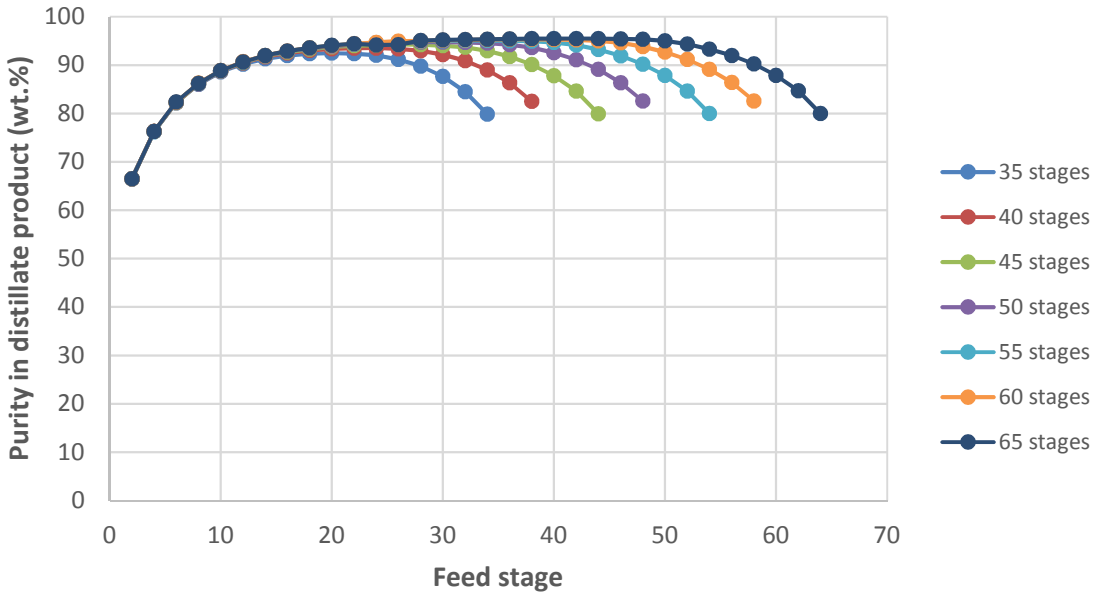

Figure 46: Effect of oil stream feed stage on limonene purity in distillate product for various number of stages

Effect of entrainer feed location

The effect of variation in entrainer feed stage on limonene purity is shown in Figure 47. It can be seen that the purity of limonene decreases as the entrainer is fed further down the column for all number of stages. This can be attributed to the reduction in the number of contact stages for the entrainer and the oil feed, and possible increased vapourisation of the entrainer as the feed stage approaches closer to the reboiler. It can also be seen that feeding below stage 2 results in a limonene purity that is way below the targeted 95%. It can therefore be concluded that the entrainer should be fed on stage 2.

Effect of entrainer flow rate

Figure 48 shows the effect of variation in entrainer flow rate on the purity of limonene. It can be seen that the limonene purity increases with increasing entrainer flow rate, as the capacity for impurities extraction is increased. At 50 stages and above, a purity of 95% can be achieved at entrainer flow rates of around 460-500 kg/hr, whereas entrainer flow rates of up to about 700 kg/hr are required at number of stages lower than 50. Further increases in entrainer flow rates above these values has minimal effect on limonene purity.

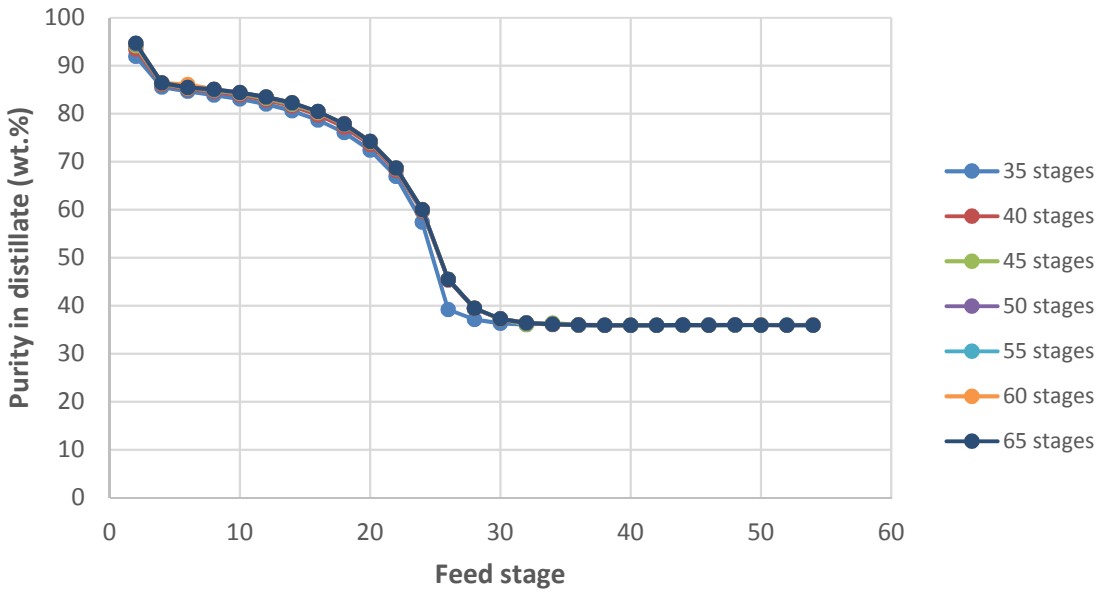

Figure 47: Effect of entrainer feed location on limonene purity in distillate product at various number of stages

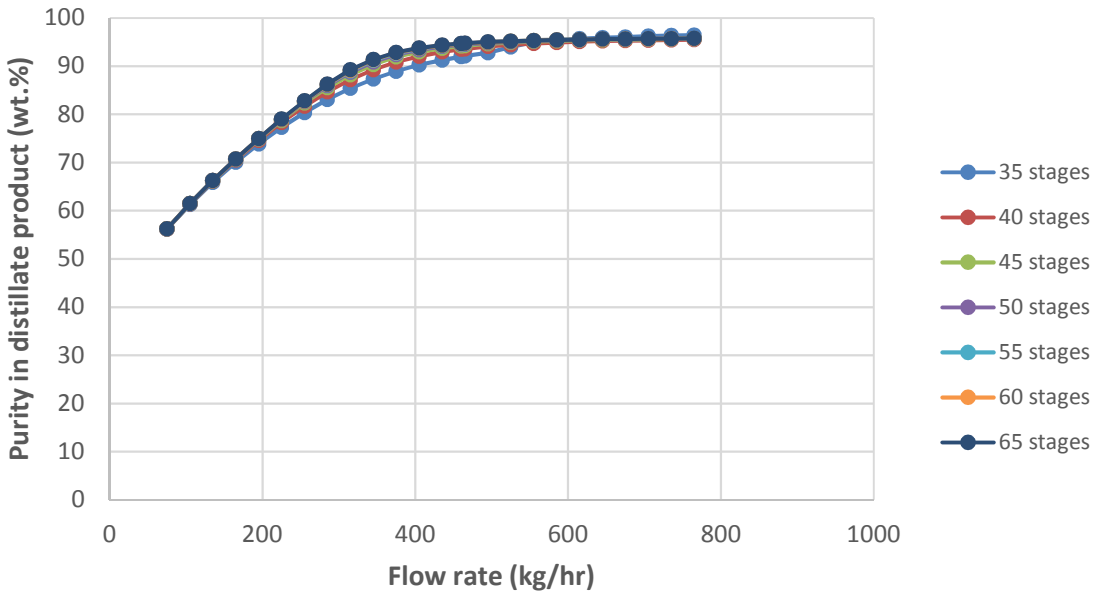

Figure 48: Effect of entrainer flow rate on limonene purity in distillate product for various number of stages

Effect of entrainer feed temperature

Figure 49 shows the effect of variation in entrainer feed temperature on the purity of limonene. The purity increases with an increase in feed temperature up to 110 °C for all number of stages and then decreases with a further increase in temperature. This could be attributed to an increasing extraction capacity of the entrainer with increasing temperature. A further increase in entrainer temperature would then vapourise part of the aromatic impurities causing them to be recovered with limonene as distillate. Entrainer feed temperatures of between 95 and 110 °C are required to achieve maximum limonene purity.

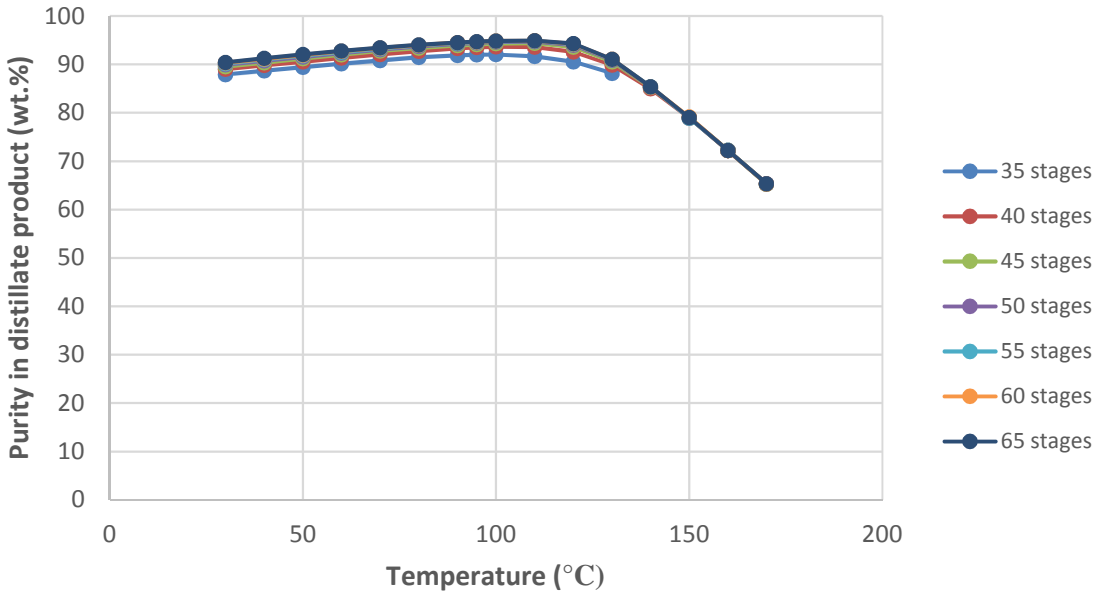

Figure 49: Effect of entrainer temperature on limonene purity in distillate product for various number of stages

The final column parameters for T-103 are determined through calculation of annualised costs for different number of stages that could achieve the minimum required limonene purity of 95 wt.%, shown in Figure 50. It can be seen that the lowest annualised costs are obtained at 50 stages, which was the minimum number required to achieve the desired purity, as shown by the sensitivity analysis. Based on Figure 50, it can be inferred that lower number of stages would yield lower TAC values; however, the limonene purity specification would not be met at lower number of stages. As such, the final T-103 specification was set at 50 stages; the final optimised column parameters for T-103 (that correspond to 50 stages) are shown in Table 31.

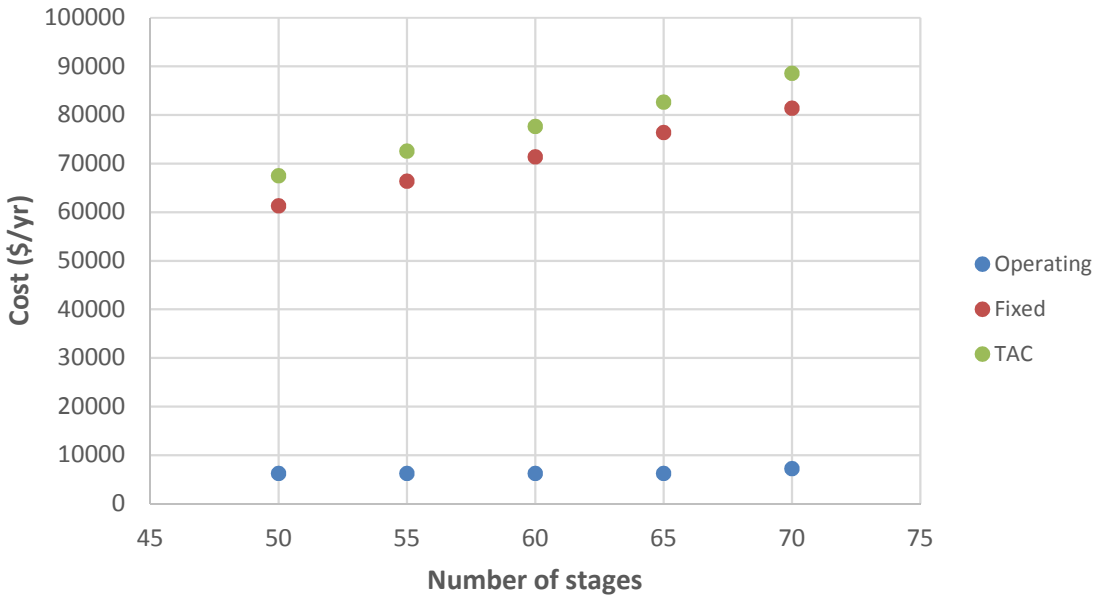

Figure 50: Annualised costs for T-103 at different number of stages

Table 31: Final column parameters for T-103

Parameter	Value
Number of stages	50
Reflux ratio	1
Distillate flow rate	28 kg/h
Oil feed stage	30
Oil feed temperature	177 °C
Entrainer feed stage	2
Entrainer flow rate	465 kg/h
Entrainer feed temperature	100 °C

Operation of T-103

T-103 was also modelled as a structured packed column, with a specified pressure drop of 50 Pa/stage. The pressurised limonene-rich stream (S121) is fed into the column on stage 30, and it is vapourised by the hot vapours from the reboiler. DEG (S124) is fed on stage 2, and the solvent contacts the oil feed counter-currently. Most of the aromatic impurities are extracted from the oil vapours, thereby enriching the limonene content of the rising vapours. A stream of around 95 wt.% limonene purity is recovered as distillate product (S125), at a rate of 28 kg/h; a limonene recovery of 96% is achieved in the distillate product. T-103 condenser has a duty of -4 kW, which is only 2% of the total cooling

requirements of all 4 columns. The small duty can be attributed to a small vapour flow rate and the high purity of limonene in the vapour overhead which would mean that the vapour temperature will almost be similar to the boiling point of limonene.

The solvent-rich stream, with most of the aromatic compounds, is recovered as the bottoms product (S126), and it is sent to T-104 for solvent regeneration. A duty of 29 kW is required for T-103 reboiler to provide the heat requirements for T-103; the reboiler accounts for 14% of the total process steam usage. The final mass balance around T-103 is shown in Table 32.

Table 32: Final mass balance for T-103

Stream number	S121	S124	S125	S126
Mass flow (kg/hr)	71.6	464.5	28.0	508.2
Mole flow (kmol/hr)	0.5	4.4	0.2	4.7
Temperature (°C)	177.0	100.0	173.5	193.3
Pressure (kPa)	105.0	100.0	100.0	102.5
Vapour fraction	0.00	0.00	0.00	0.00
Limonene purity (wt.%)	38.8	0.0	95.1	0.2
Impurities composition (wt.%)	61.2	1.0	0.7	9.5
DEG purity (wt.%)	0.0	99.0	4.2	90.3

T-104

The objective of T-104 is to regenerate the (DEG) solvent used for extraction in T-103, by stripping off the (mostly aromatic) impurities entrained in the solvent-rich stream from T-103 (S126). The aromatic impurities are collected as distillate product, and the solvent is recovered as bottoms product. The separation target in T-104 is a recovery and (mass) purity of at least 99% for diethylene glycol, in the solvent recycle stream. A high recovery and purity of the solvent minimises solvent loss and build-up of impurities in the system.

T-104 was also modelled using the RADFRAC column model. The initial input parameters for T-104 were also adopted from the study by Ngwetjana (2017). The initial column parameters are shown in Table 33. The initial parameters were then used to perform sensitivity analysis to generate a set of optimum column parameters that could achieve the desired separation objective at various number of stages. The sensitivity analysis was performed similarly to that of T-103. For T-104 sensitivity analysis at various number of stages, the reflux ratio, boil-up ratio, feed location, and temperature of

the feed stream were varied. The effects of varied parameters on the recovery and mass purity of DEG in the bottoms stream, and the reboiler energy usage were observed. The results of T-104 sensitivity analysis are given in Appendix C.5.

Table 33: Initial RADFRAC model input parameters for T-104 (adopted from Ngwetjana, 2017)

Parameter	Value
Number of stages	10
Reflux ratio	1.6
Boil-up ratio	0.0371
Feed stage	4

From the results of sensitivity analysis, it was observed that a trade-off exists between recovery and purity for most of the various varied parameters. The recovery of DEG in the bottoms product increases with increasing reflux ratio, as cooling of the rising vapours is increased. The recovery decreases with increasing boil-up ratio, as the increased heat input increases vapourisation of the solvent. The opposite trends are observed for the purity, with regards to both the reflux and boil-up ratios. It could be concluded that a maximum reflux ratio of 2, and a maximum boil-up ratio of 0.5 would give optimum recovery and purity at most number of stages. The final reflux and boil-up ratios are determined by a column design specification that is used to ensure 99% of both recovery and purity.

It could also be seen that T-104 temperature should be kept at the value of T-103 bottoms stream (193 °C), as noticeable changes in recovery and purity are observed at temperatures values that would require additional heating or cooling equipment, which would add to capital and maintenance costs. The effects of feed location on recovery, purity, and energy usage were negligible with the initial parameters, as such, the final feed location for each number of stages was set at the value that gave the lowest energy consumption with the reflux and boil-up ratios from the design specification.

The final number of stages were chosen based on analysis of annualised costs using the optimum values at each number of stages; the results of annualised costs are shown in Figure 51. It can be seen that 10 stages give the lowest annualised costs for this separation. As such, 10 stages were specified for T-104; this corresponds to a reflux ratio of 1.73, a boil-up ratio of 0.47, and feed location at stage 5. It can be noted from Figure 51 that even though fixed costs are lowest at 5 stages, the resulting reflux and boil-up ratios (20.5 and 1.74 respectively) required to achieve the targeted recovery and

purity result in very high operating costs. In reality, high reflux and/or boil-up ratios could also result in column problems such as flooding or weeping, which would decrease separation efficiency (Sinnott and Towler, 2009). The final column parameters for T-104 are given in Table 34.

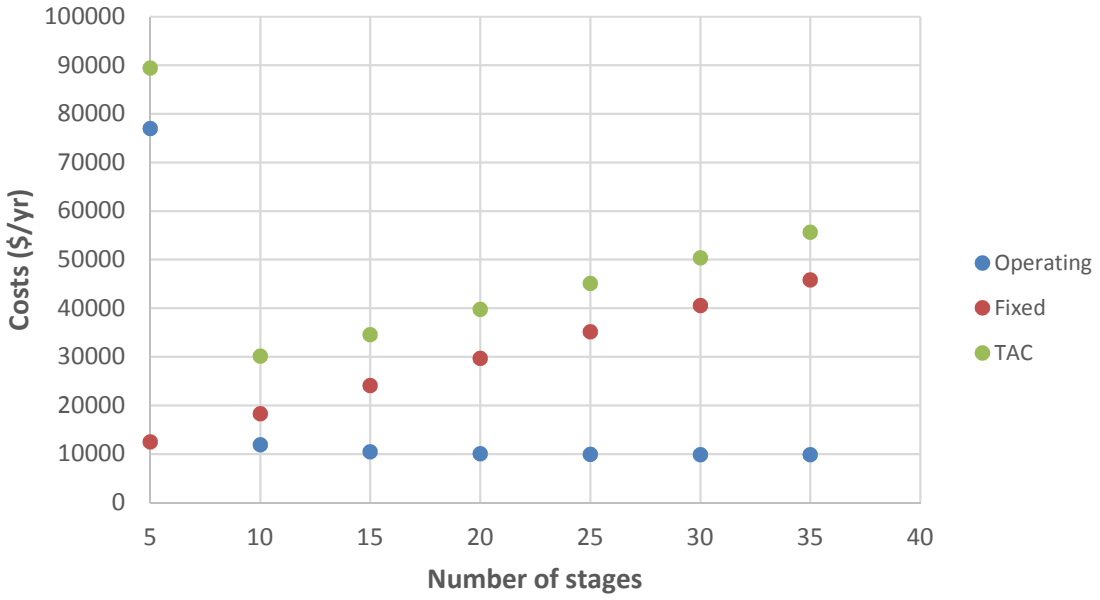

Figure 51: Annualised costs for T-104 at various number of stages

Table 34: Final optimised column parameters for T-104

Parameter	value
Number of stages	10
Reflux ratio	1.73
Boil-up ratio	0.47
Feed stage	5

Operation of T-104

T-104 was also modelled as a structured packed column with a specified pressure drop of 50 Pa/stage. The aromatics entrained in the solvent are recovered as distillate product (S127), and the regenerated solvent is recovered as bottoms product (S128). The distillate product is combined with the liquid distillate from T-101 and the bottoms product from T-102 in MX-102; the combined stream (S131) is cooled down to 35 °C in EX-104, and stored as TDO product (S132).

T-104 condenser requires a duty of -13 kW to condense the column overheads, which represents 6% of the cooling requirements in the separation section, and 3% of the overall process cooling

requirements. The reboiler in T-104 requires a duty of 31 kW to provide the energy needed to drive the separation, which represents 16% of the steam requirement in the separation section, and 4% of the overall process steam requirements. In cooling down S131, a duty of -28 kW is required in EX-104, which accounts for 13% of the cooling requirements in the separation section, and 6% of the overall process cooling requirements.

The solvent recovered (S128) is purged (1%) by SPLT-101 to avoid build-up of impurities in the system, as the solvent is recycled. The solvent recycle stream (S130) is combined with a solvent make-up stream (S122) in MX-103, and the combined stream (S123) is cooled down in EX-103 to the desired solvent feed temperature for T-103 (100 °C). A design specification (DEG-FLOW) is used to control the flow rate of DEG in the solvent stream fed to T-103 (S124) to 460 kg/hr, by manipulating the flow rate of the solvent make-up stream.

EX-103 (duty of -42 kW) accounts for 19% of the cooling requirements of the separation system, and 9% of overall cooling requirements; this can be attributed to a high temperature of S130 (238 °C) as the solvent has to be fed to T-103 at 100 °C for optimum extraction. The final mass balance around T-104, together with that of the solvent make-up stream is shown in Table 35.

Table 35: Final mass balance of T-104 and the solvent make-up stream

Stream number	S122	S126	S127	S128
Mass flow (kg/hr)	10.3	508.2	49.3	458.8
Mole flow (kmol/hr)	0.1	4.7	0.4	4.3
Temperature (°C)	25.0	193.3	175.0	244.5
Pressure (kPa)	100.0	102.5	100.0	100.5
Vapour fraction	0.00	0.00	0.0	0.0
Impurities composition (wt.%)	0.0	9.5	88.3	1.0
DEG purity (wt.%)	100.0	90.3	9.3	99.0

4.6. Design of energy recovery system

From the PFDs of Wojtowicz and Serio (1996), Fels and Pegg (2009) and Pilusa *et al.* (2014) (reviewed in section 3.5), it could be concluded that in literature, the most common way of utilising the pyrolysis gas produced is to combust the gas for reactor heating with any excess gas flared off. None of Wojtowicz and Serio (1996), Fels and Pegg (2009) and Pilusa *et al.* (2014) reviewed the potential of energy recovery from the flue gases generated. Only Fels and Pegg (2009) considered using part of the excess gas produced, to provide energy for drying. According to information obtained from two

REDISA-affiliated operational tyre pyrolysis plants, the possibility of any form of heat recovery from flue gases generated from reactor heating or burning excess pyrolysis gas is often difficult, due to low energy gains per unit of currency invested (Jefferies, 2017; Wiese, 2017).

The process developed in this study requires the use of high pressure steam in the reboilers of the distillation columns in the separation system. In this study, the possibility of using the pyrolysis gas generated in the process to provide energy for reactor heating, and subsequent heat recover by steam generation from the flue gases will be preliminarily investigated. For the preliminary investigation, it is assumed that all the gas is combusted to meet the reactor heating requirements (only the combustion chamber of the reactor is required), and if there is any excess heat generation (above the reactor heating requirements), it is used for steam generation.

A preliminary economic evaluation will be performed for the energy recovery scenario (in chapter 5), assuming that the only additional equipment required is for steam generation, and that any excess steam above process requirements can be sold at the purchase price of high pressure steam. A final decision on whether heat recovery should be further investigated in this study, is taken based on the overall effect of the current proposed heat recovery system on process economics. The PFD and stream names of the proposed heat recovery system are shown in Figure 52 and Table 36 respectively.

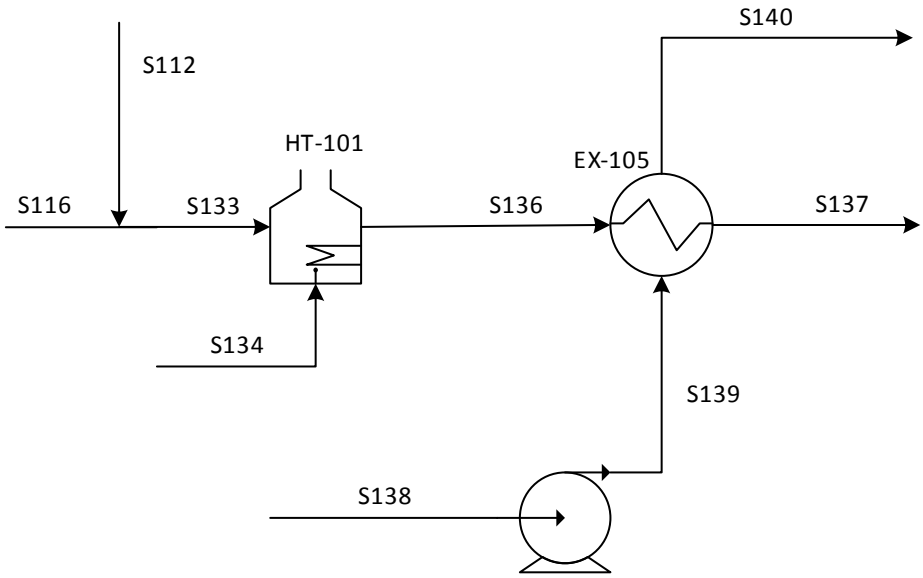

Figure 52: PFD of the heat recovery system

Table 36: Stream names of the heat recovery system

Stream name	Description
S112	Pyrolysis gas
S116	T-101 vapour distillate
S133	Fuel gas to RX-101
S134	Combustion air
S136	Hot flue gas
S137	Flue gas discharge
S138	Boiler feed water
S139	Pressurised boiler feed water
S140	HP steam

In the PFD shown in Figure 52, non-condensable pyrolysis gas from the pyrolysis section (S112 in Figure 27) is combined with the vapour distillate from T-101 in the separation system (S116 from Figure 36), and are combusted in the reactor heating chamber. The flue gases that are generated are used to generate high pressure steam, after which they are discharged via a stack.

4.6.1. Aspen Plus® simulation of the heat recovery system

The Aspen Plus® flowsheet and stream table of the heat recovery system are shown in Figure 53 and Table 37 respectively.

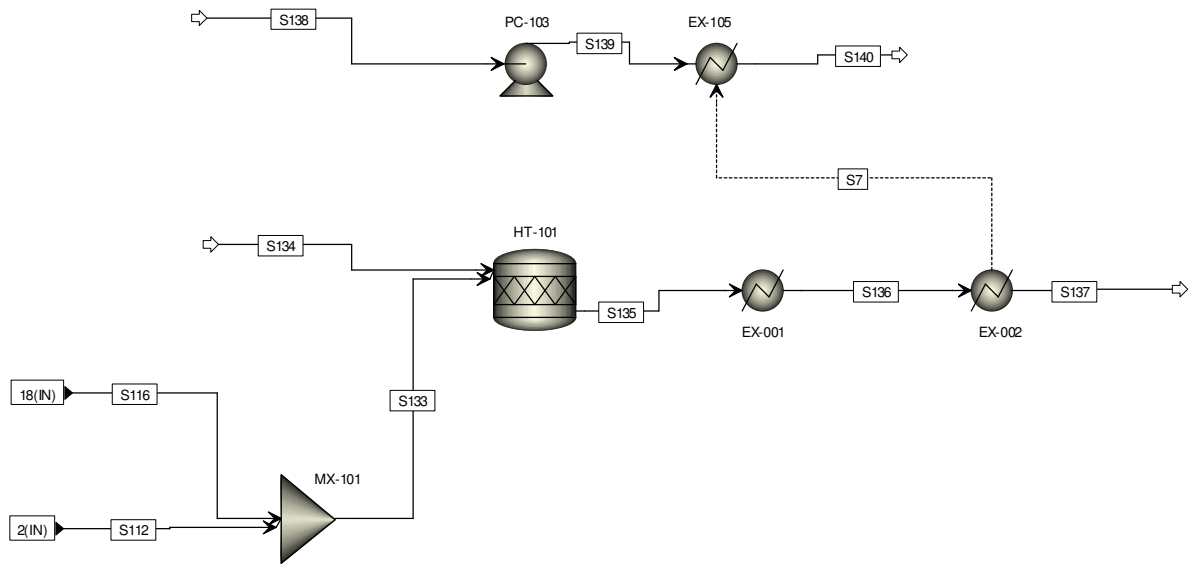

Figure 53: Aspen Plus® flowsheet of the heat recover system

Table 37: Stream table for the heat recovery system

Stream number	S112	S116	S133	S134	S135	S136	S137	S138	S139	S140
Mass flow (kg/hr)	231	14	246	12712	12957	12957	12957	2881	2881	2881
Mole flow (kmol/hr)	6	0	6	441	450	450	450	160	160	160
Temperature (°C)	35	50	36	25	800	672	150	80	83	255
Pressure (kPa)	100	100	100	100	100	100	100	100	4300	4300
Vapour fraction	1	1	1	1	1	1	1	0	0	1

Table 37 continued: Stream table for the heat recovery system

Stream number	S112	S116	S133	S134	S135	S136	S137	S138	S139	S140
CO_2 content (wt.%)	0.00	0.00	0.00	0.00	5.76	5.76	5.76	0.00	0.00	0.00
SO_2 content (wt.%)	0.00	0.00	0.00	0.00	0.06	0.06	0.06	0.00	0.00	0.00
NO_2 content (wt.%)	0.00	0.00	0.00	0.00	0.00	0.00	0.00	0.00	0.00	0.00

Pyrolysis gas from the pyrolysis system (S112) is combined with the vapour distillate from T-101 (S116) in MX-101 and the combined stream (S133) is combusted in the combustion chamber of the pyrolysis reactor. The combustion chamber of the pyrolysis reactor is represented by HT-101 which has been modelled as an adiabatic RSTOIC reactor modelled following what has normally been done in literature studies for modelling of biomass boilers (Nsaful, 2012; Naleli, 2016). Combustion air (S134) is supplied at atmospheric conditions and is fed in excess in order to maintain the temperature of HT-101 outlet stream (S135) at 800 °C. The flow rate of air is controlled by a design specification (DS-AIR) in order to control the outlet temperature of HT-101. An HT-101 outlet temperature of 800 °C was chosen assuming a reactor and flue gas system of stainless steel 304 that has a maximum working temperature of around 850 °C – 900 °C; stainless steel 304 is the most commonly used type of stainless steel in industry (Sinnott and Towler (2009).

S135 (at 800 °C) passes through EX-001 which models heating of the reactor, a (negative) heaty duty equivalent to the heat duty of the pyrolysis reactor (RX-101 in Figure 27) was specified for EX-001. The flue gases (S136) at 672 °C are then used to generate 43 bar steam in EX-105, which is then used in the column reboilers in the separation section. The temperature of the flue gas outlet stream (S137) is specified at 150°C, similarly to that of the study by Ringer *et al.* (2006). A heat stream (S7) is used to model the transfer of heat from flue gases to boiler feed water for steam generation.

Boiler feed water (S138) at 80 °C and 100 kPa is pressurised to 4300 kPa (43 bar) in PC-103, which is the pressure of the steam required to meet reboiler heating requirements in the separation system. A boiler feed water temperature of 80 °C was adopted from the study of Nsaful (2012). The amount of steam generated (S140) is controlled by a design specification (BFW-FLOW), which manipulates the flow rate of S138 in order to achieve a temperature of 255 °C in S140 (the temperature at which steam is required in the reboilers of the separation system). Steam is generated at a rate of 2881 kg/h from the system in Figure 53, which is enough to cover the 258 kg/h required in the reboilers and leave an excess of 2623 kg/h, which can then be sold to generate income.

Even though steam is produced in excess, the final choice of inclusion of the heat recovery system in the overall PFD of the process for converting tyres into limonene will be guided by the overall effect of heat recovery on process economics.

4.7. Final PFD of the waste tyres to limonene process

The final PFD of the base case waste tyres to limonene process scenario is shown in Figure 54. The heat recovery system is not included in the final PFD, as it is commonly not included in typical waste tyre pyrolysis flowsheets; heat recovery is also only preliminarily considered in this study. The pyrolysis gas from the pyrolysis section (S112) and the vapour distillate of T-101 (S116) are combined to make “fuel gas”. A portion of the fuel gas (S133) is sent to the reactor for reactor heating and the rest is sent to a flare (S141). The final stream table, equipment list and stream names are provided in Table 38, Table 39, and Table 40 respectively. The stream names and equipment list apply to all PFDs and Aspen Plus flowsheets developed in chapter 4.

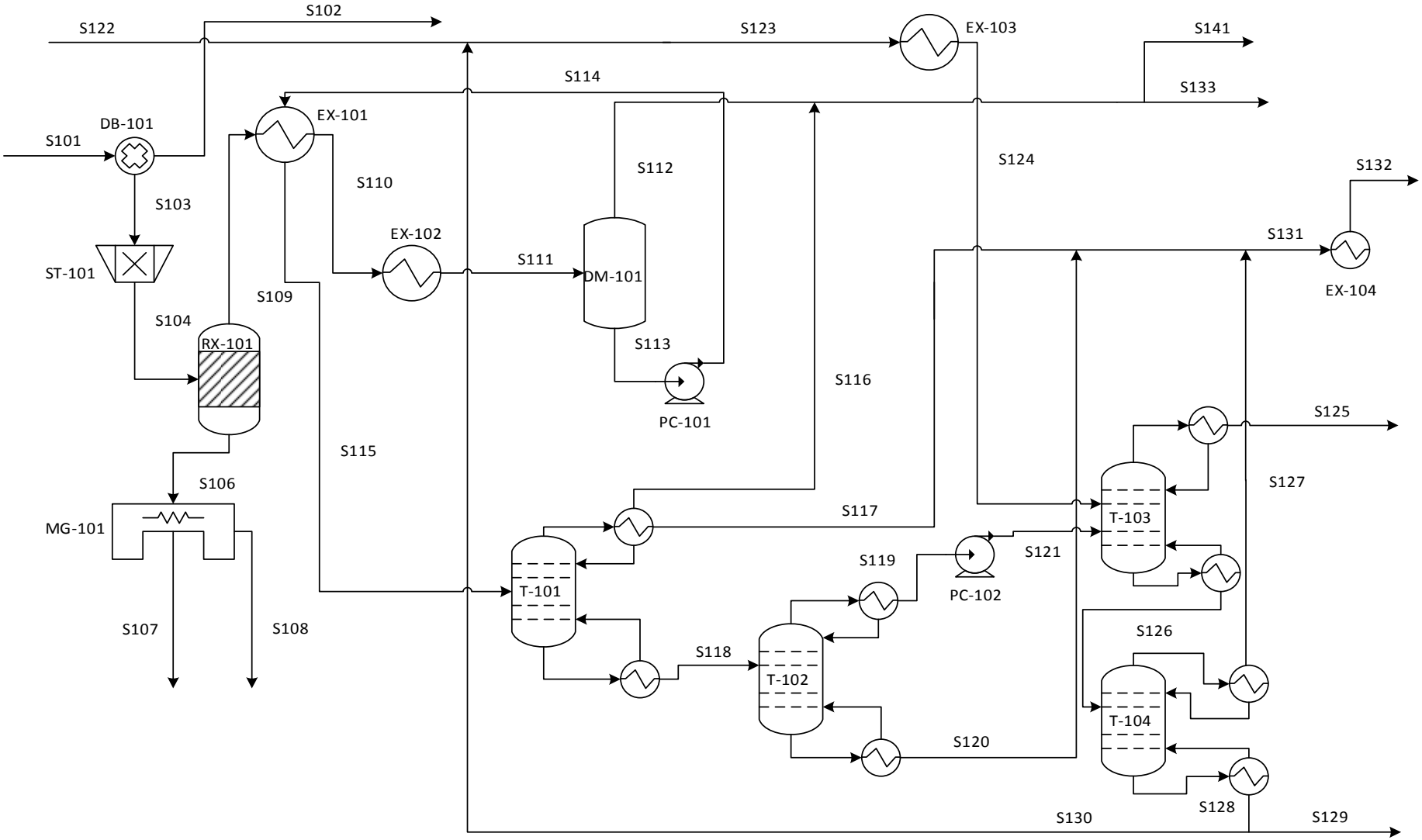

Figure 54: Final PFD of the waste tyres to limonene base case process scenario

Table 38: Final stream table for the tyres to limonene process

Stream number	S101	S102 + S108	S104	S107	S109	S110	S111	S112	S113	S114	S115	S116	S117
Mass flow (kg/hr)	1250.0	125.0	1125.0	405.6	719.4	719.4	719.4	231.3	488.1	488.1	488.1	14.2	187.3
Mole flow (kmol/hr)					10.0	10.0	10.0	5.7	4.3	4.3	4.3	0.2	2.1
Temperature (°C)	25.0	25.0	25.0	500.0	500.0	465.8	35.0	35.0	35.0	35.2	105.0	49.7	49.7
Pressure (kPa)	100.0	100.0	100.0	100.0	100.0	100.0	100.0	100.0	100.0	200.0	200.0	100.0	100.0
Vapour fraction	0.0	0.0	0.0	0.0	1.0	1.0	0.6	1.0	0.0	0.0	0.1	1.0	0.0

Table 38 continued: Final stream table for the tyres to limonene process

Stream number	S118	S119	S120	S121	S122	S123	S124	S125	S126	S127	S128	S129	S130
Mass flow (kg/hr)	286.5	71.6	214.9	71.6	10.3	464.5	464.5	28.0	508.2	49.3	458.8	4.6	454.2
Mole flow (kmol/hr)	1.9	0.5	1.4	0.5	0.1	4.4	4.4	0.2	4.7	0.4	4.3	0.0	4.3
Temperature (°C)	208.2	177.0	229.9	177.0	25.0	234.2	100.0	173.5	193.3	175.0	244.5	238.4	238.4
Pressure (kPa)	103.2	100.0	102.5	105.0	100.0	100.0	100.0	100.0	102.5	100.0	100.5	100.5	100.5
Vapour fraction	0.0	0.0	0.0	0.0	0.0	0.0	0.0	0.0	0.0	0.0	0.0	0.0	0.0

Table 38 continued: Final stream table for the tyres to limonene process

Stream number	S131	S132	S133 + S141
Mass flow (kg/hr)	451.6	451.6	245.5
Mole flow (kmol/hr)	3.9	3.9	6.0
Temperature (°C)	123.6	35.0	35.8
Pressure (kPa)	100.0	100.0	100.0
Vapour fraction	0.3	0.0	1.0

Table 39: Equipment list of the waste tyres to limonene process scenario

Equipment name	Description
DB-101	Tyre de-beader
ST-101	Tyre shredder
RX-101	Pyrolysis reactor
MG-101	Magnetic separator
EX-000	Tube side of EX-101
EX-101	T- 101 feed preheater
EX-102	Reactor volatiles condenser
DM-101	Volatiles condenser knockout drum
PC-101	Lights remover feed pump
T-101	Light hydrocarbon remover
T-102	Limonene-rich cut purifier
PC-102	Limonene column feed pump
EX-103	DEG cooler
T-103	Limonene recovery column
T-104	DEG regeneration column
EX-104	TDO cooler
HT-101	RX-101 combustion chamber
EX-001	RX-101 heating
EX-002	EX-105 shell side
PC-103	Boiler feed water pump
EX-105	Steam generator

Table 40: Stream names for the waste tyres to limonene process scenario

Stream name	Description
S101	Whole tyre feed
S102	Bead wire steel
S103	Whole tyres
S104	Tyre chips
S105	Pyrolysis reactor product
S106	Char and steel
S107	Char product
S108	Steel
S109	Reactor volatiles
S110	Slightly cooled volatile product
S111	Condensed volatiles
S112	Pyrolysis gas
S113	Pyrolysis oil
S114	Pressurised pyrolysis oil
S115	Warm pyrolysis oil feed
S116	T-101 vapour distillate
S117	T-101 liquid distillate
S118	T-101 bottoms product
S119	Limonene-rich stream
S120	T-102 bottoms product
S121	Pressurised limonene-rich stream
S122	DEG make-up
S123	Hot DEG feed
S124	Cool DEG feed
S125	Limonene product
S126	DEG-rich stream
S127	Aromatics product
S128	DEG product
S129	DEG purge
S130	DEG recycle

Table 40 continued: Stream names for the waste tyres to limonene process scenario

Stream name	Description
S131	Hot TDO product
S132	Cool TDO product
S133	Fuel gas to RX-101
S134	Combustion air
S135	Hot flue gas
S136	Hot flue gas
S137	Flue gas discharge
S138	Boiler feed water
S139	Pressurised boiler feed water
S140	HP steam
S141	Fuel gas to flare

4.8. Summary

In chapter 4, a conceptual base case process scenario for upgrading waste tyres to limonene was developed. It was shown that, by using adapted process steps involved in typical waste tyre pyrolysis flowsheets, and an adapted version of a process for TDO fractionation for valuable chemicals recovery as basis, a flowsheet for upgrading waste tyres to limonene can be successfully developed. A waste tyre feed rate of 30 tons/day was found to be a suitable design flow rate for the developed process.

The literature work by Choi *et al*. (2014) was found to be a suitable source selection of operating conditions for the pyrolysis reactor, yields of main product fractions, and calculation of yields of individual components identified. A pyrolysis reactor temperature of 500 °C and pressure of 100 kPa were found to give the maximum yield of limonene, and they were subsequently chosen as the reactor operating conditions for the base case process.

Aspen Plus® simulation of the base case process revealed that the process can produce a limonene stream of 95 wt.% limonene purity at a rate of 28 kg/hr, with an overall limonene recovery of around 95%. It was also found that there is error in predicting the equilibrium phase behaviour of some TDO compounds using the PR-BM and NRTL thermodynamic models chosen for the simulation, due to lack of readily available experimentally obtained binary interaction parameters. As such, the need for experimentally determined phase equilibrium parameters of TDO compounds was highlighted. Nevertheless, the PR-BM and NRTL property gave acceptable results for the purposes of this study.

The major cooling utility consumers were found to be the reactor volatiles condenser, condenser of the light hydrocarbon removal column, and the solvent cooler. The pyrolysis reactor represented the highest heating requirements of any kind, whereas the reboiler of the light hydrocarbon removal column had the most requirements for the high pressure steam used in the process.

Sensitivity analysis of major column parameters for optimisation (at various number of stages) proved to be a successful method for allowing selection of optimum column parameters while minimising total annualised costs. Detailed economics of the process scenario developed in chapter 4 are discussed in chapter 5.

CHAPTER 5: EVALUATION AND COMPARISON

Overview

In this chapter, objective 4 of this study (evaluation of the developed process scenarios from techno-economic and energy utilisation viewpoints) is addressed. Detailed procedure for determination of each component of economic evaluation, and the results of economic evaluation are presented in the respective subsections. This chapter is subdivided into 8 sections. Section 5.1 outlines the economic model used in this study. Section 5.2 discusses determination of total capital investment. Section 5.3 discusses how the operating costs were estimated. Section 5.4 provides information on determination of revenue. Profitability analysis is performed in section 5.5. Section 5.6 presents comparison of economic performance of the base case scenario with other pre-treatment scenarios and the pyrolysis for TDO scenario. Sensitivity analysis of key economic parameters for the most profitable scenario is discussed in section 5.7. A summary of the chapter is given in section 5.8.

5.1. Economic model used in this study

In order to evaluate the economic feasibility of the 30 tons/day process for upgrading waste tyres to limonene in this study, an economic model was developed, which takes into account changes in the main process. An overview of the proposed economic model is provided in Figure 55. The different components of the model are detailed in the numbers (sections) shown in brackets.

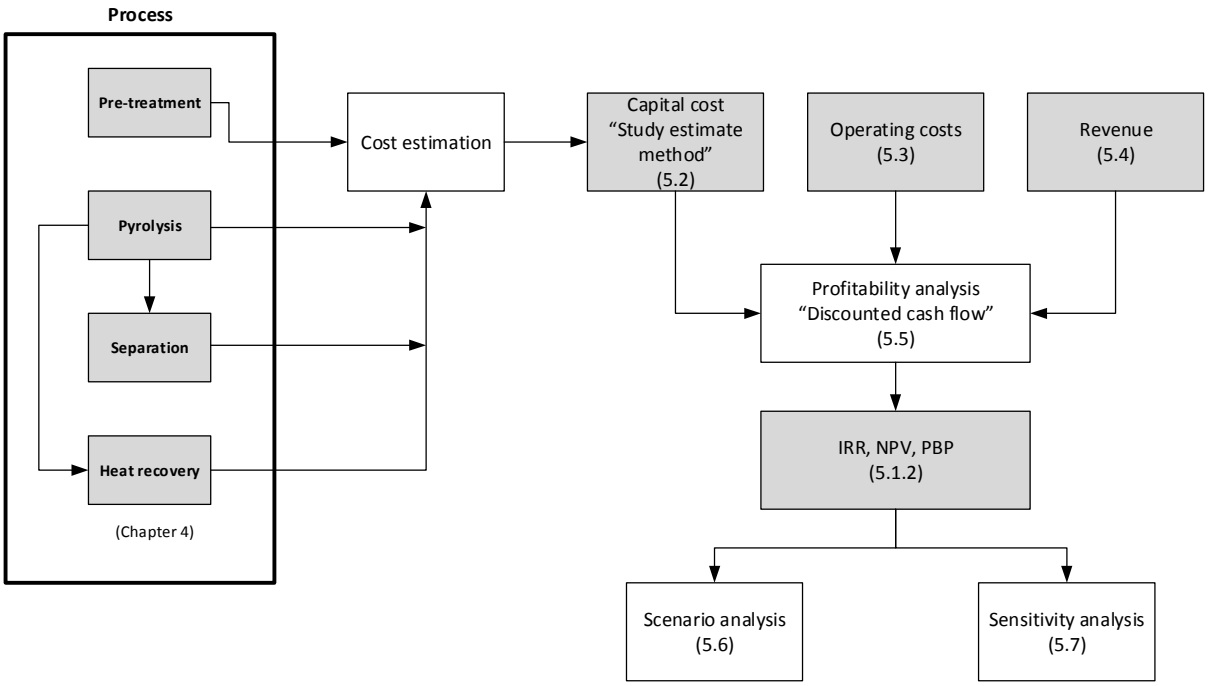

Figure 55: Overview of the economic model used for evaluation of the waste tyres to limonene process

In the economic model shown in Figure 55, the equipment requirement, and utilities and/or chemicals usage associated with each individual section of the process is used for estimation of the capital and operating costs. The resulting (capital and operating) cost estimates are combined with the revenue estimate and then used as input for a discounted cash flow analysis to determine profitability. The output of the cash flow analysis is the key economic indicators (KEI), which are used as a measure of profitability, and form a basis for comparison of the various scenarios considered in this study. The KEI also form the basis of economic sensitivity analysis for the most profitable scenario.

5.1.1. Main assumptions

The discounted cash flow rate of return (DCFROR) analysis is used for profitability analysis in this study. Profitability can be evaluated on a discounted or a non-discounted basis. A discounted basis takes the effects of time into account, whereas a non-discounted basis does not account for the effects of time (Seider *et al.*, 2004; Turton *et al.*, 2009). The discounted profitability analysis was chosen in this study as it provides a much better view of the profitability of the project over the entire project life (Seider *et al.*, 2004).

All cash flow analyses in this study are on a nominal term basis, which means that the effects of inflation on future revenues and expenses are not taken into account.

A base year of 2016 is used for all cost estimates in this study. Cost indices will be used to adjust for equipment whose original costs are of a different base year, such that their 2016 costs can be obtained. Various cost indices such as Chemical Engineering plant cost index, Nelson-Farrar refinery construction index, Marshall and Swift process industry index, and the Engineering News record construction index can be used to account for inflation (Turton *et al.*, 2009). These indices show similar inflationary trends with time; the Chemical Engineering plant cost index (CEPCI) is commonly used (Turton *et al.*, 2009). A cost index of 556.8 is used for the year 2016 in this study, which was obtained from Chemengonline (2016).

In this study, all equipment cost estimations based on costs of similar equipment of different capacities were performed using the sixth-tenths-factor rule. According to Peters and Timmerhaus (1991), cost estimation for an equipment that has no available cost data for a particular operating capacity can be performed (with good accuracy) using known cost data for a similar equipment of a different capacity. This can be achieved using a logarithmic relationship known as the sixth-tenths-factor rule (shown in Equation 3), provided that the two pieces of equipment are within a tenfold capacity range of each other.

$$New\ cost = Original\ cost * \left(\frac{New\ capacity}{Original\ capacity}\right)^{n}$$

Equation 3

n is the exponential factor, which is typically taken as 0.6.

Project lives of 10, 12, and 15 years are typically used for profitability analysis of chemical plants (Turton *et al.*, 2009). For this study, a project life of 10 years is chosen, as the project evaluated is a small plant that should be expected to show reasonable profitability at the minimum project life possible. A waste tyre pyrolysis study by Pilusa *et al.* (2014) showed reasonable profitability within a project life of 5 years even though only primary products were produced. It is also assumed that the plant in this study will be constructed and started-up within 1 year as it is a small plant. The plant in the study by Pilusa *et al.* (2014) was also assumed to be constructed and started up within 6 months of delivery of process equipment. The plant in this study will operate for 8000 hours/year, following guidelines by Sinnott and Towler (2009), and what has been done in other literature studies for continuous pyrolysis plants (Nsaful, 2012; Naleli, 2016).

Cash flow generation takes into account taxation and depreciation of the equipment. A tax rate of 28% is used in this study, which is the tax rate set for businesses in South Africa (South African Revenue Services, 2016).

The depreciation method chosen for this study is the straight-line depreciation method over a period of 10 years. Straight-line depreciation is the simplest and most common method of depreciation, and it has been used in several pyrolysis economic evaluation studies (Nsaful, 2012; Dutta *et al.*, 2015; Naleli, 2016). The plant equipment is depreciated to its salvage value at the end of project life. A salvage value of zero is used in this study, as the salvage value is difficult to estimate, and a salvage value of zero is usually assumed (Seider *et al.*, 2004; Turton *et al.*, 2009).

In this study, it is assumed that the project will be fully equity financed, which means that there is no loan payment (principal debt and interests) expenses. Equity financing is less risky as there exists no obligation to repay the money invested (Marsh, 1982).

For all cases where conversion is made between the South African rand and the USA dollar, an average conversion rate of R15/$ is used based on exchange rate trends for the year 2016, obtained from the South African Reserve bank (2016). The 2016 exchange rate graph is shown in Figure D1 (Appendix D).

5.1.2. Key economic indicators (KEI)

The KEI typically used in DCFROR analysis are: payback period (PBP), net present value (NPV), and internal rate of return (IRR). The profitability analysis in this study will be based on these KEIs. Each of the indicators is discussed briefly:

- The PBP is the required time after start-up to recover the total depreciable capital. This is the point at which the sum of the annual earnings equals the total depreciable capital. It is used in early stages to compare alternatives. A PBP of less than 2 years is desired for high risk projects, and PBP should typically not exceed 4 years for a project to be attractive.
- The NPV is the current worth of all cash flow in the project throughout the project life. The cash flows at the end of each time period are discounted (at a desired discount rate), summed up and brought back to the first time period. This accounts for time value of money, and an NPV of above zero indicates profitability, while an NPV of less than zero indicates otherwise.
- The IRR is the discount rate at which the NPV equals zero. This indicates the maximum rate at which money can be borrowed and the project still breaks even at the end of project life. An IRR of less than the lending rate results in a negative NPV (non-profitable) while an IRR greater than lending rates results in a positive NPV (profitable).

The different items that are required for DCFROR in order to generate the KEIs are discussed in section 5.2 to section 5.4.

5.2. Capital cost estimation

The total capital investment (TCI) represents a once-off expense for the design, construction, and start-up of a new plant or modifications on an existing plant (Seider *et al.*, 2004). TCI is the sum of total fixed capital investment (TFCI), land, and working capital (WC).

Different methods of estimating TCI are available based on the level of information available, and the different estimation methods yield varying levels of accuracy. According to Peters and Timmerhaus (1991), there are five methods of estimation that are normally used for process design purposes. These methods of estimation are: order-of-magnitude (±30% accuracy), study estimate (±30% accuracy), preliminary estimate (±20% accuracy), definitive estimate (±10% accuracy) and detailed estimate (±5% accuracy).

In this study, the study estimate method will be used for capital cost estimation. The study estimate method requires knowledge of the major process equipment e.g pumps, compressors, columns and vessels, heat exchangers etc. Each equipment is (roughly) sized, and an approximate cost is

determined; a factor is then applied on the total cost of equipment to give an estimate of capital cost (Peters and Timmerhaus, 1991; Turton *et al.*, 2009). The study estimate method was chosen for capital cost estimation in this study based on the availability of estimated equipment cost for the different sections of the process in this study. The study estimate method has been used for economic evaluation of various biomass pyrolysis processes (Wright *et al.*, 2010; Dutta *et al.*, 2015; Naleli, 2016).

The approach used for TCI estimation in this study is adopted from the studies of Wright *et al.* (2010), Dutta *et al.* (2015), and Naleli (2016), in which the sum of installed cost of all equipment in the main manufacturing process is calculated and is referred to as inside battery limits (ISBL). ISBL covers the costs associated with purchase, installation, piping, instrumentation and controls of each process equipment (Seider *et al.*, 2004; Naleli, 2016). In this study, ISBL covers equipment in the pre-treatment section, pyrolysis section, separation section and the energy recovery section (for the scenario with energy recovery). Table 41 shows the ISBL for the base case waste tyres to limonene process.

Table 41: ISBL for the waste tyres to limonene base case process

Equipment item	Installed cost (MM$)	Source
Pre-treatment equipment	0.21	Jiangyin Xinda Machinery (2016)
Reactor system	1.26	Pyrocrat Systems LLP (2016)
Heat exchangers	0.27	Aspen Plus® Economic Analyzer
Pumps	0.053	Aspen Plus® Economic Analyzer
Drums	0.11	Aspen Plus® Economic Analyzer
Columns	1.87	Aspen Plus® Economic Analyzer, Turton *et al.* (2009)
ISBL	**3.77**	

From Table 41, it can be seen that the major contributors to ISBL are the distillation columns and reactor system at 50% and 33% contribution respectively. The installed cost for the columns in Table 41 includes the cost of the towers and all the equipment associated with the columns i.e. condensers, reboilers, reflux pumps, and condenser accumulators. The distillation columns have a high installed cost due to the number of theoretical stages required for most of the columns, and the large number of individual equipment associated with the columns. The high installed cost for the reactor system can be attributed to the size and operating temperature of the reactor which in turns requires materials of construction that can withstand the particular operating temperature.

The purchased cost of pre-treatment equipment and the pyrolysis reactor system were obtained from Jiangyin Xinda Machinery (2016) and Pyrocrat Systems LLP (2016) respectively. Installation factors of 3.02 and 3 were applied respectively, to give the total installed costs of pre-treatment and pyrolysis reactor shown in Table 41. The installation factors of 3.02 and 3 were obtained from Wright *et al.* (2010) and Jones *et al.* (2013). Equipment costs quoted for capacities different from this study were adjusted to obtain costs for the corresponding capacity in this study, using the sixth-tenth-factor rule from Peters and Timmerhaus (1991).

The Economic Analyzer of Aspen Plus® V8.6 was used to calculate the purchased and installed costs of minor equipment such as pumps, heat exchangers, and vessels. For equipment costs to be estimated in Aspen Plus®, equipment sizing results should be within particular sizing parameters predetermined by Aspen Plus®. However, other costing techniques such as the Guthrie method are available in literature, which give equipment costs that are just as acceptable as those from Aspen Plus®. Consequently, the purchased and installed costs of distillation column towers used in this study were obtained using the bare module costing technique of Guthrie reported in Turton *et al.* (2009).

ISBL is then used to calculate the total direct cost (TDC) of capital investment by addition of costs for additional piping, site development, and warehouse. These additional costs are calculated as percentages of ISBL, as shown by Wright *et al.* (2010), Dutta *et al.* (2015) and Naleli (2016). The individual components of TDC and their actual amounts for the base case scenario are shown in Table D1 (in Appendix D). The TDC for the base case scenario is 4.43 MM$.

TDC is then used to calculate the total indirect cost (TIC) of capital investment. TIC represents the non-construction costs typically associated with project management and engineering, procurement, and construction services (Dutta *et al.*, 2015). TIC is divided into 5 components (prorateable expenses, field expenses, home office and construction, project contingency and other costs for start-up, permits etc.), which are calculated as percentages of TDC (Wright *et al.*, 2010; Dutta *et al.*, 2015). Table D2 in Appendix D shows the different components of TIC and their actual values for the base case scenario. The TIC for the base case scenario is estimated at 2.66 MM$.

After TIC has been estimated, the remaining components of TCI are total fixed capital investment (TFCI), the cost of land, and working capital (WC). TFCI is the sum of TDC and TIC (Dutta *et al.*, 2015). The cost of land is 2% of TFCI, and WC is normally estimated to be 5% of TFCI (Seider *et al.*, 2004; Jones *et al.*, 2013; Naleli, 2016). The working capital together with the cost of land are recovered at the end

of the project life. The remaining components of TCI together with the TCI for the base case scenario are shown in Table D3 in Appendix D.

From Table D3, it can be seen that the TFCI is estimated at 7.1 MM$, the cost of land is 0.14 MM$, working capital is estimated at 0.35 MM$, and it can be concluded that total capital investment of 7.6 MM$ will be required for the base case scenario.

5.3. Operating cost estimation

The operating cost is the amount of money associated with the day-to-day running of the plant (Turton *et al.*, 2009). The operating cost can be divided into variable and fixed operating costs. The variable operating costs are directly related to production rate, and incurred only during operation, whereas the fixed operating costs are incurred irrespective of the production rate (Turton *et al.*, 2009).

5.3.1. Variable operating costs

The variable operating costs evaluated in this study are the cost of utilities and diethylene glycol (DEG). The cost of whole tyres is not considered, as it is assumed that a REDISA accredited transporter will supply the tyres. The utilities considered in this study are cooling water, steam, electricity, and boiler feed water (for energy recovery). Utilities may be purchased from public or private utility companies, or a company may build their own facilities. The purchased utilities are based on consumption, and purchase of utilities can be assumed for early estimates (Seider *et al.*, 2004). Only the steady-state makeup cost of DEG is considered in this study, as the solvent is recycled. The unit cost of each utility and DEG is given in Table 42. The annual cost of each utility for the base case scenario is given in Table 43.

Table 42: Unit cost of utilities and DEG

Utility	Unit	Unit price ($)	Reference
Cooling water	m^3	1.33[a]	City of Cape Town municipality (2016)
Boiler feed water	Ton	2.45	Turton *et al.* (2009)
HP steam	Ton	12.1	Seider *et al.* (2004)
Electricity	Kwh	0.098[a]	City of Cape Town municipality (2016)
DEG	kg	1.2	Alibaba Group (2016)

[a]Converted from Rands to $

Table 43: Annual cost of variable expenses for base case scenario

Utility	Total cost ($/yr)
Cooling water	275 176
Boiler feed water	
HP steam	24 948
Electricity	104 319
DEG	98 880
Total	**503 323**

From Table 43, it can be seen that cooling water contributes the most to variable operating expenses (±55%), which is due to a high unit cost of cooling water and high process demand for cooling water. The cooling water demand can be attributed to the fact that most of the heat exchangers in the process are coolers/condensers, and a lot of cooling water is also required to condense the reactor volatiles. The cost of electricity is the second highest contributor to the variable costs (±21%), which is largely due to the power requirements of the size reduction (shredding) equipment in the pre-treatment section. From Table 43, it can then be concluded that in order to minimise the variable operating costs, cooling water usage has to be kept as minimum as possible.

5.3.2. Fixed operating costs

The other factor contributing to operating cost is fixed costs. The fixed costs considered in this study are salaries, maintenance and property insurance and taxes; these were adapted from studies by Jones *et al.* (2013) and by Dutta *et al.* (2015).

The total cost of salaries can be estimated based on the cost of operating labour (OL) (Peters and Timmerhaus, 1991). In this study, the amount of operating labour required was adapted from the study done by Muzenda and Popa (2015) and from information obtained from an operational tyre pyrolysis plant in South Africa (Wiese, 2017). Muzenda and Popa (2015) reported that an operational tyre pyrolysis plant in South Africa created sustainable jobs for about 22 people (information about the respective positions they occupied in the plant was not provided). It has been suggested that an average of 4-5 people are typically required per reactor per shift (mostly for a batch plant) (Wiese, 2017). In this study, it is assumed that a total of 4 operators will be required per shift since it is a continuous plant. According to Seider *et al.* (2004) and Turton *et al.* (2009), 5 shifts are required for a chemical plant to account for leave, sick leave and working hours. As such, 5 shifts were considered in

this study to determine the total OL required. The cost of OL in this study is obtained from PayScale (PayScale, 2016).

The different components of fixed operating costs considered in this study are shown in Table 44, and the actual cost of each component, together with total operating cost are shown in Table 45.

Table 44: Components of fixed operating costs used in this study

Item	Value ($/yr)	Reference
OL	7916[a] (per operator)	PayScale (2016)
Supervisor and clerical expenses	15% of OL	Peters and Timmerhaus (1991)
Laboratory charges	15% of OL	Peters and Timmerhaus (1991)
Maintenance	3% of ISBL	Jones *et al.* (2013), Dutta *et al. (*2015)
Property insurance and tax	0.7% of TFCI	Jones *et al.* (2013), Dutta *et al.* (2015)

[a]Converted from Rands to $

Table 45: Actual fixed costs and total operating cost for the base case scenario

Item	Total cost ($/yr)
OL	158 315
Supervisor and clerical expenses	23 747
Laboratory charges	23 747
Maintenance	113 209
Property insurance and tax	49 661
Total fixed costs	**368 679**
Total operating cost	**872 002**

From Table 45, it can be seen that labour cost is the largest contributor to the fixed operating cost (43%), which is largely due to the number of personnel required. An overall total of $872 002 will be required to cover operating costs for the base case process which is largely composed of the costs of cooling water (32%), OL (18%), maintenance (13%), and electricity (12%).

5.4. Estimation of revenue

In this study, revenue is generated from the sale of limonene, crude char, steel, and TDO. Excess steam will be regarded as a saleable product when energy recovery is considered, in order to determine if there is any economic benefit to energy recovery. The price of tyre-derived limonene in this study is

estimated using the price of citrus-derived limonene of the same purity. An average limonene selling price or $12/kg was used in this study based on prices of 95% purity limonene shown in Figure 56. All prices in Figure 56 are 2016 prices unless otherwise indicated.

The prices of char, steel, and TDO were adopted from a waste tyre pyrolysis economic evaluation by Muzenda and Popa (2015). The char is sold in its crude form without any upgrading, and the steel is sold as scrap steel. The different fractions of pyrolysis oil that are recovered from the distillation columns are combined and sold as TDO. The selling price of each product is shown in Table 46. A breakdown of revenue generated by the waste tyre to limonene process is shown in Table 47.

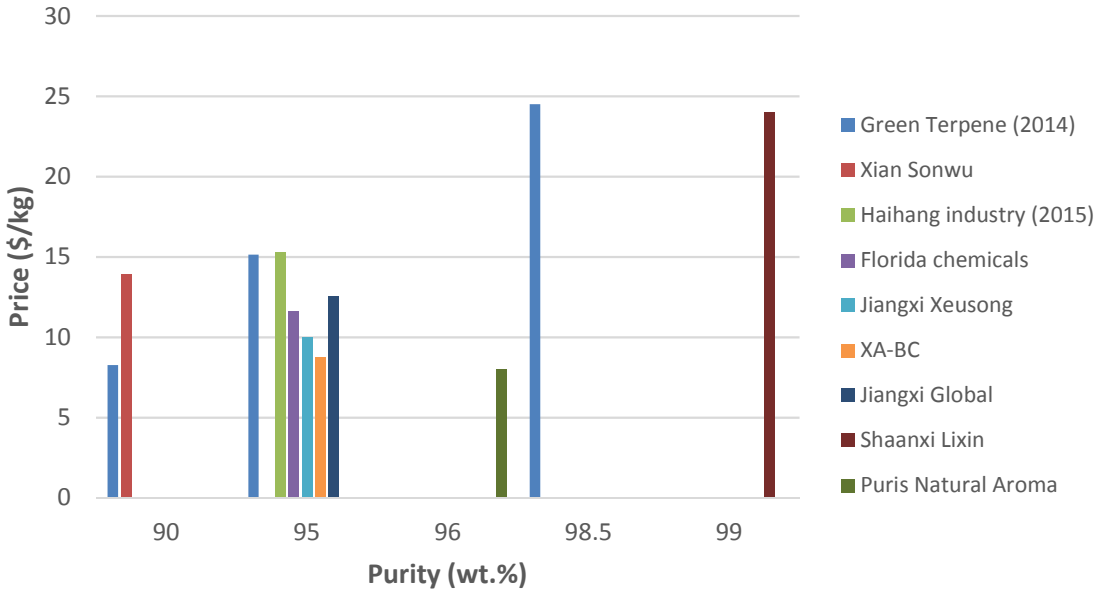

Figure 56: Limonene prices from various suppliers

Table 46: Product selling prices

Product	Unit	Unit price ($)	Reference
Limonene	Kg	12	Florida Chemicals (2016)
Char	Kg	0.037[a]	Muzenda and Popa (2015)
Steel	Kg	0.047[a]	Muzenda and Popa (2015)
TDO	L	0.27[a]	Muzenda and Popa (2015)
Steam	Ton	12.1	Seider *et al.* (2004)

[a]Converted from Rands to $

Table 47: Revenue generation for the base case waste tyre to limonene process

Product	Revenue generated ($/yr)
Limonene	2 688 000
Char	119 093
Steel	46 667
TDO	1 115 733
Steam	
Total	**3 969 493**

From Table 47, it can be seen that the total annual sales for the base case scenario are just below 4 MM$. Table 47 also shows that even though limonene is produced in small quantities (28 kg/h) compared to other products, it is the highest contributor to the revenue stream (±68%), which can be attributed to its high selling price, due to the purity achieved in this study. It can therefore be concluded that the success of the process in this study will be highly dependent on the purity and amount of limonene produced.

Table 47 also shows that TDO contributes the second most to the revenue stream (±28%), despite a low selling price of $0.27/L (R4/L). High revenue contribution from TDO sales can be attributed to a high TDO production volume, as only a small fraction of the oil condensed from the reactor volatiles is lost to the limonene stream. It therefore shows that combining the residual liquid streams from the distillation columns to form the TDO product has a positive impact on revenue generation of the process. Table 47 also shows that steel sales contribute the least (±1%) to the revenue stream, which can be attributed to a low selling price and a lower production rate as compared to char and TDO.

5.5. Profitability analysis

In this study, a conservative prime interest rate linked minimum IRR of 12% is adopted for determination of feasibility, based on historical trends from the South African Reserve bank (2016). However, in order to encourage investors to invest in a project, an IRR larger than the prime interest rate needs to be achieved; 25% is typically a rate that investors would look for (Richardson *et al.*, 2007; Robus, 2013). An IRR of 25% is adopted in this study as being the target for all scenarios to show attractiveness to investors.

In this study, the NPV will be evaluated between 12% and 25% DCFROR to determine economic feasibility, and to determine economic attractiveness respectively. The results of profitability analysis for the base case scenario are shown in Table 48.

Table 48: Key economic indicators for the base case scenario

KEI	PBP (years)	NPV at 12% DCFROR (MM$)	NPV at 15% DCFROR (MM$)	NPV at 20% DCFROR (MM$)	NPV at 25% DCFROR (MM$)	IRR (%)
Value	2.9	6.3	4.7	2.7	1.1	30

The KEIs presented in Table 48 show that the base case process evaluated in this study will be both economically feasible and economically attractive, owing to the positive NPV value at 12% DCFROR and an IRR higher than 25%. The economic attractiveness of the base case scenario can be attributed to high revenue generation from the sales of the high value limonene, and the fact that the residual TDO adds to the revenue stream, in addition to sales of char and steel. It can also be seen that the base case scenario meets the desired PBP requirement of less than 4 years (3 years), which would increase its attractiveness to investors.

The IRR and PBP shown in Table 48 are comparable to those of the study by Pilusa *et al.* (2014) who obtained an IRR of 29% and a PBP of between 2 and 3 years for their 30 tons/day process aimed at producing light-diesel equivalent fuel and refined carbon black as the main products. In the process of Pilusa *et al.* (2014), 465 L/hr of the light-diesel equivalent fuel were produced, and sold for $0.52-0.55/L, whereas 458 kg/hr of refined carbon black were produced, and sold for $0.27- 0.29/kg.

5.6. Scenario analysis and comparison

In this section, the base case scenario that was evaluated in sections 5.2 to 5.5 is compared with other several scenarios. These scenarios are: the addition of an energy recovery section to the base case scenario (energy recovery), other pre-treatment scenarios (pre-treatment to crumb and no pre-treatment/crumb purchase), and the process scenario of waste tyre pyrolysis for TDO production (TDO production). In this study, comparison of the base case scenario with the other scenarios was performed on the basis of TCI, operating costs, revenue, and profitability (KEIs used for profitability).

In the “no pre-treatment/crumb purchase” scenario, a crumb flow rate of 30 tons/day is used (fed to the reactor), which is similar to the 30 tons/day flow rate of whole tyres used for the other scenarios (although only 90% is fed to the reactor in the other scenarios). For comparison of operating costs,

the cost of crumb has to be taken into account for the crumb purchase scenario, in addition to the items in Table 42 and Table 44. The cost of crumb was obtained from Dawhi Rubber Recycling (2016), Energia Rubber Tech (2016), and Mathe Group (2016), as shown in Figure D2 (in Appendix D); an average value of R3.5/kg ($0.23/kg) was used in this study. Comparison of the different scenarios is shown in Table 49.

Table 49: Comparison of the different scenarios

Scenario	Base case	Energy recovery	Pre-treatment to crumb	No pre-treatment	TDO production
TCI (MM$)	7.6	8.2	9.1	7.4	3.3
Variable operating costs ($/yr)	503 323	545 763	887 875	2 748 803	247 941
Fixed operating costs ($/yr)	368 679	381 557	400 118	355 594	277 381
Total operating costs ($/yr)	872 002	927 320	1 287 993	3 104 397	525 323
Revenue ($/yr)	3 969 493	4 222 269	3 969 493	4 360 560	1 392 427
IRR (%)	30	27	20	8	17
NPV at DCFROR (MM$)					
12%	6.3	5.6	3.4	-1.1	0.71
15%	4.7	4	2	-1.9	0.25
20%	2.7	2	0	-2.8	-0.35
25%	1.1	0.45	-1.3	-3.5	-0.8
30%	0	-0.72	-2.3	-4	-1.1
PBP (years)	2.9	3.2	3.9	6.1	4.4

From Table 49, it can be seen that capital investment of 8.2 MM$ (8% higher than base case) will be required if the energy recovery section is added to the base case scenario, which is due to additional equipment required for boiler feed water supply and steam generation. It can also be seen that the pre-treatment to produce (steel-free) crumb scenario has the most TCI requirements (about 9 MM$), due to additional equipment required to reduce the size of tyre chips to crumb size. It can also be seen that even though there is no pre-treatment equipment required for the no pre-treatment scenario, the TCI requirement is only about 2% lower than for the base case scenario. The difference is only 2%

as equipment cost in the crumb purchase scenario was scaled up (sixth-tenth-factor rule) to account for an increase in flow rate from the value of the base case scenario. A slight increase in equipment cost (to account for the slightly increased flow rate) would cancel out the cost savings from having no pre-treatment equipment, as the major contributors to TCI are present even in the crumb purchase scenario. Table 49 also shows that the TCI requirement for the TDO production scenario is 43% of the TCI for the base case scenario, as no distillation columns are required for the TDO production scenario.

On the basis of operating costs, Table 49 shows that the total operating cost of the base case scenario increase by 6% with addition of the energy recovery section, which is due to slightly higher electricity costs (7%) from additional requirements by the boiler feed water pump. The cost of boiler feed water also increases the total operating cost with energy recovery, as steam is generated in excess to utilise all possible recoverable energy in the flue gas. The operating cost of the pre-treatment to crumb scenario is 48% higher than the cost of the base case scenario, which is due to additional electricity costs incurred from crumbing the tyre chips, as tyre size reduction applications are energy intensive. Table 49 also shows that the no pre-treatment scenario has the largest operating cost (3.1 MM$/year), which is largely due to the cost of crumb. The cost of crumb contributes 74% to the total operating cost for the no pre-treatment (crumb purchase) scenario. It can also be seen that the operating cost of the TDO production scenario is 38% lower than of the base case scenario. The lower operating cost of the TDO production scenario is due to less utility requirements as compared to the base case scenario, as TDO production involves less unit operations.

Evaluation of revenue generation shows that adding the energy recovery section to the base case scenario increases the revenue by 6% (to 4.22 MM$) due to addition of steam sales, as steam is generated in excess (relative to process requirements). Table 49 shows that the revenue generated from the crumb purchase scenario is 10% higher than the base case scenario even though there are no steel sales in the crumb purchase scenario. A slightly higher revenue in the crumb purchase scenario can largely be attributed to an increased production of limonene, since 10% more material is available for conversion to limonene. It can also be noted that the revenue generated in the TDO production scenario is considerably (65%) lower than the revenue generated in the limonene production scenario. The lower revenue generated is a result of no limonene sales in the TDO production scenario (in the limonene production scenario, the sales of limonene contribute about 65% of the revenue even though the limonene flow rate is considerably lower compared to the TDO flow rate). Even though revenue generation of some other scenarios is different from the base case scenario, the true effects of the various scenarios can only be ascertained through profitability evaluation.

In terms of profitability, it can be seen from Table 49 that the base case scenario is the best performing scenario, whereas the no pre-treatment scenario is the worst performing scenario and will not be economically feasible as the IRR achieved is less than 12%. The no pre-treatment scenario also has a PBP of 6.1 years, which also makes it unattractive for investment. It can also be seen that, of the other 3 scenarios (besides the base case scenario), addition of the energy recovery section to the base case scenario is the only other scenario that achieves economic attractiveness (IRR≥25%). It can also be concluded that there currently is no economic benefit to energy recovery in the waste tyre pyrolysis process, as the profitability of the base case scenario decreased from 30% to 27% with addition of the energy recovery section.

Table 49 also shows that the PBP of the pre-treatment to crumb and TDO production scenarios are 3.9 and 4.4 years respectively, which further shows that they will be economically unattractive (maximum PBP of 4 years is typically desired for a chemical plant to be economically attractive). The additional cost of crumbing in the pre-treatment to crumb scenario makes the process economically unattractive even though economic feasibility is still achieved. The absence of sales of the high value limonene in the TDO contribute largely to the economic unattractiveness of the TDO production scenario as demonstrated by the low revenue shown in Table 49.

On the basis of the IRR values shown in Table 49, the limonene product would have to be sold at $14.2/kg in order to achieve economic attractiveness (IRR=25%) for the pre-treatment to crumb scenario. In order for the crumb purchase (no pre-treatment) scenario to attain economic feasibility (IRR=12%), the limonene product would have to be sold at $13.3/kg, or the crumb would have to be purchased at $0.2/kg (R3/kg). The crumb purchase scenario will then only attain economic attractiveness if the limonene product is sold at $17.7/kg or if the crumb feed is purchased at $0.09/kg (R1.4/kg). For the TDO production scenario, the TDO selling price will have to be set at $0.33/L (R5/L) in order for the process to achieve economic attractiveness.

5.7. Sensitivity analysis

The results of KEIs shown in Table 49 only indicate profitability at fixed/base economic conditions adopted for this study. Sensitivity analysis then becomes necessary to determine how a particular process performs with variations in key economic parameters (Robus, 2013). In this study, an economic sensitivity analysis was performed to study the effects of variation in key parameters on the economic viability of the base case scenario (best performing scenario). The parameters that have been selected for sensitivity analysis in this study are reactor system cost, distillation columns cost, operating expenditure/cost (OPEX), limonene price, TDO price, limonene yield, exchange rate and the

discount rate. A parameter variation of ±50% of the respective base case values has been investigated in this study. The base case value of each parameter investigated is shown in Table 50.

According to Turton *et al.* (2009), any economic indicator can be used as a measure of profitability; however, according to Seider *et al.* (2004), NPV and IRR are effective measures of profitability. In this study, sensitivity analysis was performed to study the effects of variation of the various key parameters on the NPV and IRR. For the discount rate, only the effect on NPV is considered.

Table 50: Base case values for key parameters used for sensitivity analysis in this study

Parameter	Value	Unit
Reactor system cost	1.26	MM$
Distillation columns cost	1.87	MM$
OPEX	872 002	$/yr
Limonene price	12	$/kg
TDO price	0.27	$/L
Limonene yield	2.52	Wt.%
Exchange rate	15	R/$
Discount rate	12	%

The effect of variation of each key parameter on the NPV is shown in Figure 57. The effect of variation on the NPV is expressed as a percentage deviation from the NPV at base case conditions.

It is clear from Figure 57 that the process is more sensitive to changes in the cost of distillation columns, limonene selling price, and the yield of limonene, based on the slopes of the curves (both positive and negative). The high sensitivity of the process towards the cost of distillation columns could be due to the fact that column costs contributed the most (50%) to the ISBL in this study, from which the capital cost was calculated. It should also be noted that capital cost is an expense incurred in the very beginning of the project, and exerts a high negative influence on the discounted cash flow as subsequent cash flows are increasingly discounted the further from the beginning they are. It can thus be expected that items that have a huge influence on the TCI will also have a noticeable impact on the economics of the process, since TCI is a large value compared to other expenses and cash flow in this study.

Limonene sales contributed about 68% of the revenue generated in this study, which could explain the high sensitivity of the process towards the selling price of limonene, as revenue represents the

largest positive aspect of cash flow. The curve of limonene price superimposes on the limonene yield curve (only the limonene price curve is visible in Figure 57), as any changes made to the amount of limonene produced has the same effect as changing the limonene price by the same factor.

Figure 57 also shows that the process is least sensitive to changes in the OPEX and the exchange rate. This pattern could be explained by the low operational costs incurred in this study (compared to TCI and revenue), and the fact that the major contributor to revenue (limonene) is not affected by the rand/dollar conversion, as the price was sourced in dollars in this study. It can also be noted that the process does show some considerable sensitivity towards the TDO selling price, probably due to the large amount of TDO produced, which generates about 28% of the revenue.

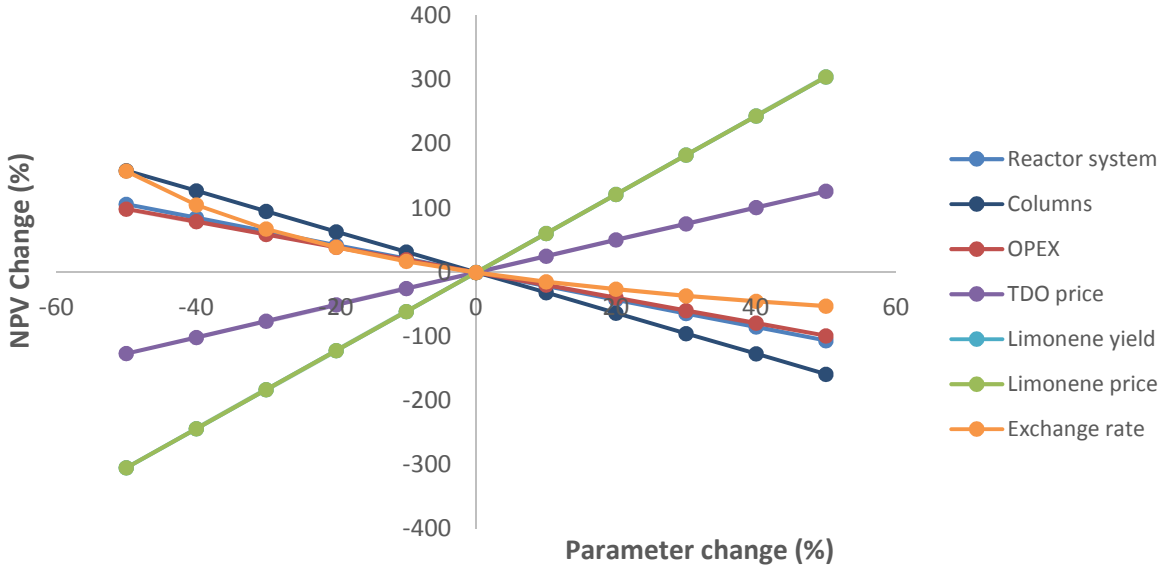

Figure 57: Effect of variation of key parameters on NPV at 25% DCFROR

The actual effect of each parameter shown in Figure 57 on IRR is shown in Figure 58. The minimum acceptable discount rates required for feasibility (12%) and to attract investors (25%) are shown on the graph as well.

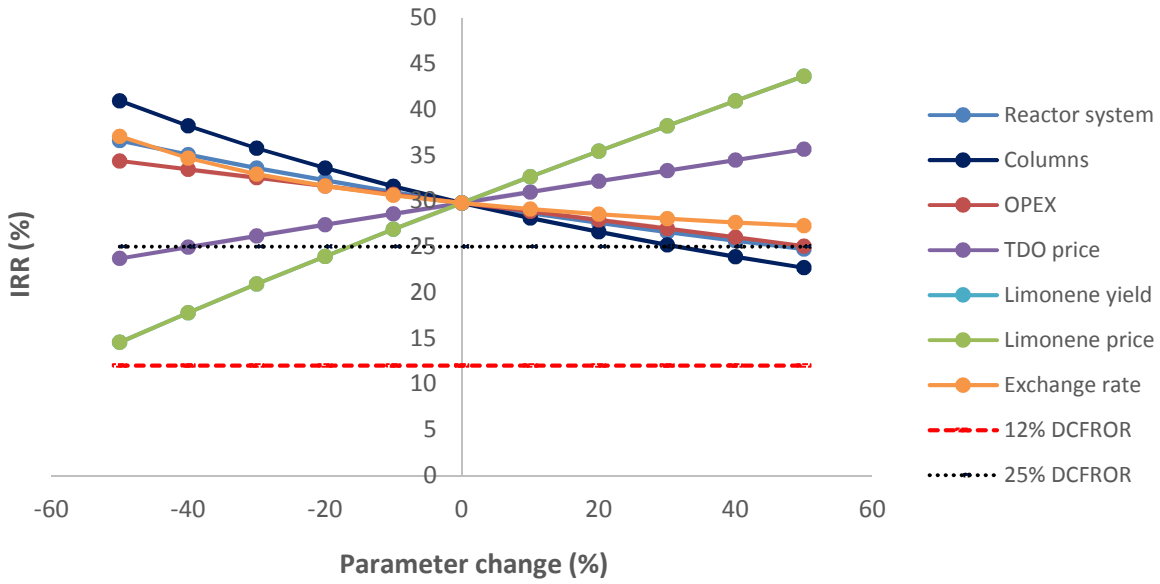

Figure 58: Effect of variation of key parameters on the IRR

From Figure 58, it can be seen that the greatest values of IRR can be achieved by varying the cost of columns, limonene selling price, and the limonene yield (as also observed in Figure 57). It can be seen that an IRR of as high as 41% can be achieved with a -50% change in the cost of columns whereas the IRR drops to 23% with an increase of 50%. To achieve an IRR of 25% (to attract investors), a maximum (installed) cost of $2 466 429 (31% increase) can be spent on the distillation columns, whereas a maximum cost of $5 280 878 (181% increase) should be spent to ensure 12% IRR. For the reactor system (another TCI component varied), it has been calculated that a maximum (purchased) cost of $1 533 339 (271% increase) can be afforded to ensure the minimum acceptable IRR of 12%, whereas a maximum of $615 543 (47% increase) should be spent to ensure 25% IRR.

Figure 58 also shows that a 50% drop in limonene price or limonene yield does not render the process economically infeasible (IRR<12%), whereas an IRR of 44% can be achieved with a 50% increase in either parameter. A price or yield drop of 58% is required to reduce the IRR of the process to below 12%. It can also be seen that a price or yield drop of more than 16% results in an IRR of less than 25%, which would not be desirable for investors. A minimum limonene selling price of $5.1/kg is required to maintain an IRR of 12%, whereas a minimum selling price of $10/kg is required for the process to maintain 25% IRR. The process requires a minimum limonene yield of 1.1 wt.% (on the basis of a steel-free tyre feed) to achieve 12% IRR, whereas a minimum yield of 2.1 wt.% is required to attain 25% IRR. At the base case limonene price and yield, a minimum overall limonene recovery (in the limonene product stream) of 40% is required to achieve 12% IRR, whereas a minimum overall recovery of 79%

is required to ensure 25% IRR. The overall limonene recoveries of 40% and 79% are based on the limonene produced in the pyrolysis reactor.

It is also evident from Figure 58 that even though the selling price of TDO does not exert much effect on the IRR, a change of more than -40% in the TDO price will cause the IRR of the process to fall below 25%, which would not be desirable. A minimum TDO selling price of $0.16/L (R2.4/L) is required to ensure 25% IRR, whereas the minimum acceptable IRR of 12% can be achieved even without any TDO sales (17% IRR). It can also be seen that it would take an increase of around 50% for either the OPEX or the exchange rate to really influence the economic attractiveness of the process. The process would remain attractive to investors up to an exchange rate of R41/$ (173% increase), largely to a huge drop in the resulting cost (in dollars) of cooling water and electricity, coupled with that the limonene price in this study is independent of the exchange rate.

Due to the difficulty in predicting future economic conditions (which would influence the minimum acceptable IRR), a sensitivity analysis of the discount rate was performed to investigate the effect it has on NPV as shown in Figure 59. A discount rate range of 5-35% was considered in this study. It can be seen from Figure 59 that the NPV decreases sharply with increasing discount rate and it can also be concluded that above a discount rate of 30%, the project will start running at a loss.

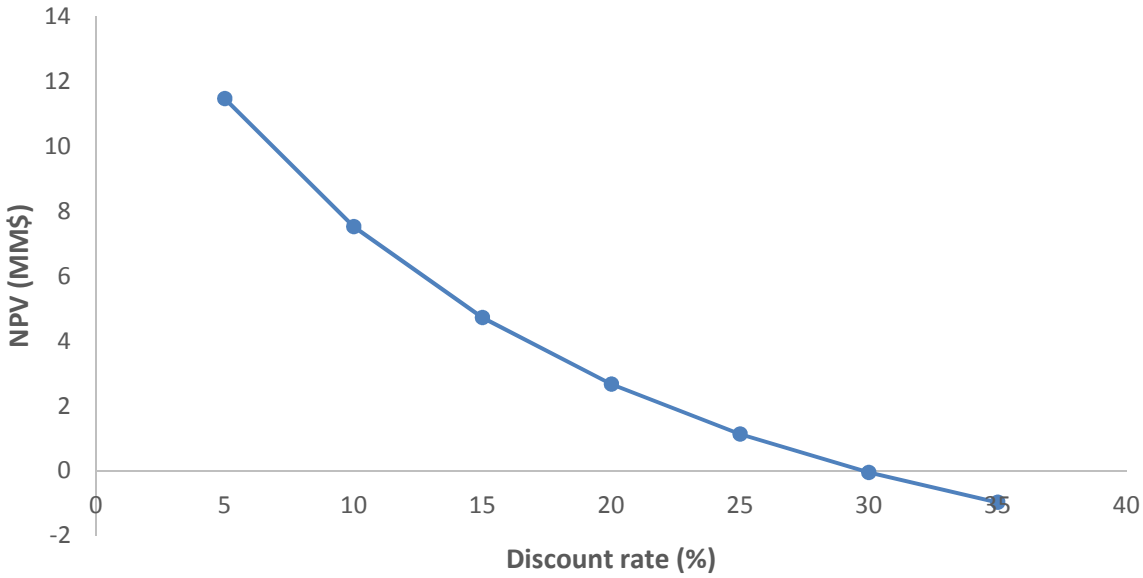

Figure 59: Effect of discount rate on NPV for base case scenario

In this study, it was deemed necessary to also investigate the effect of production capacity on the IRR of the process, to determine the feed rates necessary to ensure the minimum acceptable 12% IRR and the 25% IRR required to attract investors. The effect of feed rate was investigated within a tyre feed

range of 10 -100 tons/day, which is a range that has been used for waste tyre pyrolysis studies in literature (Wojtowicz and Serio, 1996; Muzenda and Popa, 2015).

For scaling of the process to determine the flow rates required for 12% and 25% IRR, the capital and operating costs, and the revenue generated were adjusted by a factor equivalent to dividing the new flow rate by 30 tons/day (base case flow rate). The TCI was adjusted through equipment costs by using the sixth-tenth-factor rule. Consequently, fixed operating costs that are calculated as percentages of components of the TCI were also automatically adjusted through changes in the TCI. The variable operating costs and revenue were directly multiplied by the resultant factor, to obtain corresponding values for a particular new flow rate. The effect of variation in production capacity on the IRR is shown in Figure 60.

From Figure 60, it can be seen that the IRR shows a sharp increase with increasing production capacity, especially at higher feed rates, which could be attributed to the effects of economy of scale at higher feed rates. The increase in TCI is not linear since it was adjusted using the sixth-tenth-factor rule, and it can be expected that the benefits of increased limonene production will far outweigh the increased TCI at higher feed rates. Figure 60 also shows that a minimum tyre feed rate of just over 20 tons/day (23 tons/day) is required to ensure that the process is economically attractive to investors. It can also be seen that a minimum flow rate of just over 10 tons/day is required to ensure that the process achieves the minimum acceptable IRR.

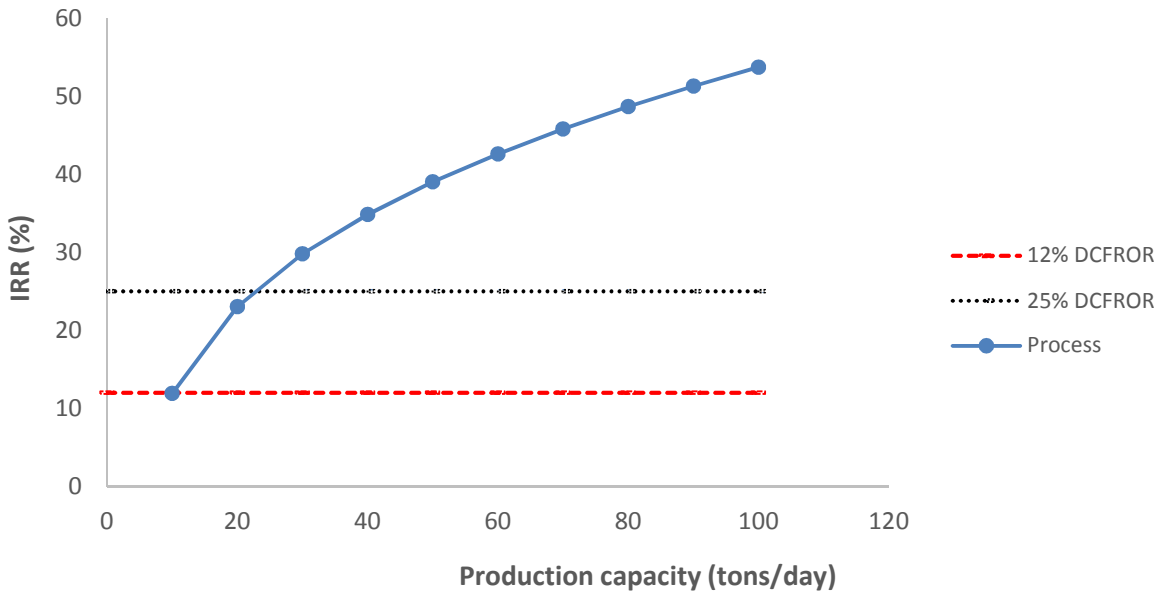

Figure 60: Effect of production capacity on IRR

Figure 60 also shows that an IRR as high as 54% can be achieved at a feed rate of 100 tons/day, however, high feed rates might not be sustainable, which would greatly affect the profitability of the process. According to information received from two operational REDISA-affiliated tyre pyrolysis plants that process 20 - 30 tons/day of tyres each, tyre supply is one of the bottlenecks encountered, as REDISA is responsible for setting up a network of tyre collectors and suppliers (Jefferies, 2017; Wiese, 2017). Information received from REDISA about waste tyre collection and processing in the Western Cape for the period December 2014 to June 2016 (Figure D4 in Appendix D) also shows that 993 tons/month (33 tons/day) was the average difference between the amount of tyres collected and the amount processed (Seebran, 2016).

It can thus be argued that at the current moment (also taking into account that the waste tyre recycling industry in South Africa is in its infancy stages), high tyre feed rates such as 100 tons/day might not be sustainable. As such, profitability projections based on such high flow rates would most likely be negatively affected as there might not be enough revenue generation to overcome the increased TCI associated with the high flow rates. It can also be argued that with a better-developed/improved waste tyre recycling industry, scale-ups of the current 30 tons/day process to higher tyre feed rates could be possible, and as such, could be recommended in future.

5.8. Summary

In this chapter, the base case conceptual process scenario for limonene recovery from waste tyre pyrolysis was evaluated on the basis of economic performance. TCI, operating costs, revenue generation, profitability and sensitivity analysis were evaluated for the process. The base case process scenario was then compared with the energy recovery scenario, other pre-treatment scenarios and the process scenario of waste tyre pyrolysis for TDO production.

The base case scenario for limonene recovery was found to be economically feasible at current economic conditions when considering a 30 tons/day process. The base case scenario had a PBP of just under 3 years, an IRR of 30% with an NPV of 6.3 MM$ at the minimum acceptable IRR of 12%. It was also found that sales of the residual TDO collected during the process are also vital in ensuring that the base case scenario remains attractive to investors. Sensitivity analysis of KEIs showed that changes in the cost of distillation columns, limonene selling price, and the yield of limonene are the main factors influencing the profitability of the process. A minimum tyre flow rate of 23 tons/day is required in order for the process to be economically attractive to investors (25% IRR).

Scenario comparison showed that addition of an energy recovery section to the base case scenario served to bring a negative overall effect on profitability, as the additional capital and operating costs outweigh the additional benefits brought by steam sales. Comparison of the base case scenario with other pre-treatment scenarios indicated that the pre-treatment option used in this study is the most economical of the scenarios. The no pre-treatment scenario (crumb purchase) showed to be the least economical pre-treatment option, largely due to the cost of crumb. The no pre-treatment scenario fails to meet the 12% minimum acceptable IRR criteria as it only achieves an IRR of 8%.

When comparing the base case scenario with the tyre pyrolysis for TDO production scenario, it was demonstrated that the TCI and operating cost of producing TDO are notably lower than for limonene recovery. Revenue generation from the TDO production scenario is also considerable lower than for limonene recovery, as there are no sales of the high value limonene. The TDO production scenario showed that it would not be economically attractive for investment under the current TDO selling price of $0.27/L, with an IRR of 17%, even though the IRR generated is higher than the minimum required IRR of 12%.

CHAPTER 6: CONCLUSIONS AND RECOMMENDATIONS

6.1. Conclusions

The aim of this study was to evaluate the economic feasibility of recovering valuable chemicals from waste tyres through different pyrolysis and separation processes. The aim was set out to be achieved through addressing the following objectives:

Objective 1: Investigating current technologies available to convert waste tyres into various valuable chemicals

A thorough literature review of various current methods/technologies used as pathways for dealing with the waste tyre generation problem was conducted in this study. The analysis demonstrated that the most common pathways include methods such as direct disposal, material recovery and recycling and thermal treatment. Direct disposal includes landfilling and stockpiling, material recovery commonly includes crumbing, milling/grinding, re-treading, devulcanisation and civil engineering applications whereas thermal treatment mainly includes incineration with energy recovery, gasification and pyrolysis. Of all these current methods for dealing with waste tyres, it was concluded that the pyrolysis technology is the most suitable pathway for converting waste tyres into various valuable chemicals. It was found that the liquid product fraction of waste tyre pyrolysis contains potentially valuable chemicals such as the BTX compounds, styrene, ethylbenzene and limonene, which makes pyrolysis the ideal technology.

Objective 2: Proposing and developing various conceptual process scenarios for converting waste tyres into targeted valuable chemicals

Limonene was selected as the valuable chemical of interest in this study based on its wide industrial uses and the high selling price that it could potentially command. This study therefore focused on developing a process that would enable the recovery of limonene from waste tyres via the pyrolysis technology.

A conceptual base case process scenario was proposed and developed by adapting typical process steps of waste tyre pyrolysis processes and combining them with an adapted version of the process developed by Ngwetjana (2017) for recovering limonene from TDO using diethylene glycol. The typical process steps involved in waste tyre pyrolysis were adapted from pyrolysis processes developed in several literature studies; the steps were considered up to recovery of primary pyrolysis products. It was concluded that the following process steps are required for the base case scenario: pre-treatment,

pyrolysis, magnetic separation of char and steel, condensation of reactor volatiles, fractional distillation, extractive distillation using a solvent and solvent regeneration. Pre-treatment included de-beading and shredding of whole tyres to form tyre chips, fractional distillation was required to produce a limonene-rich stream whereas diethylene glycol was used as the solvent for extractive distillation. It was determined that energy recovery from combustion of the pyrolysis gas does not form part of the base case scenario and could only be considered for preliminary economic investigation purposes.

Four other process scenarios were proposed that were just either alternatives of the pre-treatment step of the base case scenario or alternatives of the whole base case scenario (pre-treatment to form crumb, no pre-treatment, addition of an energy recovery section and pyrolysis for TDO production). No additional PFDs were developed for these other proposed scenarios as their PFDs could just be derived from the PFD of the base case process scenario. It was concluded that the other scenarios would be for economic comparison purposes with the base case scenario.

Objective 3: Developing Aspen Plus® models/simulations for the different scenarios developed

A model of the base case process scenario was developed and evaluated using Aspen Plus® V8.6. Physical properties for all conventional components were estimated using the PR-BM thermodynamic model except for the solvent extraction and solvent regeneration columns in which the NRTL and UNIFAC property models were used. For non-conventional components, enthalpy and density were calculated using the HCOALGEN and DCOALIGT property models.

Validation of the PR-BM and NRTL thermodynamic models by comparing model-predicted thermodynamics with literature experimental data revealed that there was some error in predicting the pure component heat capacities with use of the PR-BM model. Both the PR-BM and NRTL models also showed some error in predicting the equilibrium phase distribution of some compounds within the TDO, due to prediction of binary interaction parameters using Aspen Plus®. A need for experimentally determined phase equilibrium parameters of TDO compounds was highlighted.

Simulation results indicated that the process was able to produce a limonene stream of 95.1 wt.% limonene purity at a flow rate of 28 kg/hr. The limonene purity achieved was sufficient to meet the market product specification of 95 wt.% limonene purity required for technical grade limonene. A limonene recovery of 96% was achieved in the limonene stream on the basis of the limonene-rich stream feed, which translated to an overall limonene recovery of 94% on the basis of the limonene produced in the pyrolysis reactor. Normal distillation was able to separate the solvent used and the

entrained impurities; the solvent was recycled back at sufficient recovery and purity (99%), which reduced the demand for make-up solvent.

Objective 4: Evaluation of the various scenarios from techno-economic and energy utilisation viewpoints

A discounted cash flow analysis was performed for the various scenarios (base case, pre-treatment to crumb, no pre-treatment, energy recovery and TDO production) and compared on the basis of IRR, PBP and NPV. Economic analysis showed that the base case scenario was both feasible and attractive for investment with an IRR of 30%, a PBP of 2.9 years, and NPV values of 6.3 and 1.1 MM$ at 12% and 25% IRR respectively. The base case scenario was found to require TCI of 7.6 MM$, total operating cost of $872 002/year and generated 4 MM$/year. It was also demonstrated that TDO sales are also necessary to ensure the process remained economically attractive.

Economic comparison of the base case scenario with the other scenarios revealed that the base case scenario was the best performing scenario. The worst performing scenario was found to be the no pre-treatment scenario with an IRR of 8%, a PBP of 6.1 years and an NPV of -1.3 MM$ at 12% IRR. Evaluation of the energy recovery scenario indicated that addition of an energy recovery section to the base case scenario had an overall negative effect on the profitability of the process. From evaluation of the TDO production scenario, it was concluded that waste tyre pyrolysis for limonene recovery (with residual TDO sold as fuel) is more economically feasible than selling all the TDO produced as fuel.

Sensitivity analysis of the base case scenario (best performing scenario) showed that the process is mostly influenced by changes in the cost of distillation columns, limonene selling price and the yield of limonene. In order to remain economically attractive to investors (25% IRR), the process required a minimum limonene selling price of $10/kg, which was 83% of the assumed price of citrus-derived limonene used as reference. A minimum limonene yield of 2.1 wt.% (on a steel-free basis) was required for the process to achieve 25% IRR for economic attractiveness, which is within the common limit of limonene yield found in literature. It was also found that changes in OPEX and the exchange rate affect the feasibility of the process the least.

With respect to energy utilisation, an evaluation of the energy requirements of each process equipment of the base case scenario was performed with the aid of Aspen Plus® V8.6 and supplier quotes. It was found that the pyrolysis reactor accounted for 73% (544 kW) of the total heating requirements of the process. The pyrolysis reactor volatiles condenser had the most requirement for

cooling utilities (235 kW) which represented 52% of the total cooling requirements of the process. Heating of the oil feed stream to the first separation column with hot reactor volatiles was found to reduce the demand for both heating and cooling utilities by 19 kW, with annual savings of $14 000 in utility costs. With addition of an energy recovery section to the base case scenario, it was found that the process was able to supply the heating requirements of the pyrolysis reactor and all the steam requirements.

6.2. Recommendations

The limonene product recovered in this study represented less than 7% of the pyrolysis oil produced, with the majority of the remaining oil fraction sold as a low value TDO product. The sales of TDO represented 28% of the revenue generated in this study, which demonstrated the importance of the residual TDO to the economic success of the limonene recover process. Further work could consider conversion of the residual TDO into carbon black that could be used in the tyre manufacturing process (carbon black would have higher market value than TDO as a fuel).

The current study demonstrated economic feasibility of a process that targeted the recovery of a single valuable compound only (limonene) from the pyrolysis oil produced. Further work could look at expanding the scope of the current study by evaluating the recovery of other high value compounds in the oil that are usually present in large quantities, like the BTX compounds and styrene, in addition to limonene. Styrene could be re-used in the manufacturing of styrene-butadiene rubber that could be used in tyre formulation, thereby forming a tyre raw material recycle loop.

Due to a wide variety of chemical compounds in pyrolysis oil, prediction of product distribution was limited to compounds for which polynomial equations could be developed. Further work could consider generation of reaction kinetic data that would be used to develop kinetic models of formation of targeted (valuable) compounds. Prediction of product distribution based on kinetic models could greatly improve the accuracy of simulation results, which would lead to improved equipment sizing results. The kinetic models developed could also then be implemented in optimisation of pyrolysis conditions depending on targeted (valuable) compounds.

REFERENCES

Abdelouahed, L., Authier, O., Mauviel, G., Corriou, J.P., Verdier, G. and Dufour, A. 2012. Detailed modeling of biomass gasification in dual fluidized bed reactors under Aspen Plus. *Energy & Fuels*, *26*(6), pp.3840-3855.

Adeyemi, I. and Janajreh, I. 2015. Modeling of the entrained flow gasification: Kinetics-based ASPEN Plus model. *Renewable Energy*, 82, pp.77–84.

Adhikari, B., De, D. and Maiti, S. 2000. Reclamation and recycling of waste rubber. *Progress in Polymer Science (Oxford)*, 25(7), pp.909–948.

Aguado, J., Serrano, D.P. and Escola, J.M. 2008. Fuels from waste plastics by thermal and catalytic processes: A review. *Industrial and Engineering Chemistry Research*, 47(21), pp.7982–7992.

Ahmed, A.M.A., Salmiaton, A., Choong, T.S.Y. and Azlina, W.W. 2015. Review of kinetic and equilibrium concepts for biomass tar modeling by using Aspen Plus. *Renewable and Sustainable Energy Reviews*, *52*, pp.1623-1644.

Al Amoodi, N., Kannan, P., Al Shoaibi, A. and Srinivasakannan, C. 2013. Aspen Plus simulation of polyethylene gasification under equilibrium conditions. *Chemical Engineering Communications, 200*(7), pp.977-992.

Alibaba Group ®.2016. [Online] Available from http://www.alibaba.com/. [Accessed on: 22 August 2016].

Alqahtani, A., Hellgardt, K., Holdich, R. and Cumming, I. 2007. Integrated knowledge based system for process synthesis. *Computer Aided Chemical Engineering*, *24*, p.437

Alsaleh, A. and Sattler, M.L., 2014. Waste Tire Pyrolysis: Influential Parameters and Product Properties. *Current Sustainable/Renewable Energy Reports*, 1(4), pp.129–135.

Altayeb, R.K. 2015. Liquid fuel production from pyrolysis of waste tires : process simulation , exergetic analysis , and life cycle assessment, MSc thesis, Department of Chemical Engineering, American University of Sharjah

Amari, T., Themelis, N.J. and Wernick, I.K., 1999. Resource recovery from used rubber tires. *Resources Policy*, 25(3), pp.179–188.

Ambrose, D. and Hall, D.J. 1981. Thermodynamic properties of organic oxygen compounds L. The vapour pressures of 1,2-ethanediol (ethylene glycol) and bis(2-hydroxyethyl) ether (diethylene glycol). *The Journal of Chemical Thermodynamics*, *13*(1), pp.61-66.

Arabiourrutia, M., Lopez, G., Elordi, G., Olazar, M., Aguado, R. and Bilbao, J. 2007. Product distribution obtained in the pyrolysis of tyres in a conical spouted bed reactor. *Chemical Engineering Science*, *62*(18), pp.5271-5275.

Ashour, I., Fatemi, A., Vakili-Nezhaad, G. and Al-Rawahi, N. 2011. *Applications of Equations of State in the Oil and Gas Industry* (pp. 165-178). INTECH Open Access Publisher.

ASPEN TECHNOLOGY. 2009. Aspen Simulation User guide. Burlington, MA: Aspen Technology.

ATA Engineering. 2015. Conceptual design. [Online] Available from: http://www.ata-e.com/-http://www.ata-e.com/services/conceptual. [Accessed: 18 April 2015].

Aydin, H. and Ilkiliç, C. 2012. Optimization of fuel production from waste vehicle tires by pyrolysis and resembling to diesel fuel by various desulfurization methods. *Fuel*, 102, pp.605–612.

Aydın, H. and İlkılıç, C., 2015. Analysis of combustion, performance and emission characteristics of a diesel engine using low sulfur tire fuel. *Fuel*, 143, pp.373–382.

Aylón, E., Fernández-Colino, A., Navarro, M.V., Murillo, R., García, T. and Mastral, A.M. 2008. Waste tire pyrolysis: comparison between fixed bed reactor and moving bed reactor. *Industrial & Engineering Chemistry Research*, *47*(12), pp.4029-4033.

Bajus, M. and Olahová, N. 2011. Thermal conversion of scrap tyres. *Petroleum and Coal*, 53(2), pp.98–105.

Barlaz, M.A., Eleazer, W.E. and Whittle, D.J.1993. Potential to use waste tires as supplemental fuel in pulp and paper mill boilers, cement kilns and in road pavement. *Waste management & research*, *11*(6), pp.463-480.

Banar, M., Akyıldız, V., Özkan, A., Çokaygil, Z. and Onay, Ö. 2012. Characterization of pyrolytic oil obtained from pyrolysis of TDF (Tire Derived Fuel). *Energy Conversion and Management*, *62*, pp.22-30.

Bassano, C., Deiana, P. and Girardi, G. 2014. Modeling and economic evaluation of the integration of carbon capture and storage technologies into coal to liquids plants. *Fuel*, 116, pp.850–860.

Benallal, B., Roy, C., Pakdel, H., Chabot, S. and Poirier, M.A. 1995. Characterization of pyrolytic light naphtha from vacuum pyrolysis of used tyres comparison with petroleum naphtha. *Fuel, 74*(11), pp.1589-1594.

Bender, D.L. 2007. Tire retreading - the rationale and a review of technologies. *Rubber World*, 236(6), pp.34–40.

Bennett, G. 1993. Scrap tire technology and markets: by US Environmental Protection Agency and C. Clark, K. Meardon and D. Russell of Pacific Environmental Services, Noyes Data Corp., Park Ridge, NJ, ISBN 0-8155-1317-8, 1993, 316 pp., $54.

Berrueco, C., Esperanza, E., Mastral, F.J., Ceamanos, J. and García-Bacaicoa, P. 2005. Pyrolysis of waste tyres in an atmospheric static-bed batch reactor: Analysis of the gases obtained. *Journal of Analytical and Applied Pyrolysis*, *74*(1), pp.245-253.

Boxiong, S., Chunfei, W., Binbin, G. and Rui, W. 2007. Pyrolysis of waste tyres with zeolite USY and ZSM-5 catalysts. *Applied Catalysis B: Environmental*, *73*(1), pp.150-157.

Brondani, L.B., Flores, G.B. and Soares, R.P. 2015. Modeling and Simulation of a Benzene Recovery Process By Extractive Distillation. *Brazilian Journal of Chemical Engineering*, 32(1), pp.283–291.

CARiD™. 2016. [Online] Available from: https://www.carid.com/articles/the-hidden-secrets-of-tires.html. [Accessed on: 16 October 2016].

Carlson, E.C. 1996. *Don't gamble with physical properties for simulations. Chemical Engineering Progress, 92*(10), pp.35-46.

Chao, L.I., Dai, Z.H., Ji, Y.A.N.G., Yu, G.S. and Wang, F.C. 2015. Modelling and energy analysis of an integrated coal gasification and pyrolysis system for synthetic natural gas. *Journal of Fuel Chemistry and Technology*, *43*(7), pp.779-789.

Chaala, A. and Roy, C. 1996. Production of coke from scrap tire vacuum pyrolysis oil. *Fuel Processing Technology*, 46(3), pp.227–239.

Chemengonline. 2016. [Online] Available from: http://www.chemengonline.com/current-economic-trends-march-2016/?printmode=1. [Accessed on: 10 August 2016].

ChemSpider. 2016. 1, 1, 6-Trimethyl-1, 2-dihydronaphthalene. [Online] Available from: http://www.chemspider.com/Chemical-Structure.108567.html. [Accessed on: 01 November 2016].

ChemSpider. 2016. 1, 2, 4-Trimethylenecyclohexane. [Online] Available from: http://www.chemspider.com/Chemical-Structure.496197.html. [Accessed on: 01 November 2016].

ChemSpider. 2016. 1, 2, 5, 5-Tetramethyl-1, 3-cyclopentadiene. [Online] Available from: http://www.chemspider.com/Chemical-Structure.497460.html. [Accessed on: 01 November 2016].

Chen, C.C. and Mathias, P.M. 2002. Applied thermodynamics for process modeling. *AIChE Journal*, *48*(2), pp.194-200.

Chen, F. and Qian, J. 2002. Studies on the thermal degradation of cis-1, 4-polyisoprene. *Fuel*, *81*(16), pp.2071-2077.

Cheung, K.Y., Lee, K.L., Lam, K.L., Chan, T.Y., Lee, C.W. and Hui, C.W. 2011. Operation strategy for multi-stage pyrolysis. *Journal of Analytical and Applied Pyrolysis*, *91*(1), pp.165-182.

Chickos, J.S. and Acree, W.E. 2003. Enthalpies of vaporization of organic and organometallic compounds, 1880-2002. *Journal of Physical and Chemical Reference Data*, 32(2), pp.519–878.

Chien, J.C.W. and Kiang, J.K.Y. 1979. Polymer reactions—X thermal pyrolysis of poly (isoprene). *European Polymer Journal*, *15*(11), pp.1059-1065.

Ciriminna, R., Lomeli-Rodriguez, M., Carà, P.D., Lopez-Sanchez, J.A. and Pagliaro, M. 2014. Limonene: a versatile chemical of the bioeconomy. *Chemical Communications, 50*(97), pp.15288-15296.

City of Cape Town. 2016. Electricity tariffs. [Online] Available from:

https://www.capetown.gov.za/en/electricity/Elec%20Tariffs%20201617/ElectricityConsumptiveTariffs-1617.pdf. [Accessed on: 16 August 2016].

City of Cape Town. 2016. Water and sanitation tariffs. [Online] Available from:

https://www.capetown.gov.za/en/Budget/Budget%20201516%20Final/Utility%20Services%20-%20Water%20and%20Sanitation%20-%20Water%20-%20Consumptive%20(20%20percent).pdf. [Accessed on: 16 August 2016].

Choi, G.G., Jung, S.H., Oh, S.J. and Kim, J.S., 2014. Total utilization of waste tire rubber through pyrolysis to obtain oils and CO 2 activation of pyrolysis char. *Fuel Processing Technology*, *123*, pp.57-64.

Clará, R.A., Marigliano, A.C.G. and Sólimo, H.N. 2009. Density, viscosity, and refractive index in the range (283.15 to 353.15) K and vapor pressure of α-pinene, d-limonene,(±)-linalool, and citral over the pressure range 1.0 kPa atmospheric pressure. *Journal of Chemical & Engineering Data*, *54*(3), pp.1087-1090.

Conesa, J.A., Martin-Gullon, I., Font, R. and Jauhiainen, J. 2004. Complete study of the pyrolysis and gasification of scrap tires in a pilot plant reactor. *Environmental science & technology*, *38*(11), pp.3189-3194.

Conesa, J.A., Gálvez, A., Mateos, F., Martín-Gullón, I. and Font, R. 2008. Organic and inorganic pollutants from cement kiln stack feeding alternative fuels. *Journal of Hazardous Materials*, *158*(2), pp.585-592.

Cunliffe, A.M. and Williams, P.T., 1998a. Composition of oils derived from the batch pyrolysis of tyres. *Journal of Analytical and Applied Pyrolysis,* 44(2), pp. 131-152.

Cunliffe, A.M. and Williams, P.T. 1998b. Properties of Chars and Activated Carbons Derived from the Pyrolysis of Used Tyres. *Environmental Technology*, 19(12), pp.1177–1190.

Curry, J. 2010. The Engineering method and Skill development. [Online] Available: http://www.eng.usyd.edu.au/webnet/ENGG1803/UserFiles/File/wk 2-2 Eng Method.pdf [Accessed: 16 December 2010].

Dabić-Ostojić, S. *et al.*, 2014. Applying a mathematical approach to improve the tire retreading process. *Resources, Conservation and Recycling*, 86, pp.107–117.

Dabić-Ostojić, S., Miljuš, M., Bojović, N., Glišović, N. and Milenković, M. 2014. Applying a mathematical approach to improve the tire retreading process. *Resources, Conservation and Recycling*, *86*, pp.107-117.

Danon, B., Van Der Gryp, P., Schwarz, C.E. and Görgens, J.F. 2015. A review of dipentene (dl-limonene) production from waste tire pyrolysis. *Journal of Analytical and Applied Pyrolysis*, *112*, pp.1-13.

Diederichs, G.W. 2015. Techno-economic assessment of processes that produce jet fuel from plant-derived sources, MEng thesis, Department of Process Engineering, Stellenbosch University.

Dıez, C., Martınez, O., Calvo, L.F., Cara, J. and Morán, A. 2004. Pyrolysis of tyres. Influence of the final temperature of the process on emissions and the calorific value of the products recovered. *Waste Management*, *24*(5), pp.463-469.

Díez, C., Sánchez, M.E., Haxaire, P., Martínez, O. and Morán, A. 2005. Pyrolysis of tyres: A comparison of the results from a fixed-bed laboratory reactor and a pilot plant (rotatory reactor). *Journal of Analytical and Applied Pyrolysis*, *74*(1), pp.254-258.

Douglas, J.M. 1988. *Conceptual design of chemical processes*. McGraw-Hill.

Dũng, N.A., Klaewkla, R., Wongkasemjit, S. and Jitkarnka, S., 2009. Light olefins and light oil production from catalytic pyrolysis of waste tire. *Journal of Analytical and Applied Pyrolysis*, *86*(2), pp.281-286.

Dutta, A., Sahir, A., Tan, E., Humbird, D., Snowden-Swan, L. J., Meyer, P., Ross, J., Sexton, D., Yap, R. 2015. Process Design and Economics for the Conversion of Lignocellulosic Biomass to Hydrocarbon Fuels. Thermochemical Research Pathways with In Situ and Ex Situ Upgrading of Fast Pyrolysis Vapors. , (March 2015), p.275.

Edwards, D.W., Danon, B., van der Gryp, P. and Görgens, J.F., 2016. Quantifying and comparing the selectivity for crosslink scission in mechanical and mechanochemical devulcanization processes. *J. Appl. Polym. Sci. 43932 doi: 10.1002/app.43932*

Edwards, J.H., Smith, I.W. and Tyler, R.J. 1980. Flash pyrolysis of coals: comparison of results from 1 gh− 1 and 20 kg h− 1 reactors. *Fuel*, *59*(10), pp.681-686

Emets, S. V., Hoo, K.A. and Mann, U. 2006. A modified hierarchy for designing chemical processes. *Industrial and Engineering Chemistry Research*, 45(14), pp.5037–5043.

Emun, F., Gadalla, M., Majozi, T. and Boer, D. 2010. Integrated gasification combined cycle (IGCC) process simulation and optimization. *Computers & chemical engineering*, *34*(3), pp.331-338

Eriksson, L., Arnhold, T., Beck, B., Fox, T., Johansson, E. and Kriegl, J.M. 2004. Onion design and its application to a pharmaceutical QSAR problem. *Journal of chemometrics*, *18*(3-4), pp.188-202.

Fels, M. and Pegg, M. 2009. A techno-economic and environmental assessment of a tire pyrolysis plant Mort Fels and Michael Pegg Chemical Engineering; Dalhousie University Halifax, NS; Canada. *Carbon*, (2009), pp.2–7.

Fernández, A.M., Barriocanal, C. and Alvarez, R. 2012. Pyrolysis of a waste from the grinding of scrap tyres. *Journal of Hazardous Materials*, 203–204, pp.236–243.

Florida Chemical Co., 1991a. Marketing Data Sheet: d-limonene. Lake Alfred, FL.

Florida Chemical Co., 1991b. Product Data Sheet: d-limonene. Lake Alfred, FL.

Florida Chemical Co., 1991c. Material Safety Data Sheet: d-limonene. Lake Alfred, FL.

Foo, D.C.Y., Selvan, M. and McGuire, M.L. 2005. Integrate process simulation and process synthesis. *Chemical engineering progress*, *101*(10), pp.25-29

François, J., Abdelouahed, L., Mauviel, G., Patisson, F., Mirgaux, O., Rogaume, C., Rogaume, Y., Feidt, M. and Dufour, A. 2013. Detailed process modeling of a wood gasification combined heat and power plant. *Biomass and bioenergy*, *51*, pp.68-82.

François, J., Mauviel, G., Feidt, M., Rogaume, C., Rogaume, Y., Mirgaux, O., Patisson, F. and Dufour, A. 2013. Modeling of a biomass gasification CHP plant: influence of various parameters on energetic and exergetic efficiencies. *Energy & Fuels*, *27*(12), pp.7398-7412.

Frigo, S., Seggiani, M., Puccini, M. and Vitolo, S. 2014. Liquid fuel production from waste tyre pyrolysis and its utilisation in a Diesel engine. *Fuel*, *116*, pp.399-408.

Garcia, P.S., de Sousa, F.D.B., de Lima, J.A., Cruz, S.A. and Scuracchio, C.H. 2015. Devulcanization of ground tire rubber: Physical and chemical changes after different microwave exposure times. *Express Polym. Lett.*, *9*, pp.1015-1026.

Giugliano, M., Cernuschi, S., Ghezzi, U. and Grosso, M. 1999. Experimental evaluation of waste tires utilization in cement kilns. *Journal of the Air & Waste Management Association*, *49*(12), pp.1405-1414.

GoIndustry Dovebid SA (Pty) Ltd. 2016. [Online]. Available from: http://international.go-dove.com/data/Auctions/Auction19472/documents/Tyre%20Plant%20Visitor%20Presentation5.pdf. [Accessed on 02 January 2017].

González, J.F., Encinar, J.M., Canito, J.L. and Rodríguez, J.J. 2001. Pyrolysis of automobile tyre waste. Influence of operating variables and kinetics study. *Journal of Analytical and Applied Pyrolysis*, *58*, pp.667-683.

Gopaul, S.G., Dutta, A. and Clemmer, R. 2014. Chemical looping gasification for hydrogen production: A comparison of two unique processes simulated using ASPEN Plus. *International Journal of Hydrogen Energy*, 39(11), pp.5804–5817.

Görling, M., Larsson, M. and Alvfors, P. 2013. Bio-methane via fast pyrolysis of biomass. *Applied Energy*, 112, pp.440–447.

Green Terpene™.2014. [Online] Available from: www.greenterpene.com. [Accessed on 20 June 2014].

Grieco, E., Bernardi, M. and Baldi, G. 2008. Styrene-butadiene rubber pyrolysis: Products, kinetics, modelling. *Journal of Analytical and Applied Pyrolysis*, 82(2), pp.304–311.

Grossmann, I.E., Caballero, J.A. and Yeomans, H. 2000. Advances in mathematical programming for the synthesis of process systems. *Latin American Applied Research*, *30*(4), pp.263-284.

Gu, W., Wang, K., Huang, Y., Zhang, B., Chen, Q. and Hui, C.W. 2015. Energy Optimization for a Multistage Crude Oil Distillation Process. *Chemical Engineering & Technology*, *38*(7), pp.1243-1253

Hammer, N.L., Boateng, A.A., Mullen, C.A. and Wheeler, M.C. 2013. Aspen Plus® and economic modeling of equine waste utilization for localized hot water heating via fast pyrolysis. *Journal of environmental management*, *128*, pp.594-601.

Handbook—Fundamentals, A.S.H.R.A.E., 2005. SI edition. *Atlanta, GA: American Society of Heating, Refrigerating and Air-Conditioning Engineers, Inc*.

Handbook—Fundamentals, A.S.H.R.A.E., 2013. SI edition. *Atlanta, GA: American Society of Heating, Refrigerating and Air-Conditioning Engineers, Inc*.

He, C., Feng, X. and Chu, K.H. 2013. Process modeling and thermodynamic analysis of Lurgi fixed-bed coal gasifier in an SNG plant. *Applied Energy*, 111, pp.742–757.

Henley, E.J., Seader, J.D. and Roper, D.K. 2011. *Separation Process Principles*. New York: Wiley.

Hita, I., Arabiourrutia, M., Olazar, M., Bilbao, J., Arandes, J.M. and Sánchez, P.C. 2016. Opportunities and barriers for producing high quality fuels from the pyrolysis of scrap tires. *Renewable and Sustainable Energy Reviews*, *56*, pp.745-759.

Infrastructurene. 2016. Waste tyres. [Online] Available from: http://www.infrastructurene.ws/2016/02/24/waste-tyres-the-new-coal/. [Accessed on: 16 October 2016]

Islam, M.R., Joardder, M.U.H., Hasan, S.M., Takai, K. and Haniu, H. 2011. Feasibility study for thermal treatment of solid tire wastes in Bangladesh by using pyrolysis technology. *Waste management*, *31*(9), pp.2142-2149.

Islam, M.R., Tushar, M.S.H.K. and Haniu, H. 2008. Production of liquid fuels and chemicals from pyrolysis of Bangladeshi bicycle/rickshaw tire wastes. *Journal of Analytical and Applied Pyrolysis*, 82(1), pp.96–109.

Ismail, H.Y., Abbas, A., Azizi, F. and Zeaiter, J. 2017. Pyrolysis of waste tires: A modeling and parameter estimation study using Aspen Plus®. *Waste Management*, *60*, pp.482-493.

Jacob, P., Kashyap, P., Suparat, T., and Visvanathan, C. 2014. Dealing with emerging waste streams: Used tyre assessment in Thailand using material flow analysis. *Waste Management & Research*, 32(August), pp.918–926.

Jaksland, C.A., Gani, R. and Lien, K.M., 1995. Separation process design and synthesis based on thermodynamic insights. *Chemical Engineering Science*, *50*(3), pp.511-530.

Janajreh, I. & Raza, S.S. 2015. Numerical simulation of waste tyres gasification. *Waste Management & Research*, 33(5), pp.460–468.

Jones, S., Meyer, P., Snowden-Swan, L., Padmaperuma, A., Tan, E., Dutta, A., Jacobson, J., Cafferty, K. 2013. Process Design and Economics for the Conversion of Lignocellulosic Biomass to Hydrocarbon Fuels Fast Pyrolysis and Hydrotreating. *PNNL Report*, PNNL-23053, p.97.

Jefferies, T. 2017, Personal interview. 5 january, Stellenbosch.

Kääntee, U., Zevenhoven, R., Backman, R. and Hupa, M. 2004. Cement manufacturing using alternative fuels and the advantages of process modelling. *Fuel Processing Technology*, *85*(4), pp.293-301.

Kaminsky, W. and Mennerich, C. 2001. Pyrolysis of synthetic tire rubber in a fluidised-bed reactor to yield 1,3-butadiene, styrene and carbon black. *Journal of Analytical and Applied Pyrolysis*, 58–59, pp.803–811.

Kaminsky, W., Mennerich, C. and Zhang, Z. 2009. Feedstock recycling of synthetic and natural rubber by pyrolysis in a fluidized bed. *Journal of Analytical and Applied Pyrolysis*, 85(1–2), pp.334–337.

Kandasamy, J. and Gökalp, I. 2014. Pyrolysis , Combustion , and Steam Gasi fi cation of Various Types of Scrap Tires for Energy Recovery. *Energy & Fuels*, 29, pp.346–354.

Kar, Y. 2011. Catalytic pyrolysis of car tire waste using expanded perlite. *Waste Management*, 31(8), pp.1772–1782.

Ko, D.C., Mui, E.L., Lau, K.S. and McKay, G. 2004. Production of activated carbons from waste tire–process design and economical analysis. *Waste Management*, *24*(9), pp.875-888.

Ko, M.S., Na, S. and Kim, H. 2002. Simulation of the aromatic recovery process by extractive distillation. *Korean Journal of Chemical Engineering*, 19(6), pp.996–1000.

Kong, X., Zhong, W., Du, W. and Qian, F. 2014. Compartment modeling of coal gasification in an entrained flow gasifier: A study on the influence of operating conditions. *Energy Conversion and Management*, *82*, pp.202-211.

Kusiak, A. and Finke, G. 1987. Hierarchical approach to the process planning problem. *Discrete applied mathematics*, *18*(2), pp.175-184.

Kwon, E. and Castaldi, M.J. 2009. Fundamental understanding of the thermal degradation mechanisms of waste tires and their air pollutant generation in a N2 atmosphere. *Environmental Science and Technology*, 43(15), pp.5996–6002.

Kyari, M., Cunliffe, A. and Williams, P.T., 2005. Characterization of oils, gases, and char in relation to the pyrolysis of different brands of scrap automotive tires. *Energy and Fuels,* 19(3), pp. 1165-1173.

Lamprecht, S.M. 2010. Establishing a facility to measure packed column hydrodynamics, MSc thesis, Department of Process Engineering, Stellenbosch University.

Lamprecht, S.M. 2010. Establishing a facility to measure packed column hydrodynamics, MSc thesis, Department of Process Engineering, Stellenbosch University.

Laresgoiti, M.F., Caballero, B.M., de Marco, I., Torres, A., Cabrero, M.A. and Chomón, M.J. 2004. Characterization of the liquid products obtained in tyre pyrolysis. *Journal of Analytical and Applied Pyrolysis*, *71*(2), pp.917-934.

Lebreton, B. and Tuma, A. 2006. A quantitative approach to assessing the profitability of car and truck tire remanufacturing. *International Journal of Production Economics*, 104(2), pp.639–652.

Lee, J.M., Lee, J.S., Kim, J.R. and Kim, S.D. 1995. Pyrolysis of waste tires with partial oxidation in a fluidized-bed reactor. *Energy*, *20*(10), pp.969-976.

Leung, D.Y. and Wang, C. 1998. Kinetic study of scrap tyre pyrolysis and combustion. *Journal of Analytical and Applied Pyrolysis*, 45(2), pp.153–169.

Leung, D.Y.C. and Wang, C.L. 1999. Kinetic modeling of scrap tire pyrolysis. *Energy and Fuels*, 13(2), pp.421–427.

Leung, D.Y.C. and Wang, C.L. 2003. Fluidized-bed gasification of waste tire powders. *Fuel Processing Technology*, 84(1–3), pp.175–196.

Li, Q., Zhang, Y. and Hu, G. 2015. Techno-economic analysis of advanced biofuel production based on bio-oil gasification. *Bioresource Technology*, 191, pp.88–96.

Li, S., Jin, H. and Gao, L. 2014. Coal Based Cogeneration System for Synthetic/Substitute Natural Gas and Power With CO_2 Capture After Methanation: Coupling Between Chemical and Power Production. *Journal of Engineering for Gas Turbines and Power*, 136(9), p.91501.

Li, S.Q., Yao, Q., Chi, Y., Yan, J.H. and Cen, K.F. 2004. Pilot-scale pyrolysis of scrap tires in a continuous rotary kiln reactor. *Industrial & engineering chemistry research*, *43*(17), pp.5133-5145.

Li, X. and Kraslawski, A. 2004. Conceptual process synthesis: past and current trends. *Chemical Engineering and Processing: Process Intensification*, *43*(5), pp.583-594

Linninger, A.A. 2002. Metallurgical Process Design A Tribute to Douglas' Conceptual Design Approach. *Industrial & engineering chemistry research*, *41*(16), pp.3797-3805.

Liu, B., Yang, X., Song, W. and Lin, W. 2011. Process simulation development of coal combustion in a circulating fluidized bed combustor based on Aspen Plus. *Energy & Fuels*, *25*(4), pp.1721-1730.

Lopez, G., Olazar, M., Aguado, R., Elordi, G., Amutio, M., Artetxe, M. and Bilbao, J. 2010. Vacuum pyrolysis of waste tires by continuously feeding into a conical spouted bed reactor. *Industrial & Engineering Chemistry Research*, *49*(19), pp.8990-8997.

López, G., Olazar, M., Aguado, R. and Bilbao, J. 2010. Continuous pyrolysis of waste tyres in a conical spouted bed reactor. *Fuel*, *89*(8), pp.1946-1952.

de Marco Rodriguez, I., Laresgoiti, M.F., Cabrero, M.A., Torres, A., Chomon, M.J. and Caballero, B. 2001. Pyrolysis of scrap tyres. *Fuel processing technology*, *72*(1), pp.9-22.

Mahlangu, M.L. 2009. Waste tyre management problems in South Africa and the possible opportunities that can be created through the recycling thereof, MA thesis, Department of Environmental Sciences, University of South Africa

Mandegari, M.A., Farzad, S. and Görgens, J.F. 2016. Process Design, Flowsheeting, and Simulation of Bioethanol Production from Lignocelluloses. *Biofuels: Production and Future Perspectives*, p.255.

Mapamba, L.S., 2012. Simulation of the Copper-chlorine Thermochemical Cycle, MEng thesis, School of Chemical and Minerals Engineering, North-West University.

Marsh, P. 1982. The choice between equity and debt: An empirical study. *The Journal of finance*, *37*(1), pp.121-144.

Martínez, J.D., Murillo, R., García, T. and Veses, A. 2013. Demonstration of the waste tire pyrolysis process on pilot scale in a continuous auger reactor. *Journal of hazardous materials*, *261*, pp.637-645.

Martínez, J.D., Puy, N., Murillo, R., García, T., Navarro, M.V. and Mastral, A.M. 2013. Waste tyre pyrolysis–a review. *Renewable and Sustainable Energy Reviews*, *23*, pp.179-213

Mastral, A.M., Murillo, R., Callén, M.S. and Garcıa, T. 1999. Application of coal conversion technology to tire processing. *Fuel processing technology*, *60*(3), pp.231-242.

Mastral, A.M., Murillo, R., Callen, M.S., Garcia, T. and Snape, C.E. 2000. Influence of process variables on oils from tire pyrolysis and hydropyrolysis in a swept fixed bed reactor. *Energy & Fuels*, *14*(4), pp.739-744.

Mastral, A.M., Murillo, R., Callen, M.S. and Garcia, T. 2000. Optimisation of scrap automotive tyres recycling into valuable liquid fuels. *Resources, Conservation and Recycling*, *29*(4), pp.263-272.

Mazloom, G., Farhadi, F. and Khorasheh, F. 2009. Kinetic modeling of pyrolysis of scrap tires. *Journal of Analytical and Applied Pyrolysis*, 84(2), pp.157–164.

McDonald, R.A., Shrader, S.A. and Stull, D.R. 1959. Vapor Pressures and Freezing Points of Thirty Pure Organic Compounds. *Journal of Chemical and Engineering Data*, *4*(4), pp.311-313.

Messerly, J.F., Guthrie Jr, G.B., Todd, S.S. and Finke, H.L. 1967. Low-temperature thermal data for pentane, n-heptadecane, and n-octadecane. Revised thermodynamic functions for the n-alkanes, C5-C18. *Journal of Chemical and Engineering Data*, *12*(3), pp.338-346.

Mirmiran, S., Pakdel, H. and Roy, C. 1992. Characterization of used tire vacuum pyrolysis oil: Nitrogenous compounds from the naphtha fraction. *Journal of Analytical and Applied Pyrolysis*, 22(3), pp.205–215.

Mitta, N.R., Ferrer-Nadal, S., Lazovic, A.M., Perales, J.F., Velo, E. and Puigjaner, L. 2006. Modelling and simulation of a tyre gasification plant for synthesis gas production. *Computer Aided Chemical Engineering*, *21*(B), p.1771.

Mix, T.J., Dweck, J.S., Weinberg, M. and Armstrong, R.C., 1978. Energy conservation in distillation. *Chemical Engineering Progress, 74*(4), pp.49-55.

Mocke, F.J., 2013. Implementation of membrane technology in a base metal refinery, MEng thesis, Faculty of Chemical and Minerals Engineering, North-West University.

Mtui, P. 2013. Gasification And Combustion Of Waste Tires For Process Heat And Power Generation. , 2(12), pp.38–46.

Murugan, S., Ramaswamy, M.C. and Nagarajan, G. 2008. The use of tyre pyrolysis oil in diesel engines. *Waste Management*, 28(12), pp.2743–2749.

Muzenda, E. and Popa, C. 2015. Waste Tyre Management in Gauteng , South Africa : Government , Industry and Community Perceptions. , 6(4).

Naeem, M., Al-Arabia, A.A. and Mughees, W. 2014. Process Simulation of 1-Butene and N- Butane Separation By Extractive Distillation. , 3(6), pp.747–750.

Naim, A., Mourad, B., Khaled, L., Sary, A. and Mohand, T. 2017. Heating rate effects on pyrolytic vapors from scrap truck tires. *Journal of Analytical and Applied Pyrolysis*, *123 (2017),* pp. 419–429

Naleli, K. 2016. Process Modelling In Production of Biobutanol from Lignocellulosic Biomass via ABE Fermentation, MEng thesis, Department of Process Engineering, Stellenbosch University.

Narayanasamy, L. and Murugesan, T. 2014. Degradation of Alizarin Yellow R using UV/H2O2 advanced oxidation process. *Environmental Progress & Sustainable Energy*, *33*(2), pp.482-489.

Nayak, R. and Mewada, R. 2011. Simulation of Coal Gasification Process using ASPEN PLUS. *International conference of current trends in technology*, pp.8–10.

Ngwetjana, M.M., 2017. Fractionation of tyre derived oil (TDO), MEng thesis, Department of Process Engineering, Stellenbosch University.

Nikoo, M.B. and Mahinpey, N. 2008. Simulation of biomass gasification in fluidized bed reactor using ASPEN PLUS. *Biomass and Bioenergy*, 32(12), pp.1245–1254.

Nkosi, N. and Muzenda, E. 2014. A review and discussion of waste tyre pyrolysis and derived products.

Nkosi, N., Muzenda, E., Zvimba, J. and Pilusa, J. 2013. The current waste generation and management trends in South Africa: a review.

Nsaful, F., 2012. Process modelling of sugar mill biomass to energy conversion processes and energy integration of pyrolysis, MEng thesis, Department of Process Engineering, Stellenbosch University.

Nsaful, F., Görgens, J.F. and Knoetze, J.H. 2013. Comparison of combustion and pyrolysis for energy generation in a sugarcane mill. *Energy Conversion and Management*, 74, pp.524–534.

Oden, J., Belytschko, T., Fish, J., Hughes, T., Johnson, C., Keyes, D., Laub, A., Petzold, L., Srolovitz, D. and Yip, S. 2006. Revolutionizing Engineering Science through Simulation. Simulation-based engineering science. National Science Foundation.

Olazar, M., Aguado, R., Arabiourrutia, M., Lopez, G., Barona, A. and Bilbao, J. 2008. Catalyst effect on the composition of tire pyrolysis products. *Energy & Fuels*, *22*(5), pp.2909-2916.

Oliver, G.D., Eaton, M. and Huffman, H.M. 1948. The Heat Capacity, Heat of Fusion and Entropy of Benzene1. *Journal of the American chemical society*, *70*(4), pp.1502-1505.

Pakdel, H., Magdalena, D.and Roy, C. 2001. Production of dl -limonene by vacuum pyrolysis of used tires. , 57, pp.91–107.

Pakdel, H. and Roy, C. 1994. Simultaneous gas chromatographic-Fourier transform infrared spectroscopic-mass spectrometric analysis of synthetic fuel derived from used tire vacuum pyrolysis oil, naphtha fraction. *Journal of Chromatography A*, 683(1), pp.203–214.

Pattabhi Raman, K., Walawender, W.P. and Fan, L.T., 1981. Gasification of waste tires in a fluid bed reactor. *Conservation and Recycling*, 4(2), pp.79–88.

Payscale Human Capital. 2016. [Online] Available from:http://www.payscale.com/. [Accessed on 18 August 2016].

Pehlken, A. and Müller, D.H., 2009. Using information of the separation process of recycling scrap tires for process modelling. *Resources, Conservation and Recycling*, 54(2), pp.140–148.

Perales, A.V., Valle, C.R., Ollero, P. and Gómez-Barea, A. 2011. Technoeconomic assessment of ethanol production via thermochemical conversion of biomass by entrained flow gasification. *Energy*, *36*(7),

pp.4097-4108.Peters, J.F., Iribarren, D. and Dufour, J., 2014. Predictive pyrolysis process modelling in Aspen Plus. In pp. 352–368.

Perry, R.H. and Green, D.W. 1997. Perry's chemical engineers' handbook. New York: McGraw-Hill.

Peters, M.S. and Timmerhaus, K .D. 1991. *Plant Design and Economics for Chemical Engineers*. New York: McGraw-Hill.

Pilusa, J. and Muzenda, E. 2013. Qualitative analysis of waste rubber-derived oil as an alternative diesel additive. International Conference on Chemical and Environmental Engineering (ICCEE'2013).

Pilusa, J., Shukla, M. & Muzenda, E., 2014. Economic Assessment of Waste Tyres Pyrolysis Technology : A Case study for Gauteng Province, South Africa. *International Journal of Research in Chemical, Metallurgical and Civil Engineering*, 1(1), pp.41–49.

Pipilikaki, P., Katsioti, M., Papageorgiou, D., Fragoulis, D. and Chaniotakis, E. 2005. Use of tire derived fuel in clinker burning. *Cement and Concrete Composites*, *27*(7), pp.843-847.

PPC Ltd. 2014. [Online] Available from: http://www.ppc.co.za/media/101384/Environmental-Review.pdf. [Accessed on: 16 October 2016].

Puig-Arnavat, M., Bruno, J.C. and Coronas, A., 2010. Review and analysis of biomass gasification models. *Renewable and Sustainable Energy Reviews*, 14(9), pp.2841–2851.

Qu, W., Zhou, Q., Wang, Y.Z., Zhang, J., Lan, W.W., Wu, Y.H., Yang, J.W. and Wang, D.Z. 2006. Pyrolysis of waste tire on ZSM-5 zeolite with enhanced catalytic activities. *Polymer Degradation and Stability*, *91*(10), pp.2389-2395.

Quek, A. and Balasubramanian, R. 2013. Liquefaction of waste tires by pyrolysis for oil and chemicals - A review. *Journal of Analytical and Applied Pyrolysis*, 101, pp.1–16.

Rahman, A., Rasul, M.G., Khan, M.M.K. and Sharma, S. 2015. Recent development on the uses of alternative fuels in cement manufacturing process. *Fuel*, *145*, pp.84-99.

Raj, R.E., Kennedy, Z.R. and Pillai, B.C. 2013. Optimization of process parameters in flash pyrolysis of waste tyres to liquid and gaseous fuel in a fluidized bed reactor. *Energy Conversion and Management*, *67*, pp.145-151.

Ramanathan, S.P., Mukherjee, S., Dahule, R.K., Ghosh, S., Rahman, I., Tambe, S.S., Ravetkar, D.D. and Kulkarni, B.D. 2001. Optimization of continuous distillation columns using stochastic optimization approaches. *Chemical Engineering Research and Design*, *79*(3), pp.310-322

Ramzan, N., Ashraf, A., Naveed, S. and Malik, A. 2011. Simulation of hybrid biomass gasification using Aspen plus: A comparative performance analysis for food, municipal solid and poultry waste. *Biomass and Bioenergy*, *35*(9), pp.3962-3969.

REDISA . 2012. Integrated Industry Waste Tyre Management Plan. Government Gazette Staatskoerant. *Government Gazette*, 583(37230), pp.1–4.

REDISA NPC. 2016. [Online]. Available from: http://www.redisa.org.za/Satellite/Redisa%20Home%20Page.html. [Accessed on 02 January 2017].

Richardson, J.W., Lemmer, W.J. and Outlaw, J.L. 2007. Bio-ethanol production from wheat in the winter rainfall region of South Africa: a quantitative risk analysis. *International Food and Agribusiness Management Review, 10*(2), pp.181-204.

Ringer, M., Putsche, V. and Scahil, J. 2006. *Large-Scale Pyrolysis Oil Production: A Technology Assessment and Economic Analysis. Golden (CO): National Renewable Energy Laboratory; 2006 Nov. Report No*. NREL/TP-510-37779. Contract No.: DE-AC36-99-GO10337.

Robus, C.L.L. 2013. Production of Bioethanol from Paper Sludge using Simultaneous Saccharification and Fermentation, MSc thesis, Department of Process Engineering, Stellenbosch University.

Rofiqul Islam, M., Haniu, H. and Rafiqul Alam Beg, M. 2008. Liquid fuels and chemicals from pyrolysis of motorcycle tire waste: Product yields, compositions and related properties. *Fuel*, 87(13–14), pp.3112–3122.

Roy, C., Darmstadt, H., Benallal, B. and Amen-Chen, C. 1997. Characterization of naphtha and carbon black obtained by vacuum pyrolysis of polyisoprene rubber. *Fuel processing technology*, *50*(1), pp.87 - 103.

SA Tyre Recyclers. 2017. [Online]. Available from: http://satyrerecyclers.co.za/satyre/. [Accessed on 02 January 2017].

Sampaio, M.O. and de Castro, C.N. 1998. Heat capacitiy of liquid terpenes. *Fluid phase equilibria*, *150*, pp.789-796.

Sánchez, Ó.J. and Cardona, C.A. 2012. Conceptual design of cost-effective and environmentally-friendly configurations for fuel ethanol production from sugarcane by knowledge-based process synthesis. *Bioresource technology*, *104*, pp.305-314.

Seader, J.D., Seider, W.D. and Lewin, D.R. 2006. *Using process simulators in Chemical Engineering*. New York: Wiley

Seebran, N. 2016, Personal interview. 2 August, Stellenbosch.

Seghar, S., Ait Hocine, N., Mittal, V., Azem, S., Al-Zohbi, F., Schmaltz, B. and Poirot, N. 2015. Devulcanization of styrene butadiene rubber by microwave energy: Effect of the presence of ionic liquid. *Express Polym. Lett*, *9*, pp.1076-1086.

Seidelt, S., Müller-Hagedorn, M. and Bockhorn, H. 2006. Description of tire pyrolysis by thermal degradation behaviour of main components. *Journal of Analytical and Applied Pyrolysis*, 75(1), pp.11- 18.

Seider, W.D., Seader, J.D. and Lewin, D.R. 2004. *Product and process design principles: synthesis, analysis and evaluation*. New York: Wiley and Sons.

Senneca, O., Salatino, P. and Chirone, R., 1999. Fast heating-rate thermogravimetric study of the pyrolysis of scrap tyres. *Fuel*, 78(13), pp.1575–1581.

Shah, J., Jan, M.R. and Mabood, F., 2009. Recovery of value-added products from the catalytic pyrolysis of waste tyre. *Energy Conversion and Management*, 50(4), pp.991–994.

Sharma, V.K., Fortuna, F., Mincarini, M., Berillo, M. and Cornacchia, G. 2000. Disposal of waste tyres for energy recovery and safe environment. *Applied Energy*, *65*(1), pp.381-394.

Shelley, M.D. and El-Halwagi, M.M., 1999. Journal of Elastomers and Plastics. *Journal of Elastomers and Plastics*, 31, pp.232–254.

Shemfe, M.B., Gu, S. and Ranganathan, P. 2015. Techno-economic performance analysis of biofuel production and miniature electric power generation from biomass fast pyrolysis and bio-oil upgrading. *Fuel*, 143, pp.361–372.

Shoaib, M.W., Wukovits, W. and Gul, S. 2014. Review of process simulation and simulation software-open source software development. In *2nd Conference on Sustainability in Process Industry (SPI)* (pp. 45-49).

Shu, X. and Huang, B. 2013. Recycling of waste tire rubber in asphalt and portland cement concrete: An overview. *Construction and Building Materials*, 67, pp.217–224.

Sienkiewicz, M., Kucinska-Lipka, J., Janik, H. and Balas, A. 2012. Progress in used tyres management in the European Union: a review. *Waste Management*, *32*(10), pp.1742-1751.

Siirola, J.J. and Rudd, D.F. 1971. Computer-aided synthesis of chemical process designs. From reaction path data to the process task network. *Industrial & Engineering Chemistry Fundamentals*, *10*(3), pp.353-362.

Singh, S., Nimmo, W., Gibbs, B.M. and Williams, P.T. 2009. Waste tyre rubber as a secondary fuel for power plants. *Fuel*, *88*(12), pp.2473-2480.

Sinnott, R.K. and Towler, G. 2009. *Chemical engineering design*. Amsterdam. Elsevier, Butterworth-Heinemann.

Smith, R., 1995. *Chemical process design*. McGraw- Hill, New York.

South African Reserve Bank. 2016. Exchange rates. [Online] Available from:

http://www.resbank.co.za/Research/Rates/Pages/SelectedHistoricalExchangeAndInterestRates.aspx . [Accessed on 09 August 2016].

South African Reserve Bank. 2016. Prime lending rates. [Online] Available from: https://www.resbank.co.za/Research/Rates/Pages/SelectedHistoricalExchangeAndInterestRates.aspx. [Accessed on: 09 August 2016].

South African Revenue Services. 2016. Corporate Income Tax. [Online] Available from: http://www.sars.gov.za/TaxTypes/CIT/Pages/default.aspx. [Accessed on: 09 August 2016].

Sreejith, C.C., Muraleedharan, C. and Arun, P. 2013. Performance prediction of steam gasification of wood using an ASPEN PLUS thermodynamic equilibrium model. *International Journal of Sustainable Energy*, 33(2), pp.416–434.

Stanciulescu, M. and Ikura, M. 2007. Limonene ethers from tire pyrolysis oil. Part 2: Continuous flow experiments. *Journal of Analytical and Applied Pyrolysis*, 78(1), pp.76–84.

Stanciulescu, M. and Ikura, M. 2006. Limonene ethers from tire pyrolysis oil: Part 1: Batch experiments. *Journal of Analytical and Applied Pyrolysis*, 75(2), pp.217–225.

Steele, W.V., Chirico, R.D., Cowell, A.B., Knipmeyer, S.E. and Nguyen, A. 2002. Thermodynamic properties and ideal-gas enthalpies of formation for methyl benzoate, ethyl benzoate,(R)-(+)-limonene, tert-amyl methyl ether, trans-crotonaldehyde, and diethylene glycol. *Journal of Chemical & Engineering Data*, *47*(4), pp.667-688.

Taylor, R., Ray, R. and Chapman, C. 2013. Advanced thermal treatment of auto shredder residue and refuse derived fuel. *Fuel*, 106, pp.401–409.

Tong, Z. F., Yang, Z. Y., Liao, D. K., Wei, T. Y. and Chen, X. P. 2009. Measurement and correlation of VLE data for α-pinene+ limonene and p-cymene+ limonene systems under atmospheric pressure. *J Chem Ind and Eng (China)*, *60*(8), pp.1877-1882.

Turton, R., Baile, R.C., Whiting, W.B. and Shaeiwitz, J.A. 2009. *Analysis, synthesis, and design of chemical processes*. Prentice Hall international series in the physical and chemical engineering sciences. Upper Saddle River, NJ: Prentice Hall.

Ucar, S., Karagoz, S., Ozkan, A.R. and Yanik, J. 2005. Evaluation of two different scrap tires as hydrocarbon source by pyrolysis. *Fuel*, *84*(14), pp.1884-1892.

United States Department of Agriculture. 2016. Citrus: World Markets and Trade. [Online] Available from: http://apps.fas.usda.gov/psdonline/circulars/citrus.pdf. [Accessed on: 26 October 2016].

Van der Merwe, A.B. 2010. Evaluation of Different Process Designs for Biobutanol Production from Sugarcane Molasses, MSc thesis, Department of Process Engineering, Stellenbosch University.

VENKATARAMAN, S. 1996. Process enhancement by process simulation and multiobjective optimization, MSc thesis, Faculty of the Graduate College, Oklahoma State University.

Visconti, A., Miccio, M. and Juchelková, D. 2015. An aspen plus tool for simulation of lignocellulosic biomass pyrolysis via equilibrium and ranking of the main process variables. *International Journal of Mathematical Models and Methods in Applied Sciences*, 9, pp.71–86.

Wang, S.F., Zhao, Y.H., Wen, H. and Xu, Z.H. 2008. Simulation study of a novel process co-producing synthesis gas and light olefins. *Chemical engineering & technology*, *31*(10), p.1424.

Wang, W.C., Bai, C.J., Lin, C.T. and Prakash, S. 2016. Alternative fuel produced from thermal pyrolysis of waste tires and its use in a DI diesel engine. *Applied Thermal Engineering*, *93*, pp.330-338.

Ward, J., Rasul, M.G. and Bhuiya, M.M.K. 2014. Energy recovery from biomass by fast pyrolysis. *Procedia Engineering*, *90*, pp.669-674.

WebFinance Inc. 2015. Conceptual framework. [Online] Available from: http://www.businessdictionary.com/definition/conceptual-framework.html. [Accessed: 18 April 2015].

WebFinance Inc. 2015. Framework. [Online] Available from: http://www.businessdictionary.com/definition/framework.html. [Accessed: 18 April 2015].

Wei, Y., Lei, H., Wang, L., Zhu, L., Zhang, X., Liu, Y., Chen, S. and Ahring, B. 2014. Liquid–liquid extraction of biomass pyrolysis bio-oil. *Energy & Fuels*, *28*(2), pp.1207-1212.

Weitkamp, J., Raichle, A. and Traa, Y. 2001. Novel zeolite catalysis to create value from surplus aromatics: Preparation of C2+-n-alkanes, a high-quality synthetic steamcracker feedstock. *Applied Catalysis A: General*, 222(1–2), pp.277–297.

Wiese, J. 2017, Personal interview. 6 January, Stellenbosch.

Wilkins Jr, J.S. 1999. *Limonene pesticides*. U.S. Patent 5,951,992.

Williams, P.T. 2013. Pyrolysis of waste tyres: A review. *Waste Management*, 33(8), pp.1714–1728.

Williams, P.T. and Besler, S. 1995. Pyrolysis-thermogravimetric analysis of tyres and tyre components. *Fuel*, 74(9), pp.1277–1283.

Williams, P.T., Besler, S. and Taylor, D.T. 1990. The pyrolysis of scrap automotive tyres. The influence of temperature and heating rate on product composition. *Fuel*, 69(12), pp.1474–1482.

Williams, P.T., Besler, S. and Taylor, D.T. 1993. The batch pyrolysis of tyre waste—fuel properties of the derived pyrolytic oil and overall plant economics. *Proceedings of the Institution of Mechanical Engineers, Part A: Journal of Power and Energy*, *207*(1), pp.55-63.

Williams, P.T. and Brindle, A.J. 2002. Catalytic pyrolysis of tyres: Influence of catalyst temperature. *Fuel*, 81(18), pp.2425–2434.

Williams, P.T. and Brindle, A.J., 2003a. Aromatic chemicals from the catalytic pyrolysis of scrap tyres. *Journal of Analytical and Applied Pyrolysis*, 67(1), pp.143–164.

Williams, P.T. and Brindle, A.J. 2003b. Temperature selective condensation of tyre pyrolysis oils to maximise the recovery of single ring aromatic compounds. *Fuel*, 82(9), pp.1023–1031.

Williams, P.T. and Brindle, A.J. 2003c. Fluidised bed pyrolysis and catalytic pyrolysis of scrap tyres. *Environmental technology, 24*(7), pp.921-929.

WinSim Inc. 2012. Advanced Process Simulation Solutions.

Wojtowicz, M.A. and Serio, M.A. 1996. Pyrolysis of scrap tires: Can it be profitable?. *Chemtech-Washington DC-*, *26*, pp.48-53.

Wright, M.M., Satrio, J .A., Brown, R. C., Daugaard, D.E., Hsu, D.D. 2010. *Techno-economic analysis of biomass fast pyrolysis to transportation fuels*, NREL report.

Wright, M.M., Daugaard, D.E., Satrio, J.A. and Brown, R.C. 2010. Techno-economic analysis of biomass fast pyrolysis to transportation fuels. *Fuel*, *89*, pp.S2-S10.

Xiangdong, K., Zhong, W., Wenli, D.U. and Feng, Q.I.A.N. 2013. Three stage equilibrium model for coal gasification in entrained flow gasifiers based on Aspen Plus. *Chinese Journal of Chemical Engineering*, *21*(1), pp.79-84.

Xiao, G., Ni, M.J., Chi, Y. and Cen, K.F. 2008. Low-temperature gasification of waste tire in a fluidized bed. *Energy Conversion and Management*, *49*(8), pp.2078-2082.

Yan, H.M. and Zhang, D.K. 1999. Modeling of a Low Temperature Pyrolysis Process Using Aspen Plus. *Developments in Chemical Engineering and Mineral Processing*, 7(5–6), pp.577–591.

Yang, X., Liu, B. and Lin, W., 2012. Process Simulation of Using Coal Pyrolysis Gas to Control NO and N2O Emissions during Coal Decoupling Combustion in a Circulating Fluidized Bed Combustor Based on Aspen Plus. *Energy & Fuels, 26*(8), pp.5210-5225.

Zabaniotou, A.A. and Stavropoulos, G. 2003. Pyrolysis of used automobile tires and residual char utilization. *Journal of Analytical and Applied Pyrolysis*, 70(2), pp.711–722.

Zebala, J., Ciepka, P., Reza, A. and Janczur, R. 2007. Influence of rubber compound and tread pattern of retreaded tyres on vehicle active safety. *Forensic science international*, *167*(2), pp.173-180.

Zhang, J., Toghiani, H., Mohan, D., Pittman, C.U. and Toghiani, R.K. 2007. Product analysis and thermodynamic simulations from the pyrolysis of several biomass feedstocks. *Energy & fuels*, *21*(4), pp.2373-2385.

Zhang, X., Wang, T., Ma, L. and Chang, J. 2008. Vacuum pyrolysis of waste tires with basic additives. *Waste Management*, *28*(11), pp.2301-2310.

Zhang, Y., Brown, T.R., Hu, G. and Brown, R.C. 2013. Techno-economic analysis of monosaccharide production via fast pyrolysis of lignocellulose. *Bioresource technology*, *127*, pp.358-365.

APPENDIX A: LIST OF COMPONENTS IN CURRENT SIMULATIONS

Table A1: Compounds in oil fraction used for current study from Choi *et al.* (2014) and Aspen reactor yields

Compound name in Choi et al. (2014)	Compound name Aspen used for simulation	Aspen Plus® yield (wt.%)
2-Methyl-2-aminopropane	Tert-butalymine	0.04
p-Phenylenediamine	p-Phenylenediamine	0.04
Benzothiazole	Benzothiazole	2.57
Styrene	Styrene	0.00
Xylenes	m-Xylene	1.21
Indene	Indene	0.35
Methylstyrenes	o-Methylstyrene	1.76
Trimethylbenzenes	1,2,4-Trimethylbenzene	2.62
1,2-Methylethylbenzene	2-Ethylytoluene	1.43
1,2,4-Tris(methylene)cyclohexane	3-Ethylytoluene	0.26
1,2,5,5-Tetramethyl-1,3-cyclopentadiene	1-Ethyl-4-methyl-1,3-cyclohexadiene	0.38
Limonenes	d-Limonene	2.52
Naphthalene	Naphthalene	0.00
Methylindenes	1-Methylindene	0.78
Dimethylstyrenes	2,5-Dimethylstyrene	2.13
Cymenes	p-Cymeme	1.38
Propyltoluenes	o-Propyltoluene	0.19
Tetramethylbenzenes	1,2,3,4-Tetramethylbenzene	0.40
Ethylxylenes	5-Ethyl-m-xylene	0.99
2,7-Dimethylbenzothiophene	2,7-Dimethylbenzothiophene	0.00
Methylnaphthalenes	1-Methylnaphthalene	0.84
Dimethylindenes	1,3-Dimethylindene	2.11
Dimethylindanes	1,1-Dimethylindane	0.08
2,4-Dimethylquinoline	2,5-Dimethylquinoline	1.77
1-Dodecene	1-Dodecene	0.25
Dimethylnaphthalenes	2,6-Dimethylnaphthalene	1.43
1,2,3-Trimethylindene	1,2,3-Trimethylindene	1.22

Table A1 continued: Compounds in oil fraction used for current study from Choi *et al.* (2014) and Aspen yields

Compound name in Choi et al. (2014)	Compound name Aspen used for simulation	Aspen Plus® yield (wt.%)
Methylbiphenyls	3-Methlybiphenyl	0.00
Trimethylnaphthalenes	1,2,3-Trimethylnaphthalene	1.23
Dihydrotrimethylnaphthalenes	1,1,6-Dihydro-1,2-trimethylnaphthalene	0.39
Tetramethylnaphthalenes	1,2,6,8-Tetramethylnaphthalene	0.28
Pentadecane	Pentadecane	0.21
Heptadecane	Heptadecane	0.18
n-Eicosane	n-Eicosane	2.42
Benzene	Benzene	9.67
Phenanthrene	Phenanthrene	0.97

Table A2: Original and normalised gas composition from Rodriguez *et al.* (2001) and Aspen reactor yields

Compound	Compound name used in Aspen Simulation	Composition (wt.%)	Normalised composition (wt.%)	Aspen Plus® yield (wt.%)
Hydrogen sulphide	Hydrogen sulphide	4.3	5	0.36
Carbon monoxide	Carbon monoxide	3.3	0	0.00
Carbon dioxide	Carbon dioxide	10.3	0	0.00
Methane	Methane	7.9	9.1	2.06
Ethene	Ethylene	6.6	7.6	1.72
Ethane	Ethane	6.8	7.9	1.78
Propene	Propylene	6.7	7.7	1.74
Propane	Propane	4.8	5.6	1.27
Butenes	1-Butene	24.4	28.2	6.37
Butanes	N-Butane	5.5	6.4	1.45
Pentene	1-Pentene	4.9	5.6	1.27
Pentane	N-Pentane	8.6	10	2.26
Hexene	1-Hexene	2.3	2.7	0.61
Hexane	N-Hexane	3.6	4.2	0.95

APPENDIX B: ADDITIONAL INFORMATION FOR PYROLYSIS SECTION

B.1. Mass balance equations

$$Y_i = \left(\frac{X_i G}{100}\right) * YG$$

Equation B1

$$Y_i = \left(\frac{X_i L}{100}\right) * YL$$

Equation B2

Y_i is the yield of compound *i* from tyre (wt/wt), $X_i G$ and $X_i L$ are the respective compositions (wt.%) of the gas and liquid product compounds in their respective fractions. YG and YL are the respective adjusted yields of the gas and liquid fractions from tyre (wt/wt).

$$Y_{Benzo} = \frac{(N_{tyre} - N_{volatile} - N_{char})}{d * F_{tyre}}$$

Equation B3

$$N_{tyre} = \left(\frac{b}{100}\right) * F_{tyre}$$

Equation B4

$$N_{volatile} = \sum_{i=1}^{n} a_i * Y_i * F_{tyre}$$

Equation B5

$$N_{char} = \left(\frac{c}{100}\right) * YS * F_{tyre}$$

Equation B6

Y_{Benzo} is the yield of benzothiazole from tyre (wt/wt). N_{tyre}, $N_{volatile}$ and N_{char} represent the nitrogen in the tyre feed, the volatiles (gas and liquid fractions) and the char fraction respectively. The letters a, b, c and d represent the mass fraction of nitrogen in each of the volatiles compounds, tyre feed, char and benzothiazole respectively. F_{tyre} is the flow rate of the tyre feed in kg/h.

$$Y_{H2S} = \frac{(S_{tyre} - S_{volatile} - S_{char})}{d * F_{tyre}}$$

Equation B7

$$S_{tyre} = \left(\frac{b}{100}\right) * F_{tyre}$$

Equation B8

$$S_{volatile} = \sum_{i=1}^{n} a_i * Y_i * F_{tyre}$$

Equation B9

$$S_{char} = \left(\frac{c}{100}\right) * YS * F_{tyre}$$

Equation B10

Y_{H2S} is the yield of hydrogen sulphide from tyre (wt/wt). S_{tyre}, $S_{volatile}$ and S_{char} represent the sulphur in the tyre feed, the volatiles (gas and liquid fractions) and the char fraction respectively. The letters a, b, c and d represent the mass fraction of sulphur in each of the volatiles compounds, tyre feed, char and hydrogen sulphide respectively.

$$Ash_{char} = \left(\frac{Ash_{tyre}}{YS}\right) * 100$$

Equation B11

Ash_{char} is the ash content of the char product (wt.%), Ash_{tyre} is the mass fraction of ash in the tyre feed and YS is the yield of char.

$$Y_{Benzene} = 1 - Y_{gastotal} - Y_{oiltotal} - YS$$

Equation B12

$Y_{Benzene}$ is the yield of benzene from tyre (wt/wt), $Y_{gastotal}$ and $Y_{oiltotal}$ represent the total reactor yield accounted for by the gas and oil components respectively. YS is the yield of the char product fraction.

B.2. Correlation equations for yield prediction

In this study, the correlations were developed by fitting nth order polynomial trends to plots of the literature yields from tyre (wt.%) against reactor temperature of the particular chosen compounds. The yield values (wt.%) calculated from the resultant polynomial equations were compared with the original experimental (literature) values. The sum of square of errors of the yields from the polynomial equation and literature at the different temperatures was then minimised according to Equation B13 below.

$$\mathrm{SSE} = \sum_{\mathrm{i}=1}^{\mathrm{n}} (x_{i1} - x_{i2})^2$$

Equation B13

SSE is the sum of square of errors, x_{i1} and x_{i2} are the experimental (literature) and the predicted yields (wt.%) of compound *i* respectively. Minimisation of the sum of square of errors was performed by manipulating the parameters of the initially generated polynomial equations; this generated a new set of equation parameters that were then used as the correlation parameters. The yields calculated from the newly generated equations were accepted to within a 10% error margin from the literature yields.

The task of minimising the sum of square of errors was performed in Microsoft Excel® using the SOLVER function of data analysis. The correlation equations generated are in the form of Equation B14 with the corresponding parameter values of a, b and c given in Table B1.

$$\mathrm{Y}_i = \mathrm{aT}^2 + \mathrm{bT} + \mathrm{c}$$

Equation B14

Table B1: Parameters for correlation equations

Product	a	b	c
Oil	1.600E-04	-0.2442	118.1
Trimethylbenzene	1.550E-05	-0.02182	9.660
Naphthalene	-1.200E-05	0.01825	-6.197
Dimethylstyrene	1.000E-05	-0.0147	6.984
Dimethylquinoline	1.700E-05	-0.02590	10.47
Dimethylnaphthalene	-1.100E-05	0.01416	-2.871

Table B1 continued: Parameters for correlation equations

Product	a	b	c
Indene	-5.410E-06	8.530E-03	-2.564
Methylindene	-1.010E-05	0.01631	-4.854
Tetramethylbenzene	2.860E-06	-4.390E-03	1.880
Methylnaphthalene	-2.317E-05	3.2200E-02	-9.466
Dimethylindane	3.484E-06	-3.800E-03	1.118

The expression of the yield of char is the only exception from Equation B.14, and the char yield is in the form of Equation B15. The corresponding values of a, b, c and d are -2.000E-07, 4.000E-04, -0.2584 and 90.25 respectively.

$$Y_i = aT^3 + bT^2 + cT + d$$

Equation B15

The generated correlation equations used to describe the yields of the selected compounds as functions of the reactor temperature were used to give a certain degree of predictive ability to the reactor model.

B.3. Selection of thermodynamic model

The choice of an appropriate property model is a vital decision in simulation which affects all subsequent tasks in developing accurate physical properties for simulation and has implications on the accuracy of the simulation results (Aspen Technology, 2009; Van der Merwe, 2010). Aspen Plus® uses a collection of methods and models for property models in estimation of thermodynamic and transport properties (Aspen Technology, 2009; Mapamba 2012). Aspen Plus® contains a large number of built-in property methods that cover most engineering applications (Aspen Technology, 2009).

In Aspen Plus®, a choice of property models between ideal, equation of state (EOS) and activity coefficient property models is afforded based on the type of simulation (Aspen Technology, 2009; Mapamba 2012). The composition, temperature and pressure range and availability of parameters will influence the choice of property model to be selected (Van der Merwe, 2010). An equation of state is an analytical expression that relates the pressure to volume and temperature in describing the volumetric behaviour, vapour-liquid equilibria and thermal properties for both pure components and mixtures (Ashour *et al.*, 2011; Mapamba, 2012).

The choice of thermodynamic model to be used depends on the compounds that are being handled in the model. In the current study, the introduction of extractive distillation was found to require a different thermodynamic model from the rest of the flowsheet. As such, the choice of thermodynamic model will be highlighted for other sections and for the extractive distillation separately.

Thermodynamic model for pyrolysis section, normal distillation and heat recovery

Several methods have been used in literature for selection of property methods based on different algorithms. The methods considered for evaluation in this study are the Eric Carlson method, Bob Seader method and the Aspen Plus® guidelines for property method selection (Carlson, 1996; Seader *et al.*, 2006; Aspen Technology, 2009). Each of the methods considered is discussed below. The green lines indicate the paths that were followed to get to the recommended property method(s) for each method of evaluation.

Eric Carlson method

The Eric Carlson method for selection is shown in B.12 (Carlson, 1996). According to the Eric Carlson method, the Peng-Robinson (PENG-ROB), Redlich-Kwong-Soave (RK-SOAVE), Lee-Kesler-Plocker (LK-PLOCK), Peng-Robinson with Boston-Mathias alpha function (PR-BM) and the Redlich-Kwong-Soave with Boston-Mathias alpha function (RKS-BM) are then recommended for non-polar real compounds.

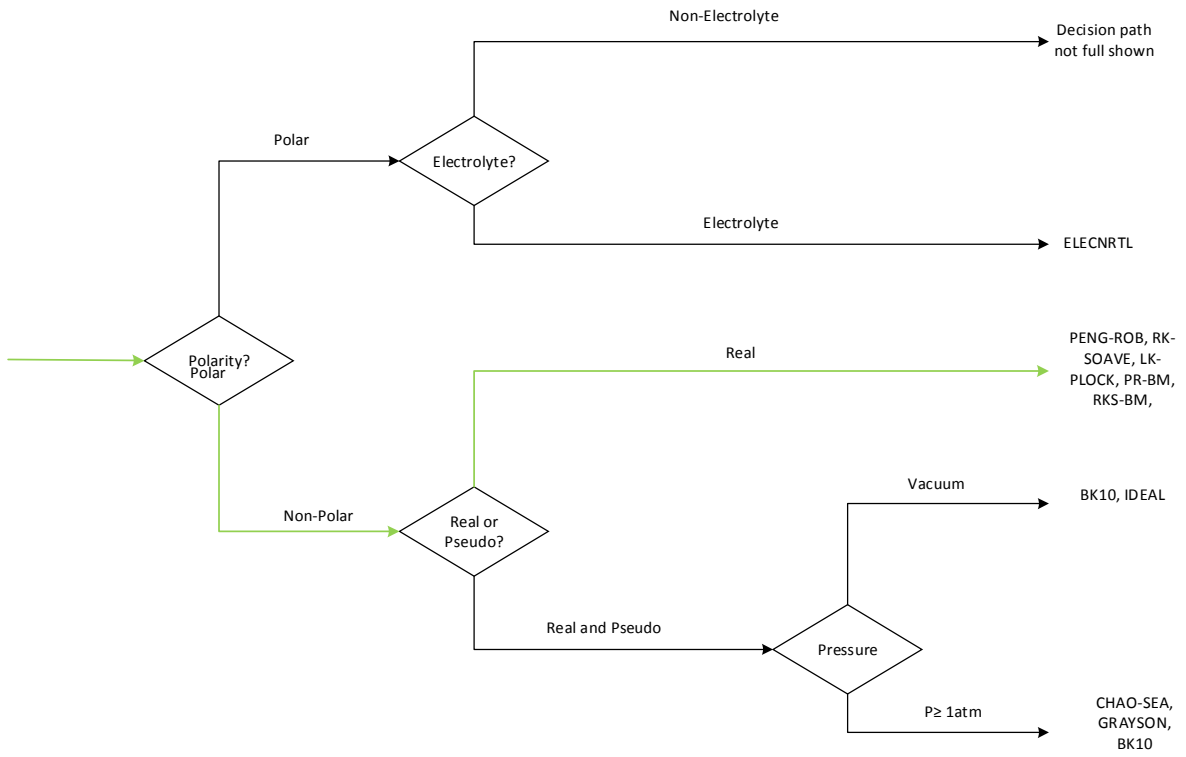

Figure B12: The Eric Carlson property method selection algorithm

Bob Seader method

The Bob Seader method for selection is shown in B.13 and B.14 (Seader *et al.*, 2006). According to the Bob Seader method, the Peng-Robinson (PR) or the Soave-Redlich-Kwong (SRK) property methods are then recommended for (non-polar) hydrocarbons (with light gases) at non-cryogenic temperatures.

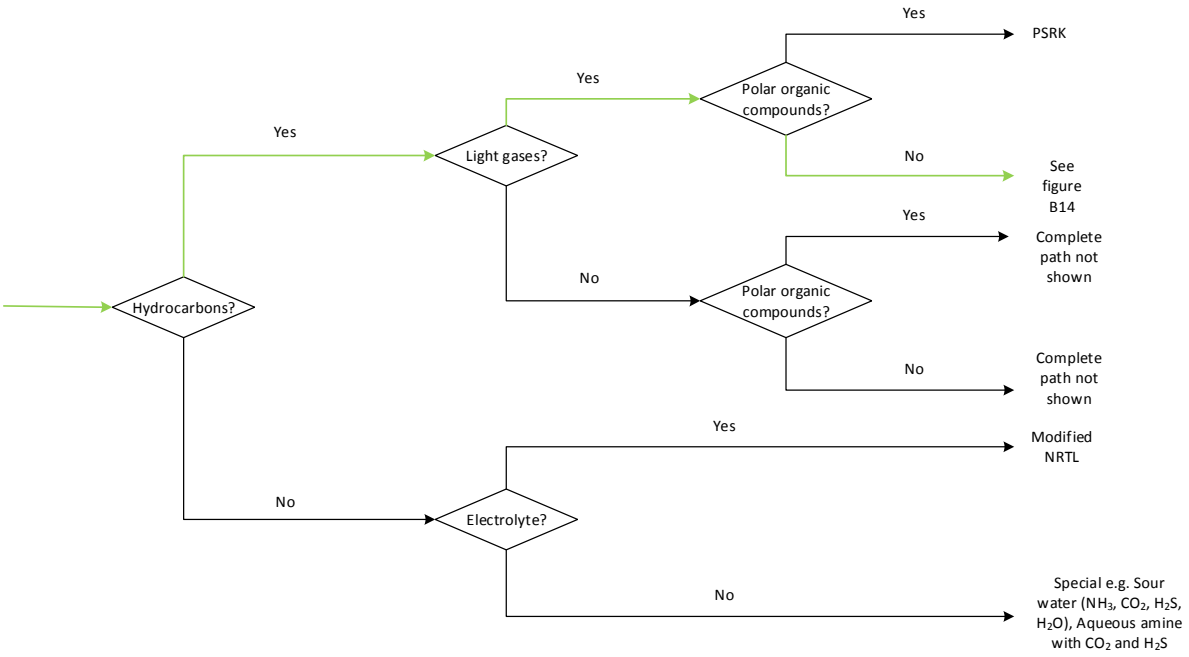

Figure B13: Bob Seader method of selection

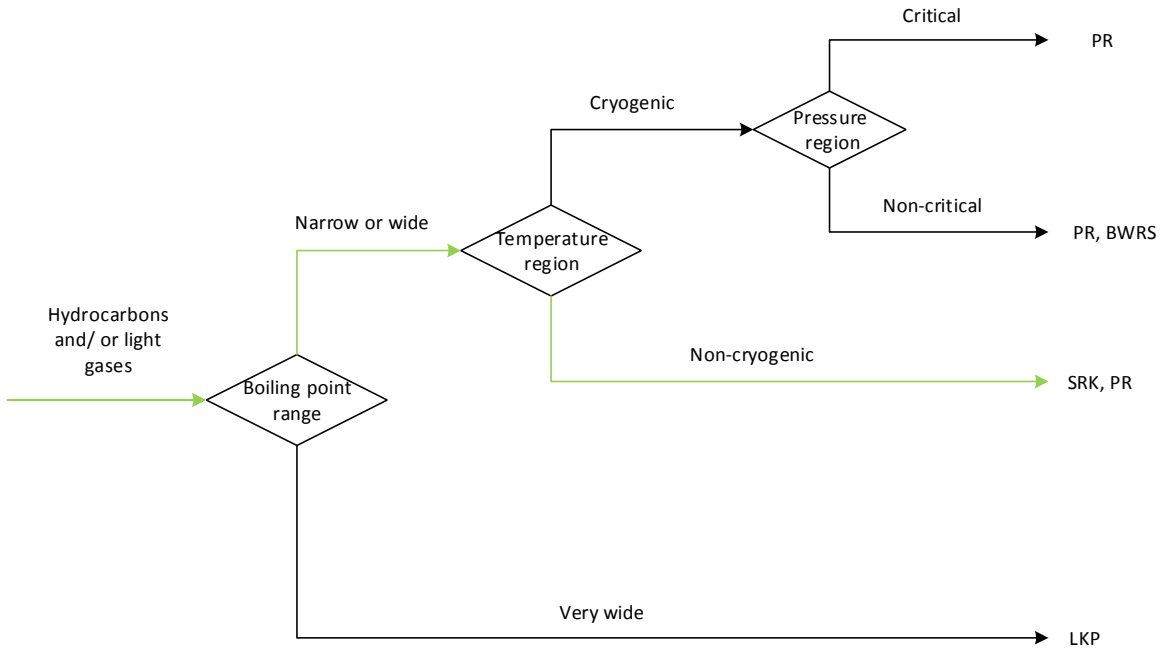

Figure B14: Extension of the Bob Seader method of selection

Aspen Plus® guideline

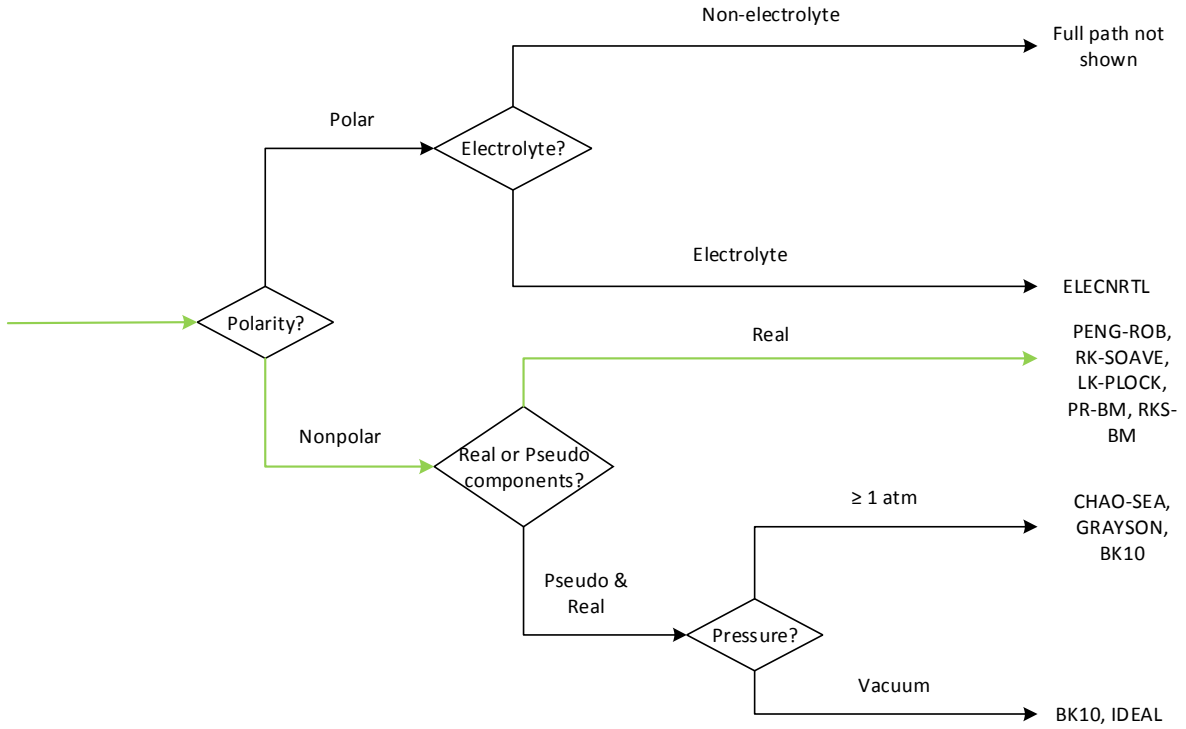

Figure B15: Aspen Plus® property method selection algorithm

The Aspen Plus® guideline for choosing a property method is indicated in B.15 (Aspen Technology, 2009). According to this algorithm, equation of state methods should be used. The Peng-Robinson (PENG-ROB), Redlich-Kwong-Soave (RK-SOAVE), Lee-Kesler-Plocker (LK-PLOCK), Peng-Robinson with Boston-Mathias alpha function (PR-BM) and the Redlich-Kwong-Soave with Boston-Mathias alpha function (RKS-BM) are then recommended for non-polar real compounds at pressures equals to or above atmospheric.

Literature recommendations

Equations of state are well suited for vapour mixtures, non-polar mixtures and slightly polar compounds (Aspen Technology, 2009; Mapamba 2012). The most commonly used equations of state are the Redlich-Kwong-Soave (RKS) and the Peng-Robinson (PR) equations of state. Both these equations of state give quite similar results for prediction of vapour-liquid equilibrium and vapour pressure comparison of several substances with the difference being that the PR EOS gives superior predictions for liquid densities (Aspen Technology, 2009; Ashour *et al.*, 2011; Mapamba 2012).

The Boston-Mathias alpha function is an alternative function to the usual PR alpha function and it is suitable for temperatures higher than critical. The PR alpha function can be used for subcritical temperatures but gives unrealistic results for light gases at high reduced temperatures (Ashour *et al.*,

2011). The PR-BM property method can be used for non-polar or mildly polar mixtures, hydrocarbons and light gases hence its relevance to the current model. It is recommended for applications of coal gasification or liquefaction of which the process of tyre pyrolysis is similar to (Aspen Technology, 2009). The PR-BM property method has been used in literature for processes simulating pyrolysis and gasification of carbonaceous material like tyres and coal (Kong *et al.*, 2013; He *et al.*, 2014; Altayeb, 2015).

Recommended property method

The Peng-Robinson with a Boston-Mathias alpha function (PR-BM) property method was chosen to calculate the physical properties for all the conventional components in the current study. The HCOALGEN and DCOALIGT property models were used to calculate the enthalpy and density of the non-conventional components (tyre and char) respectively (based on the proximate and ultimate analyses provided in Choi *et al.*, 2014).

Thermodynamic model for extractive distillation

In this study, work regarding the recovery of limonene using extractive distillation was adapted from a study by Ngwetjana (2017). As such, the thermodynamic model used in this study for the extractive section was also adopted from Ngwetjana (2017). For the solvent recovery section, the non-random two-liquid (NRTL) property model has been used for prediction of thermodynamic properties of components in this study. The universal function activity coefficient (UNIFAC) property model was used to estimate missing binary parameters for the NRTL property model in this study.

Activity coefficient property models (such as the NRTL model) are recommended for non-ideal liquid mixtures and are preferred for solvent recovery systems in literature (Chen and Mathias, 2002; Aspen Technology, 2009). When binary interaction parameters are available, activity coefficient models are accurate for phase equilibrium calculations. The UNIFAC predictive model can however be used to estimate the required parameters in the absence of vapour-liquid equilibrium (VLE) data to generate the required binary parameters (Aspen Technology, 2009). The NRTL property model has been used in literature for simulations including solvent recovery of hydrocarbons with the UNIFAC property model used to estimate missing interaction parameters (Ko *et al.*, 2002; Brondani *et al.*, 2015).

APPENDIX C: SENSITIVITY ANALYSIS OF SEPARATION COLUMNS

C.1. Determination of initial parameters for T-101 using DSTWU column model

The DSTWU column model generates the necessary parameters by performing a Winn-Underwood-Gilliland shortcut design calculation for a single-feed, two-product distillation column for the specified key components. The desired recovery of key components also has to be specified. The DSTWU model then estimates reflux ratio or number of theoretical stages given that either of the parameters is specified (Aspen Technology, 2009; Henley *et al.*, 2011).

The key components were specified as 2-ethyltoluene (light key) and limonene (heavy key) based on the desired limonene cut/fraction. The recovery of each key component was specified at 99%, as it is usually desirable to have it specified at such for target compounds (Sinnott and Towler, 2009).

The number of theoretical stages was chosen (as input) such that the resulting ratio of actual: minimum reflux ratios was around 1.15. According to literature, the ratio of actual: minimum reflux ratios should typically be between 1.05 and 1.5 (with 1.15 being a good initial estimate) for optimum column operation (Douglas, 1998; Sinnott and Towler; 2009; Henley *et al.*, 2011). The number of theoretical stages was manually changed until the ratio of 1.15 was obtained. A stage pressure drop of 0.7 kPa was specified as it is recommended for atmospheric operation (Henley *et al.*, 2011). The resulting number of stages was compared with information of some representative commercial binary distillation at atmospheric pressure (100 kPaa) of close boiling point compounds shown in Table C1.

Table C1: Representative commercial binary distillation operations (Henley *et al.*, 2011)

Binary mixture	Average relative volatility	Number of trays	Reflux: minimum reflux ratio
Vinyl acetate/ethyl acetate	1.16	90	1.15
o-Xylene/*m*-xylene	1.17	130	1.12
Methanol/ethanol	1.44	75	1.2
Water/acetic acid	1.83	40	1.35
Acetic acid/acetic anhydride	2.02	50	1.13

C.2. T-101 sensitivity analysis

Sensitivity analysis at base case number of stages

Effect of reflux ratio

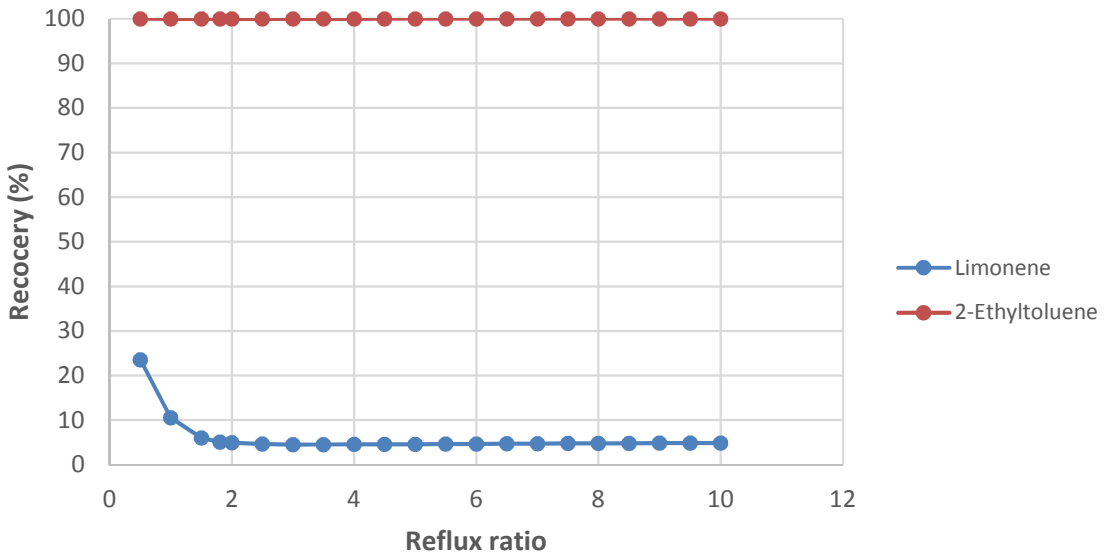

Figure C1: Recovery of key components in desired streams at various reflux ratios (base case number of stages)

The effect of variation in reflux ratio on the recovery of limonene and 2-ethyltoluene is shown in Figure C1. It can be seen that increasing the reflux ratio leads to a decrease in the recovery of limonene. This decrease can be attributed to increased vapourisation of limonene due to increased energy input from the reboiler in order to meet the increasing refluxing requirements. This leads to more stripping of the limonene, hence less recovery of limonene in bottoms product. Figure C1 also shows that variation in reflux ratio does not have an effect on the recovery of 2-ethyltoluene (as distillate product). This can be attributed to that at low reflux ratios there is little cooling of 2-ethyltoluene (vapours at the top of the column) which enhances the recovery. At higher reflux ratios, the increased energy input helps maintain the recovery in the distillate stream.

Effects of number of stages

The effect of variation in the number of stages on the recovery of limonene and 2-ethyltoluene at different reflux ratios is shown in Figure C2. It can be seen that the recovery of limonene decreases with an increase in number of stages at all reflux ratios with a rapid decrease at reflux ratios of higher than 2. The decrease in the limonene recovery is due to the addition of more stages in the stripping section (feed stage is fixed) of the column which allows for more contact with the hot rising vapours and results in increased stripping of limonene. The rapid decrease at higher reflux ratios can be attributed to increased vapour generation in the column to meet reflux requirements.

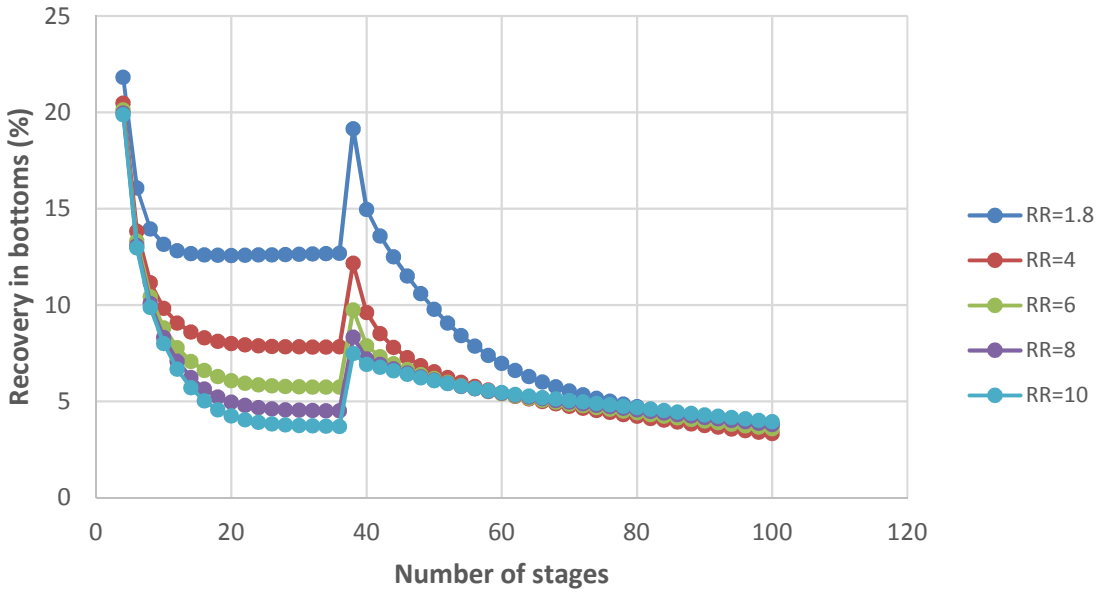

Figure C2: Effect of number of stages on recovery of limonene at various reflux ratios

Figure C3 shows the effect of variation in the number of stages on the recovery of 2-ethyltoluene. It can be seen that the recovery of 2-ethyltoluene increases with increasing number of stages at all reflux ratios as increased contact with hot vapours and increased vapour generation favours its recovery as distillate.

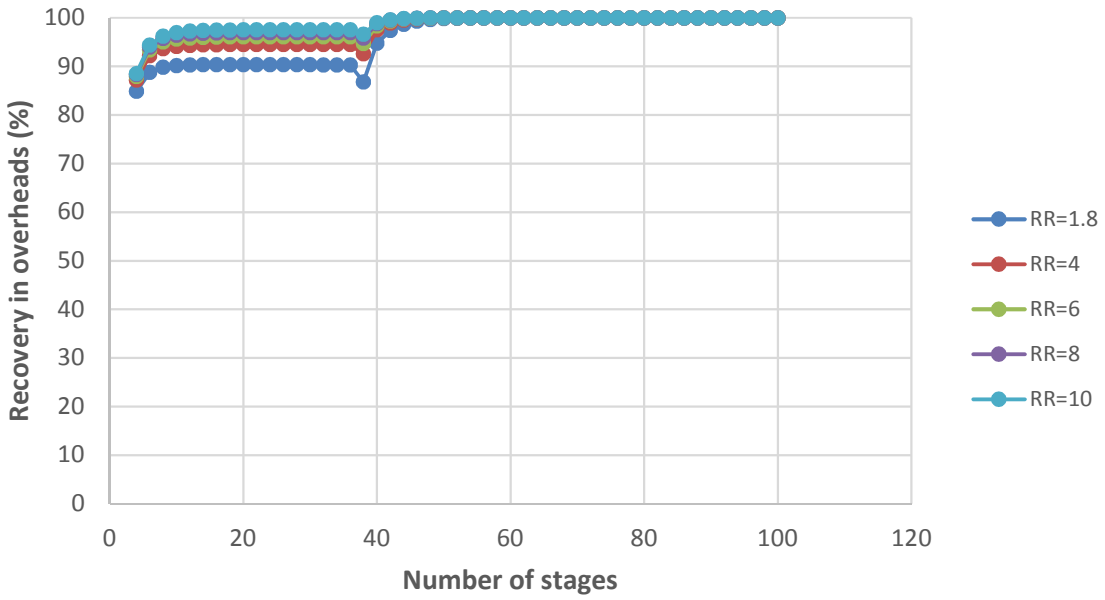

Figure C3: Effect of number of stages on recovery of 2-ethyltoluene at various reflux ratios

Effect of feed location

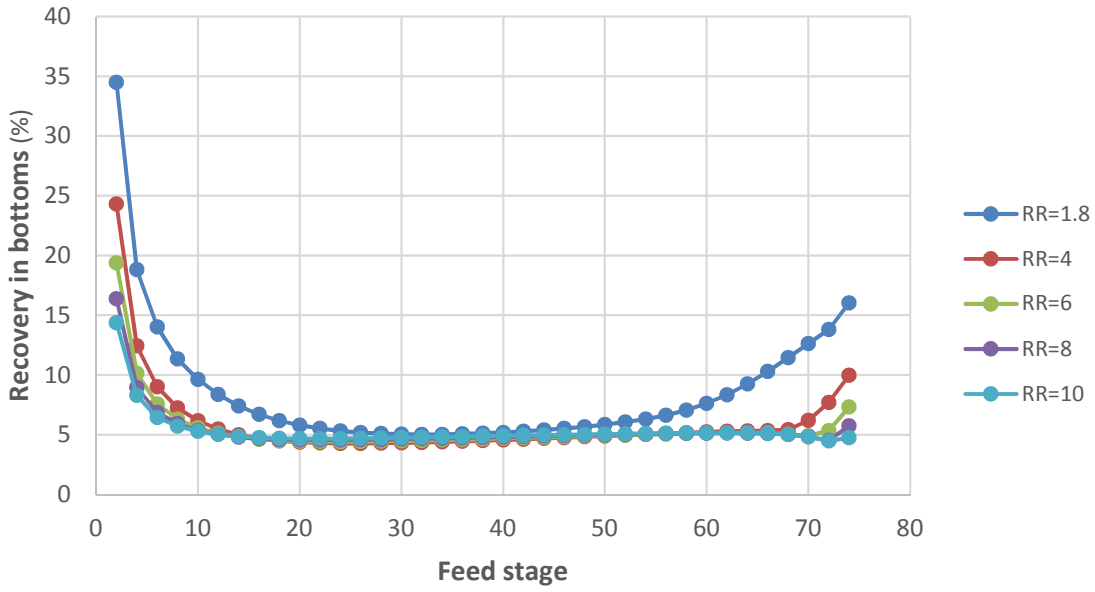

Figure C4: Effect of feed stage on the recovery of limonene at various reflux ratios

The effect of feed location on the recoveries of limonene and 2-ethyltoluene is shown for various reflux ratios in Figure C4. Figure C4 shows that the recovery of limonene decreases with increasing feed location (feeding further down the column) for all reflux ratios. Feeding further down the column facilitates more vapourisation of limonene due to increasing feed point temperature as feed is

introduced closer to the reboiler. The recovery starts increasing as the feed is introduced much closer to the reboiler as there is less room for contact of the liquid feed with the hot vapours coming from the reboiler which results in less limonene being stripped off.

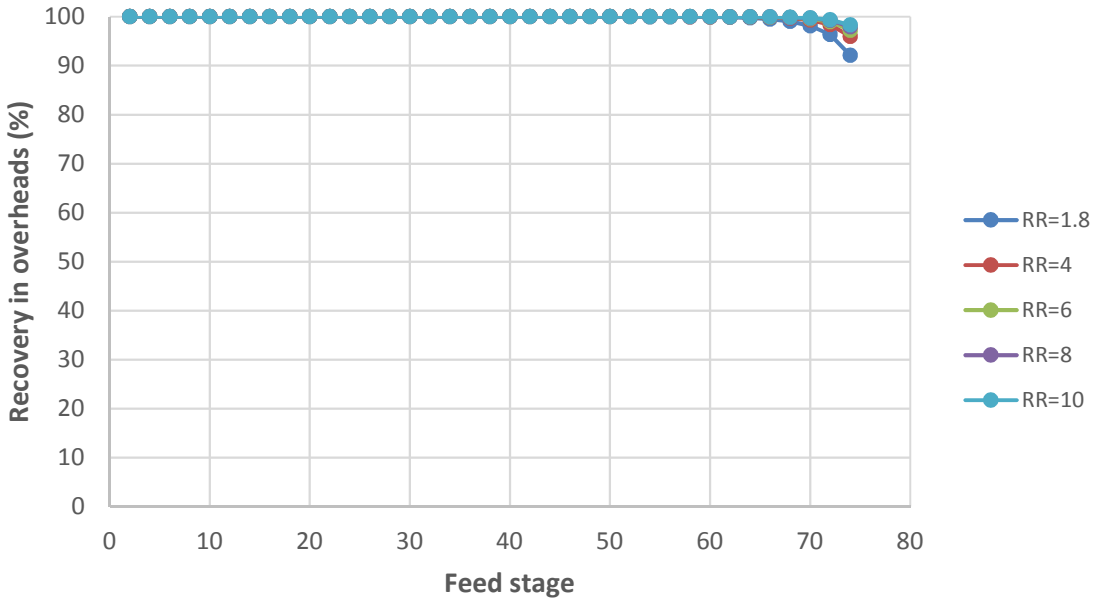

Figure C5: Effect of feed stage on the recovery of 2-ethyltoluene at various reflux ratios

Figure C5 shows that the recovery of 2-ethyltoluene remains constant for almost all feed locations except just above the reboiler as some of it flows down the column due to reduced contact stages with the vapours coming from below the feed. Feed location has no effect on the recovery of 2-ethyltoluene.

Effect of boilup ratio

The effect of boilup ratio on the recoveries of limonene and 2-ethyltoluene is shown in Figure C6 and Figure C7 respectively. Figure C6 shows that limonene recovery decreases with an increase in boilup ratio for reflux ratios below 10 as more bottoms product is vapourised and returned as boilup. At a reflux ratio of 10 there is no change in the recovery as the increased reflux ratio counteracts the effects of increased boilup and all limonene is recovered as bottoms product.

The recovery of 2-ethyltoluene increases with increasing boilup ratio for all reflux ratios as shown in Figure C7 and it can also be noted that increasing the boilup ratio above 7 no longer has an effect as almost all 2-ethyltoluene is recovered already. The recovery in the distillate is favoured by an increased boilup ratio as more material is vapourised due to increased reboiler energy input.

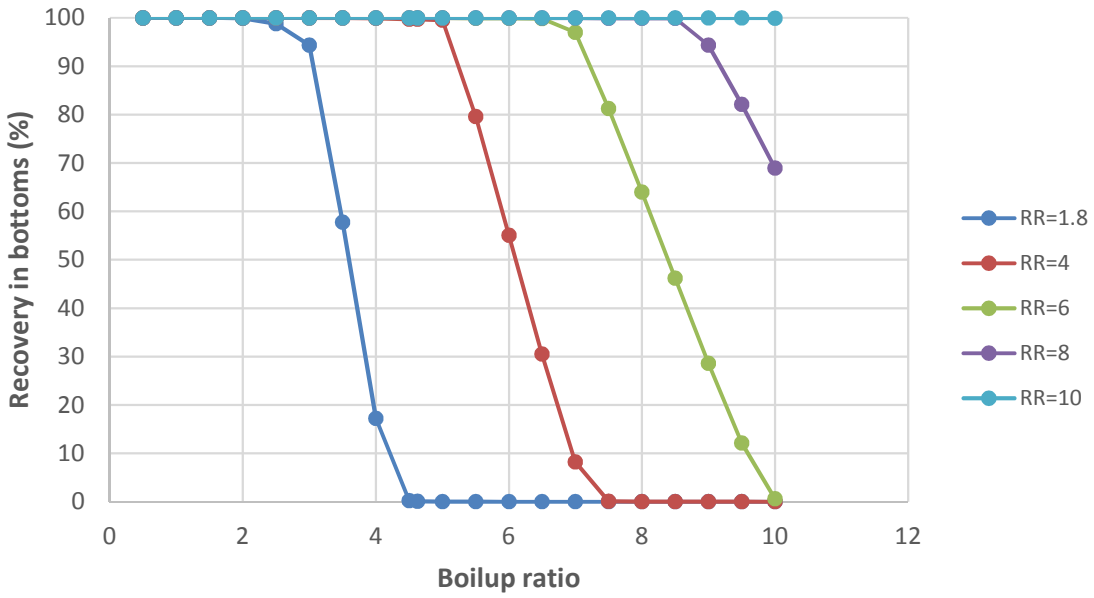

Figure C6: Effect of boilup ratio on the recovery of limonene at various reflux ratios

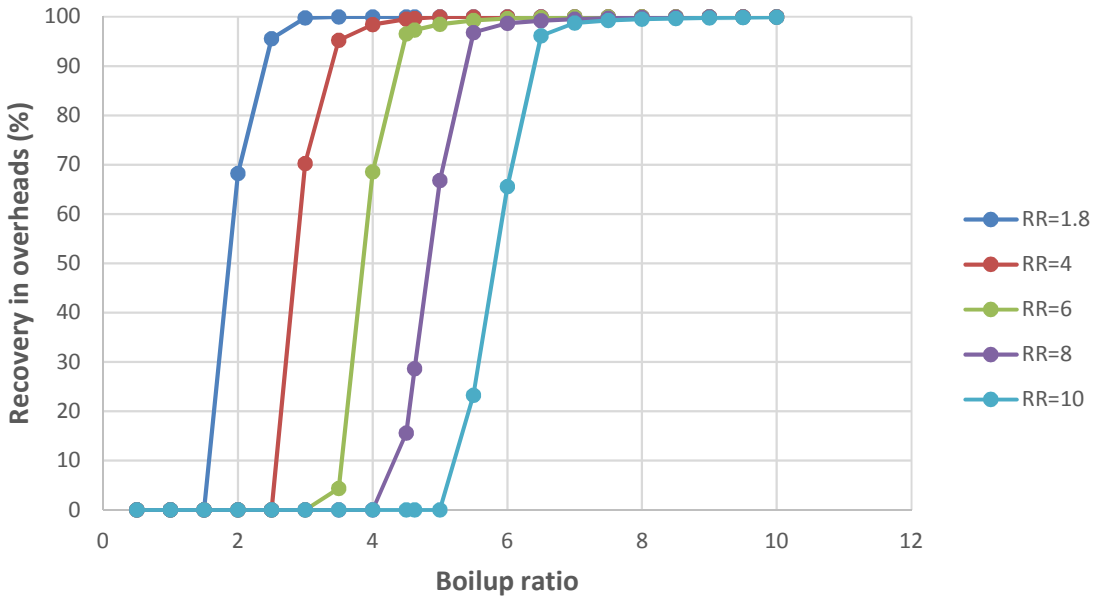

Figure C7: Effect of boilup on the recovery of 2-ethyltoluene at various reflux ratios

Effect of feed temperature

Figure C8 and Figure C9 show the effects of variation in feed temperature on the recoveries of limonene and 2-ethytoluene respectively. The variation in feed temperature has very minimal effect on the recoveries of both limonene and 2-ethyltoluene at all reflux ratios. There is only a slight increase

in limonene recovery above 120 °C at a reflux ratio of 1.8 as the effects of decreased reboiler duty slightly decrease the stripping of limonene.

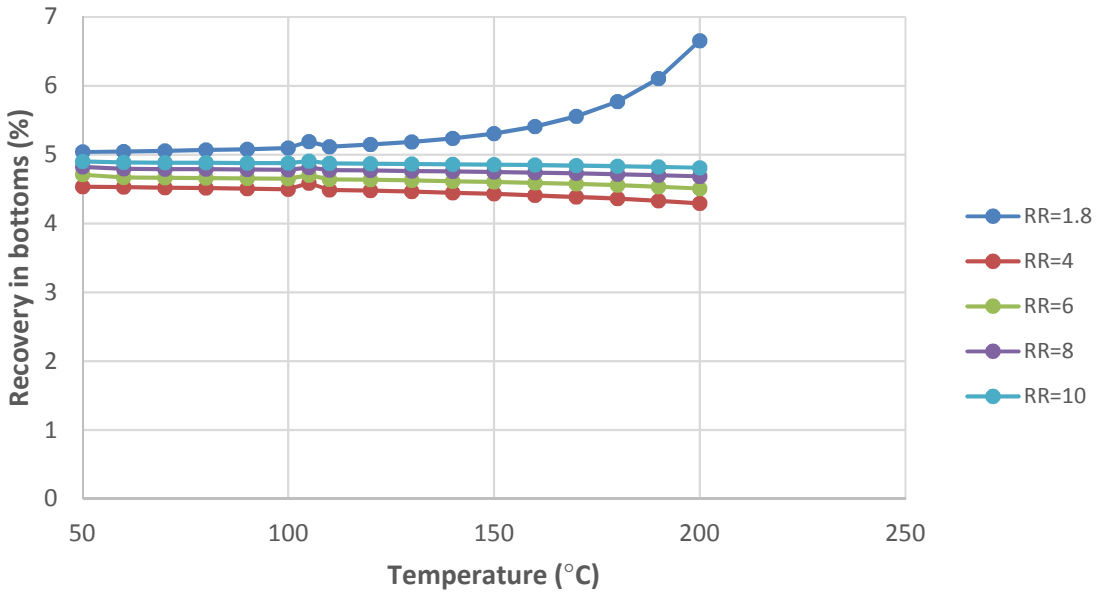

Figure C8: Effect of temperature on the recovery of limonene at various reflux ratios

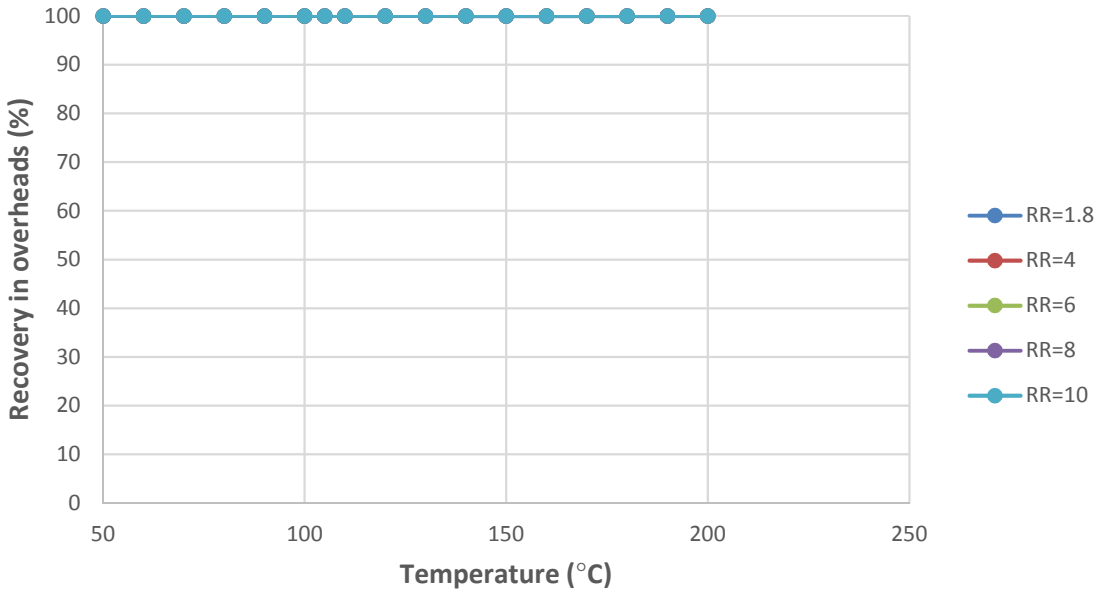

Figure C9: Effect of feed temperature on the recovery of 2-ethyltoluene at various reflux ratios

Reboiler duties

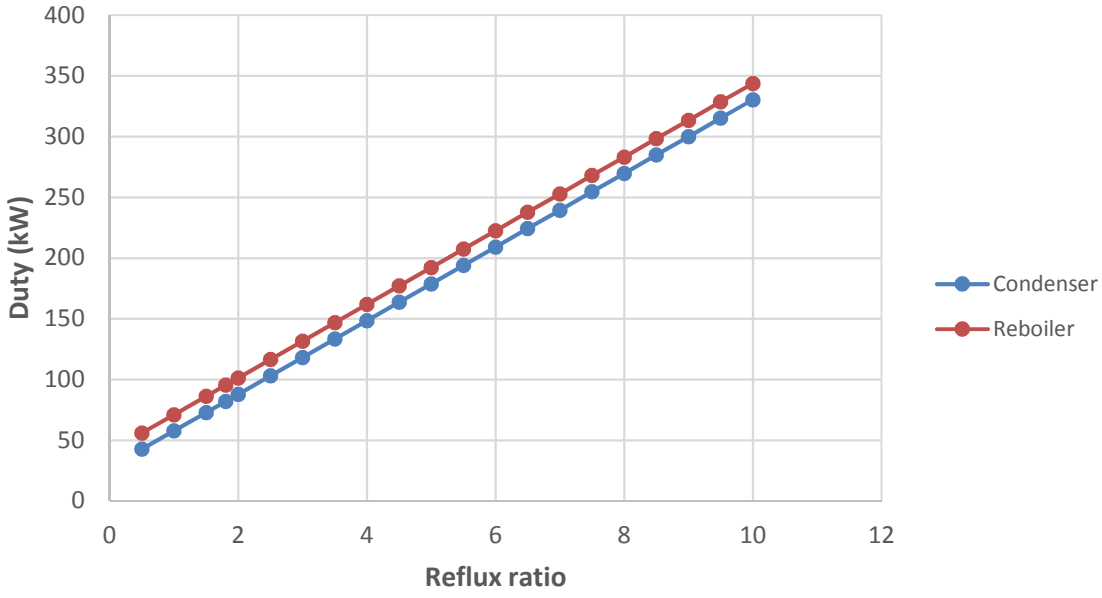

Figure C10: Effect of reflux ratio on condenser and reboiler duties at base case number of stages

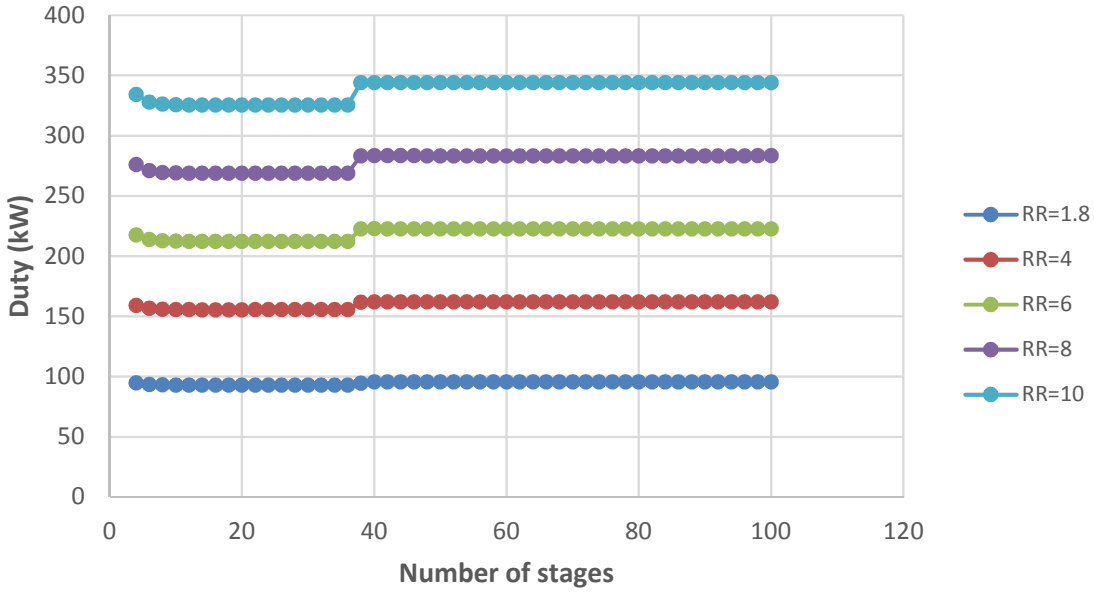

Figure C11: Effect of number of stages on reboiler duty at various reflux ratios

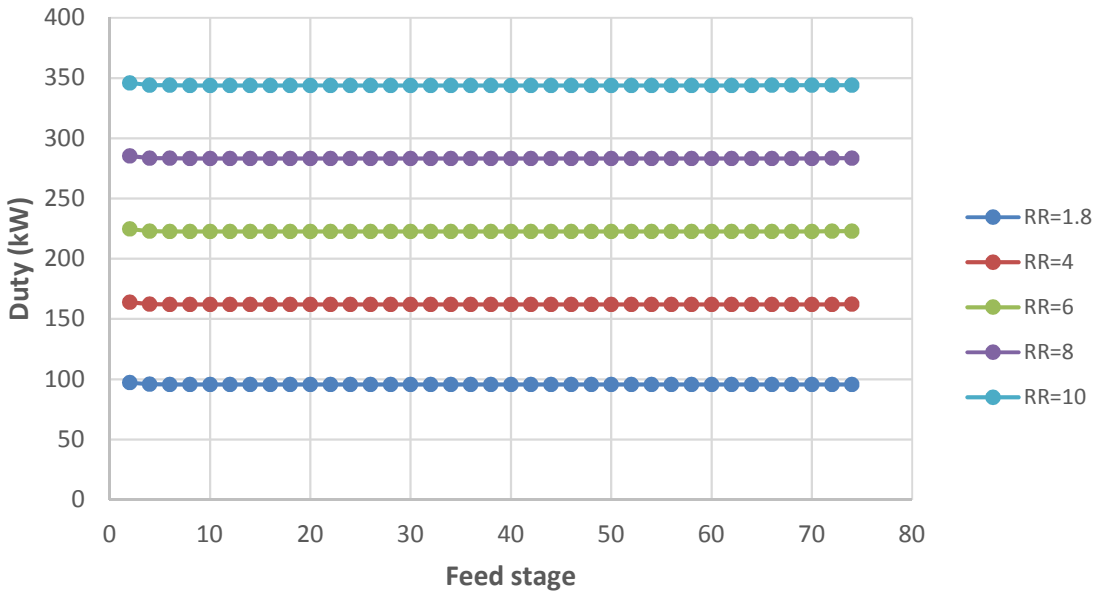

Figure C12: Effect of feed location on the reboiler duty at various reflux ratios

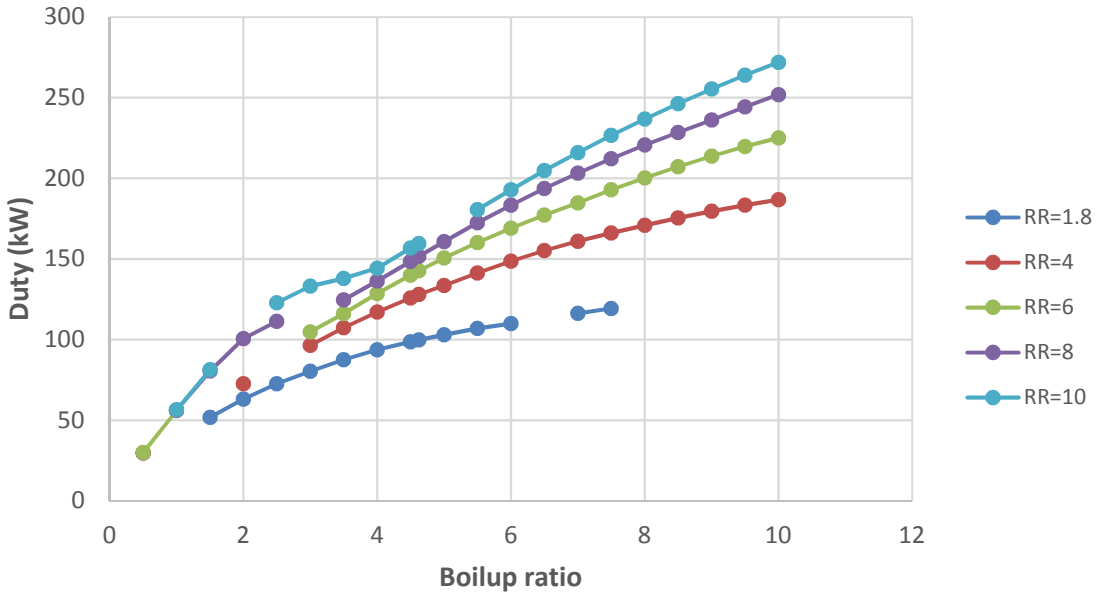

Figure C13: Effect of boilup ratio on the reboiler duty at various reflux ratios

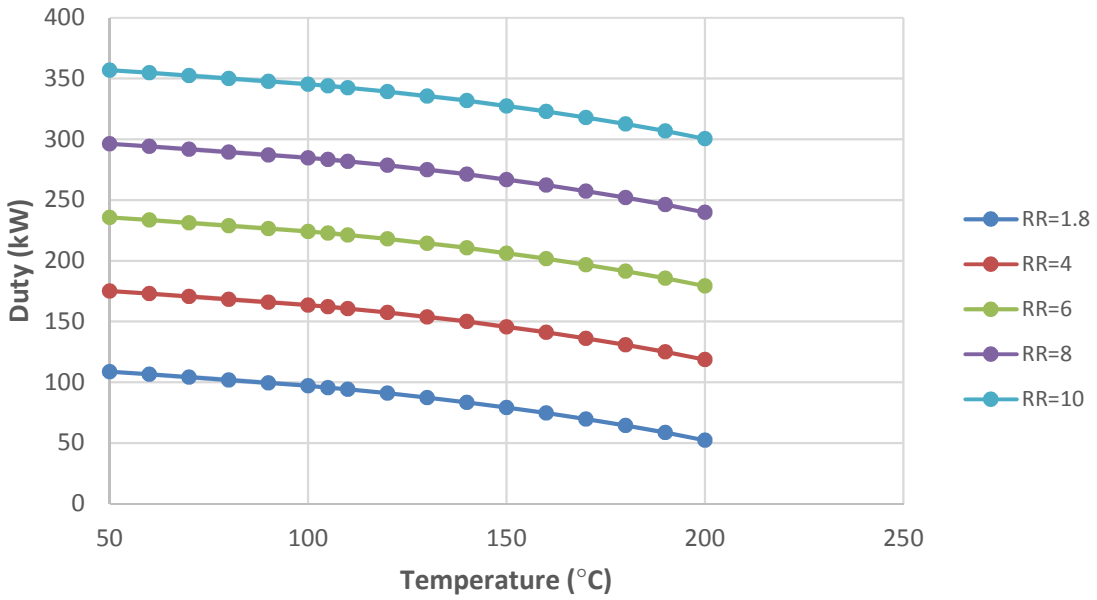

Figure C14: Effect of feed temperature on reboiler duty at various reflux ratios

Sensitivity analysis at various number of stages

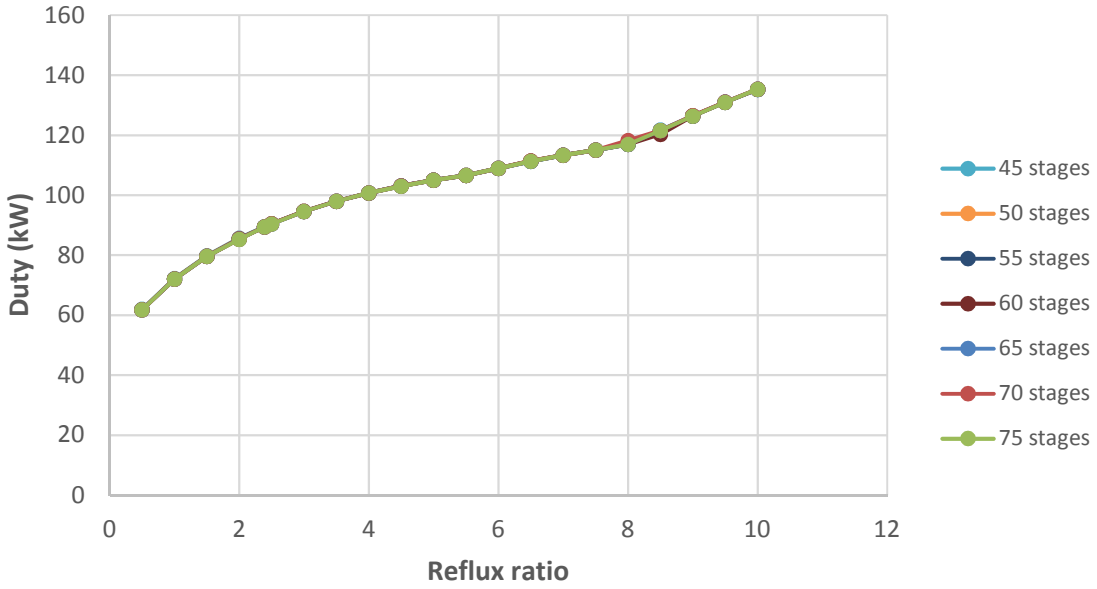

Figure C15: Effect of reflux ratio on reboiler duty at various number of stages

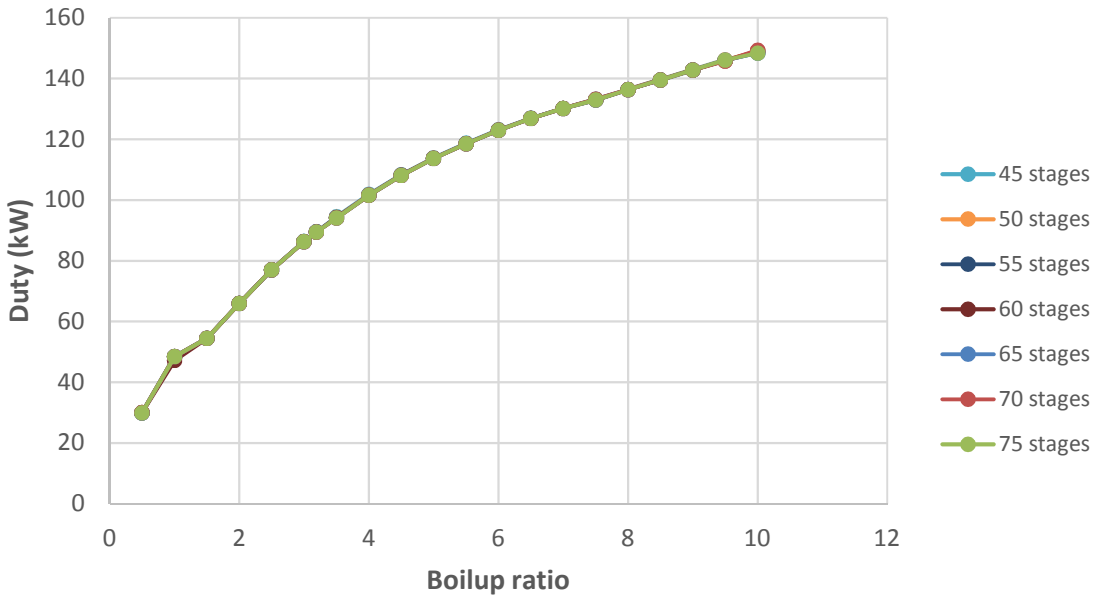

Figure C16: Effect of boilup ratio on reboiler duty at various number of stages

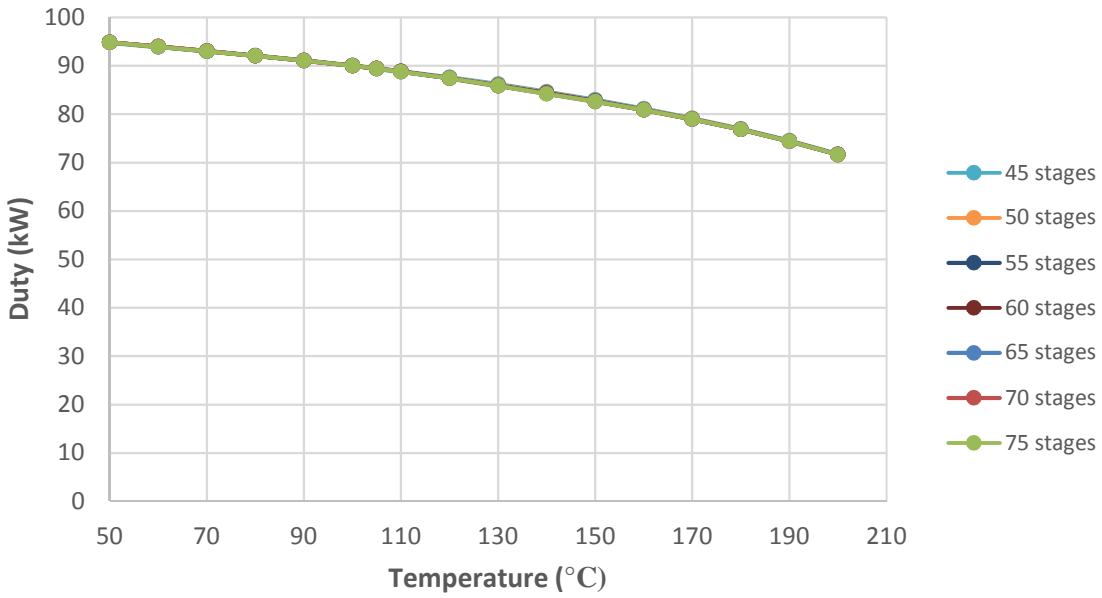

Figure C17: Effect of feed temperature on reboiler duty at various number of stages

C.3. T-102 sensitivity analysis

Sensitivity analysis at base case number of stages

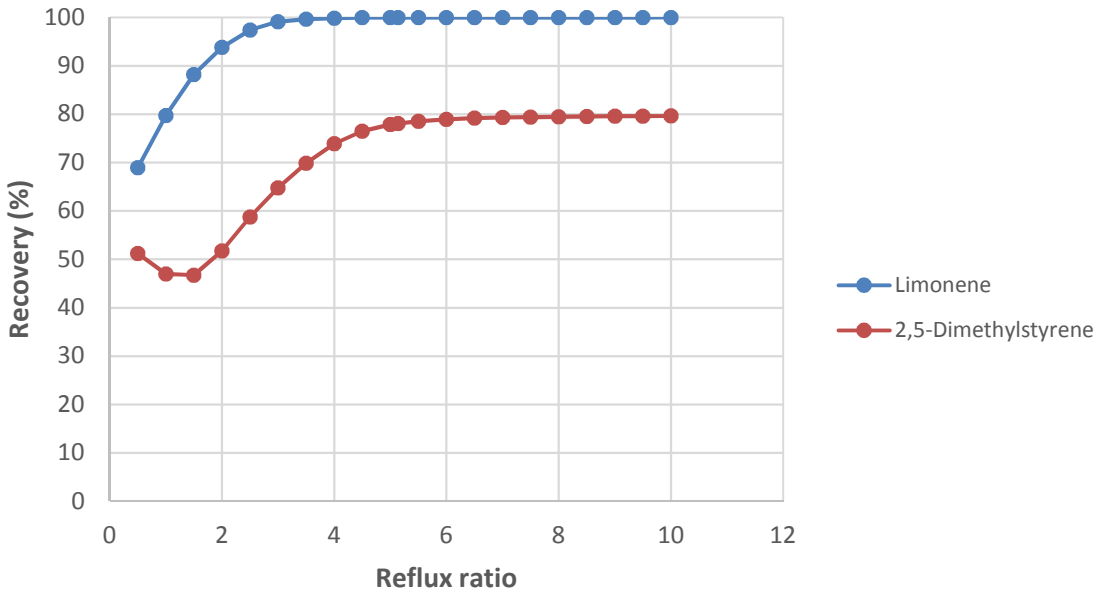

Figure C18: Recovery of key components in desired product streams at various reflux ratios at base case number of stages

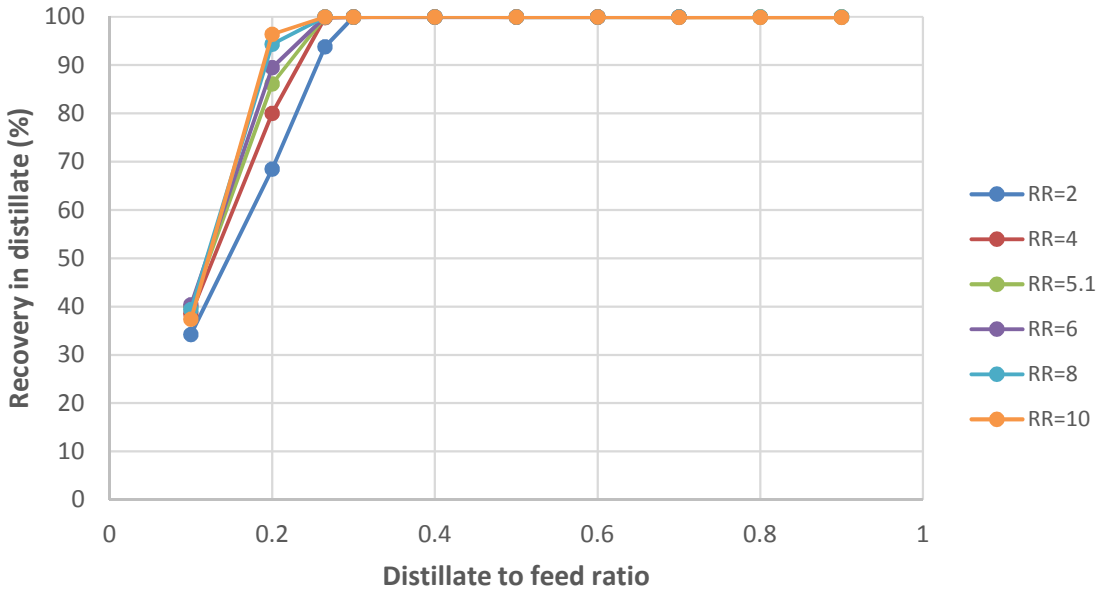

Figure C19: Recovery of limonene in distillate product at various distillate to feed ratios for base case number of stages

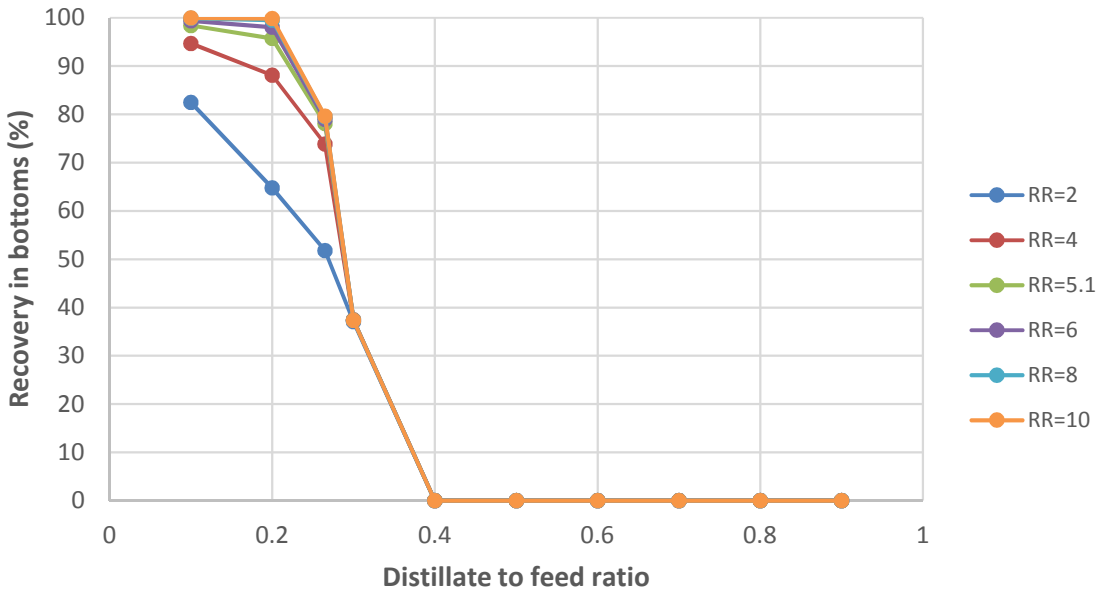

Figure C20: Recovery of 2,5-dimethylstyrene at various distillate to feed ratios for base case number of stages

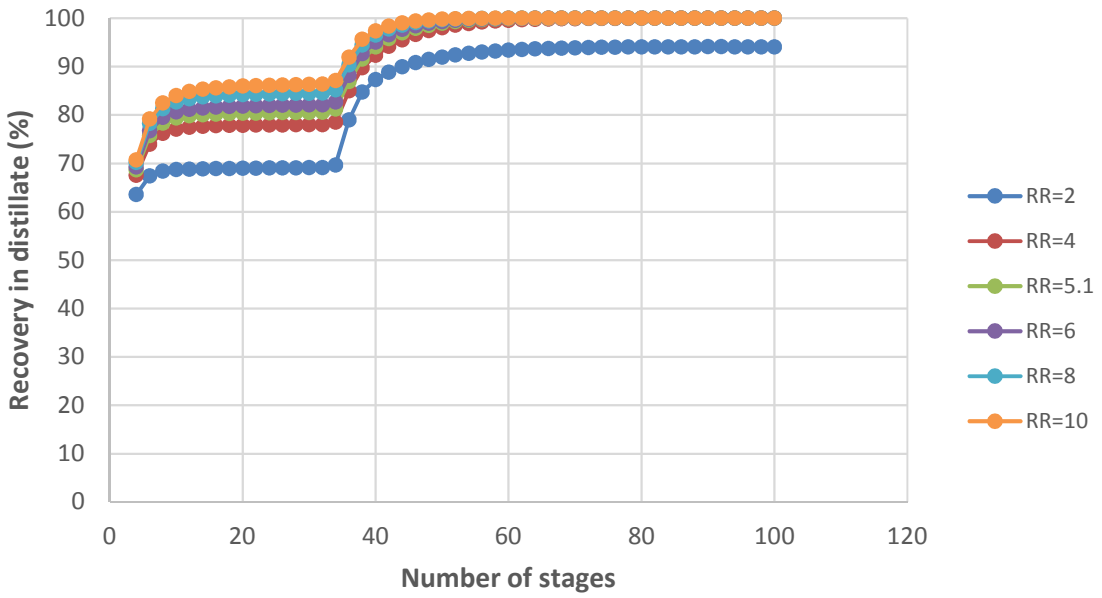

Figure C21: Effect of number of stages on recovery of limonene in distillate product at various reflux ratios

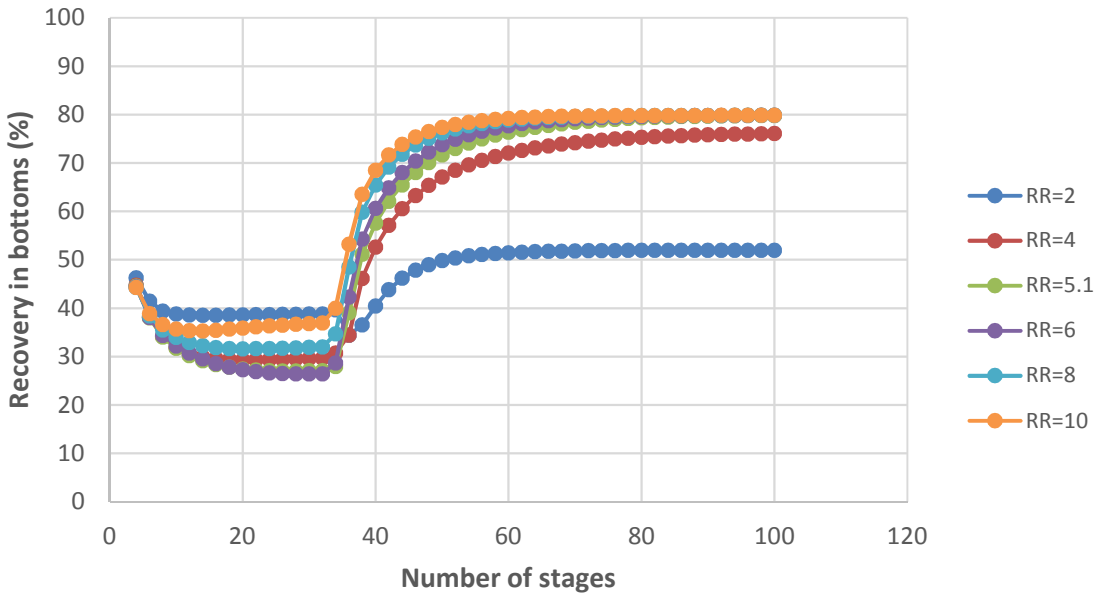

Figure C22: Effect of number of stages on recovery of 2,5-dimethylstyrene in bottoms product at various reflux ratios

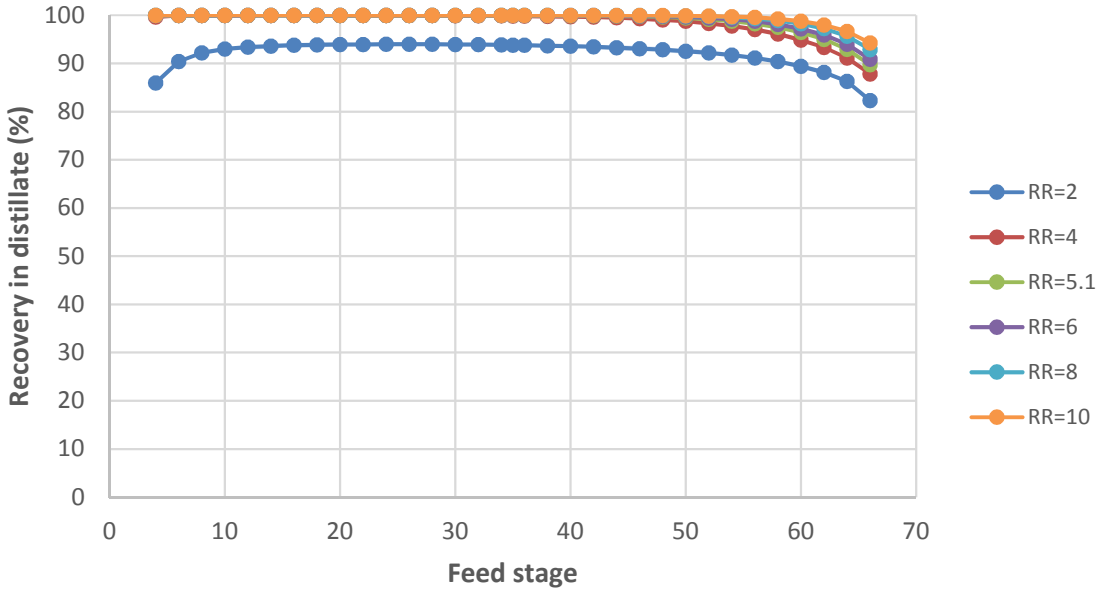

Figure C23: Effect of feed location on recovery of limonene in distillate product at various reflux ratios

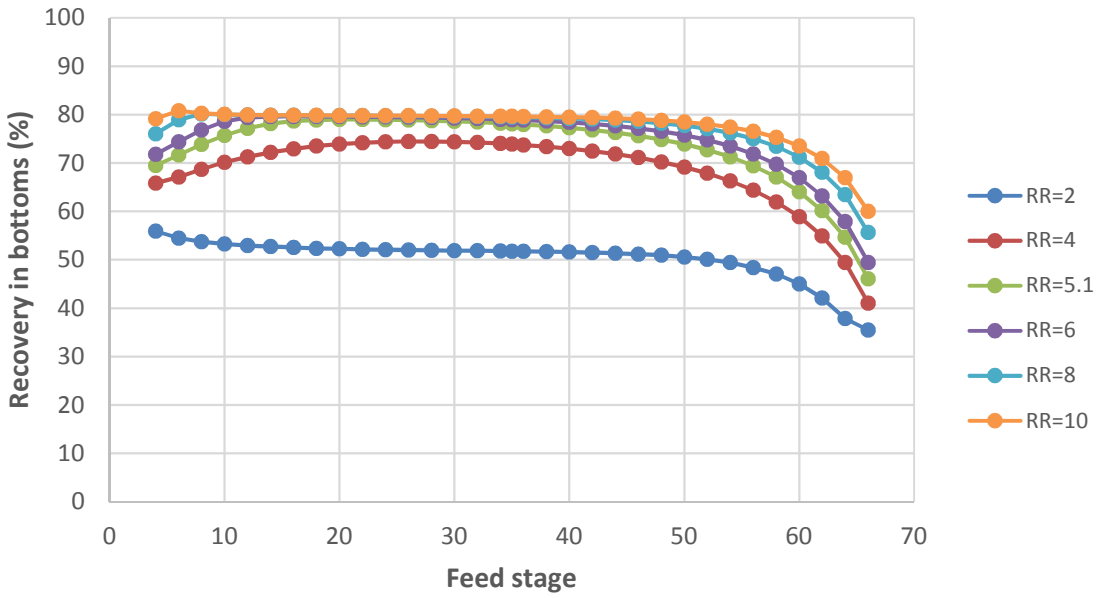

Figure C24: Effect of feed location on recovery of 2,5-dimethylstyrene in bottoms at various reflux ratios

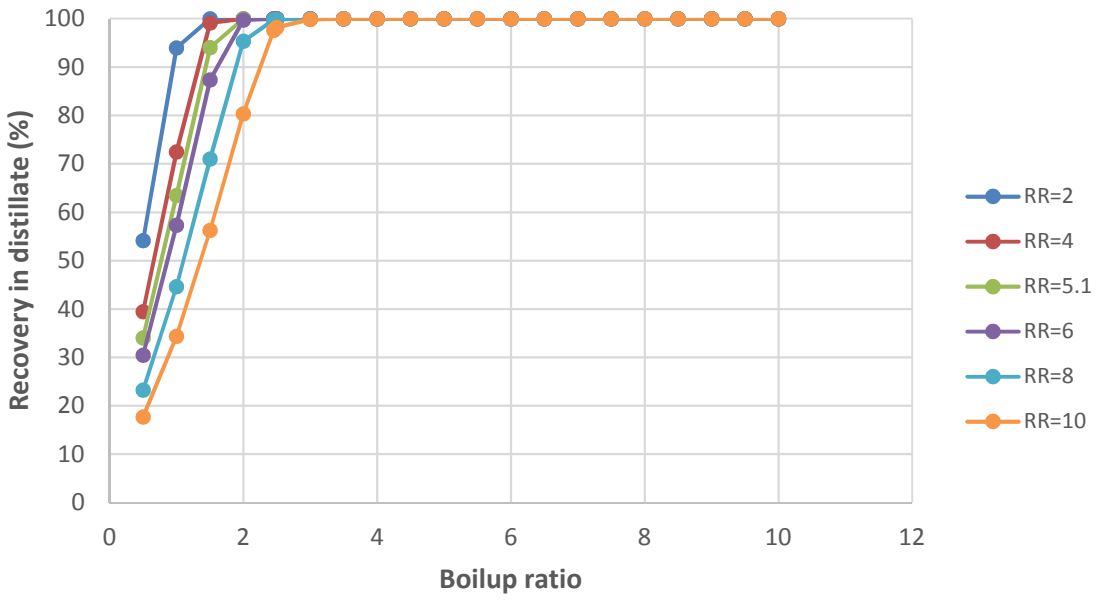

Figure C25: Effect of boil-up ratio on recovery of limonene in distillate at various reflux ratios

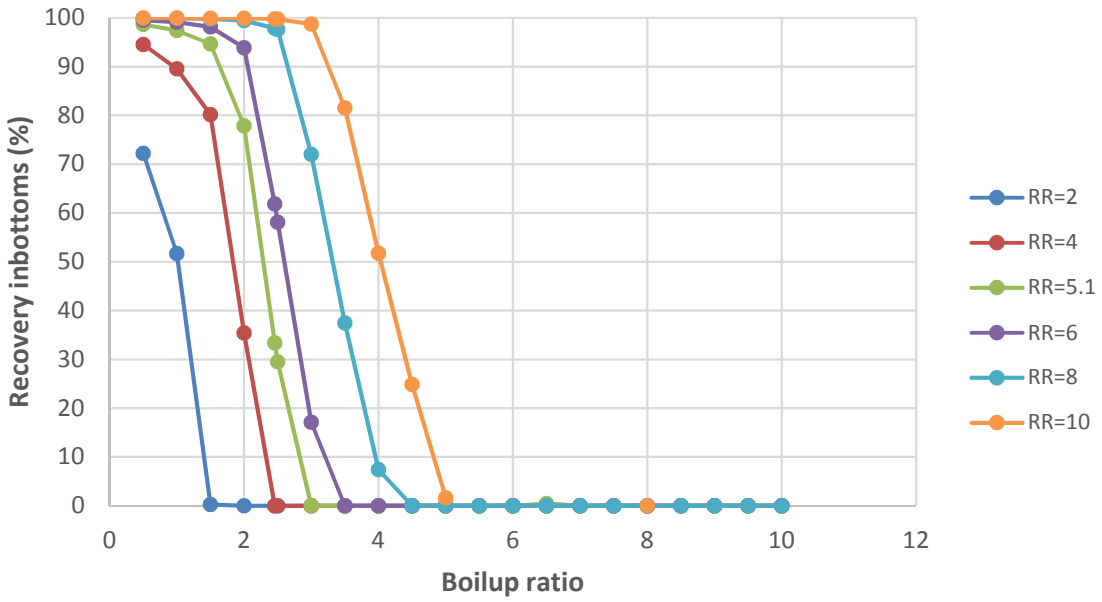

Figure C26: Effect of boil-up ratio on the recovery of 2,5-dimethylstyrene in bottoms at various reflux ratios

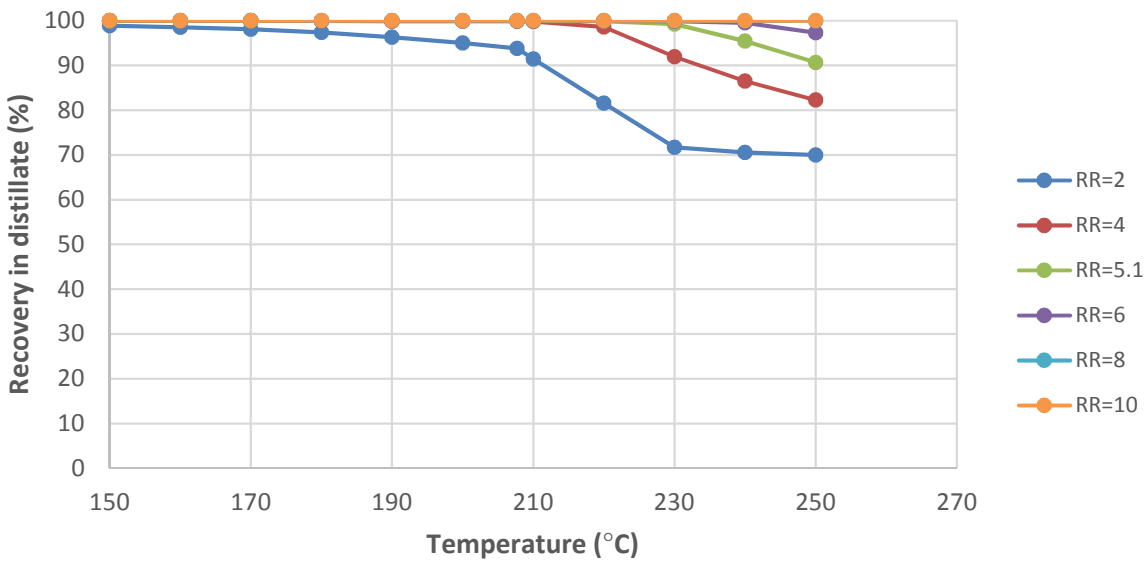

Figure C27: Effect of feed temperature on the recovery of limonene in distillate at various reflux ratios

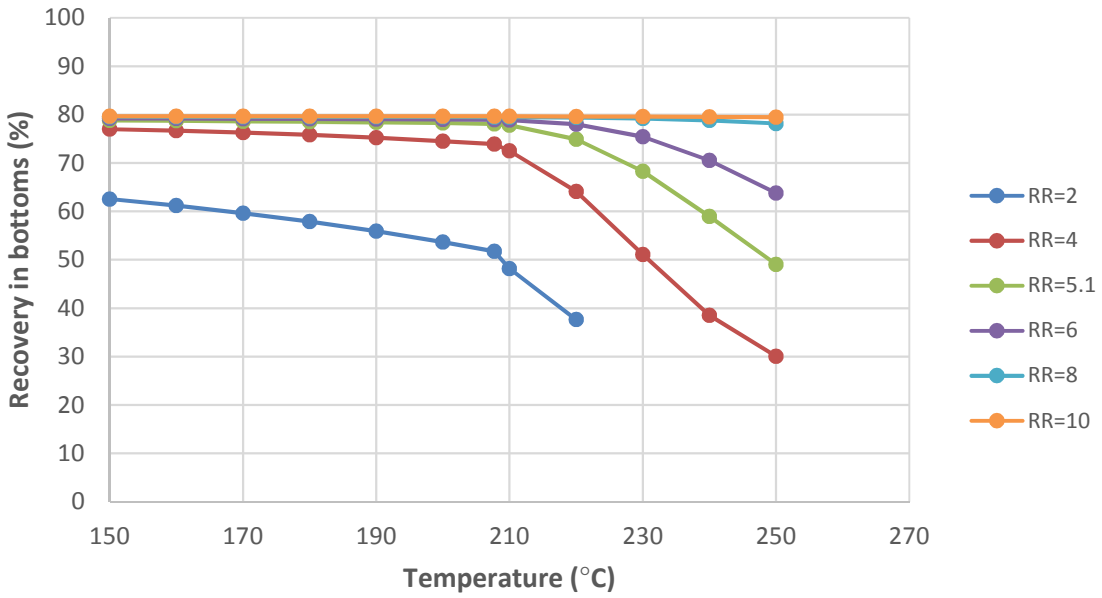

Figure C28: Effect of feed temperature on the recovery of 2,5-dimethylstyrene in bottoms at various reflux ratios

Reboiler duties

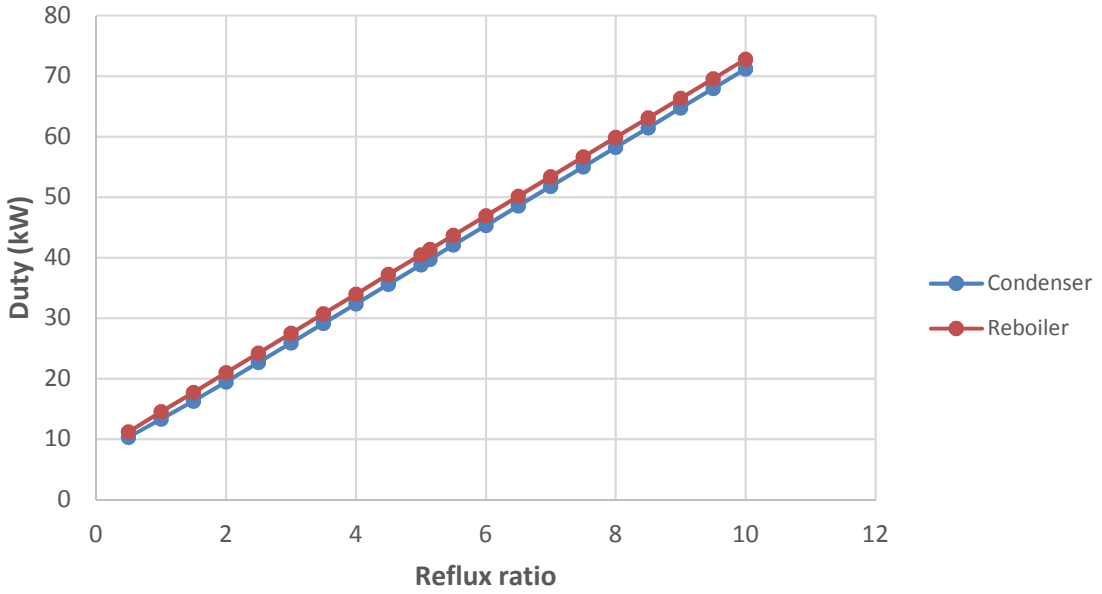

Figure C29: Effect of reflux ratio on reboiler duty at base case number of stages

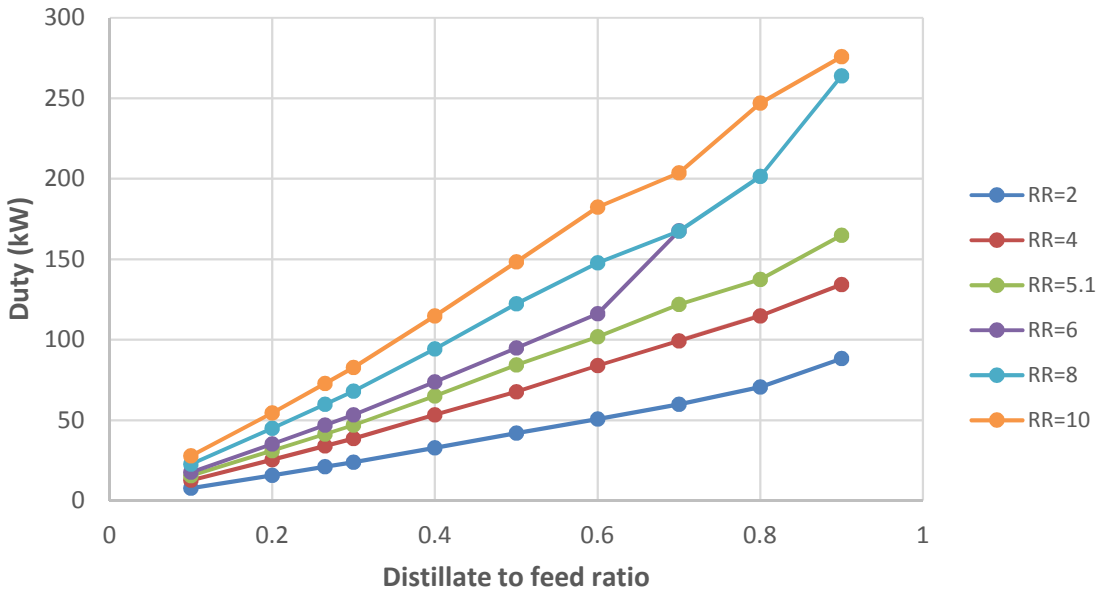

Figure C30: Effect of distillate to feed ratio on reboiler duty at various reflux ratios

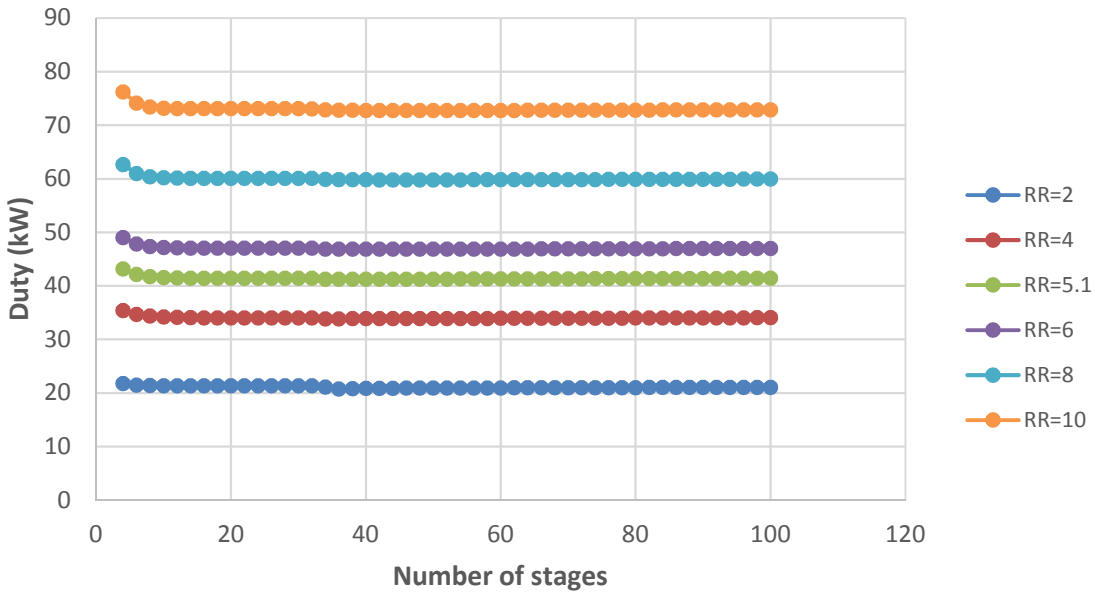

Figure C31: Effect of number of stages on reboiler duty at various reflux ratios

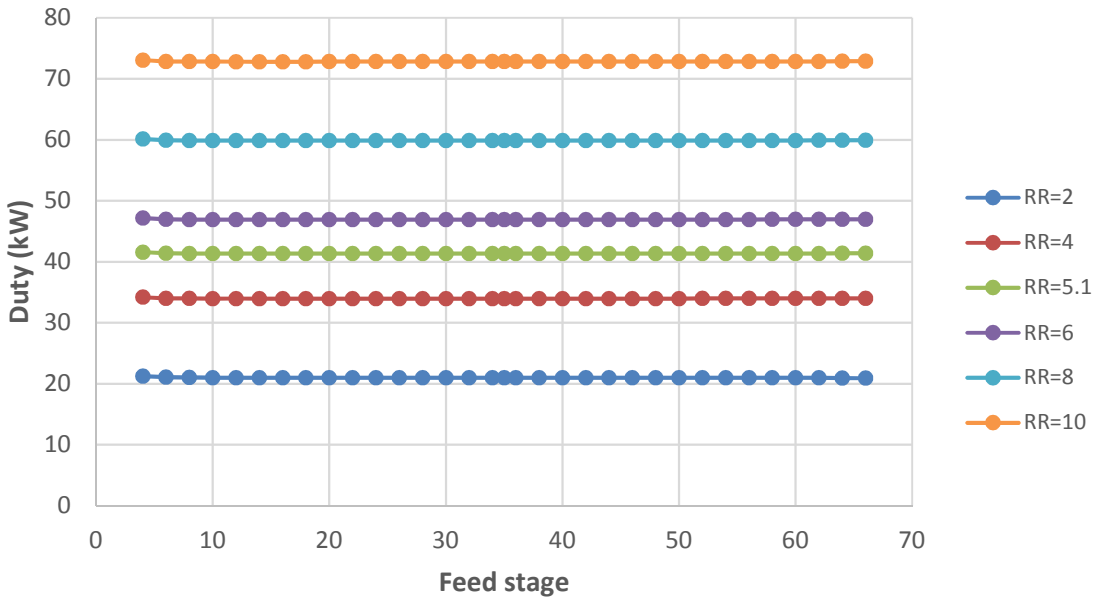

Figure C32: Effect of feed location on the reboiler duty at various reflux ratios

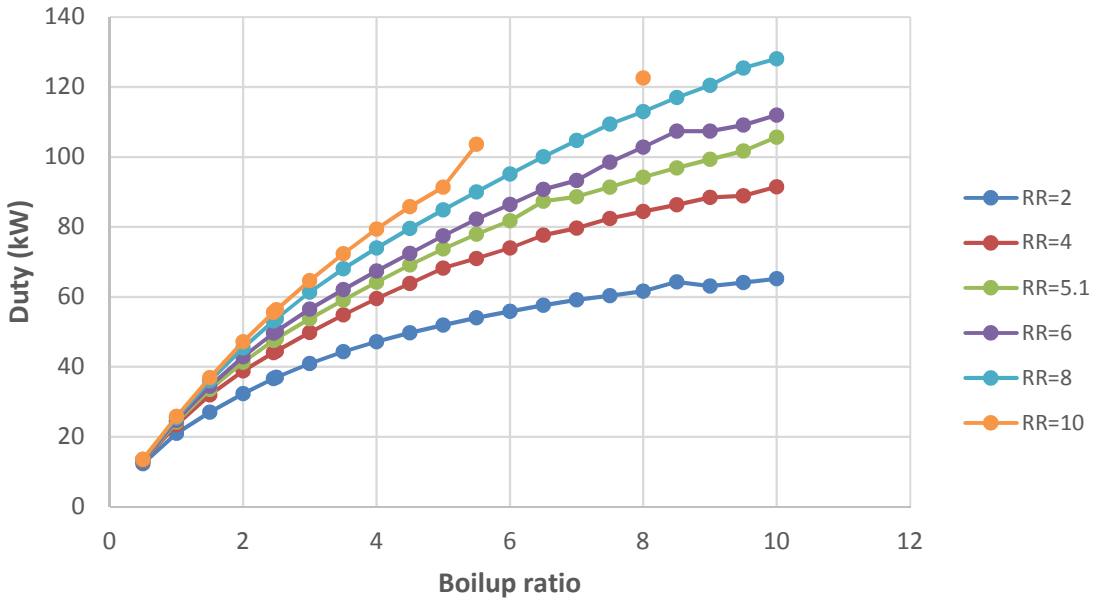

Figure C33: Effect of boilup ratio on reboiler duty at various reflux ratios

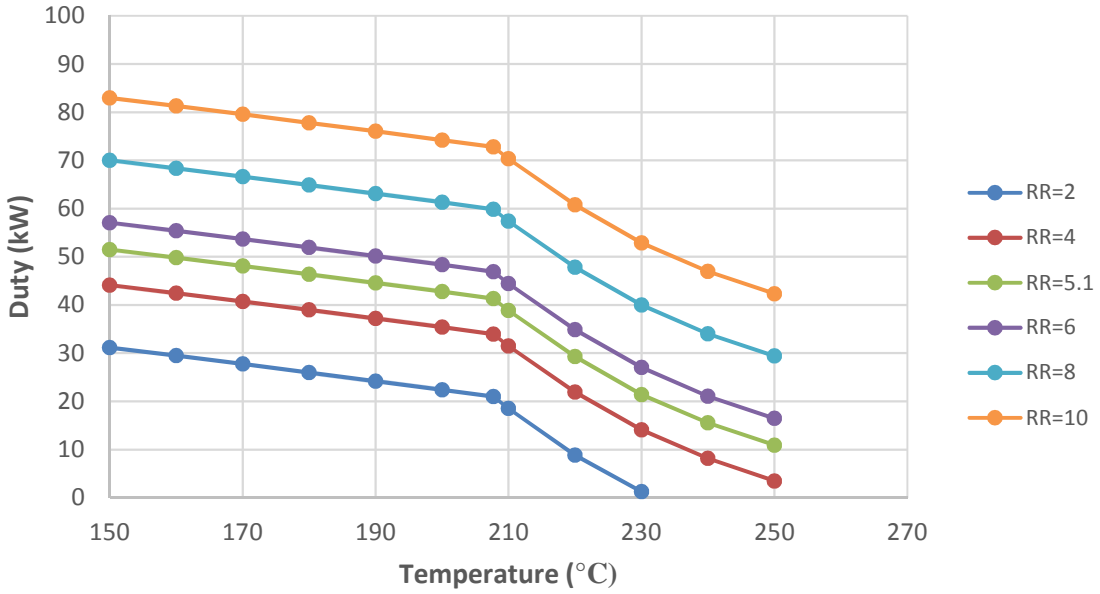

Figure C34: Effect of feed temperature on the reboiler duty at various reflux ratios

Sensitivity analysis at various number of stages

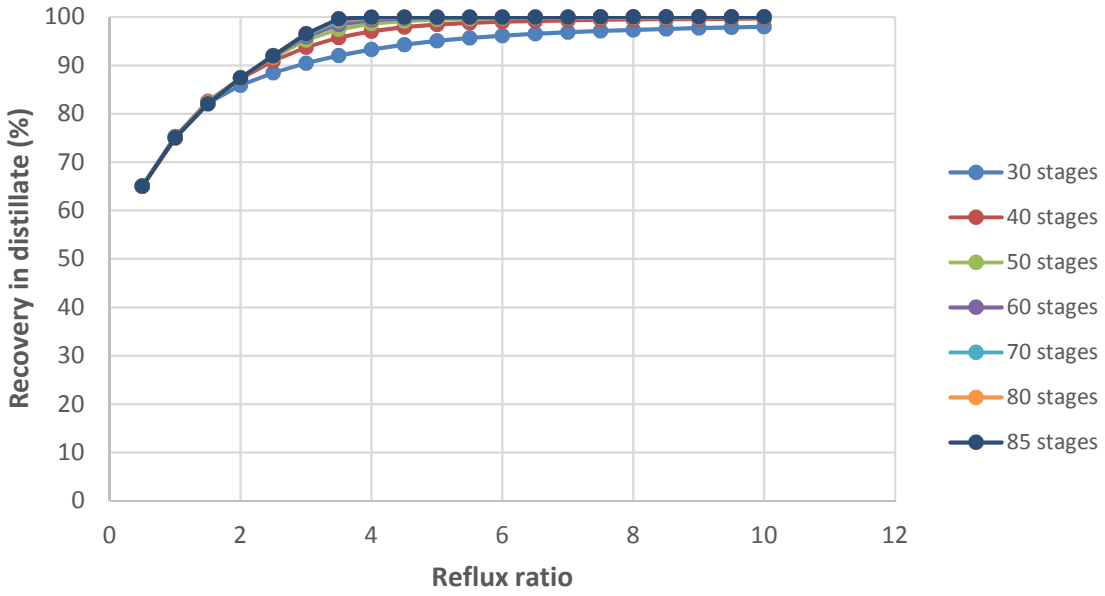

Figure C35: Effect of reflux ratio on the recovery of limonene in distillate at various number of stages

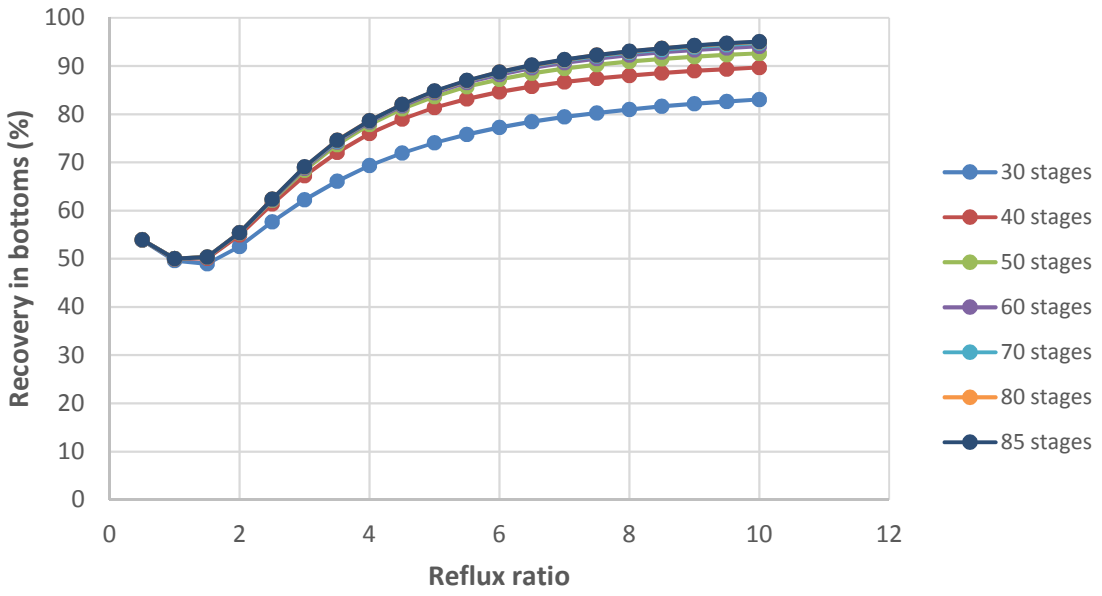

Figure C36: Effect of reflux ratio on the recovery of 2,5-dimethylstyrene in bottoms at various number of stages

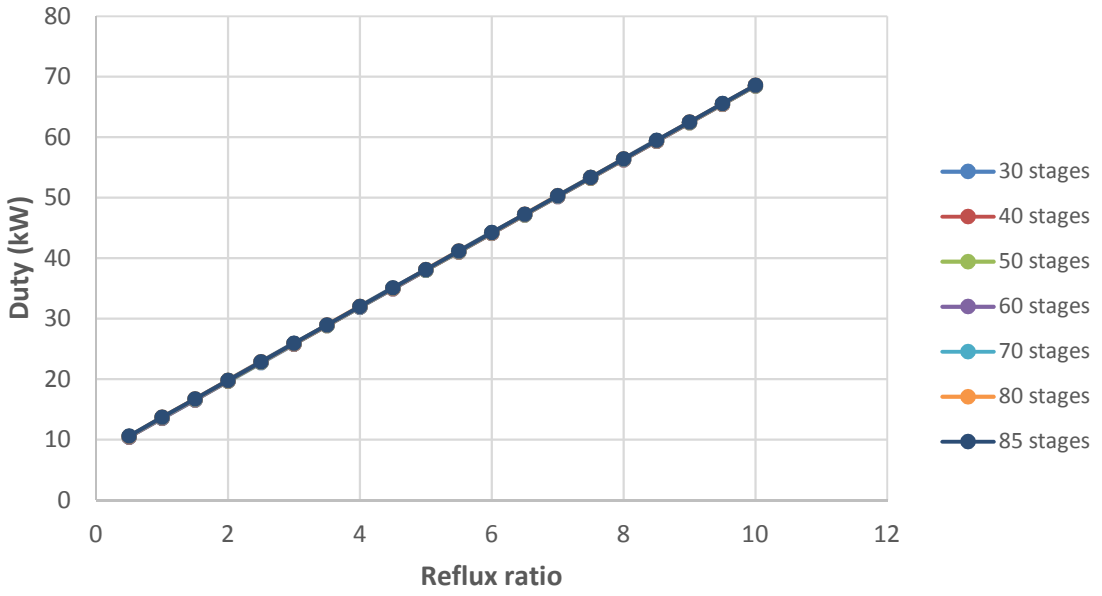

Figure C37: Effect of reflux ratio on the reboiler duty at various number of stages

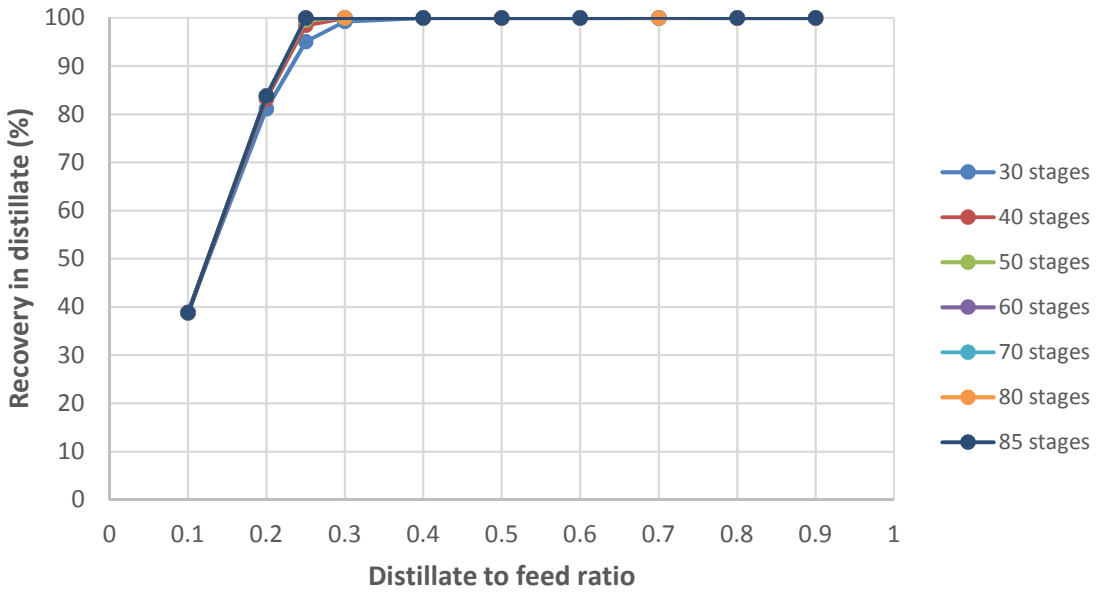

Figure C38: Effect of distillate to feed ratio on recovery of limonene in distillate at various number of stages

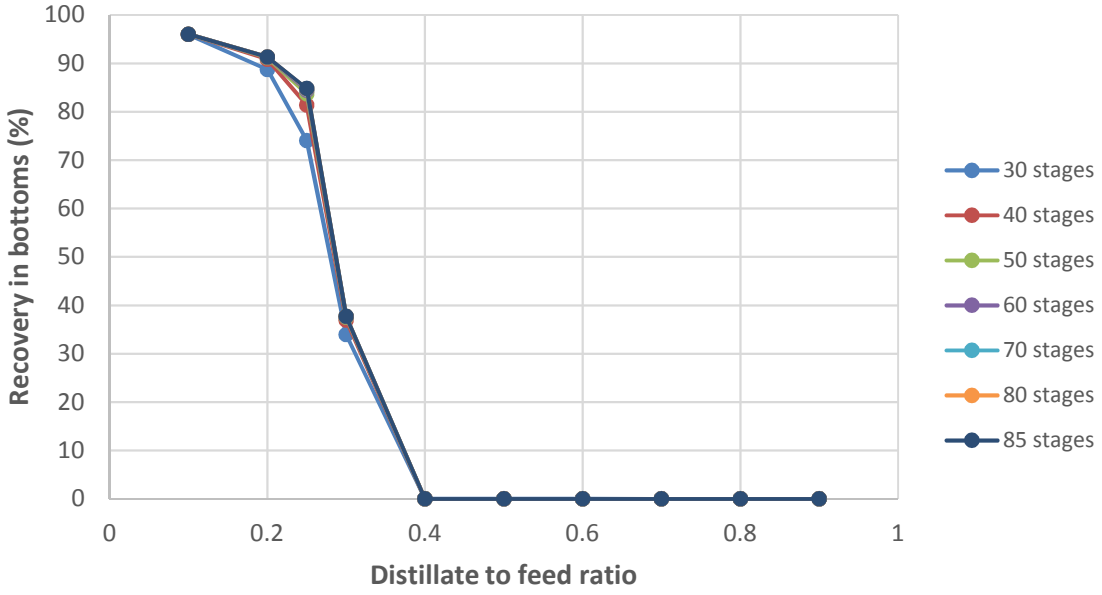

Figure C39: Effect of distillate to feed ratio on recovery of 2,5-dimethylstyrene in bottoms at various number of stages

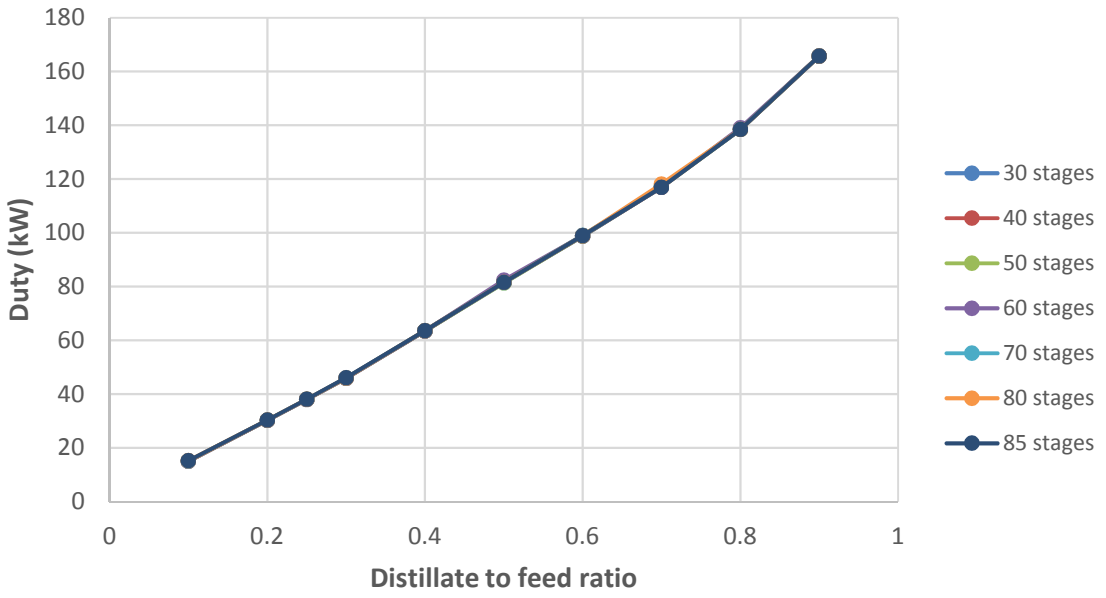

Figure C40: Effect of distillate to feed ratio on the reboiler duty at various number of stages

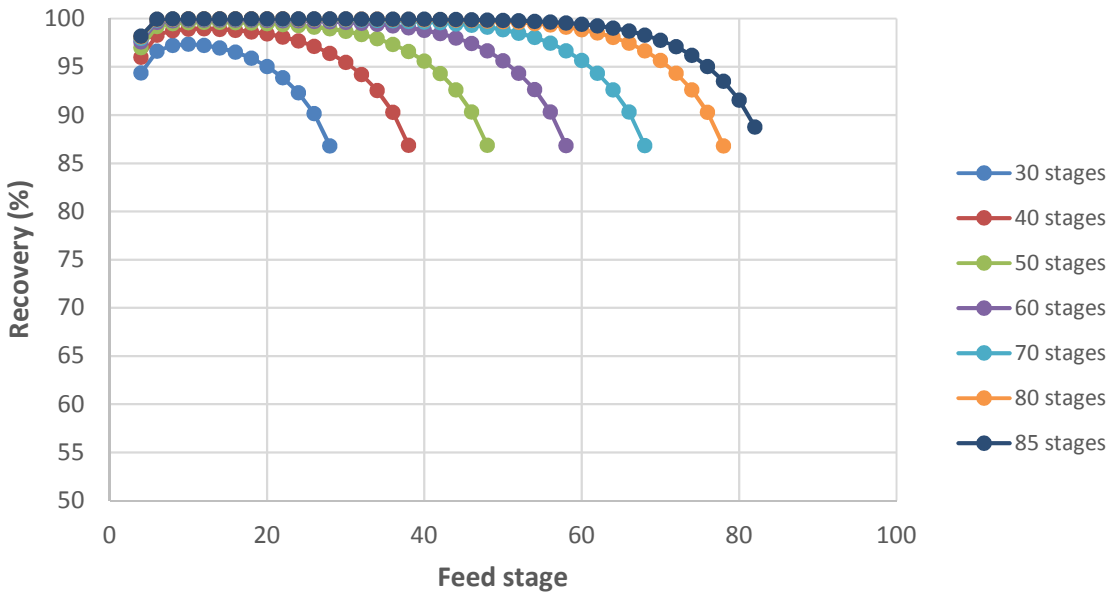

Figure C41: Effect of feed location on the recovery of limonene at various number of stages

C.4. T-103 sensitivity analysis

Effect of reflux ratio

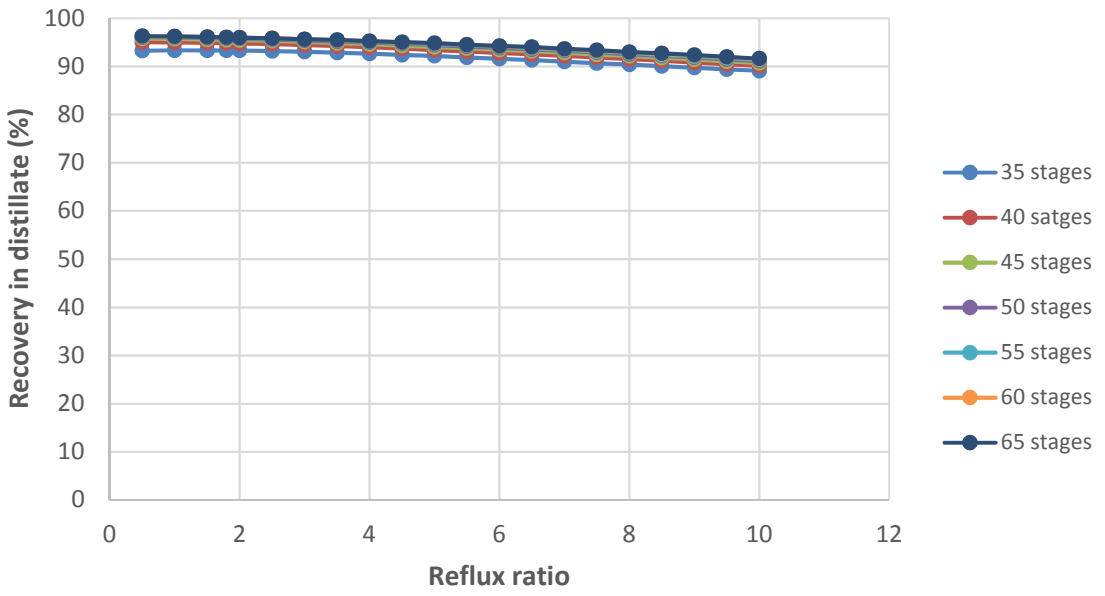

Figure C42: Effect of reflux ratio on limonene recovery in distillate product for various number of stages

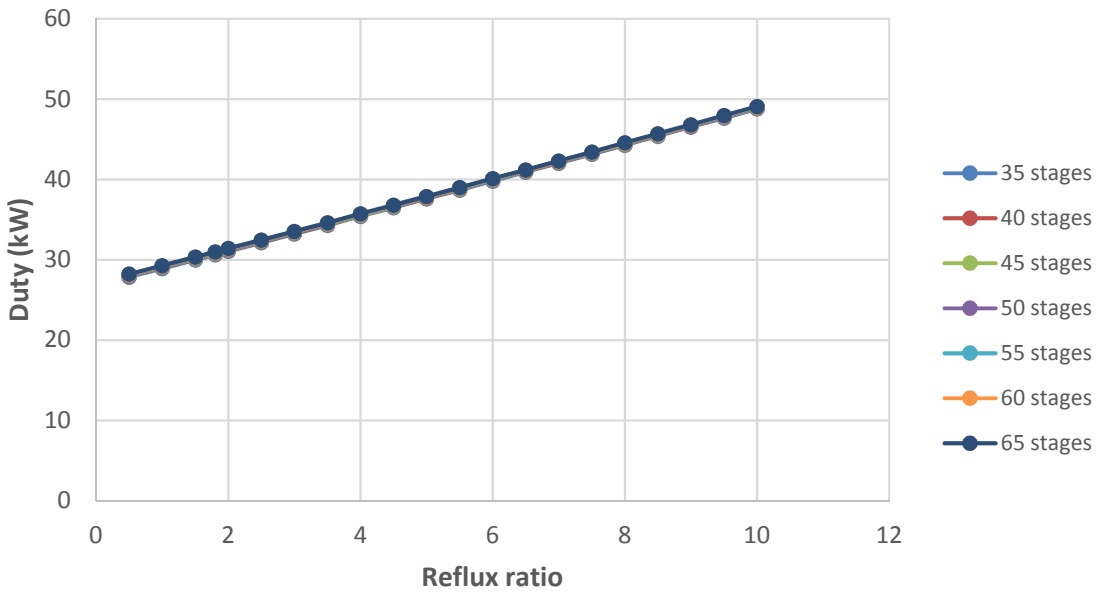

Figure C43: Effect of reflux ratio on reboiler duty for various number of stages

Effect of oil feed location

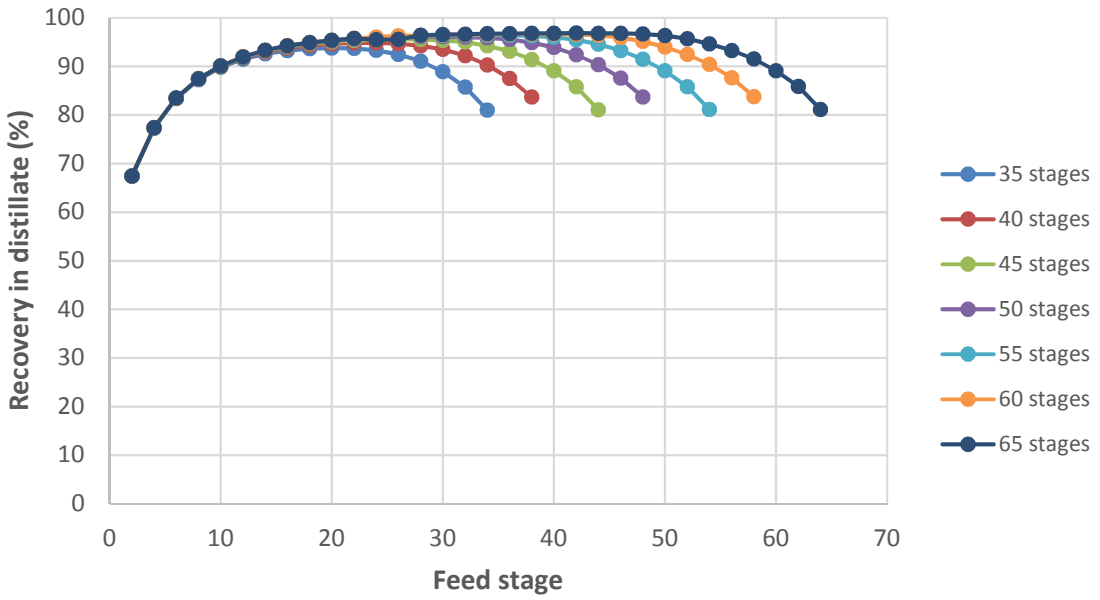

Figure C44: Effect of oil feed stage on limonene recovery in distillate product for various number of stages

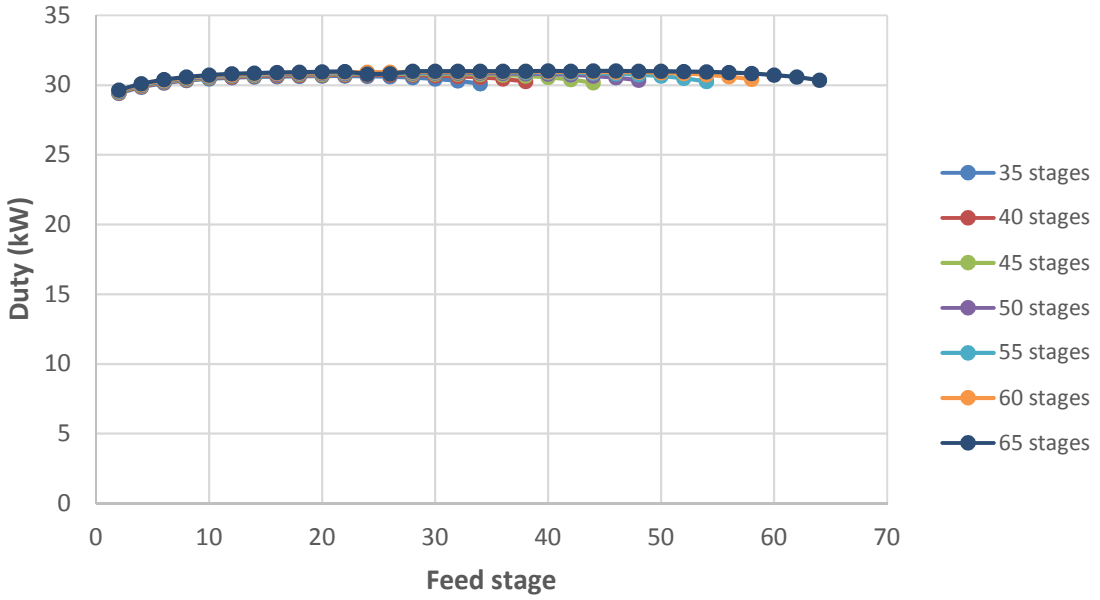

Figure C45: Effect of oil feed location on reboiler duty for various number of stages

Effect of entrainer feed location

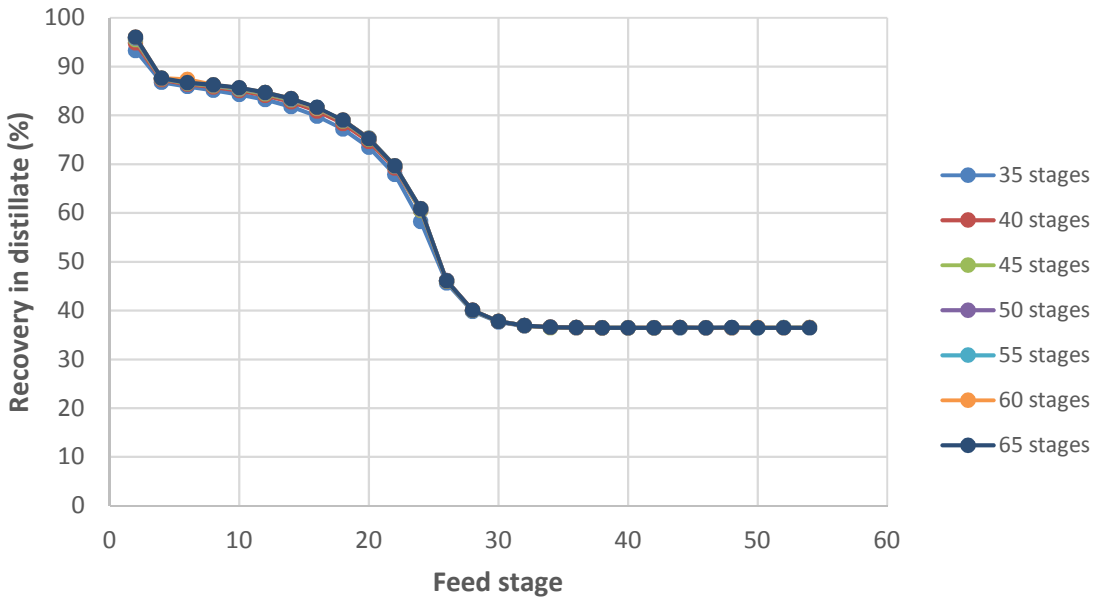

Figure C46: Effect of entrainer feed stage on limonene recovery in distillate product for various number of stages

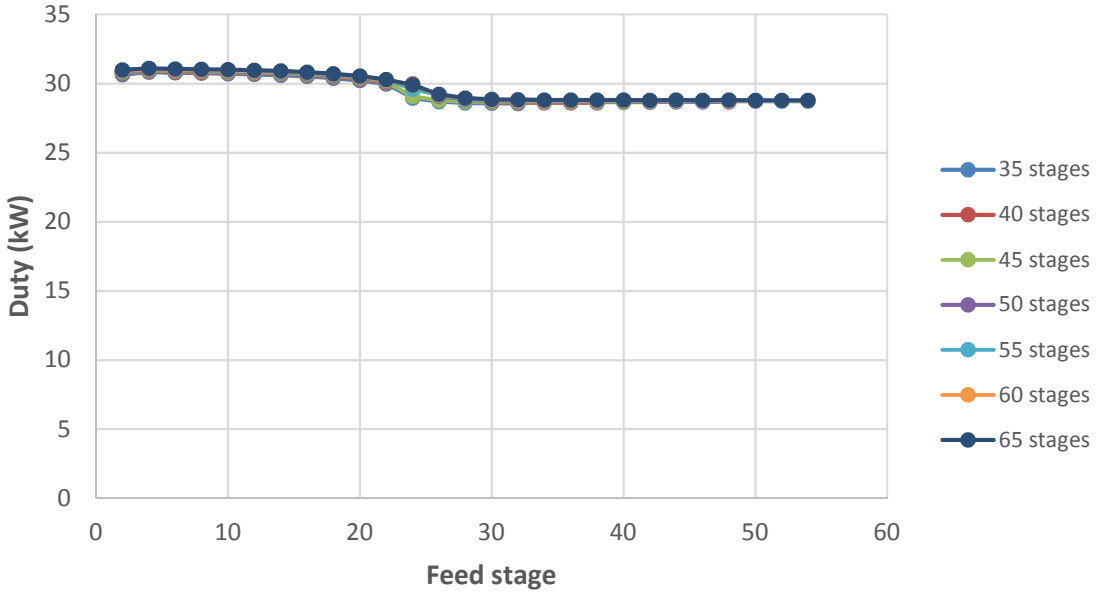

Figure C47: Effect of entrainer feed location on reboiler duty for various number of stages

Effect of entrainer flow rate

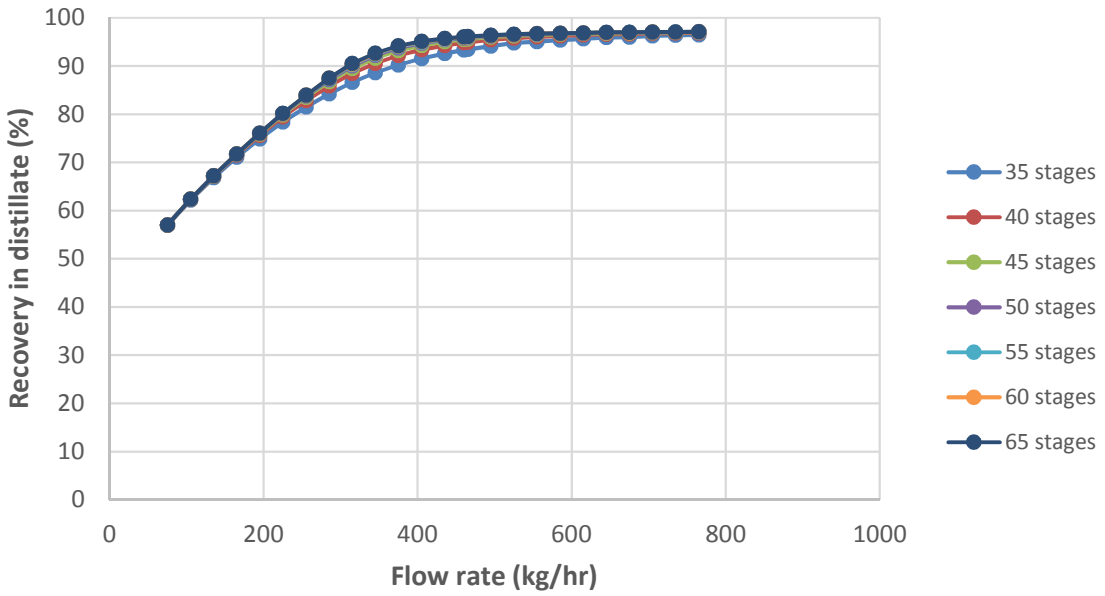

Figure C48: Effect of entrainer flow rate on limonene recovery in distillate product for various number of stages

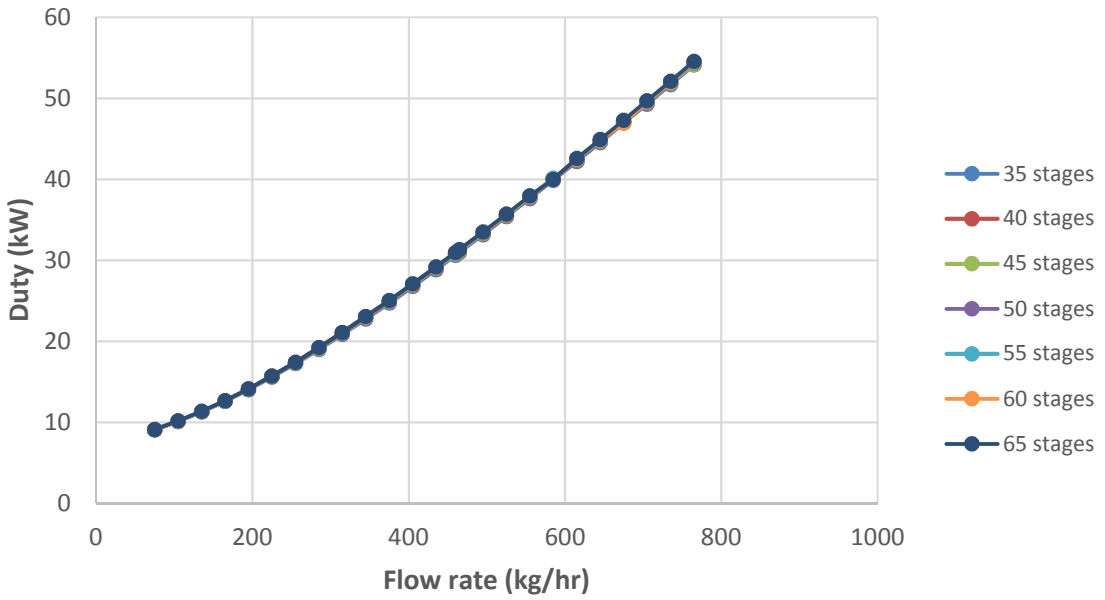

Figure C49: Effect of entrainer feed rate on reboiler duty for various number of stages

Effect of entrainer feed temperature

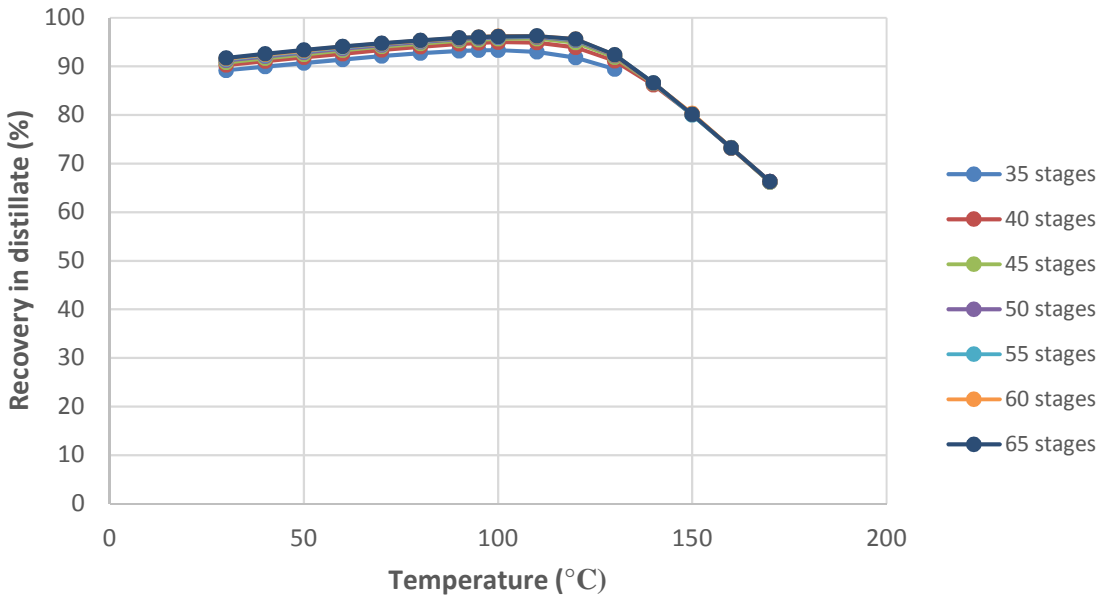

Figure C50: Effect of entrainer feed temperature on limonene recovery in distillate product for various number of stages

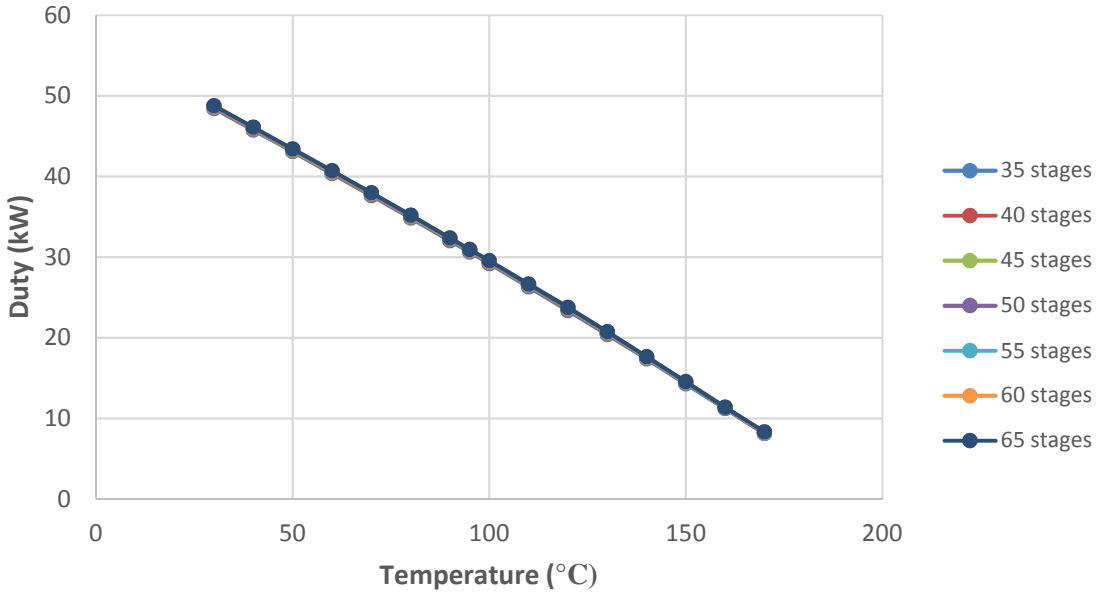

Figure C51: Effect of entrainer feed temperature on reboiler duty for various number of stages

C.5. T-104 sensitivity analysis

Effect of reflux ratio

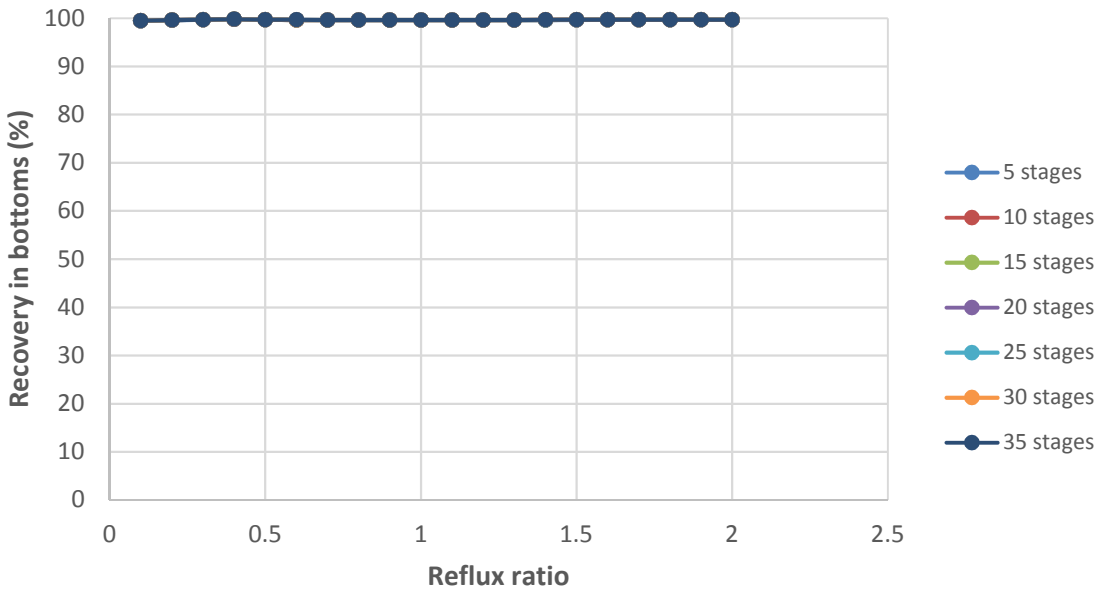

Figure C52: Effect of reflux ratio on the recovery of DEG in bottoms product for various number of stages

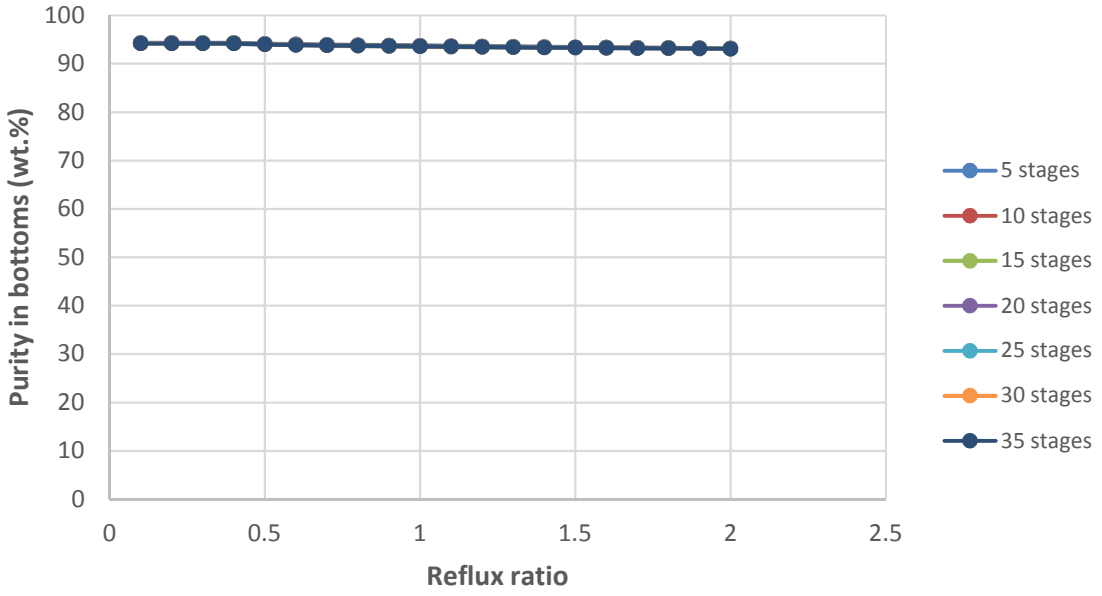

Figure C53: Effect of reflux ratio on purity of DEG in bottoms product for various number of stages

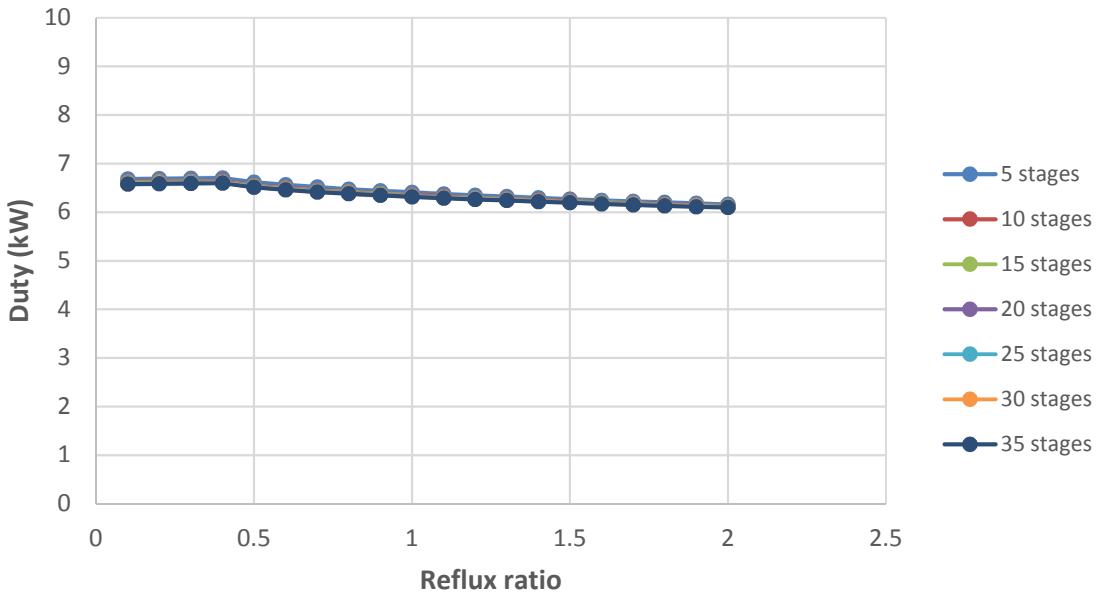

Figure C54: Effect of reflux ratio on reboiler duty for various number of stages

Effect of boilup ratio

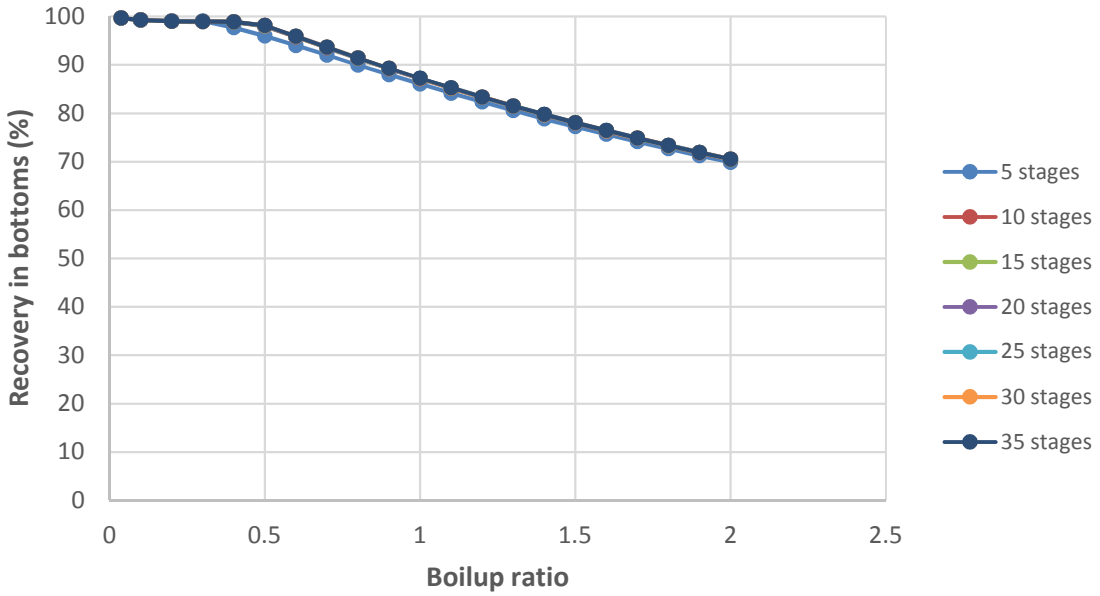

Figure C55: Effect of boilup ratio on DEG recovery in bottoms product at various number of stages

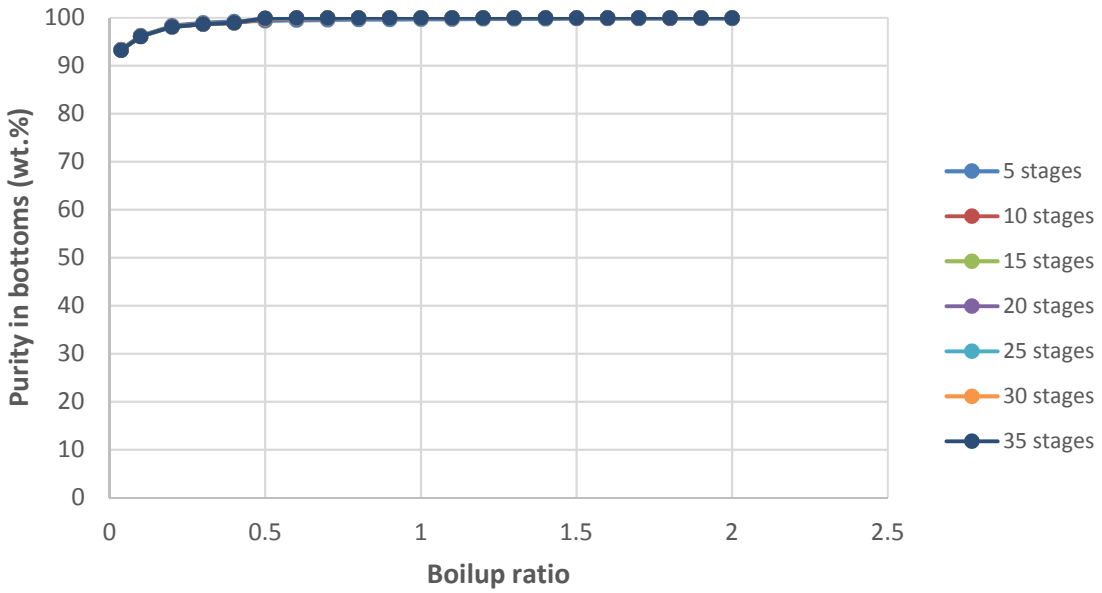

Figure C56: Effect of boilup ratio on DEG purity in bottoms product at various number of stages

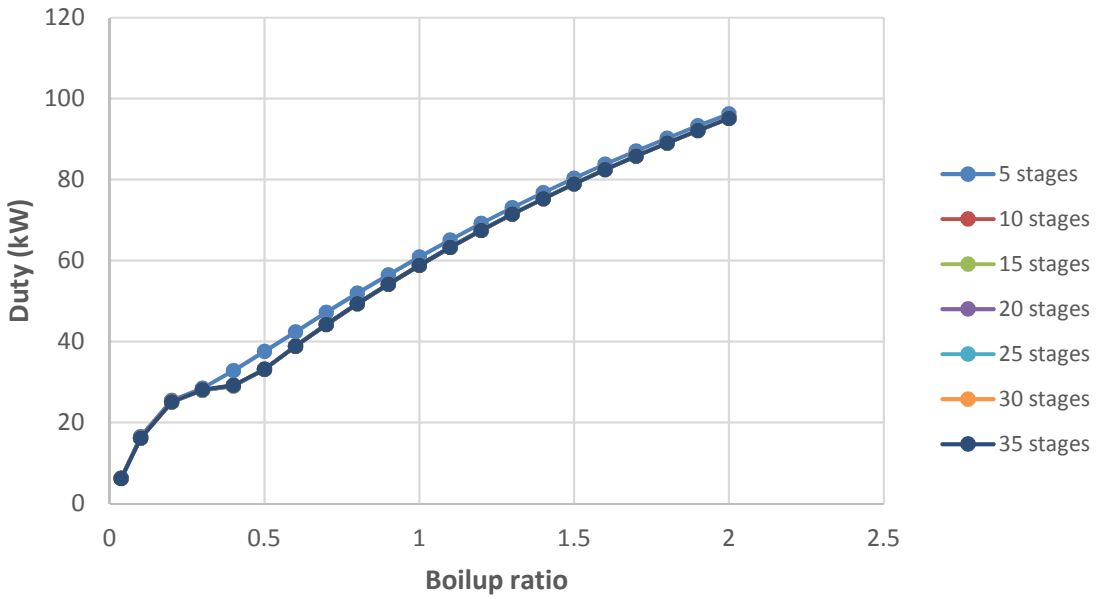

Figure C57: Effect of boilup ratio on reboiler duty at various number of stages

Effect of feed location

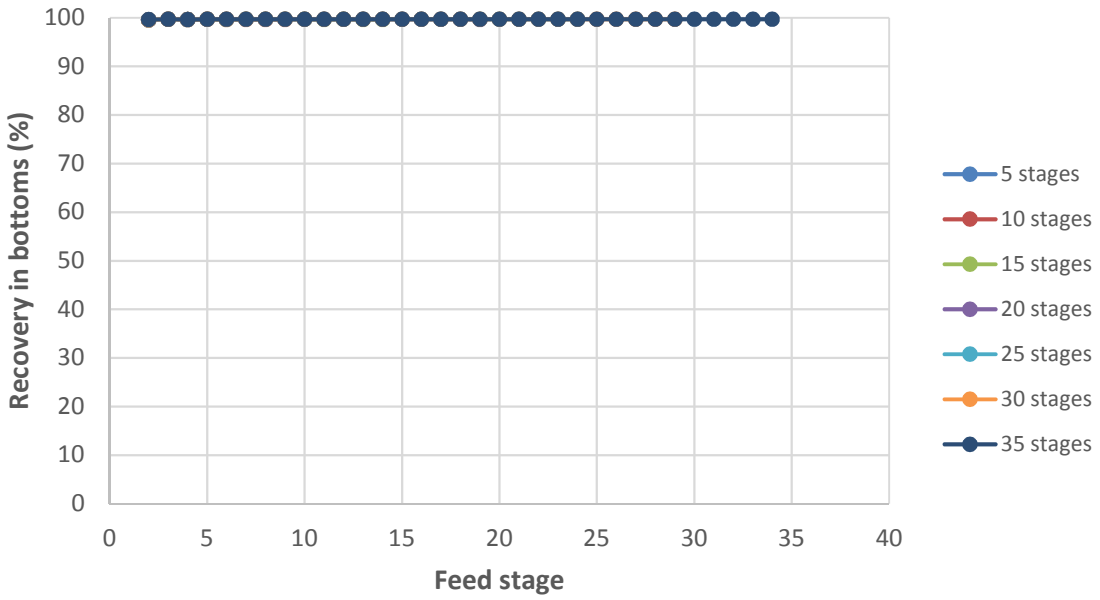

Figure C58: effect of feed location on DEG recovery in bottoms product for various number of stages

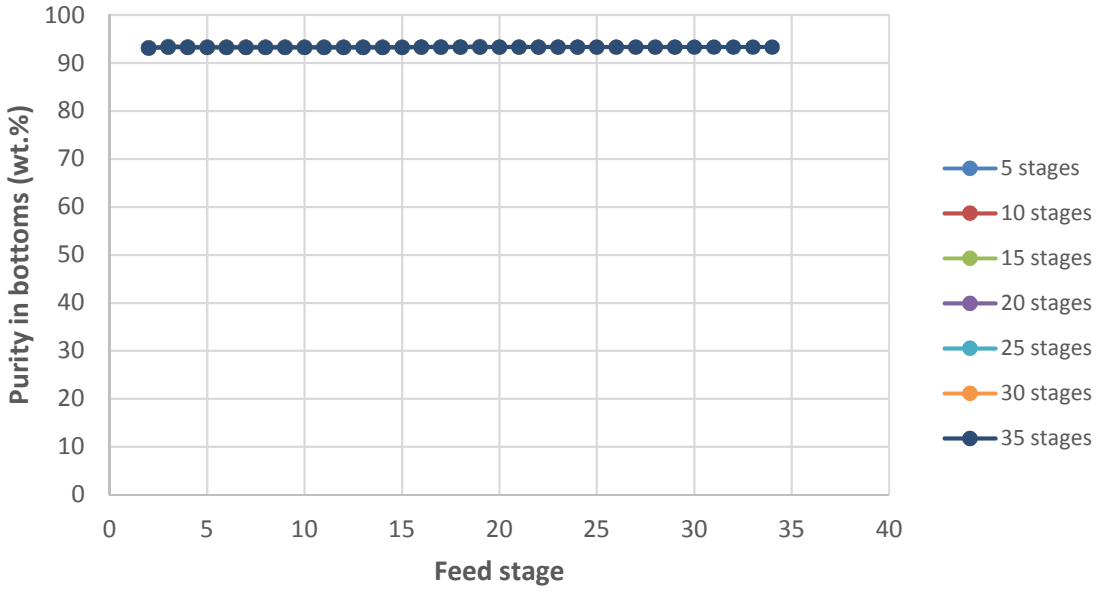

Figure C59: Effect of feed location on DEG purity in bottoms at various number of stages

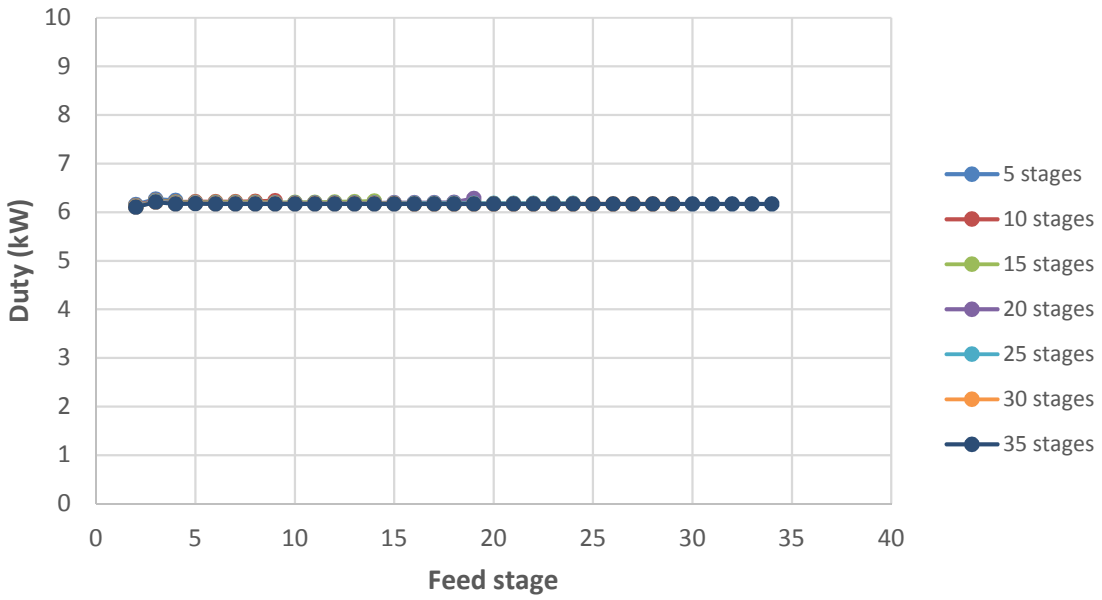

Figure C60: Effect of feed location on reboiler duty for various number of stages

Effect of feed temperature

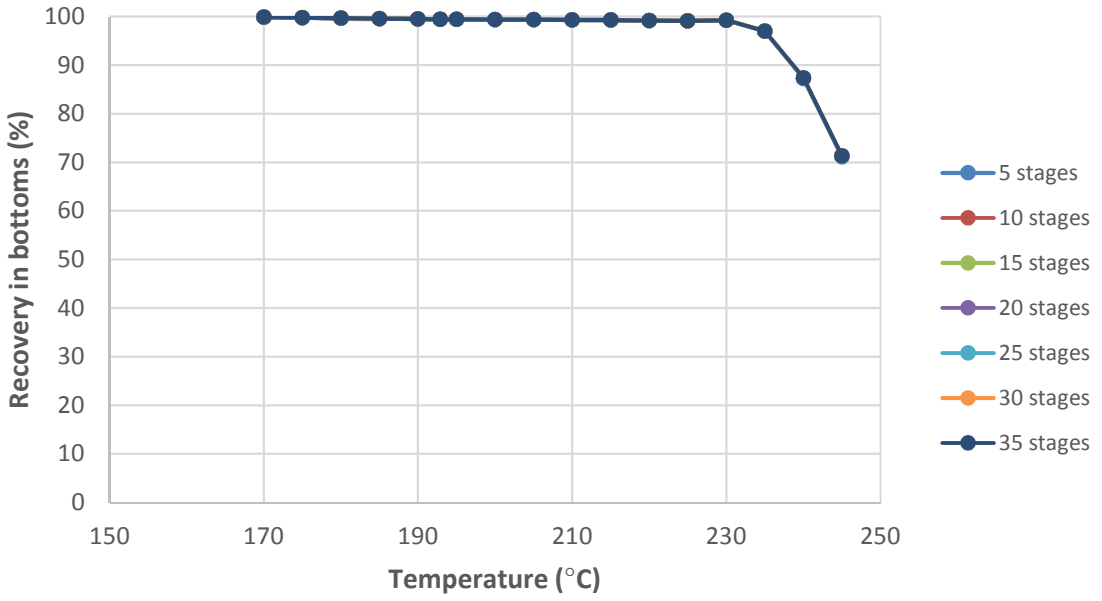

Figure C61: Effect of feed temperature on DEG recovery in bottoms product at various number of stages

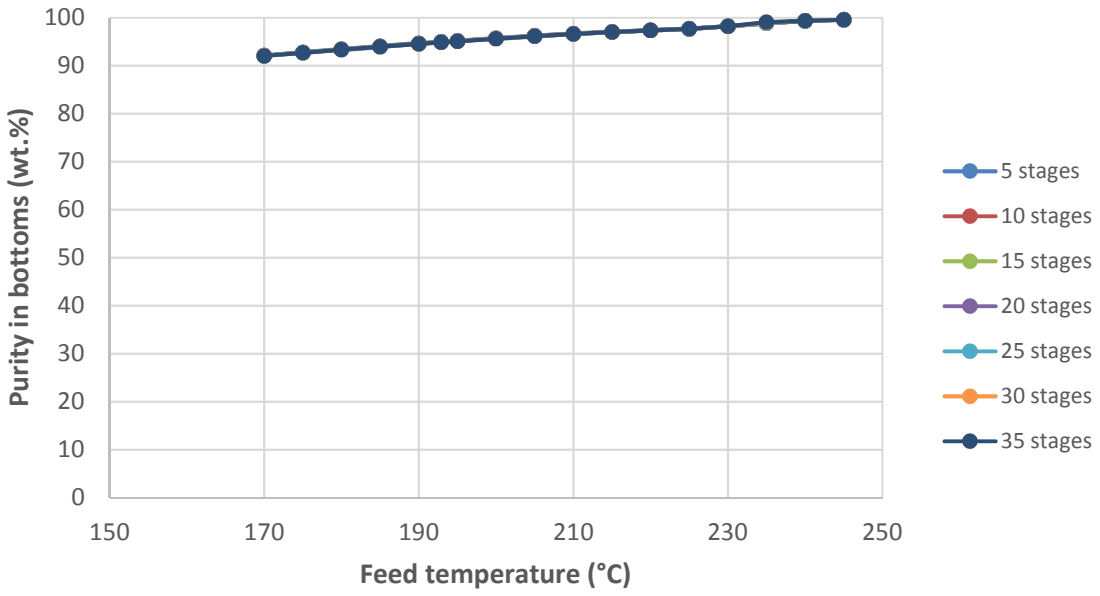

Figure C62: Effect of feed temperature on DEG purity in bottoms product for various number of stages

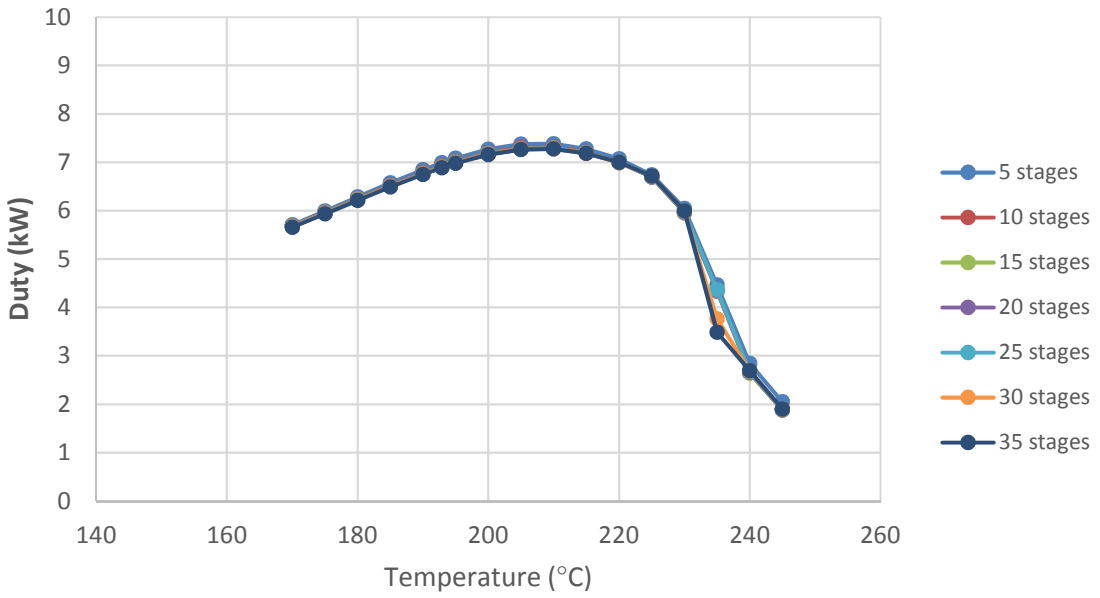

Figure C63: Effect of feed temperature on reboiler duty at various number of stage

APPENDIX D: ADDITIONAL INFORMATION FOR ECONOMIC EVALUATION

Table D1: Additional components of TDC

Component	Value (% of ISBL)	Actual amount (MM$)
Additional piping	4.5	0.17
Warehouse	4	0.15
Site development	9	0.34
Total other costs		**0.66**
TDC		**4.43**

Table D2: Components of TIC

Component	Value (% of TDC)	Actual amount (MM$)
Prorateable expenses	10	0.44
Field expenses	10	0.44
Home office and construction	20	0.88
Project contingency	10	0.44
Other costs (start-up, permits etc)	10	0.44
TIC		**2.66**

Table D3: Final components for capital cost estimation

Item	Actual amount (MM$)
TFCI	7.09
Land	0.14
WC	0.35
TCI	**7.6**

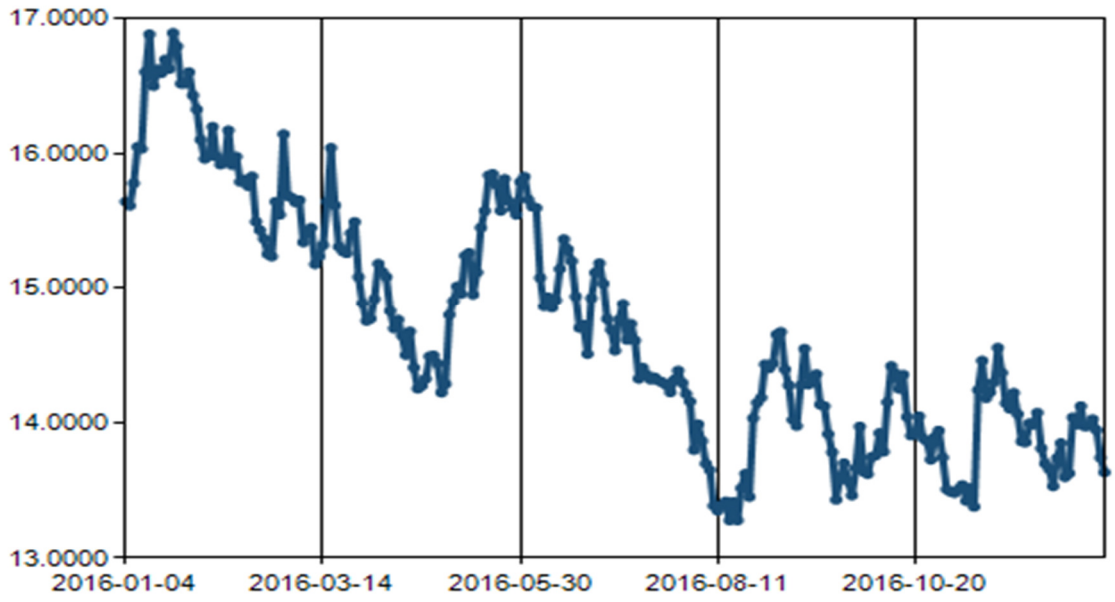

Figure D1: Rand/Dollar exchange rate trends for 2016 (from South African Reserve Bank)

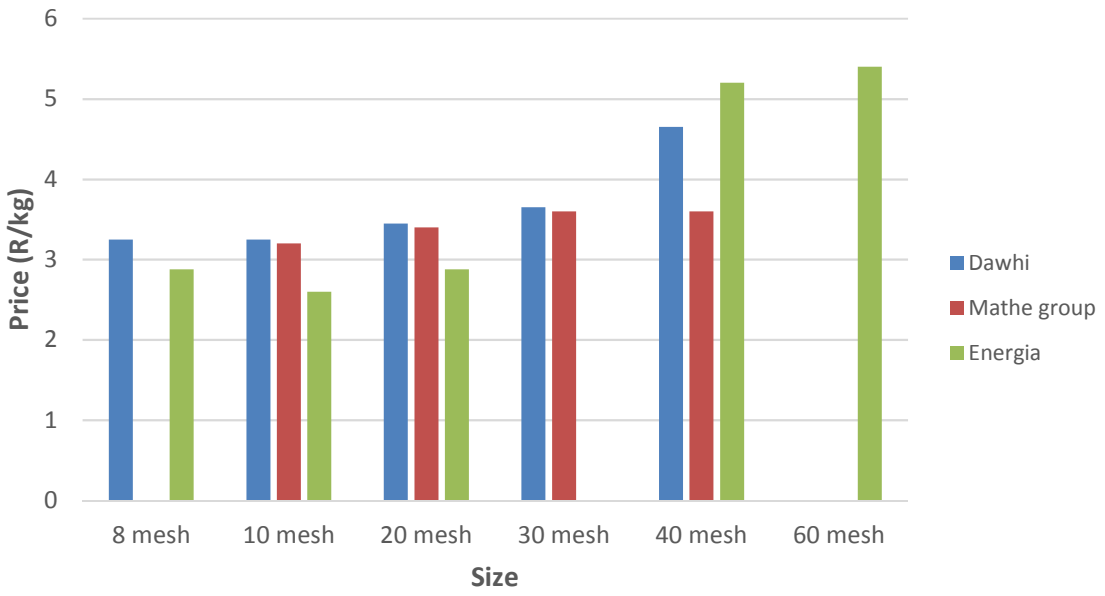

Figure D2: Crumb prices from various suppliers

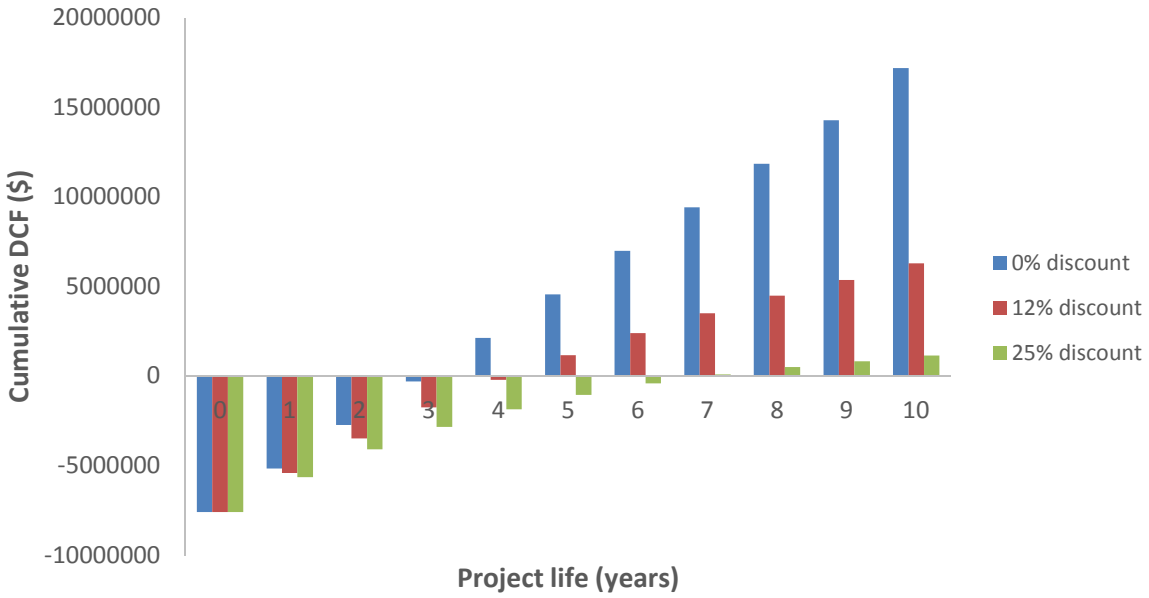

Figure D3: Discounted cash flow for the base case waste tyre to limonene process

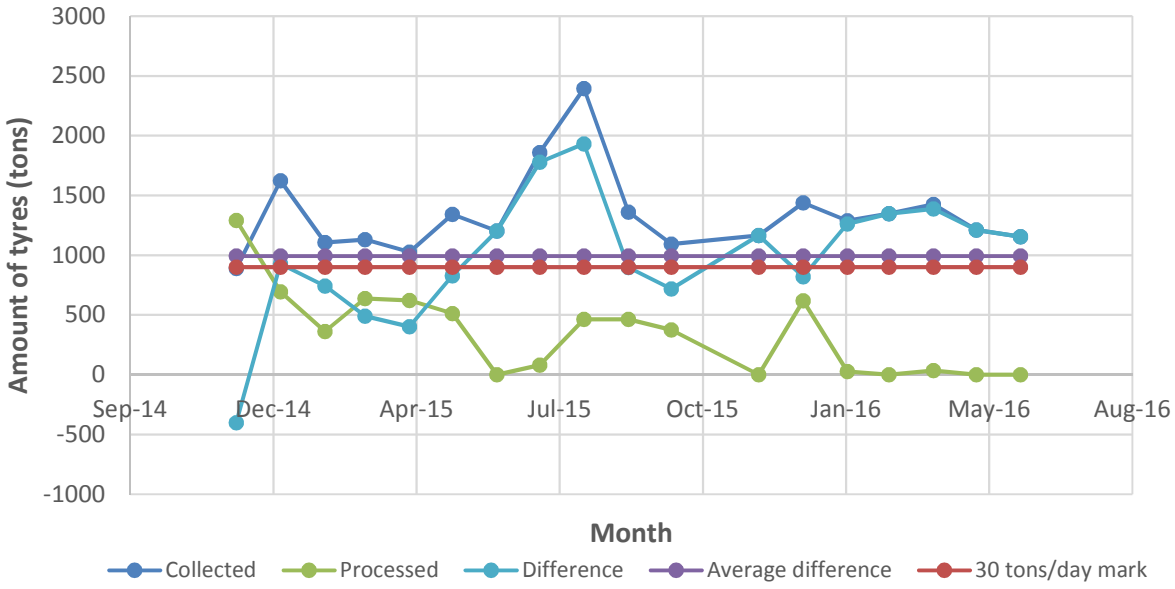

Figure D4: Waste tyres collection and processing data for Western Cape, from REDISA (Dec 2014 – Jun 2016)

APPENDIX E: INDIVIDUAL EQUIPMENT COST

Equipment name	Description	Number required	Original size parameter	Size parameter in current study	Size ratio	Size parameter units	Base year	Scaled unit purchased cost in base year (US$)	Total purchased cost in base year (US$)	Total scaled installed cost in base year (US$)	Installation factor	Total scaled installed cost in 2016 (US$)	Source
Pre-treatment													
	Single hook debeader	1					2016	8000	8000	24160		24160	
	Tyre conveyor	1					2016	4800	4800	14496		14496	
	Tyre shredder	1					2016	52200	52200	157644		157644	Jiangyin Xinda
	Tyre chip conveyer	1	1250	1250	1	kg/hr	2016	3600	3600	10872	3.02	10872	Machinery Co. Ltd
	Area total								**68600**	**207172**		**207172**	
Pyrolysis													
RX-101	Pyrolysis reactor	1	417	1250	3	kg/hr	2016	386636	386636	1159909	3.0	1159909	Pyrocrat Systems
MG-101	Magnetic separator	1	417	1250	3	kg/hr	2016	32000	32000	96000	3.0	96000	LLp
EX-102	Reactor volatiles condenser	1	235	235	1	kW	2013	14000	14000	88400	6.3	86764	Aspen Plus®
DM-101	Volatiles condenser knockout drum	1	719	719	1	kg/hr	2013	16100	16100	110500	6.9	108455	Aspen Plus®
	Area total								**448736**	**1454809**		**1451128**	

Figure D1: Individual equipment cost for pre-treatment and pyrolysis section

Equipment name	Description	Number required	Original size parameter	Size parameter in current study	Size ratio	Size parameter units	Base year	Scaled unit purchased cost in base year (US$)	Total purchased cost in base year (US$)	Total scaled installed cost in base year (US$)	Installation factor	Total scaled installed cost in 2016 (US$)	Source
Separation													
PC 101	Lights remover feed pump	1	0.6	0.6	1	m3/hr	2013	3800	3800	26600	7.0	26108	Aspen Plus®
PC 102	Limonene column feed pump	1	0.1	0.1	1	m3/hr	2013	3800	3800	27500	7.2	26991	Aspen Plus®
	T 101 reflux pump	1	0.1	0.1	1	m3/hr	2013	4300	4300	27100	6.3	26598	Aspen Plus®
	T 102 reflux pump	1	0.08	0.08	1	m3/hr	2013	4300	4300	28000	6.5	27482	Aspen Plus®
	T 103 reflux pump	1	0.01	0.01	1	m3/hr	2013	4300	4300	28000	6.5	27482	Aspen Plus®
	T 104 reflux pump	1	0.02	0.02	1	m3/hr	2013	4300	4300	28000	6.5	27482	Aspen Plus®
EX 101	T 101 feed preheater	1	19	19	1	kW	2013	9300	9300	56300	6.1	55258	Aspen Plus®
EX 103	DEG cooler	1	42	42	1	kW	2013	10400	10400	54700	5.3	53688	Aspen Plus®
EX 104	HFO cooler	1	28	28	1	kW	2013	10800	10800	80100	7.4	78617	Aspen Plus®
	T 101 condenser	1	91	91	1	kW	2013	12200	12200	81600	6.7	80090	Aspen Plus®
	T 102 condenser	1	36	36	1	kW	2013	9300	9300	53400	5.7	52412	Aspen Plus®
	T 103 condenser	1	4	4	1	kW	2016	1224	1224	7253	5.9	7253	Turton et al., 2009
	T 104 condenser	1	130	130	0.1	kW	2013	3549	3549	16905	4.8	16592	Aspen Plus®
	T 101 reboiler	1	103	103	1	kW	2013	18500	18500	79800	4.3	78323	Aspen Plus®
	T 102 reboiler	1	38	38	1	kW	2013	16800	16800	71400	4.3	70078	Aspen Plus®
	T 103 reboiler	1	29	29	1	kW	2013	12300	12300	66200	5.4	64975	Aspen Plus®
	T 104 reboiler	1	31	31	1	kW	2013	20200	20200	75100	3.7	73710	Aspen Plus®
	T 101 condenser accumulator	1	680	680	1	kg/hr	2013	15700	15700	99500	6.3	97658	Aspen Plus®
	T 102 condenser accumulator	1	430	430	1	kg/hr	2013	15700	15700	108500	6.9	106492	Aspen Plus®
	T 103 condenser accumulator	1	56	56	1	kg/hr	2013	15700	15700	108500	6.9	106492	Aspen Plus®
	T 104 condenser accumulator	1	135	135	1	kg/hr	2013	15700	15700	108500	6.9	106492	Aspen Plus®
T 101	Light hydrocarbon remover	1	0.46	0.46	1	m	2016	41027	41027	318310	7.8	318310	Turton et al., 2009
T 102	Limonene-rich cut purifier	1	0.46	0.46	1	m	2016	32731	32731	255331	7.8	255331	Turton et al., 2009
T 103	Limonene column	1	0.46	0.46	1	m	2016	32731	32731	255331	7.8	255331	Turton et al., 2009
T 104	DEG regenaration column	1	0.46	0.46	1	m	2016	9291	9291	76087	8.2	76087	Turton et al., 2009
	Area total								**327953**	**2138017**		**2115331**	

Figure D2: Individual equipment cost for the separation section

APPENDIX F: CASH FLOW ANALYSIS

Year	Fixed capital	Land	Working capital	Manufacturing costs	Revenue	Depreciation	Tax	Net income	Cash flow	Cummulative cash flow	Discounted cash flow (12%)	Cummulative discounted cash flow (12%)		Discounted cash flow (25%)	Cummulative discounted cash flow
0	-7094426	-141889	-354721						-7591035	-7591035	-7591035	-7591035		-7591035	-7591035
1				-872002	3969493	709443	668654	1719395	2428838	-5162198	2168605	-5422430		1943070	-5647965
2				-872002	3969493	709443	668654	1719395	2428838	-2733360	1936255	-3486176		1554456	-4093509
3				-872002	3969493	709443	668654	1719395	2428838	-304522	1728799	-1757377		1243565	-2849944
4				-872002	3969493	709443	668654	1719395	2428838	2124316	1543570	-213806		994852	-1855092
5				-872002	3969493	709443	668654	1719395	2428838	4553154	1378188	1164381		795882	-1059210
6				-872002	3969493	709443	668654	1719395	2428838	6981991	1230525	2394906		636705	-422505
7				-872002	3969493	709443	668654	1719395	2428838	9410829	1098683	3493589		509364	86859
8				-872002	3969493	709443	668654	1719395	2428838	11839667	980967	4474556		407491	494350
9				-872002	3969493	709443	668654	1719395	2428838	14268505	875863	5350419		325993	820343
10		141889	354721	-872002	3969493	709443	668654	1719395	2925448	17193952	941916	6292335		314118	1134461

Figure E1: Cash flow analysis for the waste tyres to limonene scenario (all values in $)